



Università
Ca'Foscari
Venezia

PHD IN ENVIRONMENTAL SCIENCES

33° CYCLE

**Chemical characterization of Arctic aerosol for
investigating the multi-annual profile of
anthropogenic and biogenic markers**

SSD: CHIM/01

Doctorate Coordinator:

Prof. Enrico BERTUZZO

Supervisor:

Prof. Andrea GAMBARO

PhD candidate:

Matteo FELTRACCO

816906

Declaration of Authorship

I, Matteo FELTRACCO, declare that this thesis titled, “Chemical characterization of Arctic aerosol for investigating the multi-annual profile of anthropogenic and biogenic markers” and the work presented in it are my own. I confirm that:

- This work was done wholly or mainly while in candidature for a research degree at this University.
- Where any part of this thesis has previously been submitted for a degree or any other qualification at this University or any other institution, this has been clearly stated.
- Where I have consulted the published work of others, this is always clearly attributed.
- Where I have quoted from the work of others, the source is always given. With the exception of such quotations, this thesis is entirely my own work.
- I have acknowledged all main sources of help.
- Where this work is based on work done by myself jointly with others, I have made clear what was done by others and what I have contributed myself.

Matteo Feltracco

For those who believed in me.

Abstract

The present PhD thesis provides a broad information about the chemical characterization of the Arctic aerosol from 2013 to early 2019 collected at Ny-Ålesund, Svalbard Island, Norway. The work aims to investigate the inter- and intra-annual variation of several water-soluble compounds in order to understand their potential sources, their transport processes and their chemical/physical transformation.

Svalbard is Norway's northernmost region, and the archipelago is one of the northernmost land-areas in the world. The Svalbard archipelago is surrounded by two different water masses: the warm Atlantic water on the western side, and the cold Arctic water on the eastern side. The coastal current is the closest water mass, originating from the cold East Spitsbergen Current (ESC) and further west, warm and saline Atlantic Water (AW) flows as the West Spitsbergen Current (WSC). For these reasons, the Svalbard region is particularly interesting in regard to climate change.

Ny-Ålesund is a research community with up to 150 people living there in the summer, while only around 20-30 permanent people are there during winter months. Pollution sources in and around Ny-Ålesund include power stations, cars, airplanes and water traffic, including small vessels and cruise ships. The limited local contamination makes Ny-Ålesund an open laboratory to investigate the long range atmospheric transport from anthropic areas and also the local biogenic sources.

Here, the size-distributions, source apportionment and transport processes of major ions, organic acids, free and combined amino acids, sugars and phenolic compounds were studied in the Arctic aerosols. This led to the characterization of more than 70 species. The thesis also aims to develop a new method for the determination of combined amino acids and photo-oxidation products of α -pinene in aerosol to understand differences and analogies with free amino acids and to understand the possible emission sources of these biomarkers. The determination of ions, carboxylic acids, free amino acids and phenolic compounds contained in the Arctic aerosol was performed using some method developed in some previous studies.

The results of this study explain that the water-soluble compounds were influenced by biomass burning events occurred in Northern Russia and Canada, together with a strong contribution from sea particles and phytoplankton bloom, especially deriving from the fjord (Kongsfjorden) which is located 1.2 km from the sampling site. It was therefore possible to investigate the degradation processes during long-range atmospheric transport and to highlight the impact of ice-free areas in summer, mainly due to the bacterial and fungal activity in the Svalbard Archipelago.

Contents

Declaration of Authorship	iii
Abstract	vii
List of papers	xv
Chapter 1 Atmospheric aerosol	1
1.1 Introduction	1
1.2 Aerosol size distribution	2
1.3 Primary and secondary organic aerosol	4
1.4 Lifetime and transport	6
1.5 Main sources of aerosols	6
1.6 Cloud condensation nuclei and ice nuclei	9
1.7 Aerosol optical proprieties	10
1.8 Health effects	11
Chapter 2 Sampling site	13
2.1 The Svalbard Archipelago	13
2.2 Ny-Ålesund	15
2.3 Gruvebadet Observatory	16
2.4 Aerosol sampling	17
2.5 State of art	19
2.5.1 Key results of Italian research	20
Chapter 3 Analytes	23
3.1 Inorganic ions	23
3.2 Water soluble organic compounds	25
3.3 Atmospheric Microbiome	29

Chapter 4	Results and discussion	31
4.1	Free and combined L- and D-amino acids in Arctic aerosol (Feltracco et al., 2019)	31
4.2	Interannual variability of sugars in Arctic aerosol: Biomass burning and biogenic inputs (Feltracco et al., 2020)	32
4.3	Year-round measurements of size-segregated low molecular weight organic acids in Arctic aerosol (Feltracco et al., 2021)	33
4.4	Airborne bacteria and particulate chemistry capture phytoplankton bloom dynamics in an Arctic Fjord (Feltracco et al., <i>submitted</i>)	34
4.5	Multi-annual trend of major ions and WSOCs	35
4.5.1	Major ions	35
4.5.2	Organic acids	40
4.5.3	Sugars	42
4.5.4	Free amino acids	43
4.5.5	Phenolic compounds	46
4.6	Novelties of the thesis and future challenges	48
	Conclusions	51
	Bibliography	53
	Appendix A	63
	Appendix B	125
	Acknowledgements	133

List of Figures

1.1	Major sources of atmospheric aerosols ^[4]	2
1.2	Schematic representation of the modes of aerosol for different particle diameters D . On the left, key chemical compounds and particle generation processes; on the right, size ranges ^[3]	3
1.3	Comparison between median particle size distributions of aerosol mass concentrations and of water-soluble compounds of aerosol collected in Mestre-Venice ^[5]	4
1.4	Atmospheric lifetime for individual particles with indicated dominant loss processes in the troposphere ^[3]	7
1.5	South Eastern Australia bushfire smoke plume (NASA, 2019)	8
1.6	Global distribution of aerosol optical depth for the years 2007 to 2011 taken from the MODIS satellite instrument (NASA)	11
2.1	Regional geographical setting of Svalbard (left) and Prevailign surface currents of the Barents Sea and North Atlantic areas (right) ^[30]	14
2.2	Ny-Ålesund and the Kongsfjorden	15
2.3	Location of Ny-Ålesund, Gruvebadet Observatory and Kongsfjorden in front of Kongsvegen glacier	17
2.4	TE-6000 PM ₁₀ Head	18
2.5	TE-235 cascade impactor	18
3.1	Comparison between size distribution of PM _{2.5} , PM ₁₀ and some PBAPs (a); comparison between the molecular weight range of water-soluble organic matter from TSP, PM _{2.5} , PM ₁₀ , and the molecular weight of amino acids, peptides, and proteins (b) ^[73]	27
4.1	Composition of water soluble fraction of PM ₁₀ in atmospheric aerosol collected.	35

4.2	Major ions concentration in PM ₁₀ of 2014, 2015 and 2018-2019.	37
4.3	Carboxylic acids concentration in PM ₁₀ of 2013, 2014, 2015 and 2018-2019. . .	41
4.4	Pinonic and pinic acids concentration in PM ₁₀ of 2013, 2014, 2015 and 2018-2019.	42
4.5	Saccharides, anhydro-sugars and alcohol-sugars concentration in PM ₁₀ of 2013, 2014, 2015 and 2018-2019.	44
4.6	FAAs concentration in PM ₁₀ of 2014, 2015 and 2018-2019.	45
4.7	PCs concentration in PM ₁₀ of 2013, 2014, 2015 and 2018-2019.	47
1	Map of the Brøgger peninsula and Kongsfjorden. The red dots indicate Ny- Ålesund, Gruvebadet Laboratory and the KB3 marine sampling site. Image courtesy of the Norwegian Polar Institute.	96
2	Relative % of major ions, FAAs and CAs.	103
3	Target compounds PM ₁₀ concentration trend (ng m ⁻³). L-FAAs/Na ⁺ is dimen- sionless. “Chl depth-int” represents the 0-100 m depth-integrated standing stocks (mg Chl <i>a</i> m ⁻²) and “Chl discr. surface” represents the 10 m surface discrete concentrations (μg Chl <i>a</i> L ⁻¹). The graphs in column A represents the compounds derived from the exponential bloom (green-shaded), while col- umn B represents the post-bloom phase (orange-shaded).	105
4	Comparisons of microbial communities between coarse and fine fractions. The Venn diagram represents the amount of unique and shared OTUs across frac- tions, while the stacked histogram represents the relative abundance of OTUs at the Class level in each of the samples over time.	106
5	Changes in biodiversity and community structure of air samples over time. .	107

List of Tables

1.1	Approximative emission fluxes from different types of primary aerosols and gaseous precursors of secondary aerosols.	5
2.1	Aerosol sampling campaign considered for this work.	18

4.1	PM ₁₀ mean concentration for major ions reported for each sampling campaign. 2018-19 sampling campaign was divided depending on the seasons. Autumn and Winter 2018-2019 are reported as "18-19". In brackets, standard deviations are shown.	38
4.2	PM ₁₀ mean concentration for relevant L- and D-FAAs reported for each sampling campaign. 2018-19 sampling campaign was divided depending on the seasons. Autumn and Winter 2018-2019 are reported as "18-19".	46
4.3	PM ₁₀ mean concentration for PCs reported for each sampling campaign. . . .	47

List of papers

This doctoral thesis is based on the following papers, which are summarized in Chapter 4 and entirely reported in Appendix A:

- Feltracco, M., Barbaro, E., Kirchgeorg, T., Spolaor, A., Turetta, C., Zangrando, R., Barbante, C., & Gambaro, A. (2019). Free and combined L- and D-amino acids in Arctic aerosol. *Chemosphere*, 220, 412–421. doi.org/10.1016/j.chemosphere.2018.12.147
- Feltracco, M., Barbaro, E., Tedeschi, S., Spolaor, A., Turetta, C., Vecchiato, M., Morabito, E., Zangrando, R., Barbante, C., & Gambaro, A. (2020). Interannual variability of sugars in Arctic aerosol: Biomass burning and biogenic inputs. *Science of the Total Environment*, 706, 136089. doi.org/10.1016/j.scitotenv.2019.136089
- Feltracco, M., Barbaro, E., Spolaor, A., Vecchiato, M., Callegaro, A., Burgay, F., Vardè, M., Maffezzoli, N., Dallo, F., Scoto, F., Zangrando, R., Barbante, C., & Gambaro, A. (2021). Year-round measurements of size-segregated low molecular weight organic acids in Arctic aerosol. *Science of the Total Environ.* 10.1016/j.scitotenv.2020.142954
- Feltracco M., Barbaro E., Hoppe C. J. M., Wolf K. K. E., Spolaor A., Layton R., Keuschnig C., Barbante C., Gambaro A., & Larose C. Airborne bacteria and particulate chemistry capture phytoplankton bloom dynamics in an Arctic Fjord. (*submitted*)

The following papers are not directly related with the present thesis:

- Feltracco, M., Barbaro, E., Contini, D., Zangrando, R., Toscano, G., Battistel, D., Barbante, C., & Gambaro, A. (2018). Photo-oxidation products of α -pinene in coarse, fine and ultrafine aerosol: A new high sensitive HPLC-MS/MS method. *Atmospheric Environment*, 180(March), 149–155. 10.1016/j.atmosenv.2018.02.052
- Barbaro, E., Feltracco, M., Cesari, D., Padoan, S., Zangrando, R., Contini, D., Barbante, C., & Gambaro, A. (2019). Characterization of the water soluble fraction in ultrafine,

fine, and coarse atmospheric aerosol. *Science of the Total Environment*, 658, 1423–1439. doi.org/10.1016/j.scitotenv.2018.12.298

- Barbaro, E., Morabito, E., Gregoris, E., Feltracco, M., Gabrieli, J., Vardè, M., Cairns, W. R. L., Dallo, F., De Blasi, F., Zangrando, R., Barbante, C., & Gambaro, A. (2020). Col Margherita Observatory: A background site in the Eastern Italian Alps for investigating the chemical composition of atmospheric aerosols. *Atmospheric Environment*, 221(September 2019). doi.org/10.1016/j.atmosenv.2019.117071
- Cesari, D., Merico, E., Dinoi, A., Gambaro, A., Morabito, E., Gregoris, E., Barbaro, E., Feltracco, M., Alebic-Juretic, A., Odorcic, D., Kontosic, D., Mifka, B., & Contini, D. (2020). An inter-comparison of size segregated carbonaceous aerosol collected by low-volume impactor in the port-cities of Venice (Italy) and Rijeka (Croatia). *Atmospheric Pollution Research*, 11(10), 1705–1714. 10.1016/j.apr.2020.06.027
- Gregoris, E., Morabito, E., Barbaro, E., Feltracco, M., Toscano, G., Merico, E., Grasso, F. M., Cesari, D., Conte, M., Contini, D., & Gambaro, A. (2020). Chemical characterization and source apportionment of size-segregated aerosol in the port-city of Venice (Italy). *Atmospheric Pollution Research*, August. doi.org/10.1016/j.apr.2020.11.007
- Chirizzi, D., Conte, M., Feltracco, M., Dinoi, A., Gregoris, E., Barbaro, E., La Bella, G., Ciccarese, G., La Salandra, G., Gambaro, A., & Contini, D. (2021). SARS-CoV-2 concentrations and virus-laden aerosol size distributions in outdoor air in north and south of Italy. *Environment International*, 146, 106255. doi.org/10.1016/j.envint.2020.106255

List of Abbreviations

BC	Black Carbon
Br_{en}	Bromine enrichment
CAs	Carboxylic Acids
CAAs	Combined Amino Acids
CCN	Cloud Condensation Nuclei
DMS	Di-Methyl Sulphide
FAAs	Free Amino Acids
IN	Ice Nuclei
LRAT	Long Range Atmospheric Transport
LOD	Limit Of Detection
LOQ	Limit Of Quantification
MDL	Method Determination Limit
MSA	MethaneSulphonic Acid
MQL	Method Quantification Limit
nss-K⁺	non-sea-salt-potassium
nss-SO₄²⁻	non-sea-salt-sulphate
OC	Organic Carbon
PCs	Phenolic Compounds
PBAP	Primary Biogenic Aerosol Particles
POA	Primary Organic Aerosol
QFF	Quartz Fiber Filter
SOA	Secondary Organic Aerosol
ss-SO₄²⁻	sea-salt-sulphate
VOCs	Volatile Organic Compounds
WSOCs	Water-Soluble Organic Compounds

Chapter 1

Atmopheric aerosol

1.1 Introduction

An aerosol is defined as a suspension of fine liquid and/or solid particles in a gas ^[1]. Aerosol is a constituent of the global atmosphere. It affect global climate via its interaction with sunlight, influence the formation of clouds, and participate in many atmospheric chemical reactions. These particles¹ can travel over distances of several thousands of kilometers and transport particulate material such as dust, sea salt, spores, pollen, bacteria, etc.

The ocean is one major source of natural aerosols with an estimated annual emission up to 10000 Tg of material ^[2]. The exchange of particulate matter between air and sea contributes to the global cycles of carbon, nitrogen, and sulphur particles. Ocean water and sea salt are transferred to the atmosphere through sea spray and air bubbles at the sea surface. Another major natural source of particulate mass is mineral dust from dry continental regions like deserts or semi-arid areas. Estimates of the global mass of dust particles released per year into the atmosphere are up to 5000 Tg ^[2]. Other significant sources of airborne particles are biomass burning from forest fires, volcanic eruptions, and anthropogenic pollution from traffic or industrial emissions.

Once airborne, particles can change their size and composition by condensation of vapour species or by evaporation, by coagulating with other particles, by chemical reaction, or by activation in the presence of water supersaturation to become fog and cloud droplets ^[3]. Particles are eventually removed from the atmosphere by two mechanisms: deposition at

¹Very often aerosol is indicated with the words "particulate matter" or "particles" even if this nomenclature does not include liquid droplets

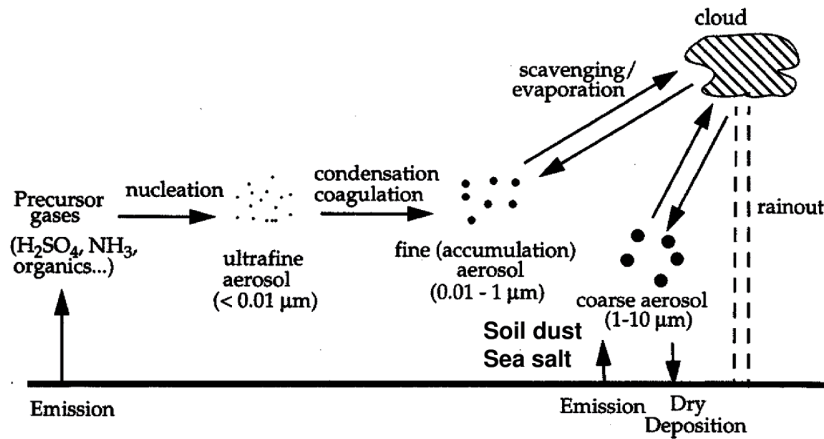


FIGURE 1.1: Major sources of atmospheric aerosols [4]

the Earth's surface (dry deposition) and incorporation into cloud droplets during the formation of precipitation (wet deposition). Because wet and dry deposition lead to short residence times in the troposphere, and because the geographic distribution of particle sources is highly non-uniform, tropospheric aerosols vary widely in concentration and composition over the Earth [4]. Whereas atmospheric trace gases have lifetimes ranging from less than a second to a century or more, residence times of particles in the troposphere vary only from a few days to a few weeks. Figure 1.1 provides an overview on the various processes and interactions.

1.2 Aerosol size distribution

A key property is the particle size, given as particle diameter D or as typical dimension in the case of irregularly shaped particles. Particle size spans over multiple orders of magnitude from a few nanometers for particles freshly produced from gaseous precursors by gas-to-particle conversion up to almost 1 mm for large dust particles. Atmospheric aerosol always contains particles of different sizes and is therefore classified as poly-disperse. At the contrary, an aerosol composed of particles of a single size would be classified as mono-disperse. Generally, the distribution of particle sizes present in an aerosol is given as the probability of occurrence of particles with diameters at certain size intervals. This property is called the particle size distribution function.

Atmospheric aerosol can be regarded as a superposition of four particle modes, each described by a single log-normal size distribution. Figure 1.2 is a schematic representation

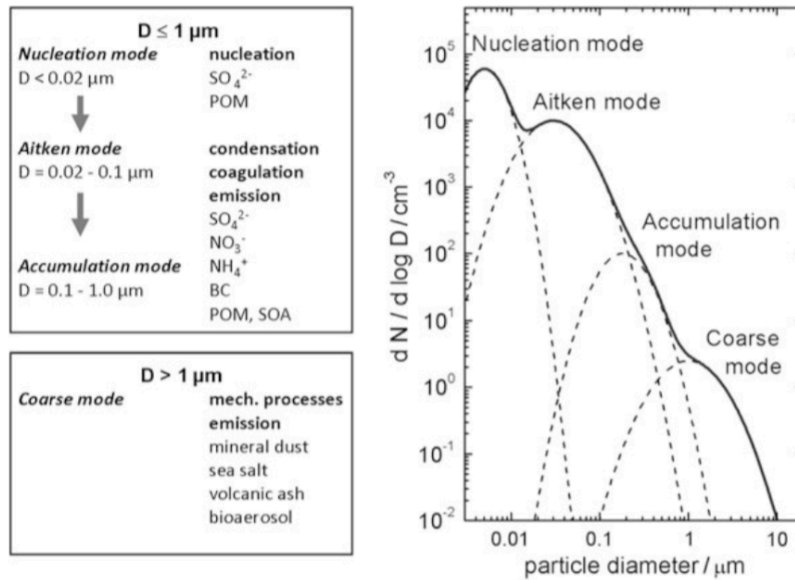


FIGURE 1.2: Schematic representation of the modes of aerosol for different particle diameters D . On the left, key chemical compounds and particle generation processes; on the right, size ranges [3].

of the modes of a generic atmospheric aerosol.

The Aitken mode includes particles formed by coagulation of nucleated particles and condensation of vapors on already existing particles, or emitted directly into the atmosphere. Nucleation mode and Aitken mode are combined by some authors into a single Aitken mode which then covers all particles smaller than 100 nm in diameter. The accumulation mode (D 0.1 - 1.0 μm) consists of particles formed from the Aitken mode by particle coagulation or particles emitted directly from primary sources like combustion of fossil fuels or vegetation; for atmospheric aerosols the accumulation mode forms the sink of particles growing from nucleation via the Aitken mode into the accumulation mode. The coarse mode contains particles larger than 1 μm ; these particles are generated mainly by mechanical processes like wind-blown dust, sea spray, or plant debris, or are emitted from volcanoes or large fires. Because of the different formation pathways, coarse mode particles are separated from smaller particles with respect to their chemical composition. Spores, bacteria or pollen are also mainly part of the coarse mode, but may be part of the accumulation mode as well. The major chemical constituents of sub- μm aerosol in the troposphere are sulphates (in particular non-sea-salt sulphate), nitrates, ammonium, black carbon (BC), and organic matter emitted directly from the source (primary organic aerosol, POA) or formed as secondary organic aerosol (SOA).

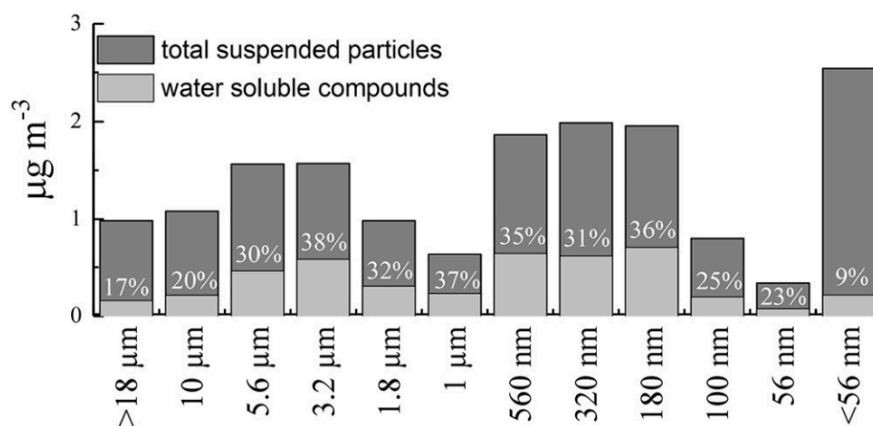


FIGURE 1.3: Comparison between median particle size distributions of aerosol mass concentrations and of water-soluble compounds of aerosol collected in Mestre-Venice [5].

A clear case-study [5] is shown in Figure 1.3. The aerosol was collected with a twelve-stage cascade impactor in Mestre-Venice and the size distribution was trimodal centred between 5.6 and 3.3 μm for the coarse particle mode, at 320 nm for the accumulation mode while nuclei mode was recognized below 56 nm.

1.3 Primary and secondary organic aerosol

Source processes for primary particles are manifold (anthropogenic fossil fuel combustion, biomass burning, volcanic eruptions, wind mobilization of soil material, wind-driven sea spray production, desert dust storm). They are mostly related to particle emissions from Earth's surface, with the exception of emissions from cruising aircraft, which is the only source of primary aerosol particles in the upper troposphere [6]. Several hundred organic compounds have been identified in primary organic aerosol emissions. In spite of this, these studies have been able to identify compounds representing only 10-40% of the emitted organic mass depending on the source.

SOA material is formed in the atmosphere by the mass transfer to the aerosol phase of low vapour pressure products. As organic gases are oxidized in the gas phase by species

TABLE 1.1: Approximative emission fluxes from different types of primary aerosols and gaseous precursors of secondary aerosols.

Aerosol type	Emission flux (per year)
<i>Natural primary aerosol</i>	
Desert dust	1000-3000 Tg
Sea spray	1000-6000 Tg
Biomass burning aerosols	20-35 Tg
Terrestrial primary biogenic aerosols	Order of 1000 Tg
Including bacteria	40-1800 Gg
Including spores	30 Tg
<i>Precursors of natural secondary aerosols</i>	
Dimethylsulphide (DMS)	20-40 Tg
Volcanic SO ₂	6-20 Tg
Terpenes	40-400 Tg
<i>Anthropogenic primary aerosols</i>	
Industrial dust	40-130 Tg
Biomass burning aerosols	50-90 Tg
Black carbon (from fossil fuel)	6-10 Tg
Organic carbon (from fossil fuel)	20-30 Tg
<i>Anthropogenic secondary aerosols</i>	
SO ₂	70-90 Tg
Volatile organic compounds (VOCs)	100-560 Tg
NH ₃	20-50 Tg
NO _x	30-40 Tg N

such as the hydroxyl radical (OH), ozone (O₃), and the nitrate radical (NO₃), their oxidation products accumulate. Some of these products have low volatilities and condense on the available particles establishing equilibrium between the gas and aerosol phases. Briefly, there are two separate steps involved in the production of secondary organic aerosol. First, the organic aerosol compound is produced in the gas phase during the reaction of parent organic gases. Then, the organic compound partitions between the gas and particulate phases, forming secondary organic aerosol. The first step depends on the gas-phase chemistry of the organic aerosol precursor, while the partitioning is a process that may involve interactions with various compounds. Table 1.1 presents data summarized on aerosol mass concentrations from different types of primary aerosols and gaseous precursors of secondary aerosols [7] [8] [9] [10] [11][12].

1.4 Lifetime and transport

The lifetime of atmospheric aerosol particles depends on their chemical nature, altitude range and size. Airborne particles in the troposphere have typical lifetimes of 3–10 days on average ^[13]. After 1 month, more than 90% of the particles are removed by coagulation with other particles or cloud drops (scavenging), and wet deposition via precipitation. Aerosol particles in the lower stratosphere have a longer lifetime of up to 1 year before they penetrate the tropopause.

Figure 1.4 shows the lifetime of individual particles for the different altitude ranges of the atmosphere ^[14]. Smaller particles are efficiently removed by coagulation and coarse particles by sedimentation, while particles of the accumulation mode size range are efficiently removed only by wet deposition via aerosol-cloud processes.

1.5 Main sources of aerosols

Aerosols can also be classified according to their origin. One can distinguish natural from anthropogenic sources. Natural sources consist of emissions from the soil, ocean, fires, vegetation, and volcanoes. Anthropogenic sources are dominated by emissions from the combustion of fossil fuels, biofuels (plant biomass including wood, vegetable oils, animal waste), or vegetation fires caused by humans.

The wind friction at the ocean surface ejects fine particles of marine water into the atmosphere. Although these particles are often called sea salt aerosols, this is yet another misuse of language because these particles may also contain biological material and other impurities (carboxylic acids, amino acids, sugars, etc). It is more appropriate to refer to "sea spray aerosols". Sea spray aerosols cover sizes that range from typically 100 nm to tens of μm . The largest particles fall back quickly to the ocean surface and are therefore of lesser climatic importance.

Intercontinental transport of particles is observed frequently associated with lifting in warm conveyor belts associated with low pressure systems and long-range atmospheric transport (LRAT) in the troposphere.

The wind friction on continental surfaces can detach soil particles and suspend them in the atmosphere. This is particularly the case in arid and semiarid regions where the wind

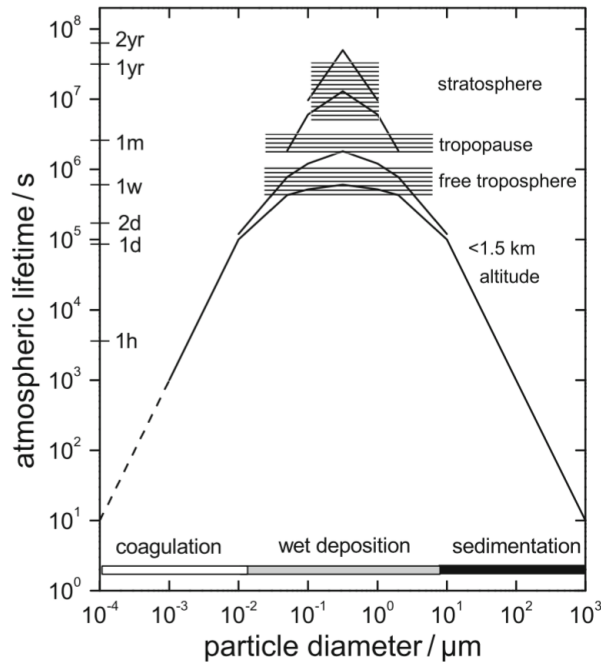


FIGURE 1.4: Atmospheric lifetime for individual particles with indicated dominant loss processes in the troposphere [3].

is not slowed down by the vegetation that is fairly sparse. As for sea spray aerosols, soil particles sizes range from typically 100 nm to tens of μm . In particular, desert dust aerosols are also called mineral dust or mineral aerosols. Emissions of desert dust depend very much on environmental and meteorological conditions.

Volcanoes can emit fragments of pulverized rocks and minerals, called volcanic ash, during explosive eruptions. These particles have sizes typically ranging from a micrometre to millimetres. Volcanic ash can be transported over distances of a few hundreds to a few thousand kilometres but being micrometric particles they tend to fall down rapidly. Hence their climate effect is limited. Volcanoes also emit sulphur-rich gases that get oxidized in the atmosphere to form submicrometric sulphate aerosols. If the eruption is powerful enough to inject the sulphur gases in the stratosphere, then the volcanic aerosols have a residence of a few months to more than a year, depending on the region and altitude of injection. Volcanic eruptions can also release free amino acids and proteinaceous materials [15] [16].

The terrestrial biosphere is a source of primary biogenic aerosol particles (PBAP). They comprise plant and insect debris, pollen, spores (present in many plants and fungi), bacteria and viruses. These particles can be transported by the wind on varying distances depending on their size. Debris are usually larger than 100 μm , pollen, spores and large bacteria are generally in the range of 1–100 μm , while small bacteria and viruses are generally smaller

than $1\ \mu\text{m}$ [17]. Seawater also can contain biological material, some of which is transferred to sea spray aerosols during the emission process. This primary organic matter is found preferentially in particles smaller than 200 nm in diameter [18] and has been found to depend on the bio-activity in ocean waters [19]. Some species of phytoplankton can produce DMS, a gaseous compound that is oxidized in the atmosphere to form sulphur-containing aerosols, for example MSA. Plants and algae emit volatile VOCs that are oxidized in the atmosphere and condense and contribute organic material to the atmospheric aerosol. These aerosols are referred to as SOA. Their sizes are typically of the order of a few tenths of a μm .

Biomass burning aerosols comprehend all organic material that comes from vegetation, dead wood, animal dung, peat, etc and can potentially burn, excluding so-called fossil fuels that are formed on geological time-scales. The burning of biomass generates primary aerosols that derive from the incomplete combustion of the organic matter. Biomass burning aerosols include organic carbon (OC) and black carbon (BC), where the carbon content is very high. These aerosols are generally submicronic and are clearly visible in smoke plumes (Figure 1.5). The sources of biomass burning aerosols are both natural and anthropogenic. The combustion of biomass can also emit gaseous compounds, such as VOCs and sulphur dioxide.

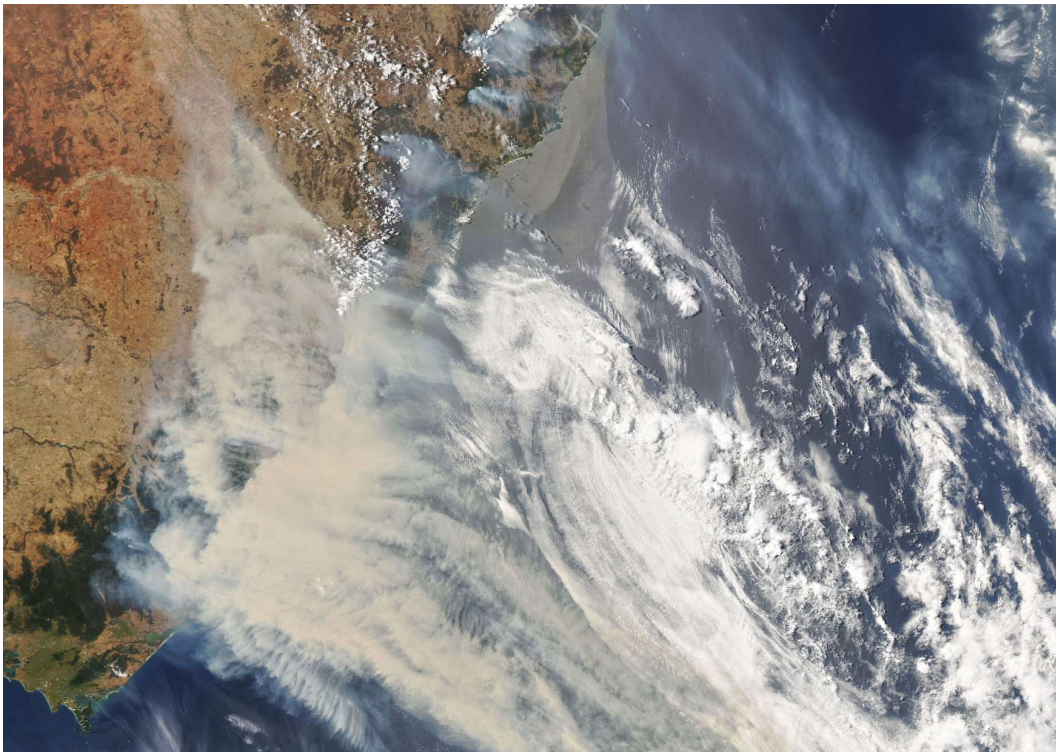


FIGURE 1.5: South Eastern Australia bushfire smoke plume (NASA, 2019)

The combustion of coal and oil derivatives produces BC and OC, as well as sulphur dioxide. These are essentially submicronic particles, that are also a source of air pollution in developing and industrialized countries. Air pollution is responsible for a wide range of adverse health and environmental effects. Effects on human health include increased respiratory and cardiovascular diseases and associated mortality. Aerosols and acidic deposition are responsible for damages on historical buildings.

1.6 Cloud condensation nuclei and ice nuclei

Aerosols particles can act as cloud condensation nuclei (CCN) so that an increase in aerosol concentrations generally leads to an increase in the concentration of CCN and in the concentration of cloud droplets. This effect can be associated to a radiative forcing calculation, at least in principle if the pre-industrial aerosol concentration is known. For a fixed cloud cover and liquid water content, an increase in cloud droplet concentration results in smaller cloud droplets but an increase in the total scattering cross section, and thus an increase in cloud reflectivity. Although only the change in cloud droplet concentration is considered in the original concept, a change in the shape (or dispersion) of the droplet size distribution that is directly induced by the aerosols may also play a role ^[20].

The major source of CCN over the oceans and in coastal areas appears to be DMS ^[21], which is produced by planktonic algae in seawater and oxidises in the atmosphere to form a sulphate aerosol. Because the reflectance of clouds (and thus the Earth's radiation budget) is sensitive to CCN density, biological regulation of the climate is possible through the effects of temperature and sunlight on phytoplankton population and DMS production.

The largest flux of DMS comes from the tropical and equatorial oceans ^[22]. This suggests that the most important climatic role of DMS is to contribute to elevated cloud over the warmest ocean regions, and thus to reduce the input of heat into the low-latitude oceans. A cooling of the oceans or a reduction in area of the tropical seas could thus lead to a smaller DMS flux, providing a negative feedback.

Aerosols also serve as ice nuclei (IN): a change in their concentration could also lead to a change in ice cloud amount and properties. Ice nuclei acting in different ways, and freezing being sometimes a slower process than condensation itself. Aerosol–cloud interactions

remain poorly understood despite a large amount of research that has been dedicated to this topic.

1.7 Aerosol optical properties

Aerosol particles can influence the radiative budget of the Earth-atmosphere system in two ways. The first is the direct effect, whereby particles scatter and absorb solar and thermal infrared radiation and thereby alter the radiative balance of the Earth-atmosphere system. Whereas scattering redirects radiation, absorption removes radiation from an incident beam. In both cases, radiation in the beam is attenuated, reducing the quantity of radiation transmitted. The sum of total light scattering in all directions and absorption is called extinction. Usually light absorption is small and the ratio of absorption to extinction coefficients is smaller than 0.1 and even 0.01 for remote polar areas. The primary absorber of light in the atmosphere is soot, in particular Fe_2O_3 and Al_2O_3 [23]. Scattering may take place by radiation reflection, refraction, or diffraction. The scattering efficiency of a particle is defined as the probability that a photon incident on the particle will be scattered.

The second are called the indirect effects, since particles modify the micro-physical and hence the radiative properties and lifetime of clouds.

The fundamental aerosol parameters governing the aerosol impact on climate forcing are the aerosol optical depth and the ratio of particle scattering to extinction at a wavelength of 550 nm. Figure 1.6 shows the global distribution of aerosol optical depth as a measure of the atmospheric aerosol load.

Radiative effects are evaluated in terms of radiative fluxes in the solar and thermal infrared spectral regions at the top of the atmosphere. If the anthropogenic aerosol or the clouds modified by the anthropogenic aerosol increase the radiative flux at the top of the atmosphere, more energy is reflected back into space than in the unperturbed case without anthropogenic aerosol in the atmosphere, and the overall effect is a cooling. If the net radiative flux is reduced by light-absorbing aerosol particles or by clouds, the resulting effect is a heating of the Earth-Atmosphere system because more radiative energy remains in the system compared to the unperturbed case.

Tropospheric aerosols, that have a substantial anthropogenic component, include black carbon, mineral dust, sulfate particles, organic carbon and nitrate aerosol. From these aerosol

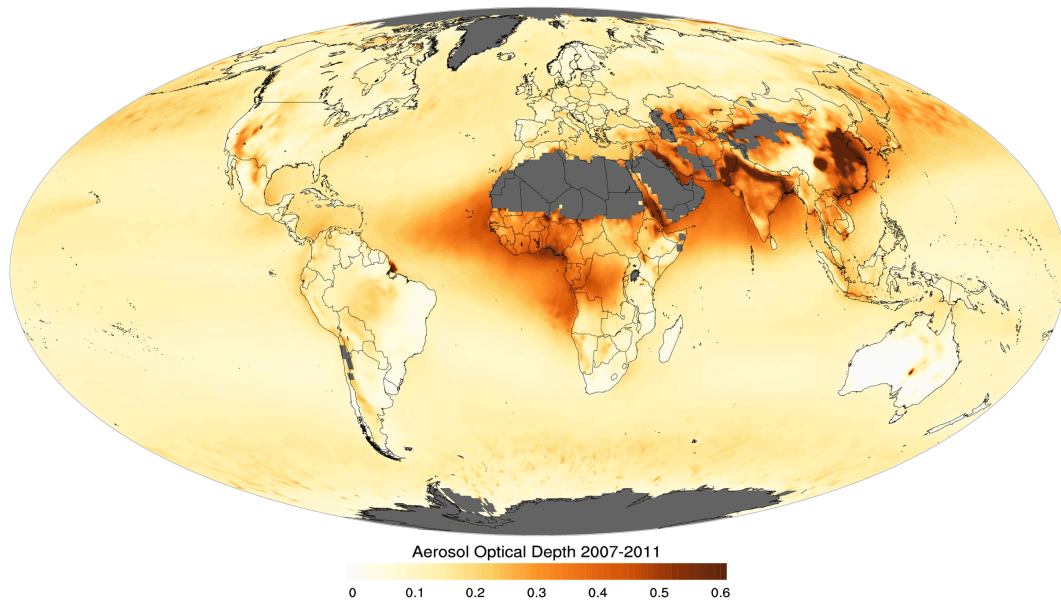


FIGURE 1.6: Global distribution of aerosol optical depth for the years 2007 to 2011 taken from the MODIS satellite instrument (NASA)

components black carbon and mineral dust are the only constituents which absorb solar radiation in the visible spectrum, while sulphate and nitrate aerosols are purely light-scattering [24].

1.8 Health effects

A strong increase of air pollutants has been observed on local, regional and global scales since the industrial revolution during the period known as the Anthropocene. High concentrations of gaseous pollutants such as ozone and nitrogen oxides are a threat to public health, as they cause adverse health effects such as respiratory, allergic and cardiovascular diseases. Particulate matter with a diameter less than $2.5 \mu\text{m}$ (PM 2.5) can be deposited deep into the lungs, inducing oxidative stress and respiratory diseases [25]. The causes of aerosol health effects are highly complex and interdisciplinary studies are required to address a wide range of length and time scales. In general, the most prominent risk factors for the global burden of disease were identified to be ambient and indoor air pollution by air particulate matter and ozone.

During the COVID-19 outbreak several studies were made to investigate the potential transmission of SARS-CoV-2 in aerosol [26] [27] [28]. The common conclusion of these studies stated that no assumptions can be made concerning the presence of the virus on particulate

matter and COVID-19 outbreak progression, so far. To confirm this, aerosol samples collected 2 to 5 m from the patients' beds were negative. In the framework of the PhD project, it was investigated outdoor concentrations and size distributions of SARS-CoV-2 in aerosol, simultaneously collected during the pandemic, in May 2020, in northern (Veneto) and southern (Apulia) regions of Italy ^[29].

Chapter 2

Sampling site

2.1 The Svalbard Archipelago

The archipelago lies on the Northwest corner of the Barents Shelf 650 km north of Norway. The name Spitsbergen was given by the Dutch captain, Barents, who is generally credited with the modern discovery of the islands in 1596 and after whom the Barents Sea is named. Barents did not know that the name Svalbard (cool coast) was mentioned in the *Islandske Annaler* in A.D. 1194 and in the *Landnámabók* from Viking exploration. Also Russian hunters are claimed to have built huts in the fifteenth century and possibly earlier. The name Spitsbergen refers to the pointed mountain peaks that the main island exhibits on approach from the sea. It had been used for the whole archipelago or for the main part of it excluding the outlying islands. Spitsbergen was the name for the whole archipelago in the Treaty of Sèvres in 1920, and in the Spitsbergen Treaty, which came into effect in 1925. The main island had been known as West Spitsbergen. The name Svalbard was formally introduced by Orvin A. K. in *Place Names of Svalbard* (1942), by the the Norwegian Polar Institute in the first systematic and descriptive gazeteer. In this book Svalbard Spitsbergen was redefined to comprise the main group of islands, excluding the outlying islands Storoya, Kong Karls Land, Hopen (Hope island) and Bjornoya (Bear Island). The nomenclature was revised again, so that Spitsbergen now refers only to the main island and excludes Nordaustlandet (North East Land), Barentsoya, Edgeoya, and Prins Karls Forland (Figure 2.1).

Longyearbyen is the largest settlement and the administrative centre of Svalbard, Norway. Polar research and tourism began in the 19th Century, and in the 20th Century, coal mining began in the region. Longyearbyen ("Longyear City") is named after John M. Longyear, an American businessman who began mining operations in 1906.

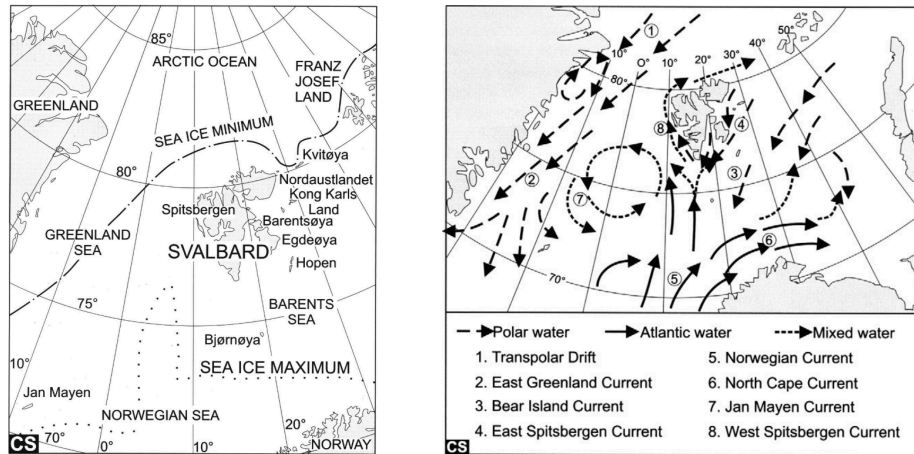


FIGURE 2.1: Regional geographical setting of Svalbard (left) and Prevailing surface currents of the Barents Sea and North Atlantic areas (right) ^[30]

The main islands stand between 76° and 81° . Many distinctive features of this Arctic environment derive from the angle of incidence of solar radiation. About 60% of Svalbard is glacier-covered, with many outlet glaciers terminating in the sea.

As a small archipelago, the climate of Svalbard is influenced by two sources of surface ocean water: the West Spitsbergen Current, is the northern-most remnant of the Gulf Stream moving relatively warm water northwards along the west coast; the East Spitsbergen Current brings cold water and ice-pack south-westwards east of Spitsbergen and the eastern islands. These currents meet off and the cold water is deflected and continues northwards between the warmer current and the coast, often carrying ice-pack with it, and causing fog.

Svalbard Islands have a mean annual air temperature of about -6°C at sea level and as low as -15°C in the high mountains ^[31]. In Longyearbyen the coldest month is February with -15.2°C , the warmest month is July with 6.2°C and the mean annual air temperature is -5.8°C (average 1975-2000). A recent study ^[32] shows how the coldest months at Ny-Ålesund in the winters 2010–2015 was January 2011 with -11.3°C and February 2015 with -9.4°C , but the minimum temperatures were recorded in March 2010 and 2013. Anomalous warm periods were recorded during winters 2012 and 2014 ^[33] with a minimum temperature of -3.2°C on January 2012 and -3.2°C on February 2014. In summer, the maximum monthly temperature ranges between 5.3°C and 7.4°C , July 2015 being the warmest summer month and July 2014 the coldest one.

Svalbard falls within the zone of continuous permafrost and periglacial and permafrost-related terrain features are widespread in areas not covered by glaciers. The formation, temperature, and depth of permafrost are the result of a complex interplay between the microclimatological conditions, the surface cover and the rock beneath, as are the movements that take place within the active zone to form many distinctive types of patterned ground. At the coasts, the thickness of permafrost is between 10 and 40 m, but increases to more than 450 m in the highlands ^[30].

Flora and fauna reflect the above physical conditions. About 150 species of flowering plants and a few other species occupy low ground and flourish in the snow-free areas in the short summer. Grasses can exceed the 10 cm height. Vegetation directly supports a variety of insects, reindeer and ptarmigan and indirectly the Arctic fox ^[30].

2.2 Ny-Ålesund

Ny-Ålesund is one of the world's northernmost year-round research stations and an important Norwegian platform for international research that has been in operation for more than 50 years (Figure 2.2). The station's High Arctic location, far from pollution sources, makes Ny-Ålesund ideal for Arctic research and monitoring of environmental change.



FIGURE 2.2: Ny-Ålesund and the Kongsfjorden

The Ny-Ålesund area consists of typical High Arctic ecosystems, with both marine and terrestrial components. It offers a variety of Arctic fjord environments, from calving glacier

fronts to sandy beaches. The terrestrial environments in the Kongsfjorden area, including several bird and plant sanctuaries, are rich in wildlife and also provide wide opportunities for research. The geology of the Kongsfjorden area is very diverse, and the area offers sites ranging from rocks and cliffs exposed to the raging Arctic seas on the tip of the Brøgger peninsula to protected coves in the inner parts of the fjord.

Ny-Ålesund is surrounded by a variety of High Arctic ecosystems typical of Svalbard, and most of the animal and plant species are to be found in the area. Along the rim of the fjord there are densely populated bird cliffs and other rock formations and islands with breeding sea birds.

The seal has important breeding and pup-rearing areas in the innermost parts of Kongsfjorden. The vegetation in the area ranges from a uniform and bleak lichen cover to lush areas further east which provide rich reindeer grazing.

Ny-Ålesund was a mining village until 1963. During the 1990's it was transformed into a multidisciplinary science settlement, and today stations from more than 10 different nations host researchers from up to 20 different countries. Italy researchers are hosted at "Dirigibile Italia" Arctic Station. It is funded and managed by the Institute of Polar Sciences - National Research Council of Italy (ISP-CNR).

2.3 Gruvebadet Observatory

The Gruvebadet atmospheric observatory (78°55'03" N, 11°53'39" E, 50 m a.s.l.) is located about 1 km far from the village of Ny-Ålesund. It is equipped to host aerosol sampling for measurements of chemical, physical and optical properties. It is managed by Institute of Polar Sciences (ISP-CNR) personnel and normally operative from March to October each year. In 2018, 2019 and 2020 the lab was operative all year long. The site has been specially identified to avoid local contamination from the village. The dominating wind pattern is east-southeast katabatic flow from Kongsvegen glacier or from northwest-erly directions as channeled by the Kongsfjord ^[34]. Katabatic wind is the generic term for down-slope winds flowing from high elevations of mountains, plateaus, and hills down their slopes to the valleys or planes below. Figure 2.3 shows the location of Ny-Ålesund, Gruvebadet and Kongsvegen glacier.

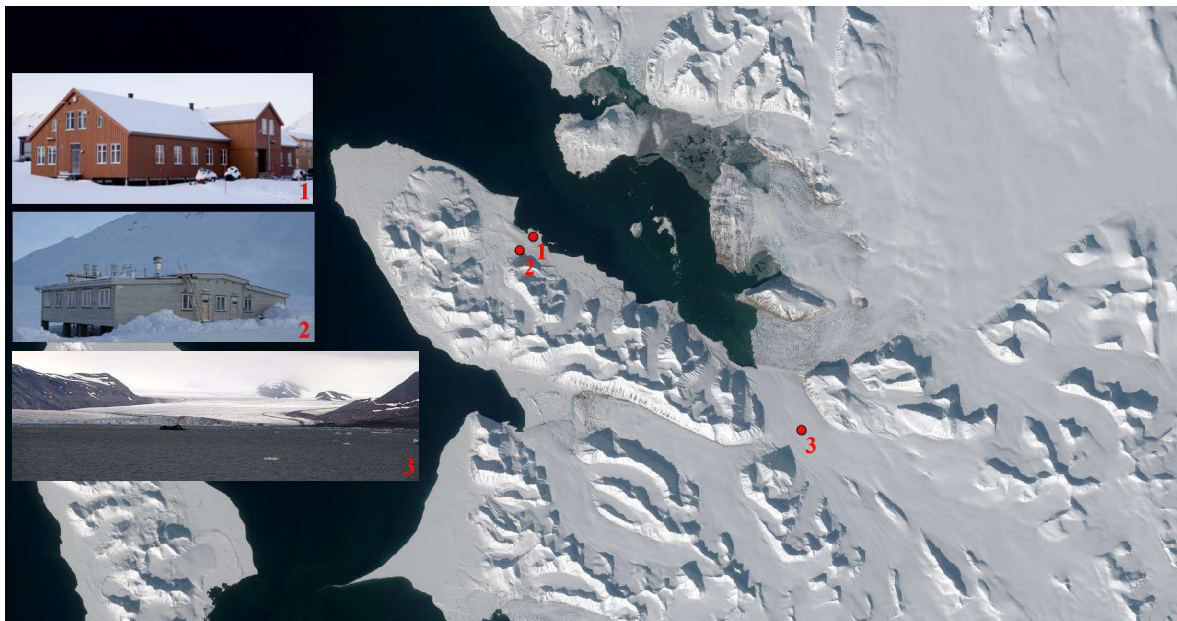
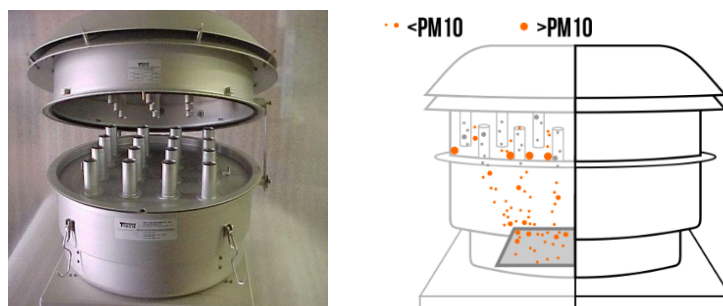


FIGURE 2.3: Location of Ny-Ålesund, Gruvebadet Observatory and Kongsfjorden in front of Kongsvegen glacier

2.4 Aerosol sampling

This thesis took into account those Arctic sampling campaigns conducted from April 2013 to February 2019 at the Gruvebadet Observatory. Each sample has a sampling time (resolution) of between 1 and 10 days, with the aim of identifying specific events, while maintaining the protocols used in previous studies ^[16] ^[35]. Samples were collected with a PM₁₀ high volume air sampler (TE-6070) at a flow rate of 68 m³ h⁻¹ equipped with a five stage high volume cascade impactor (TE-235, Tisch Environmental Inc., Cleves, OH) equipped with slotted quartz fiber filters (250 × 143 mm) and fitted with a high-volume back-up filter (203 × 254 mm) (FILTERLAB, Barcelona, Spain) to collect aerosol particles in the following size ranges: 10.0–7.2 μm, 7.2–3.0 μm, 3.0–1.5 μm, 1.5–0.95 μm, 0.95–0.49 μm, > 0.49 μm. As the particulates travel through the size selective inlet, the larger particulates are trapped inside of the inlet as the smaller PM₁₀ particulates continue to travel through the PM₁₀ inlet and are collected on the QFF (Figure 2.4).

With the TE-235 cascade impactor (Figure 2.5), suspended particulates enter through the first set of parallel slots on the first stage. Particulates that are too large to travel to the next stage are impacted on the collection substrate and the smaller particles remain in the air stream and travel to the next stage. The slots on each stage are the same width but as the particulates continue through, the slots become successively smaller and most of the

FIGURE 2.4: TE-6000 PM_{10} Head

particulates will eventually become impacted on one of the collection stages. After the last stage the smallest particles will be collected on the backup filter.

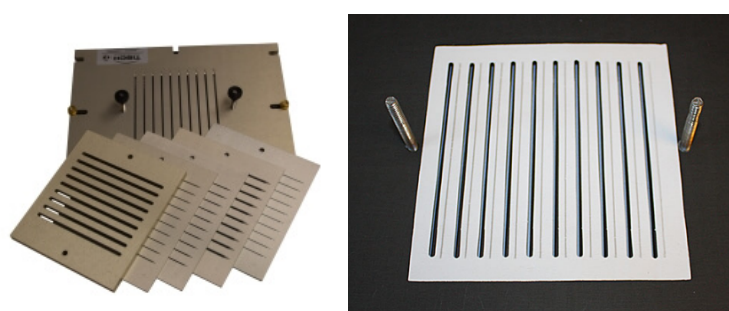


FIGURE 2.5: TE-235 cascade impactor

To test contamination, field blank samples were collected by positioning filters in the impactor plates with the sampler turned off. Filters were pre-combusted (400 °C, 4 h) before sampling and stored afterwards at -20 °C enfolded in aluminium foil. Filters were after sent in Venice to perform analysis. Table 2.1 shows all the sampling campaign considered for this work.

TABLE 2.1: Aerosol sampling campaign considered for this work.

Year	Period
2013	13 th April - 9 th September
2014	2 nd April - 29 th June
2015	4 th April - 13 th June
2016	no data
2017	no data
2018-2019	26 th February 2018 - 26 th February 2019

About 450 QFF were sampled at Gruvebadet Laboratory from 2013 to 2019, about 1000 water-extractions and 3000 instrumental injections were performed for the analysis of the compounds described in Chapter 3. This leads to around 50.000 concentration data.

2.5 State of art

In 1980 J. Heintzenberg stated that "the Arctic is one of the few areas where only very limited knowledge exists about the regional aerosol" [36]. At that time, only rather qualitative atmospheric aerosol results were given by few studies in Greenland [37] [38].

During the '70 and '80 decades there has been an increasing interest for air pollution studies in the Arctic, especially in Ny-Ålesund. To obtain new informations on both particle size distribution and optical properties of the Arctic aerosol, Heintzenberg et al. (1980) [36] conducted a field experiment near Ny-Ålesund in April-May 1979, using particle counters and a multi-wavelength integrating nephelometer. The Arctic particles were described as a aged continental aerosol that has reached the Arctic region with LRAT.

Plenty of studies were published from 1980 to 2000, studying trace metals and inorganic species [39] [40], SO_2 and SO_4^{2-} [41], hydrocarbons [42], pollutants [43], etc. These studies pointed out that pollution in the lower layers of the Arctic troposphere during winter originated from Eurasian areas, while in summer European sources were more important. Furthermore, the fine particle fraction of the Arctic aerosol is of particular significance for "Arctic haze", a polluted air mass deriving from the anthropogenic emissions from Europe and Asia that are transported and trapped in the Arctic air mass during the winter and early spring. The fine particles are mainly composed of anthropogenic pollutants during winter and they also contain high concentrations of heavy metals and persistent organic pollutants. Coarse particles on the other hand are not connected to anthropogenic pollution and consist of clay minerals, soil, and sea salt.

In the last two decades the international research in the aerosol chemistry composition has rapidly grown at Ny-Ålesund, with the aim to better understand the atmospheric transport processes and sources. Studies have been mainly focused in major ions [44] [45], black and organic carbon [46] and some biomass burning tracers [47].

Another important research station in Ny-Ålesund is the Zeppelin Observatory, located on the Zeppelin Mountain (Ny-Ålesund, 474 m a.s.l.), far away from substantial contamination sources. Owned by the Norwegian Polar Institute, it was officially opened in 1990. This station is a unique location for monitoring global atmospheric gasses and long-transported contaminants. Aerosol measurements at the observatory are collected by several research institutions, including Norsk institutt for luftforskning (NILU), Stockholm University, and the

Greek National Centre for Scientific Research (NCSR). The research at Zeppelin is mainly focused on the monitoring of a wide range of air pollutants and trace gases and on aerosol physic-chemical properties, such as the number size distribution, optical properties, and carbon partitioning. Nevertheless, research teams performed at Zeppelin Station several long-term chemistry measurements such as EC, major ions and WSOCs [46] [47] [48].

2.5.1 Key results of Italian research

Since 1997, Italy is present in Ny-Ålesund with the Dirigibile Italia Arctic Station that is managed by the Institute of Polar Sciences of CNR-Italy. Ny-Ålesund is becoming more and more valuable in the international context of Arctic research, considering the great amount of research and observations that the large international cooperation allows there. The special issue entitled "Environmental changes in the Arctic: an Italian perspective" presents a collection of reports on recent scientific achievements and provides the state-of-the-art and future perspectives of Italian research in the Arctic [49]. The study of chemical and physical properties of atmospheric aerosols is one of the main activities of the Italian teams operating at Ny-Ålesund and also includes the determination of aerosol size distributions and chemical speciation.

Zangrando et al. (2013) [50] determined for the first time phenolic biomass (PCs) markers in spring and summer 2010. PCs levels in the Ny-Ålesund atmosphere in different size fractions reflected both long-range transport linked to biomass burning and a terrigenous local source. Scalabrin et al. (2012) [16] determined free amino acids (FAAs) from 19 April until 14 September 2010 [51]. The higher amino acid concentrations were present in the ultrafine aerosol fraction and accounted for the majority of the total amino acid content. Local marine sources dominate the summer concentrations. Bazzano et al. (2015, 2016) [52] [53] analysed the lead content and isotopic composition ($^{207}\text{Pb}/^{206}\text{Pb}$ and $^{208}\text{Pb}/^{206}\text{Pb}$), along with other chemical tracers, such as aluminium and non-sea-salt sulphates. Here, the atmospheric lead reaching the Arctic during spring can be mainly related to inputs from eastern Eurasia, while North America appeared to be the major source during the summer. Turetta et al. (2016) [35] investigated the PCs, levoglucosan, acrylamide and the water-soluble fraction of trace elements, rare earth elements in size-segregated aerosol from 19 April to 14 September 2010 identifying different kind of events (volcanic eruptions and wildfire events). Udisti et al. (2016) [54] analysed PM_{10} aerosol samples for investigating ions (inorganic anions and

cations and selected organic anions) composition aiming to evaluate the seasonal pattern of sulfate. The anthropogenic input was found to be the most relevant contribution to the sulfate budget in the Ny-Ålesund aerosol in spring and summer.

After the report made by Cappelletti et al. (2016) ^[49], other papers that deal to chemical proprieties of aerosol were published, investigating biogenic aerosol ^[55] and source identification and temporal evolution of trace elements ^[56].

Chapter 3

Analytes

It has become clear in recent years that organic compounds constitute an important fraction of ambient aerosols, ranging from 20 % to 80 % according to recent literature [57] [58] [59][60]. This fraction is formed by a mixture of compounds, including aromatics, aliphatics, ketones, aldehydes, acids, alcohols, and nitrates. This project aims to study a wide range of Water Soluble Organic Compounds (WSOC) and inorganic ions, because carbonaceous aerosol species and inorganic substances such as sulphates and mineral particles could strongly affect many environmental factors, as described in Chapter 1.

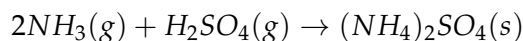
3.1 Inorganic ions

In this work we investigated the major inorganic ions such as nitrite (NO_2^-), nitrate (NO_3^-), ammonium (NH_4^+), chloride (Cl^-), sodium (Na^+), sulphate (SO_4^{2-}), phosphate (PO_4^{3-}), bromide (Br^-), iodide (I^-), potassium (K^+), and magnesium (Mg^{2+}). The analytical procedure was validated through measurement of procedural blanks, recoveries, errors, and repeatability by Barbaro et al. (2017) [61].

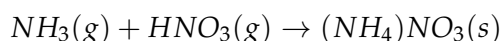
In marine aerosol the main contributors to the mass concentration are Na^+ , Cl^- , Mg^{2+} , SO_4^{2-} , K^+ , and Ca^{2+} . Apart from SO_4^{2-} , these compounds are mainly distributed in the coarse particle mode because they originate from sea salt derived from bubble bursting. Sulfate mass concentrations peak in both the coarse particle and accumulation modes.

Sulphate is one of the prime contributors to the mass concentration of atmospheric aerosols. The mass fractions of SO_4^{2-} range from 22% to 45% for continental aerosols to 75% for aerosols in the Arctic and Antarctic. Since the sulphate content of the Earth's crust is too low to explain the large percentage of sulphate in aerosols, most of it must derive from gas-to-particle conversion of SO_2 . The sulphate is contained mainly in sub-micrometer diameter

aerosols, with a peak in the accumulation mode. Ammonium (NH_4^+) is the main cation associated with SO_4^{2-} in continental and polar aerosol; it is produced by gaseous ammonia neutralizing sulphuric acid to produce ammonium sulphate.



The ratio of the molar concentrations of NH_4^+ to SO_4^{2-} ranges from 1 to 2, corresponding to an aerosol composition intermediate between that for NH_4HSO_4 and $(\text{NH}_4)_2\text{SO}_4$. Nitrate (NO_3^-) is also common in aerosols, where it extends in the coarse-particle mode. It derives mainly from the condensation of $\text{HNO}_3(g)$ onto larger and more alkaline mineral and sea-salt particles. This condensation can form ammonium nitrate from the reaction of ammonia with nitric acid via:



Other minor reactive nitrogen oxides such as N_2O_5 and NO_3 may also have a large contribution to particulate NO_3^- [62].

Over the oceans, aerosols show a deficit of Cl^- and Br^- due to the chloride and bromide depletion processes. Chloride depletion refers to the processes of chloride removal from sea salt aerosol through reactions with acidic species or their precursors. The processes of chloride depletion result in changes in the deliquescent points and optical properties of coarse aerosol particles. NO_x transforms into gaseous nitrous and nitric acids, which later react with NaCl in sea-salt aerosols. This reaction of sea salt particles, containing releases HCl . The evaluation of chloride depletion allows to estimate the amount of nitrate and sulphate formed on sea salt particles. HCl can also react with NH_3 in the gas phase to initially form gaseous NH_4Cl . The ammonium chloride can undergo the gas-to particles process, depending on the partial pressure [63].

Bromide (Br^-) depletion also occurs in sea salt particles, releasing bromine gas, through reactions with different gaseous bromine species under acidic conditions. Such reactions involving Br^- are especially important owing to subsequent effects on ozone depletion reactions [64].

Elements from the Earth's crust are also found in oceanic aerosols, even thousands of kilometres from land. The composition of continental aerosols differ appreciably from crustal

rock and average soils. The enrichment factors of some of the major elements (e.g., Si, Al, Fe) can differ by factors of 3, and some minor elements (e.g., Cu, Zn, Ag) are enriched by several orders of magnitude.

3.2 Water soluble organic compounds

Aerosols contain a wide variety of inorganic and organic compounds, and can organics account for up to 70% of the fine aerosol mass. Organic carbon is classified into two groups: water-soluble organic carbon (WSOC) and water-insoluble organic carbon (WIOC) [65]. WSOC accounts for 20–70% of organic carbon, and it is of interest because it can affect the aerosol's hygroscopicity and ability to serve as cloud condensation nuclei (CCN), and thus impacts climate change. It is well known that WSOC consists of oxygenated compounds containing functional groups such as COOH, COH, C=O, COC, CONO₂, CNO₂, and CNH₂. Sources of WSOC have been shown to be complex. They are emitted directly from combustion, industrial, and natural sources (primary) and/or formed through secondary processes such as homogeneous gas-phase and/or heterogeneous aerosol-phase oxidation (secondary) [66]. Although the primary sources such as biomass burning may be important for WSOC loadings, it is suggested that a major fraction of WSOC is from SOA formation [65].

Here, it has been investigated a broad class of organic acids, including carboxylic acids (CAs) and photo-oxidation products of α -pinene. The role of carboxylic acids as chemical constituents in the troposphere has become an important topic of growing interest. Low molecular weight carboxylic acids like formic and acetic acids have been shown to be ubiquitous components in the tropospheric aqueous and gaseous phases, and in aerosol particles. The current available data cover a large range of environments, e.g. marine, continental, urban, and remote atmospheres. Sources of carboxylic acids are now well recognised, they comprise anthropogenic and biogenic emissions and chemical transformations of precursors. In this project it has been studied the following CAs: C1-formic, C2-oxalic, C2-acetic, C2-glycolic, C3-malonic, C4-succinic, *h*C4- malic, *cis-us*C4-maleic, *trans-us*C4-fumaric, C5-glutaric, C6-adipic, C7-pimelic. In general, oxalic acid is the dominant species followed by formic, acetic, glycolic, malonic, etc. C2-oxalic is the most abundant CA over the world because is the end product of various oxidation/decomposition reactions in the atmosphere [67]. Photochemical production of alkenes released by phytoplankton produced mainly these

CAs. All acids are also mainly distributed in the fine fraction, especially in polar areas, due to their nature of secondary aerosol products in the atmosphere^[61]. The analytical procedure was validated through measurement of procedural blanks, recoveries, errors, and repeatability by Barbaro et al. (2017)^[61].

Various organic species are emitted to the atmosphere from vegetation and, on a global scale, the emission rate of VOCs from natural sources is nearly a factor of 10 greater than the emission rate from anthropogenic sources^[68]. Oxidation processes of monoterpenes in the atmosphere could influence both the SOA formation and the total amount of acid compounds. In a recent study, the present day annual biogenic SOA formation was estimated to be 61-79 Tg yr⁻¹ compared to pre-industrial emission of 17-28 Tg yr⁻¹^[69]. In many experiments^{[66][68][70][71]} the predominant aerosol products were pinic and cis-pinonic acid. In Appendix B is reported the method developed in urban aerosol for the determination and quantification of pinic and cis-pinonic acids^[72].

In the last decades, there has been an increasing interest in the occurrence of amino acids in atmospheric aerosols, either free or in combination (e.g., proteinaceous compounds). The fact that these compounds play an important role in the chemistry and physics of air particles, in atmosphere/biosphere nutrient cycling, and have a direct impact in human health, has encouraged further studies. Despite the many efforts undertaken thus far, the role and fate of these components in the atmosphere still are poorly understood. Due to their hygroscopic properties, some amino compounds may act as ice-forming and cloud condensation nuclei in the atmosphere. These components may also play an important role in the radiative forcing at the Earth's surface and, hence, in the climate. Since amino acids and proteinaceous compounds contribute to the total organic nitrogen and organic carbon fraction of atmospheric aerosols, they are likely to affect the global chemistry of aerosol particles by altering their buffering capacity and acidity/basicity. Moreover, amino acids contribute to the atmosphere-biosphere nutrient cycling, as well as the global nitrogen and carbon cycles^[73]. The presence of ozone in the atmosphere impacts the ratio of amino acids, and their oxidation products (e.g. methionine sulfoxide, half-life of 21–80 h) can be used to study aerosol aging for a specified duration and, consequently, to evaluate the particle transportation phenomena^[16]. Moreover, the origin of the amino compounds in the atmosphere can be deciphered from the ratios of some D/L amino acid enantiomers (alanine, aspartic acid, serine, and glutamic acid). For example, in nature, the D-enantiomer forms of the above mentioned four

amino acids are usually found only in the peptidoglycan layer of the bacterial membranes [74]. The concentration and type of amino compounds in atmospheric aerosols vary widely over the world, since their residence time in the atmosphere, and their spatial and temporal distributions are linked to complex systems. This variability is dependent on the origin and emission sources of these compounds to the atmosphere alongside the effect of different meteorological conditions. PBAPs are likely to be a major source of proteinaceous materials in the atmosphere. These biological aerosols include viruses, algae, fungi, bacteria, protozoa, spores and pollen, fragments of plants and insects, and epithelial cells of animals and humans [73].

Figure 3.1 provides a comparison between the sizes of some of the most common PBAPs and the different particle sizes normally under study. This figure shows a clear overlap between the size of the PBAPs and the easily breathable particles with diameter $<10\ \mu\text{m}$ (particulate matter; PM_{10}) and fine particles with diameter $<2.5\ \mu\text{m}$ ($\text{PM}_{2.5}$).

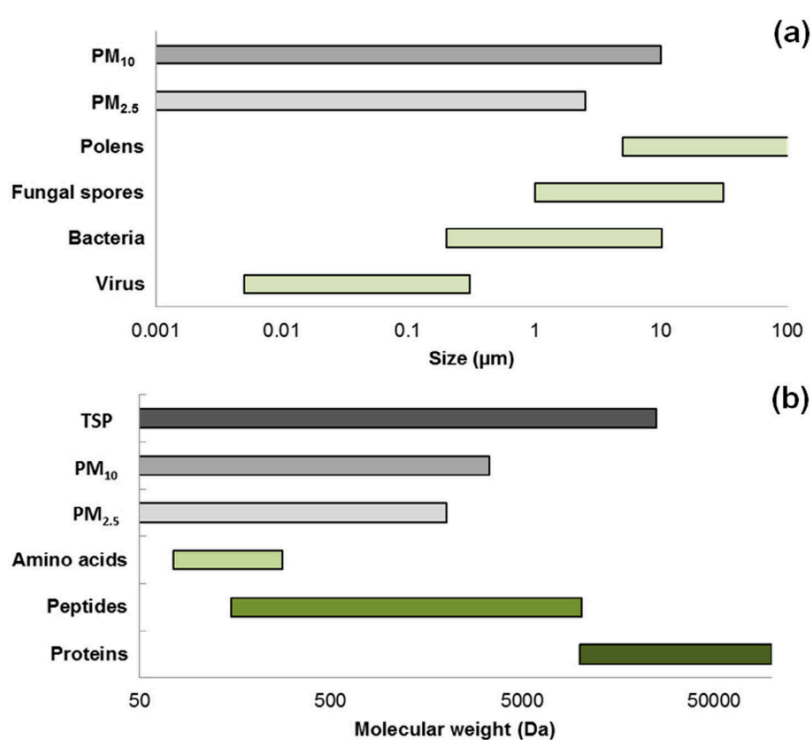


FIGURE 3.1: Comparison between size distribution of $\text{PM}_{2.5}$, PM_{10} and some PBAPs (a); comparison between the molecular weight range of water-soluble organic matter from TSP, $\text{PM}_{2.5}$, PM_{10} , and the molecular weight of amino acids, peptides, and proteins (b) [73].

In this study forty-one free amino acid standards were determined (L-/D-alanine (L-/D-Ala), L-/D-arginine (L-/D-Arg), L-/D-asparagine (L-/D-Asn), L-/D-aspartic acid (L-/D-Asp), L-/D-glutamic acid (L-/D-Glu), glycine (Gly), L-/D-glutamine (L-/D-Gln), L-/D-hydroxyproline (L-/D-Hyp), L-/D-histidine (L-/D-Hys), L-/D-isoleucine (L-/D-Ile), L-/D-leucine (L-/D-Leu), L-/D-methionine (L-/D-Met), L-/D-ornithine (L-/D-Orn), L-/D-phenylalanine (L-/D-Phe), L-proline (L-Pro), L-/D-serine (L-/D-Ser), L-/D-threonine (L-/D-Thr), L-/D-tyrosine (L-/D-Tyr), L-/D-tryptophan (L-/D-Trp), and L-/D-valine (L-/D-Val)). Moreover, twelve combined amino acids were studied (L-Ala, L-Arg, L-Asp, L-Asn, L-Glu, L-Gln, Gly, L-/D-Hys, L-/D-Leu, L-/D-Ile, L-Phe, L-Pro, L-D-/Ser, L-Thr, L-Val) [75]. Method validation was developed by Barbaro et al. (2014) [76].

The presence of sugars is being reported for aerosols taken in urban, rural, polar and marine areas. Sugars or saccharides represent the major form of photosynthetically assimilated carbon in the biosphere. They comprise up to 75 wt.% of vascular plant tissues as structural polysaccharides like cellulose, hemicellulose and pectin [77]. In aerosols, the saccharides are comprised of three main groups: 1) primary saccharides consisting of mono- and disaccharides, 2) saccharide polyols (reduced sugars), and 3) anhydrosaccharide derivatives. The dominant primary saccharides in aerosols are comprised of glucose, sucrose and fructose, with various other minor components (e.g., xylose). The sources of these compounds are innumerable and include microorganisms, plants and animals [78]. Glucose is the most common monosaccharide present in vascular plants and is an important source of carbon for soil micro-organisms, such as fungi and bacteria. Saccharide polyols are produced in large amounts by many fungi, and several functions have been proposed for these compounds, such as storage or transport carbohydrates, and intracellular osmoregulatory solutes. Polyols are also the major soluble carbohydrates in lichens, often found on the bark of trees, branches and leaves. Bacteria can also form and accumulate polyols in order to overcome osmotic stress [77]. Levoglucosan, with a minor contribute by mannosan and galactosan, are the primary thermal alteration products produced during biomass combustion of cellulose and hemicellulose and, therefore, are key tracers for smoke particulate matter from burning biomass [79]. Levoglucosan and other anhydrosaccharides produced during biomass burning have been found in aerosols over the ocean, attesting to their stability during long-range transport. In this study it were applied two sensitive HPAEC-MS methods to determine six

monosaccharides (arabinose, fructose, galactose, glucose, mannose, ribose, xylose), one disaccharide (sucrose), eight alcohol-sugars (mannitol, ribitol, sorbitol, xylitol, galactitol, erythritol, maltitol) and three anhydrosugars (levoglucosan, mannosan and galactosan). The analytical procedure was validated by Barbaro et al. (2015) [80].

Lignin, the second-most abundant naturally occurring polymer (after cellulose), is composed of collective macromolecules that form the major structure of vascular plants, contributing about 28% and 20% of softwood and hardwood biomass, respectively. Because vascular plants are exclusively terrestrial and lignin possesses greater resistance to biodegradation than hemicellulose and cellulose, it serves as an ideal unambiguous tracer of terrigenous organic matter [81]. Lignin is composed of three aromatic alcohols (p-coumaryl, coniferyl, and sinapyl alcohols) that give rise to phenolic aldehydes, ketones, and acids upon oxidation or pyrolysis. Hardwood (angiosperms) lignin is enriched in sinapyl alcohol precursors so burning produces principally syringyl and vanillyl moieties. The dominant phenolic biomarkers in deciduous tree smoke include homovanillyl alcohol, vanillic acid, vanillin, and syringic acid. Softwoods (gymnosperms) instead have high proportions of coniferyl alcohol products with minor components from sinapyl alcohol and burning produces that are primarily vanillyl moieties [50]. The dominant phenolic biomarkers in conifer smoke include vanillin, homovanillic acid, vanillic acid, and homovanillyl alcohol. In grasses p-coumaryl alcohol is the dominant lignin unit not prevalent in softwood and hardwood. Significant products from burning grasses are acetosyringone, syringic acid, vanillin and vanillic acid. In this work we determined syringic acid, isovanillic acid, homovanillic acid, p-coumaric acid, coniferyl aldehyde, vanillic acid, syringaldehyde and ferulic acid, using the method developed by Zangrando et al. (2013) [50].

3.3 Atmospheric Microbiome

Microorganisms are of particular interest in fields as diverse as epidemiology, including phytopathology, bioterrorism, forensic science and public health, and environmental sciences, like microbial ecology, meteorology and climatology. Microbial transport in the atmosphere is critical for understanding the role microorganisms play in meteorology, atmospheric chemistry and public health. For example, specific bacterial taxa (e.g., *Actinobacteria* and some *Gammaproteobacteria*) have been proposed to be preferentially aerosolized from

oceans. Once aerosolized, microbial cells enter the planetary boundary layer, defined as the air layer near the ground, directly influenced by the planetary surface, from which they might eventually be transported upwards by air currents into the free troposphere (air layer above the planetary boundary layer) or even higher into the stratosphere [82]. The composition of airborne microbial communities is closely related to the nature of the surrounding landscapes (ocean, agricultural soil, forest etc.) from which local meteorology (especially wind direction and speed) controls microbial cell emission rates. Atmospheric microbiome characterization is a powerful tool that has been recently adopted for the identification of the microbial content and diversity in atmospheric samples [82] [83]. Nevertheless, these studies are still rare, mostly due to challenges in obtaining high quality DNA amounts, and sampling limitations. Significant knowledge gap regarding aerial transport of micro-organisms through the atmosphere remains, especially in polar areas.

The main objective of this study was to investigate the potential sources of chemical and biological measurements in different size-segregated aerosol particles collected weekly at the Gruebadet atmospheric observatory. This is the first investigation that combined chemical and biological data in order to predict changes in Kongsfjorden dynamics. The experiment have been carried out using the samples collected from 26th February to 1st June 2018. DNA analysis were performed using the method developed by Dommergue et al. (2019) [84].

Chapter 4

Results and discussion

In the following sections an abstract of the published papers in chronological order are reported. Section 4.4 reports a preliminary study in which chemical and biological data are compared in order to predict changes in Kongsfjorden dynamics. After, the multi-annual trend of major ions and WSOCs is discussed. Appendix A reports the full manuscripts that are directly linked with this thesis, while Appendix B reports an ancillary study in which were developed a method to determine some organic acids.

4.1 Free and combined L- and D-amino acids in Arctic aerosol (Feltracco et al., 2019)

In this first study aerosol samples were collected with the high-volume cascade impactor described in Chapter 2 with a 10 day sampling frequency, providing the first investigation of free and combined L- and D-amino acids (FAAs and CAAs) in Arctic atmospheric particulate matter. The main aims of this study were:

- to investigate the occurrence and concentration levels of L- and D- FAAs and CAAs in atmospheric aerosol in Ny-Ålesund (Svalbard Islands) during the 2015 spring campaign (4th April - 13th June)
- to determine how these compounds are distributed in size-segregated aerosols
- to investigate the possible emission sources

This study also developed a new method for the determination of combined amino acids (CAAs) that involves a hydrolysis step to release FAAs from proteinaceous material or other polypeptides contained in the aqueous extracts obtained during sample processing. The

concentration of CAAs in each aerosol sample was calculated by subtracting the quantity of FAAs from that measured after acid hydrolysis. In general, the average concentrations of free amino compounds (amino acids and alkyl amines) were generally 4-5 times lower than those of combined amino compounds (proteins and peptides). The study of peptides and proteins in atmosphere is particularly complex, for their presence in low concentration and in composite mixtures. Moreover they can be modified by chemical and physical processes in the atmosphere.

To confirm the amino acid sources, other specific tracers were also investigated. Levoglucosan was used as a biomass burning marker, while MSA was used as an algal bloom marker. Nss-SO_4^{2-} was used to distinguish between sources. Back-trajectories analysis, MSA, nss-SO_4^{2-} and FcA were used to describe the geographic origin of the air masses and to explain how biomass burning events and phytoplankton blooms may influenced the FAAs concentration. The paper was published in *Chemosphere* ^[75] in 2019 and is reported in Appendix A.

4.2 Interannual variability of sugars in Arctic aerosol: Biomass burning and biogenic inputs (Feltracco et al., 2020)

The work aimed to study, for the first time, the intra- and inter-annual trend of sugars in the aerosol collected at Ny-Ålesund in 3 different periods:

- 13th April - 9th September 2013
- 2nd April - 29th June 2014
- 14th April - 13th June 2015

The three sampling campaigns were conducted during the spring and the sampling campaign of 2013 provided the opportunity to evaluate the impact of ice-free areas during the summer.

This work identified a reproducibility in the sugars trend during spring, while the summer data in 2013 allowed to us to demonstrate strong local inputs when the ground was

free of snow and ice. The study applied two sensitive HPAEC-MS methods developed by Barbaro et al. (2015) ^[80] to determine monosaccharides, disaccharides, alcohol-sugars and anhydrosugars in Arctic aerosol samples. As such, this study presents the first results on the sugar composition and concentrations in Svalbard aerosol.

Here we also propose the arabinose to levoglucosan (A/L) and sorbitol + galactiol to levoglucosan (S/L) ratios, according to their high correlation, as diagnostic ratios to strengthen the well know levoglucosan to mannosan ratio (L/M). Based on the results, the ratios should be used only in ice or snow-covered polar areas to avoid the contribution of local biogenic contamination.

This study demonstrates that not only is long-range atmospheric transport significant. But depending on seasonality, local inputs can also play an important role in the chemical composition of sugars in Arctic aerosol. The paper was published in *Science of the Total Environment (STOTEN)* ^[85] and is reported in Appendix A.

4.3 Year-round measurements of size-segregated low molecular weight organic acids in Arctic aerosol (Feltracco et al., 2021)

This paper wants to define the different source contributions to low molecular weight organic acids in Arctic aerosols across a full year period, from 26th February 2018 to 3rd March 2019. These compounds are poorly investigated, because of their trace concentrations in polar region. For the first time, an annual trend of carboxylic, pinic and pinonic acids in the Svalbard aerosol was shown to the scientific community.

To identify the sources of the low molecular weight organic acids sources using specific and known markers, we studied the size-segregated PM₁₀ aerosol the PMF model was performed, by including in the CAs dataset also major ions, MSA and levoglucosan, as ancillary data. The PMF identified five different possible sources: a) sea spray; b) marine primary production; c) biomass burning; d) sea ice related process and e) secondary products.

EPA's Positive Matrix Factorization (PMF) Model is a mathematical receptor model developed by EPA scientists that provides scientific support for the development and review of air and water quality standards, exposure research and environmental forensics. The PMF model reduces the large number of variables in complex analytical data sets to combinations of species called source types and source contributions. The source types are identified

by comparing them to measured profiles. Source contributions are used to determine how much each source contributed to a sample.

In addition, EPA PMF provides robust uncertainty estimates and diagnostics. The model calculates source profiles or fingerprints, source contributions, and source profile uncertainties. The PMF model results are constrained to provide positive source contributions and the uncertainty weighted difference between the observed and predicted species concentration is minimized. The paper was published in *Science of the Total Environment (STOTEN)* [86] and is reported in Appendix A.

4.4 Airborne bacteria and particulate chemistry capture phytoplankton bloom dynamics in an Arctic Fjord (Feltracco et al., *submitted*)

The paper (*submitted*) aims to investigate the potential sources of chemical and biological measurements in different size-segregated aerosol particles collected at the Gruvebadet Observatory from February 26th to June 1st 2018 with a resolution of 6 days. The study combined for the first time chemical and biological data in order to predict changes in Kongsfjorden dynamics. The surface water of the fjord varies according to complex factors including currents, precipitation, winds, water inflow from glacial melt and the coast, and sea ice drift.

This study also included the Chlorophyll-*a* to better interpret the changes in plankton. Chl *a* has been widely used as a proxy for phytoplankton biomass to explore influences of oceanic biological activity on sea salt aerosol (SSA) properties. Positive correlations between satellite-derived Chl *a* and the organic fraction of SSA were observed in the North-East Atlantic.

Using this approach, it was possible to identify blooms of rare marine microorganisms such as *Polaribacter* and *Janthinobacterium* and relate them to algal blooms. D-amino acids could serve as indications of developing marine blooms and be used to predict biological activity of the exponential phase in marine ecosystems. L-amino acids could also serve as markers for post-bloom phase in other types of archives such as ice cores. The submitted version of the paper was submitted in *Atmospheric Environment* and is reported in Appendix A.

4.5 Multi-annual trend of major ions and WSOCs

Here, unpublished data regarding the whole sampling campaigns considered in this thesis (2013,2014,2015 and 2018-19) are presented. The chemical species determined in this thesis in Arctic aerosol are displayed on pie charts in Figure 4.1. The most abundant compounds in aerosol particles are nss-SO_4^{2-} , Cl^- , Na^+ followed phenolic compounds (PCs), sugars, organic acids and free amino acids (FAAs). Not surprisingly, major ions are the most abundant compounds and this is consistent with several studies [5] [87].

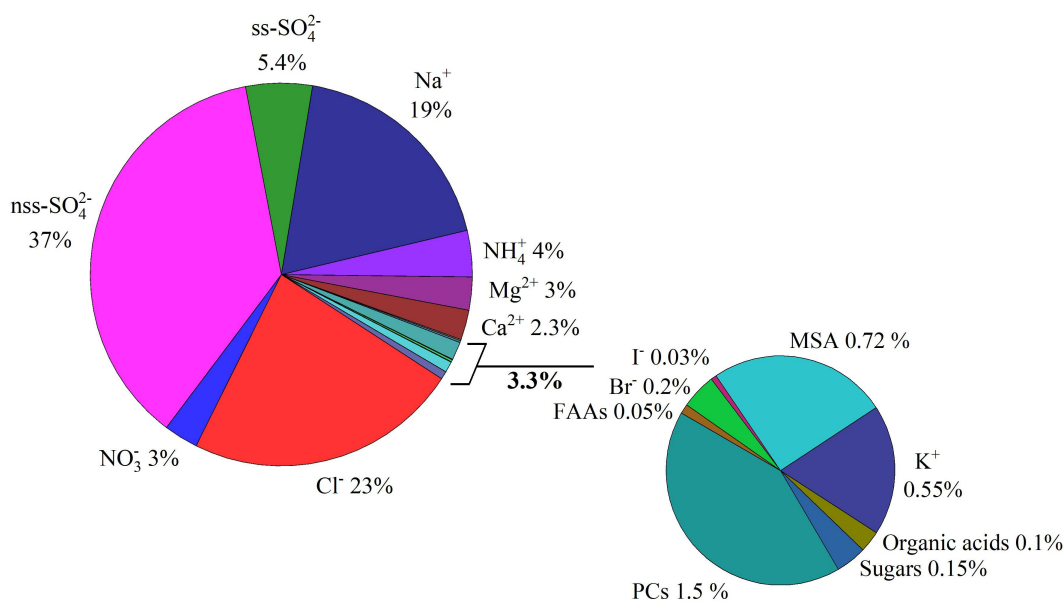


FIGURE 4.1: Composition of water soluble fraction of PM_{10} in atmospheric aerosol collected.

4.5.1 Major ions

Anions (F^- , Cl^- , NO_2^- , NO_3^- , PO_4^{3-} , Br^- , SO_4^{2-}) and cations (Na^+ , K^+ , NH_4^+ , Ca^{2+} , Mg^{2+}), are the major components of atmospheric aerosols [88] [89]. In general, the water soluble major ions account for about 60-70% of particulate mass [90]. Consequently, the ionic characterization of atmospheric particle has been studied extensively in recent years, even in polar regions. The size distributions of major ions provide detailed information on mode distributions and also give evidences on the formation and transformation of these particles in the atmosphere. However, concentrations and particulate distributions would be distinct in different regions,

because they depend heavily on local sources, weather conditions, reaction conditions, and long-range atmospheric transportation.

Several studies investigated different inorganic together with organic acids in the Svalbard atmosphere in both size-segregated and PM₁₀ aerosols [51] [54] [91] [92] [93]. The main components of Arctic aerosol are Na⁺, Cl⁻, and Mg²⁺, originated by sea spray; conversely, Ca²⁺, K⁺, and SO₄²⁻ have relevant contributions from other sources, especially crustal aerosol and anthropic emissions by long-range transport from continental regions [51] [45]. The bromine and iodine concentration trends were also studied. Both halogens present a complex photochemistry in the atmosphere [94] [95] [96], this suggests that reactive halogens also play an important role in the chemistry of the troposphere. Bromine atoms react in the atmosphere mainly with O₃ to form BrO and is associated with the presence of first-year sea ice [97] [95]. The main channel of the BrO self-reaction produces two Br atoms, a minor channel produces Br₂ [95]. Another source of bromine could be also sea spray aerosol [98]. Iodine sources in polar regions are believed to mainly be related with biological production under sea ice, with ice surface photochemistry and marine primary production [99] [100].

Here is described multi-annual variation in Arctic aerosol of major ions (Na⁺, NH₄⁺, K⁺, Mg²⁺, Ca²⁺, Cl⁻, Br⁻, I⁻, NO₃⁻, SO₄²⁻) and methanesulfonic acid (MSA) in size-segregated aerosol samples collected at Gruvebadet Laboratory, close to Ny-Ålesund (Svalbard Island). Pre-analytical procedures and instrumental analysis were validated by Barbaro et al., (2017) [61] and already reported in the published papers.

Three sampling campaign were analysed: from 2nd April to 29th June 2014, from 14th April to 13th June 2015 and 3rd March 2018 to 26th February 2019. The 2013 sampling campaign were not considered because glass fiber filters were used, instead of quartz fiber, that provided huge interferences for the quantifications of major ions.

Figure 4.2 shows the PM₁₀ concentration of 2014, 2015 and 2018-2019 sampling campaigns for major ions. The plot-markers change the size depending on the aerosol fraction. The PM₁₀ concentration was obtained by summing the values obtained from each sampling stage (6 filters with different particle diameter range). Table 4.1 shows the PM₁₀ mean concentrations for each season of each sampling campaign.

The trend concentration depends on the compound and the season. As mentioned above, Na⁺ and Cl⁻ are recognized as specific tracers of sea salt aerosol. These species are mainly distributed in the coarse fraction (D>0.95 μm) in all years, especially in the particles with

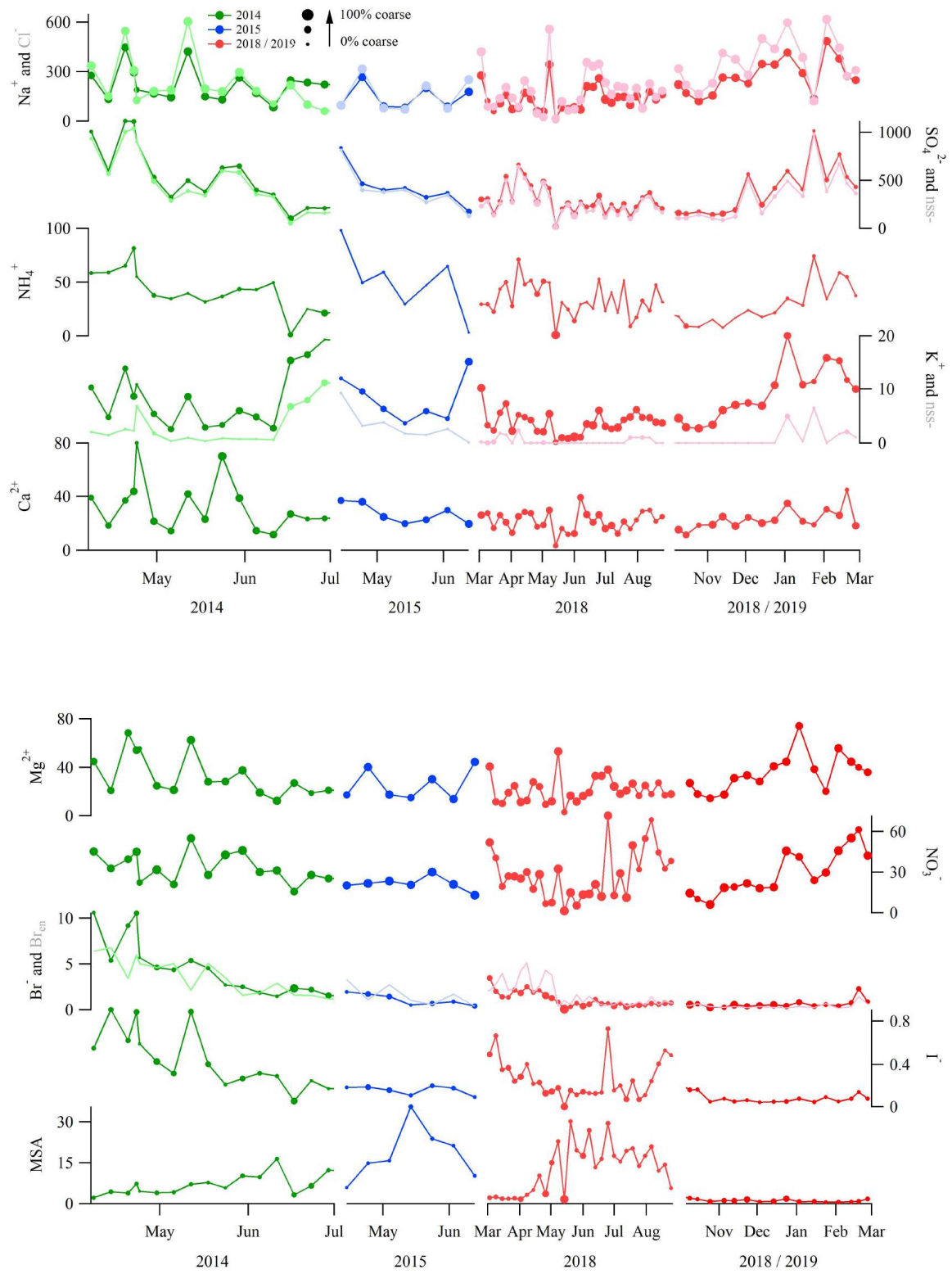


FIGURE 4.2: Major ions concentration in PM₁₀ of 2014, 2015 and 2018-2019.

TABLE 4.1: PM₁₀ mean concentration for major ions reported for each sampling campaign. 2018-19 sampling campaign was divided depending on the seasons. Autumn and Winter 2018-2019 are reported as "18-19". In brackets, standard deviations are shown.

	Na ⁺	Cl ⁻	SO ₄ ²⁻	nss-SO ₄ ²⁻	NH ₄ ⁺	K ⁺	nss-K ⁺	Ca ²⁺	Mg ²⁺	NO ₃ ⁻	Br ⁻	I ⁻	MSA
Spr 14	223 (102)	235 (142)	648 (531)	594 (525)	52 (46)	8 (5)	3 (3)	33 (19)	34 (18)	34 (11)	5 (3)	0.4 (0.3)	7 (4)
Spr 15	143 (72)	157 (101)	426 (204)	390 (210)	57 (45)	10 (9)	3 (3)	27 (7)	25 (13)	21 (5)	1 (1)	0.16 (0.04)	18 (10)
Win 18	141 (94)	183 (160)	260 (74)	225 (62)	31 (9)	5 (4)	1 (1)	24 (5)	20 (14)	35 (14)	2 (1)	0.5 (0.1)	2.1 (0.3)
Spr 18	120 (85)	171 (149)	335 (175)	305 (171)	36 (18)	3 (2)	0.3 (0.7)	21 (9)	20 (13)	17 (10)	1 (1)	0.2 (0.1)	13 (10)
Sum 18	144 (47)	193 (68)	240 (79)	204 (75)	32 (15)	4 (1)	0.4 (0.5)	22 (6)	23 (6)	40 (20)	0.6 (0.1)	0.3 (0.2)	17 (6)
18-19	270 (103)	355 (143)	402 (255)	334 (250)	29 (19)	9 (5)	1 (2)	23 (8)	35 (15)	29 (17)	0.6 (0.5)	0.09 (0.04)	1.1 (0.5)

diameters above 3 μm . Sea salt aerosol showed the highest concentrations in winter and autumn 2018-2019. In addition, during the winter season, Na⁺ also showed an increase in the finest fraction ($D < 0.49 \mu\text{m}$) at 9% (winter), while 3% of was found in spring, summer and autumn, suggesting an additional contribution by LRAT. Chlorine did not reveal the same size variability. Considering others periods, the trend seems to be driven by some meteorological events and physical transformation of aerosol (bubble bursting events due to strong winds occurrences, etc).

Nss-SO₄²⁻ (calculated as $[\text{SO}_4^{2-}] - 0.253 \times [\text{Na}^+]$) dominated the total concentration of sulphate and showed the highest concentration in spring 2014 ($1041 \pm 622 \text{ ng m}^{-3}$) and in winter 2018-2019 ($502 \pm 224 \text{ ng m}^{-3}$). Nss-SO₄²⁻ has mainly two sources: anthropogenic, from the oxidation of SO₂ [101] [102], as well as resulting from emissions from phytoplanktonic blooms [75] [103]. Oxidation of SO₂ pollution is considered to be the source of most of the nss-SO₄²⁻ [104]. To confirm this, an high correlation in spring 2014, 2015, 2018 and winter 2018, is shown with nss-K⁺ ($R^2 > 0.6$) that has long been considered as a tracer for biomass burning [13] [105]. Both tracers are mainly present in fine particles. The significant correlation with MSA in summer 2018 ($R^2 = 0.8$) suggests that nss-SO₄²⁻ derived likely from primary production.

Ammonium can be emitted during the high biological marine activity [106] in summer. Nevertheless, in winter, spring and autumn ammonium in Arctic mostly originates from anthropogenic sources in East Asia and Europe, with added contribution from boreal fire [45]. The significant correlation between NH₄⁺ and nss-SO₄²⁻ ($R^2 = 0.8$) demonstrates that sulfate is present at Ny-Ålesund also as ammonium salt. Furthermore, the distribution mainly in fine fraction of ammonia suggests a dual source: primary marine production in summer and anthropogenic contribution in spring and winter.

Ca²⁺ and Mg²⁺ had a constant trend during the four years of sampling, except for the end

of April and the end of May that showed a peak value, probably due to strong winds that contribute to the sea spray source with a minor effect compared with sea salt particles. Mg^{2+} showed a non-negligible concentration enhance in winter 2018-2019 that seems to follow the sea-salt trend.

Nitrate in aerosol samples collected near the coast was mainly found in the coarse fraction >80%. The main formation pathway was likely the interaction of nitric acid or other reactive nitrogen compounds with sea-salt particles in the Arctic atmosphere [92]. Unlike the sea salt particles, NO_3^- peaked also in summer, reaching its highest concentration ($40 \pm 20 \text{ ng m}^{-3}$). This is due to the reactions that nitric acid may undergo with some species that are condensed on the same particles. This reaction has been suggested to be the major way for the formation of coarse particles of nitrate at many coastal areas [107]. NO_x transforms into gaseous nitrous and nitric acids, which later react with NaCl in sea-salt aerosols to form $NaNO_3$ and HCl in the so-called chloride depletion reaction. The same pathway can be followed by H_2SO_4 [108]. High percentage of chloride depletion (<80%) is found for fine particles ($D < 0.95 \mu\text{m}$) and still reaches $\sim 60\%$ at $1.5 \mu\text{m}$ but decreases to $\sim 15\%$ for larger particles. It has been suggested that the surface reaction mechanism is the principal explanation for higher depletion of smaller particles [107]. Cl_{dep} also reaches values slightly lower 0% in the coarsest fraction. The size-trend suggests that nitric acid reacted with NaCl in fine particles to release HCl. The negative percentage in the coarsest mode indicates a slight excess of chlorine, which could be due to the gas-particle conversion of gaseous HCl in the atmosphere on coarse particles, or to an atmospheric pollution caused by coal combustion processes [109].

A possible connection between bromine emissions and sea ice extent has been also suggested recently. Spolaor et al., (2016) [110] hypothesised that Br^- deposition in Arctic regions and its subsequent preservation in ice cores could be used as a tracer for changes in sea ice cover. The bromine enrichment resulting from sea ice events, was calculated as calculate $Br_{\text{en}} = Br / (Na^+ \times 0.006)$. The PM_{10} trend concentration showed in Figure 4.2 confirms the enhance of Br^- springtime in the Arctic atmosphere.

Iodine followed the temporal trend of bromine during all the sampling period. Since the presence of I^- is related to marine biological production [111], the high level of I^- in springtime is may due to the sub-ice biological productivity, directly related to Arctic sea ice thinning [112] and in summer to the algae bloom involving different emission process than MSA. The I^-

and Br⁻ trends are widely discussed in the paper entitled "Year-round measurements of size-segregated low molecular weight organic acids in Arctic aerosol" [86]. A broad information about MSA characteristics have been already provided in the published papers.

4.5.2 Organic acids

The atmospheric concentrations of diacids are influenced by primary source such as motor exhausts and biomass burning [113] [114]. Secondary sources such as production from photooxidation of hydrocarbons are expected to be important, because diacids have been reported to be the oxidation products of aromatic hydrocarbons and alkanes in the laboratory studies [115] [116].

The annual trend, sources and transport of organic acids (CAs) are discussed by Feltracco et al. (2021) [86]. Here a brief summary of multi-annual concentration trend is reported. All sampling campaign were analysed: from 13th April to 9th September 2013, from 2nd April to 29th June 2014, from 14th April to 13th June 2015 and 3rd March 2018 to 26th February 2019. The filters of the 2013 sampling campaign did not show the same interferences provided by major ions.

Figure 4.3 shows the PM₁₀ concentration of 2013, 2014, 2015 and 2018-2019 sampling campaigns for carboxylic acids. The Table 1 reported in the paper entitled "Year-round measurements of size-segregated low molecular weight organic acids in Arctic aerosol" shows the the PM₁₀ mean concentrations for each season of each sampling campaign.

Spring and summer are highlighted in light grey and orange, respectively. All the detected CAs peaked in spring, in particular their concentrations started to increase significantly in March and peaked in mid April. These peaks appeared at the time of Arctic sunrise, suggesting that CAs are mainly produced in the atmosphere by photo-induced reactions. CAs in 2013 and 2018 began also to increase between July and August. This trend can be associated to the the marine primary production from adjacent sea, some biomass burning events especially from Northern Russia and also the rise in temperature that may have enhanced the photochemical transformation of organic precursors to carboxylic acids [86]. CAs were mainly distributed in the fine particles and did not show a size-variability throughout the years.

Monoterpenes are the most abundant biogenic hydrocarbons in troposphere and these compounds affect the oxidising capacity of the atmosphere [69]. In particular, α -pinene is the

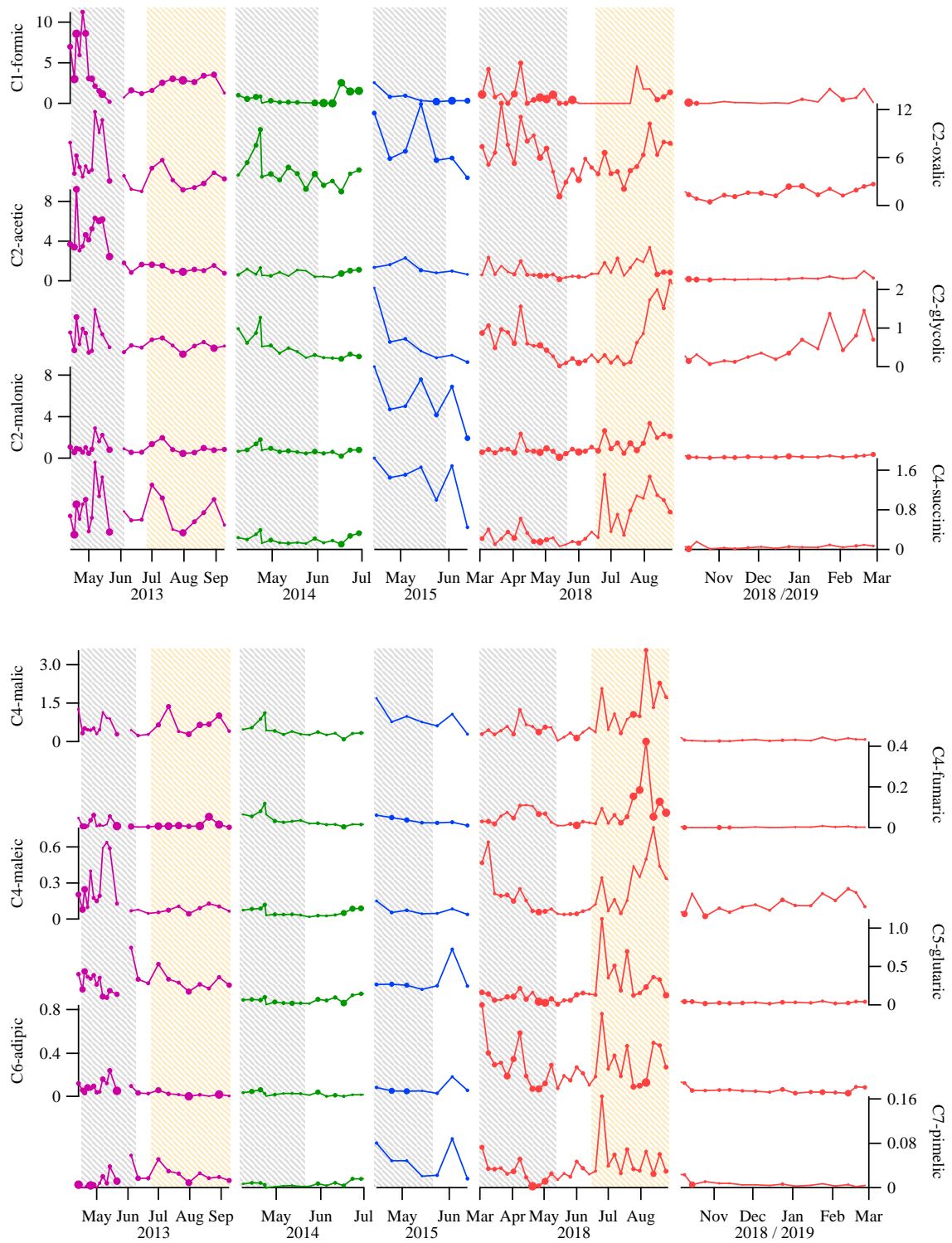


FIGURE 4.3: Carboxylic acids concentration in PM_{10} of 2013, 2014, 2015 and 2018-2019.

most important monoterpene released by biogenic sources, particularly conifers [72]. Pinonic and pinic acids are known as main products of α -pinene [117] [118]. Figure 4.4 shows the PM₁₀ concentration of 2013, 2014, 2015 and 2018-2019 sampling campaigns.

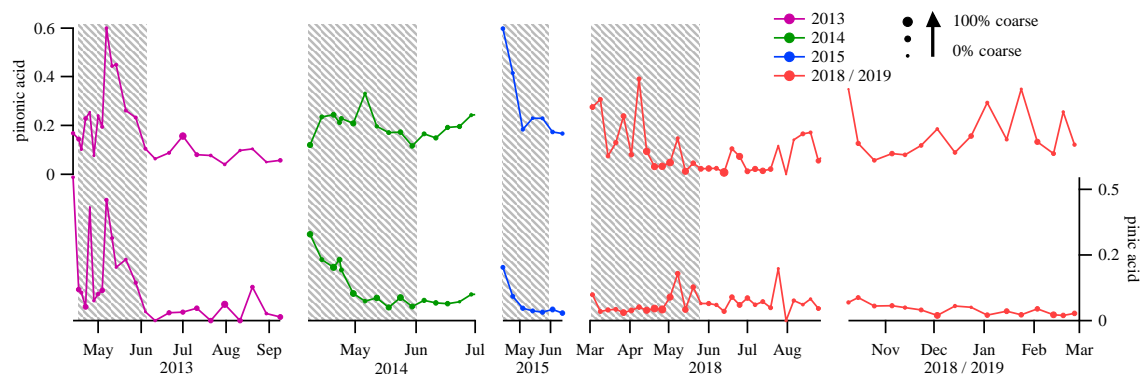


FIGURE 4.4: Pinonic and pinic acids concentration in PM₁₀ of 2013, 2014, 2015 and 2018-2019.

In Figure 4.4 springs are highlighted in light grey to bring out the contribute of these acids. Monoterpene-derived SOA tracers correlated with levoglucosan in 2018-2019 campaign) [86], indicating that biomass burning may be a source for these compounds. This is confirmed by the peak always showed in spring (except for pinic acid in spring 2018) and in winter 2018-2019 that well correlates the levoglucosan trend in this period (Figure 4.5).

The peak of these compounds in spring is also due to the strong recurring seasonality with higher number of particles in the accumulation mode (0.3 - 0.7 μm) in March and April, compared to the summer. This phenomenon is called "Arctic haze" and it is a result, visible to the naked eye, of long-range transportation of sub-micrometric particles, especially anthropogenic non-sea-salt sulphates, black carbon and heavy metals [101]. Several studies suggest that the atmospheric pollutants reaching the Arctic during spring can be mainly related to inputs from eastern Eurasia [52] [85] [101].

4.5.3 Sugars

Sugar sources to the atmosphere are diverse and include direct biogenic emissions, vegetation burning, soil dust resuspension, and bacterial and fungal spores [119] [120]. In plants, pollen accumulates starch reserves, which are converted into fructose, glucose, and sucrose [121]. The sources, transport, seasonal variation and concentrations in 2013, 2014 and 2015 are

discussed in the paper entitled "Interannual variability of sugars in Arctic aerosol: Biomass burning and biogenic inputs" [85].

Figure 4.5 shows the PM₁₀ multi annual variability of determined sugar. The improvement from the cited study [85] is provided by the year-round trend in 2018 and 2019 campaign, even though anhydro-sugars trend were entirely explained.

The concentration trend of arabitol and mannitol reflect the trend concentration of 2013 campaign, with a clear peak in summer due to the exposure of ice-free areas, confirmed also by the coarse fraction distribution of such sugars. Sorbitol and galactiol, iso-erythritol, sucrose, fructose and galactose did not show a valuable trend. On the contrary, glucose and maltitol showed a strong enhance in coarse particles in August 2018 (3.6 and 0.13 ng m⁻³). In summer, considering the ice-free areas, glucose can originate from local microorganisms, plants, and animals [78]. The same summer trend was not showed in 2013 for fructose and glucose, but summer 2013 showed a strong enrichment of arabinose. By evaluating the ratio of glucose to levoglucosan in smoke samples is also possible to exclude biomass burning as a source of glucose [77]. Medeiros et al. (2006) reported a value of about 4.5 of glucose/levoglucosan ratio for smoke-free samples, and considerably lower values of 0.9 for smoke samples. We calculated this ratio for each sample and the values were always >4, excluding smoke as major source of glucose.

4.5.4 Free amino acids

The different free amino acids (FAAs) found in continental particles are thought to have been originally produced by plants, pollens and algae, as well as fungi, bacterial spores and biomass burning [73] [122]. The amino acids were deeply studied taking into account the 2015 sampling campaign [75].

Figure 4.6 shows the PM₁₀ multi annual variability of more concentrated and interpretable L- and D-FAAs. The 2013 sampling campaign were not considered because the glass fiber filters gave again huge interferences also for the quantifications of FAAs. The mean PM₁₀ concentrations of more concentrated FAAs are reported in in Table 4.2.

Gly, D-Ala and D-Asp are always distributed in fine particles, suggesting mainly a long-range transport. The high intake of these FAAs in spring 2014, 2015 and 2018 suggests a biomass burning input from Eurasia and the algal bloom from adjacent sea. L-amino acids showed a coarser distribution, with a concentrations increase in August 2018. The presence

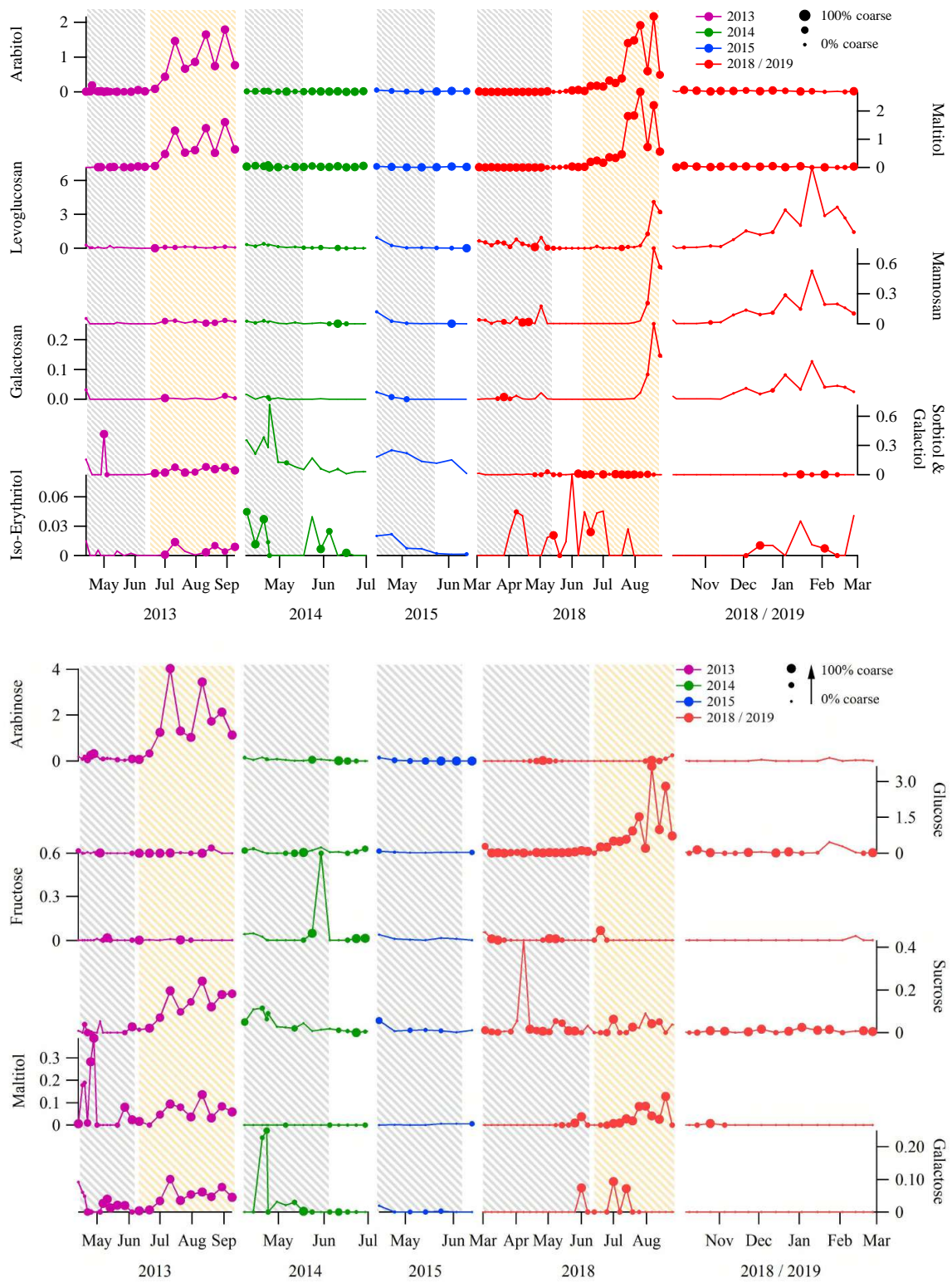


FIGURE 4.5: Saccharides, anhydro-sugars and alcohol-sugars concentration in PM₁₀ of 2013, 2014, 2015 and 2018-2019.

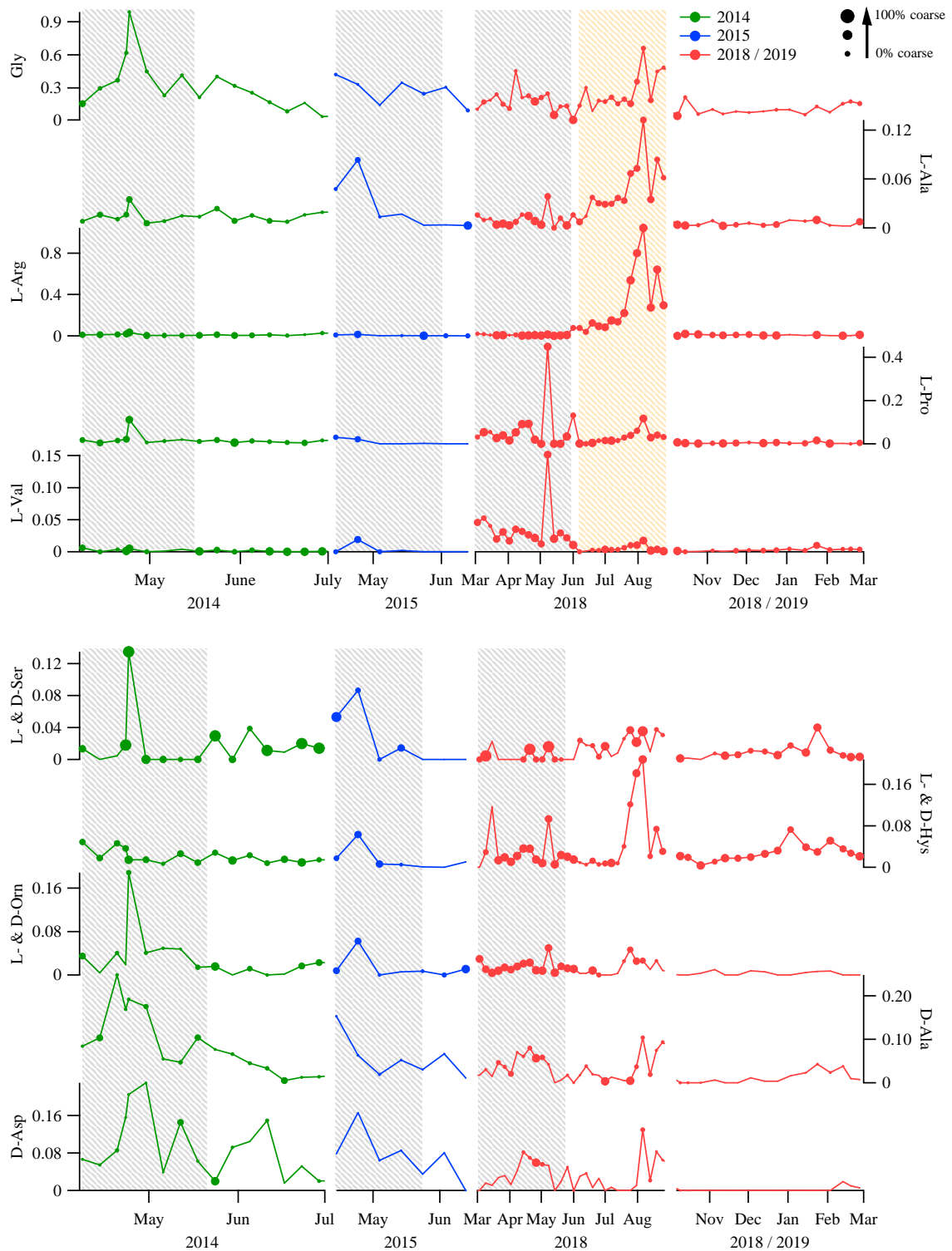


FIGURE 4.6: FAAs concentration in PM_{10} of 2014, 2015 and 2018-2019.

TABLE 4.2: PM₁₀ mean concentration for relevant L- and D-FAAs reported for each sampling campaign. 2018-19 sampling campaign was divided depending on the seasons. Autumn and Winter 2018-2019 are reported as "18-19".

	Gly	L-Ala	L-Arg	L-Pro	L-Val	LD-Ser	LD-Hys	LD-Orn	D-Ala	D-Asp
Spr 2014	0.3 (0.2)	0.01 (0.01)	0.01 (0.01)	0.02 (0.03)	0.002 (0.002)	0.02 (0.03)	0.02 (0.01)	0.03 (0.05)	0.09 (0.07)	0.09 (0.07)
Spr 2015	0.3 (0.1)	0.02 (0.03)	0.004 (0.005)	0.01 (0.01)	0.003 (0.007)	0.02 (0.03)	0.01 (0.02)	0.01 (0.02)	0.06 (0.05)	0.07 (0.05)
Win 2018	0.2 (0.1)	0.01 (0.01)	0.01 (0.01)	0.04 (0.01)	0.04 (0.01)	0.01 (0.01)	0.04 (0.05)	0.01 (0.01)	0.03 (0.01)	0.01 (0.01)
Spr 2018	0.2 (0.1)	0.01 (0.01)	0.03 (0.04)	0.1 (0.1)	0.03 (0.04)	0.01 (0.01)	0.02 (0.02)	0.01 (0.01)	0.03 (0.03)	0.04 (0.03)
Sum 2018	0.3 (0.2)	0.06 (0.03)	0.4 (0.3)	0.04 (0.03)	0.01 (0.01)	0.02 (0.01)	0.06 (0.07)	0.02 (0.02)	0.03 (0.04)	0.03 (0.04)
18-19	0.1 (0.1)	0.01 (0.01)	0.01 (0.01)	0.01 (0.01)	0.003 (0.002)	0.01 (0.01)	0.03 (0.02)	0.003 (0.004)	0.01 (0.01)	0.002 (0.005)

of these L-FAAs in the coarse fractions would suggest a local contribution. This peak is consistent with the stationary and waning stages of the algal bloom (see MSA, Figure 4.2, during which phytoplankton release proteins, amongst other molecules. These results can not exclude a biomass burning contributions also in summer 2018, as suggested in the 2015 campaign [75] and in a previous study [122], due to good overlap with anhydro-sugar peak occurred in the same period (Figure 4.5).

4.5.5 Phenolic compounds

Phenolic compounds (PCs) produced from lignin combustion have been observed in high concentrations in combustion plumes and are specific molecular markers that can assess combustion sources. Lignin is a biopolymer that constitutes approximately 20-30% of dry wood mass and is derived from three main aromatic alcohols: p-coumaryl, coniferyl, and sinapyl alcohols [79]. The pyrolysis products of these aromatic alcohols are classified as coumaryl, vanillyl, and syringyl moieties. The dominant phenolic biomarkers in deciduous tree smoke include homovanillyl alcohol, vanillic acid, vanillin, and syringic acid [123]. The dominant phenolic biomarkers in conifer smoke include vanillin, homovanillic acid, vanillic acid, and homovanillyl alcohol [124]. Significant products from burning grasses are acetosyringone, syringic acid, vanillin and vanillic acid [125]. We determined eight PCs: vanillin (VAN), vanillic acid (VA), homovanillic acid (HA), p-cumaric acid (PA), syringic acid (SyA), coniferyl aldehyde (CAH), ferulic acid (FA).

Figure 4.7 shows the PM₁₀ multi annual variability of PCs above the detection limit. The mean PM₁₀ concentrations of relevant PCs are reported in in Table 4.3. These results were not yet published.

The majority of PCs in Ny-Ålesund occur in the fine fraction, where this distribution is consistent with long range transport [50] [126] [127]. Even though the majority of PCs occur

TABLE 4.3: PM₁₀ mean concentration for PCs reported for each sampling campaign.

	VA	VAH	FA	CAH	PA	VAC
Spring 2013	3 (4)	4 (8)	0.1 (0.2)	2 (4)	0.3 (0.4)	0.04 (0.07)
Summer 2013	0.8 (0.7)	0.1 (0.2)	0.01 (0.01)	0	0	0.002 (0.006)
Spring 2014	0.4 (0.9)	5 (3)	0.2 (0.4)	0.1 (0.2)	0	0.2 (0.3)
Spring 2015	2 (3)	2 (2)	0.1 (0.2)	0	0	0.2 (0.4)
Winter 2018	2 (1)	11 (9)	0	0	0.05 (0.07)	0.01 (0.01)
Spring 2018	2 (1)	9 (7)	0.2 (0.3)	0	0.02 (0.05)	0.02 (0.03)
Summer 2018	1 (1)	8 (7)	0	0	7 (3)	0.4 (0.7)
Aut & Win 2018-19	2 (2)	4 (3)	0	0.1 (0.1)	4 (2)	0.1 (0.1)

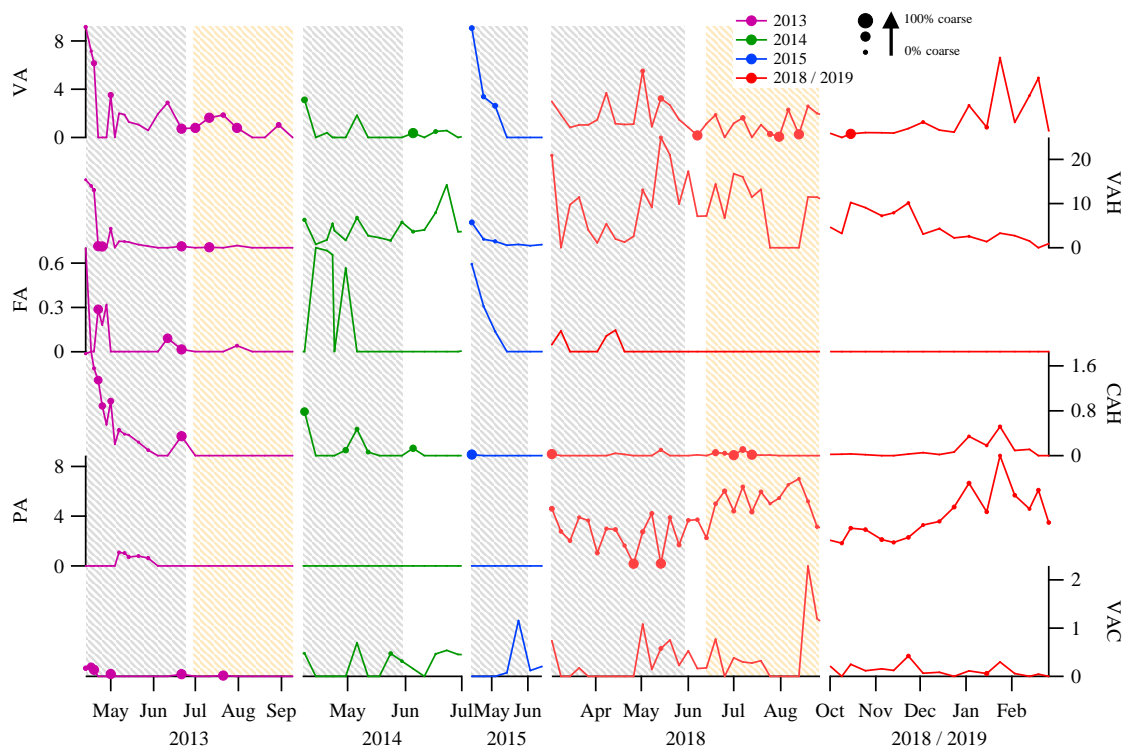


FIGURE 4.7: PCs concentration in PM₁₀ of 2013, 2014, 2015 and 2018-2019.

in the fine fraction, PCs are sporadically present in the coarse fraction. Knowing that PCs are semivolatile species, they can volatilize and re-condense on coarse particles ^[128] during long range transport. As reported in Table 4.3, VAH results the more abundant PCs (60 %) followed by VA (18 %), PA (17 %), CAH (3 %), VAC (1.5 %) and FA (0.9%).

In spring 2013, 2014, 2015 and 2018, highlighted in light-grey (Figure 4.7), PCs peaked demonstrating that the biomass burning sources already explained above are also detectable with these markers. The same source is identifiable in winter 2018-19, in which the trend concentration of PCs are well overlapped with levoglucosan. In summer 2013 and more frequently in summer 2018, it was found a non-negligible presence of VA, VAH, PA and VAC. Some studies reported the possibility that phytoplankton could be the source of PCs ^[129]. It has to be noted that a limited number of studies report the profile of PCs in phytoplankton, but numerous PCs (among them VA and PA) have been observed in extracts and exudates of diatoms ^[130]. Again, a possible source in summer 2018 could be due to the strong biomass burning event occurred in Northern Russia ^[86], but it is necessary to study PCs concentrations in seawater and in aerosol under a variety of atmospheric conditions in order to better understand their applicability as reliable markers of biomass burning, anthropogenic activity or biogenic activity.

4.6 Novelties of the thesis and future challenges

The compounds studied in this thesis in the Arctic are particularly concentrated in winter and spring. The finding of Northern-Russia as a major source region for biomass burning markers and the comparison with the free amino acids trend in spring 2015 has allowed to identify wildfires as possible source of FAAs. Spring emissions were better interpreted also with major ions that helped to differentiate between marine, crustal and anthropogenic source. For example, the MSA trend suggested the primary marine production as a source for some FAAs and some carboxylic acids that indicates the high complexity of marine inputs.

The determination of some sugars (i.e. arabitol and mannitol) were associated primarily with coarse aerosols in summer, suggesting local transport, while these compounds do not show significant concentrations in other seasons. A wide and multi annual investigation of WSOCs has never been done before in the Ny-Ålesund atmosphere and the results achieved here are overriding also for future collaboration and data-sharing.

While a number of studies of Arctic aerosol have focused mainly on physical properties and size distribution without a deep investigation of the chemical composition, there are still lack answers to a long-term monitoring of airborne WSOCs and how they interact with the environment.

Careful consideration is needed to understand the influence of various processes as sea spray, sea ice thinning and atmospheric stratifications, with a inter-comparison studies taking into account the study of particles physical properties, nano-particles investigation, snow-atmosphere interaction and oceanography. The measurement of other climatically relevant parameters (CCN and IN) has been performed only during spot campaigns. The study of cloud condensation and ice nuclei should be done in parallel with ongoing observations, as long term monitoring. Very similar suggestions are reported in the SESS report 2020 ^[131].

Conclusions

Through the multi-annual studies conducted in this PhD thesis it has been possible to demonstrate the applicability of a wide range of environmental markers in analytical studies with the aim of environmental characterization of aerosol. It has been demonstrated that environmental markers play a crucial role to better understand the transport processes and the sources in the Arctic area, strongly characterized by both natural inputs and anthropic inputs, depending on the season.

Four sampling campaigns, from 2013 to early 2019 permitted the investigation of the chemical composition and particle size distribution of aerosol. Furthermore, for the first time in the Italian station were studied the behaviour of environmental markers during the polar night in winter 2018-2019. A wide range of markers were detected: ionic species, organic acids, sugars, free and combined amino acids and phenolic compounds.

The particle size-distribution of molecular markers were also investigated in order to identify different emission sources and to discriminate between local source and long range transport. Transport and dispersion simulations were conducted using a Lagrangian dispersion model, Hybrid Single-Particle Lagrangian Integrated Trajectory (HYSPLIT) model.

To sum up, the general conclusion of this PhD thesis is the extensive utility of environmental markers in the Arctic aerosol: 1) they can discriminate the sources also integrating the determination with the particles size distribution; 2) the markers well describe the seasonal variation; 3) they can be used as support data for other disciplines. To confirm the third point, a combination among chemical and biological data was studied to predict changes in fjord dynamics in front of Ny-Ålesund. Fourthly, the results of this thesis have serious implications for paleoclimatic studies, since the achieved knowledge permits to better understand the environmental meaning of the target markers.

Bibliography

- [1] J. M. Prospero et al. "The atmospheric aerosol system: An overview". In: *Reviews of Geophysics* 21.7 (1983), pp. 1607–1629. ISSN: 19449208. DOI: 10.1029/RG021i007p01607.
- [2] F. Raes et al. "Formation and cycling of aerosols in the global troposphere". In: *Developments in Environmental Science* 34 (2002), pp. 519–563. ISSN: 14748177. DOI: 10.1016/S1474-8177(02)80021-3.
- [3] U. Schumann. *Atmospheric Physics*. 2012, p. 877. ISBN: 9783642301827. DOI: 10.1007/978-3-642-29190-6.
- [4] J. H. Seinfeld and S. N. Pandis. *Atmospheric chemistry and physics: from air pollution to climate change*. 2006. ISBN: 9780471720171.
- [5] E. Barbaro et al. "Characterization of the water soluble fraction in ultrafine, fine, and coarse atmospheric aerosol". In: *Science of the Total Environment* 658 (2019), pp. 1423–1439. ISSN: 18791026. DOI: 10.1016/j.scitotenv.2018.12.298. URL: <https://doi.org/10.1016/j.scitotenv.2018.12.298>.
- [6] N. Sharma et al. *Air pollution and control*. 2018, p. 260. ISBN: 9789811071843. DOI: 10.1007/978-981-10-7185-0_6.
- [7] S. M. Burrows et al. "Bacteria in the global atmosphere – Part 2: Modelling of emissions and transport between different ecosystems". In: *Atmospheric Chemistry and Physics Discussions* 9.3 (2009), pp. 10829–10881. ISSN: 1680-7375. DOI: 10.5194/acpd-9-10829-2009.
- [8] F. Dentener et al. "Emissions of primary aerosol and precursor gases in the years 2000 and 1750 prescribed data-sets for AeroCom". In: *Atmospheric Chemistry and Physics* 6.12 (2006), pp. 4321–4344. ISSN: 16807324. DOI: 10.5194/acp-6-4321-2006.
- [9] A. Guenther, C. Hewitt, and D. Erickson. "A global model of natural volatile organic compound emissions". In: *Journal of Geophysical Research* 100.94 (1995), pp. 8873–8892. URL: <http://www.agu.org/pubs/crossref/1995/94JD02950.shtml>.
- [10] C. L. Heald and D. V. Spracklen. "Atmospheric budget of primary biological aerosol particles from fungal spores". In: *Geophysical Research Letters* 36.9 (2009), pp. 1–5. ISSN: 00948276. DOI: 10.1029/2009GL037493.
- [11] R. Jaenicke. "Abundance of cellular material and proteins in the atmosphere". In: *Science* 308.5718 (2005), p. 73. ISSN: 00368075. DOI: 10.1126/science.1106335.
- [12] J.E. Penner et al. *Aerosols, their Direct and Indirect Effects, in: Climate Change 2001: The Scientific Basis, Contribution of Working Group I to the Third Assessment Report of the Intergovernmental Panel on Climate Change*. Tech. rep. 2001.

- [13] M. O. Andreae. "Emission of trace gases and aerosols from biomass burning". In: *Global Biogeochemical Cycles* 15.4 (2001), pp. 955–966.
- [14] R. Jaenicke. "Atmospheric aerosol and global climate". In: *J. Aerosol Sci.* 11 (1980), pp. 577–588.
- [15] L. M. Mukhin. "Volcanic processes and synthesis of simple organic compounds on primitive earth". In: *Origins of life* 7.4 (1976), pp. 335–368.
- [16] E. Scalabrin et al. "Amino acids in Arctic aerosols". In: *Atmospheric Chemistry and Physics* 12.21 (2012), pp. 10453–10463. ISSN: 16807316. DOI: 10.5194/acp-12-10453-2012.
- [17] O. Boucher. *Atmospheric Aerosols. Properties and climate impacts*. Vol. 53. 9. 2013, p. 311. ISBN: 9788578110796. DOI: 10.1017/CB09781107415324.004. arXiv: arXiv:1011.1669v3.
- [18] C. Leck and E. K. Bigg. "Comparison of sources and nature of the tropical aerosol with the summer high Arctic aerosol". In: *Tellus, Series B: Chemical and Physical Meteorology* 60 B.1 (2008), pp. 118–126. ISSN: 02806509. DOI: 10.1111/j.1600-0889.2007.00315.x.
- [19] M. C. Facchini et al. "Primary submicron marine aerosol dominated by insoluble organic colloids and aggregates". In: *Geophysical Research Letters* 35.17 (2008), pp. 1–6. ISSN: 00948276. DOI: 10.1029/2008GL034210.
- [20] Y. Liu and P. H. Daum. "Anthropogenic aerosols: indirect warming effect from dispersion forcing". In: *Nature* 419.4 (2002), pp. 580–581. ISSN: 1943281X. DOI: 10.1521/00332747.1963.11023367.
- [21] R.J. Charlson et al. "Ocean phytoplankton, atmospheric sulfur, cloud albedo and climate". In: *Nature* 326.16 (1987), pp. 665–661. ISSN: 08866236. DOI: 10.1029/2003GB002183.
- [22] P. Buat-Ménard. *The Role of Air-Sea Exchange in Geochemical Cycling*. 1986, p. 549. ISBN: 9789401086066. DOI: 10.1007/978-94-009-4738-2.
- [23] Alexander A. Kokhanovsky. *Aerosol optics: Light absorption and scattering by particles in the atmosphere*. Vol. 46. 03. Springer, 2008, p. 154. ISBN: 9783540237341. DOI: 10.5860/choice.46-1543.
- [24] A. Petzold et al. "Perturbation of the European free troposphere aerosol by North American forest fire plumes during the ICARTT-ITOP experiment in summer 2004". In: *Atmospheric Chemistry and Physics* 7.19 (2007), pp. 5105–5127. ISSN: 16807324. DOI: 10.5194/acp-7-5105-2007.
- [25] M. Shiraiwa et al. "Aerosol Health Effects from Molecular to Global Scales". In: *Environmental Science and Technology* 51.23 (2017), pp. 13545–13567. ISSN: 15205851. DOI: 10.1021/acs.est.7b04417.
- [26] S. Faridi et al. "A field indoor air measurement of SARS-CoV-2 in the patient rooms of the largest hospital in Iran". In: *Science of the Total Environment* 725 (2020), pp. 1–5. ISSN: 18791026. DOI: 10.1016/j.scitotenv.2020.138401.
- [27] S. Flaxman et al. "Estimating the effects of non-pharmaceutical interventions on COVID-19 in Europe". In: *Nature* (2020). ISSN: 14764687. DOI: 10.1038/s41586-020-2405-7.
- [28] Y. Liu et al. "Aerodynamic analysis of SARS-CoV-2 in two Wuhan hospitals". In: *Nature* 86.21 (2020), p. 2020.03.08.982637. ISSN: 0028-0836. DOI: 10.1038/s41586-020-2271-3. URL: <http://www.nature.com/articles/s41586-020-2271-3>.

- [29] D. Chirizzi et al. "SARS-CoV-2 concentrations and virus-laden aerosol size distributions in outdoor air in north and south of Italy". In: *Environment International* 146 (2021), p. 106255. ISSN: 18736750. DOI: 10.1016/j.envint.2020.106255. URL: <https://doi.org/10.1016/j.envint.2020.106255>.
- [30] W. B. Harland. *The geology of Svalbard*. 1998, p. 521. ISBN: 1897799934.
- [31] O. Ingolfsson. "Outline of the geography and geology of Svalbard". In: (2000), p. 12.
- [32] M. Mazzola et al. "Atmospheric observations at the Amundsen-Nobile Climate Change Tower in Ny-Ålesund, Svalbard". In: *Rendiconti Lincei* 27.1 (2016), pp. 7–18. ISSN: 17200776. DOI: 10.1007/s12210-016-0540-8.
- [33] M. Maturilli, A. Herber, and G. König-langlo. "Surface Radiation Climatology for Ny-Ålesund, Svalbard (78.9° N), Basic Observations for Trend Detection Corresponding Author: short- and longwave radiation are operated since August 1992 in the frame of the Baseline since August 1993." In: *Theor Appl Climatol* 120 (2015), pp. 331–339. DOI: 10.1594/PANGAEA.150000..
- [34] J. Heintzenberg et al. "New particle formation in the Svalbard region 2006-2015". In: *Atmospheric Chemistry and Physics* 17.10 (2017), pp. 6153–6175. ISSN: 16807324. DOI: 10.5194/acp-17-6153-2017.
- [35] C. Turetta et al. "Water-soluble trace, rare earth elements and organic compounds in Arctic aerosol". In: *Rendiconti Lincei* 27 (2016), pp. 95–103. ISSN: 17200776. DOI: 10.1007/s12210-016-0518-6.
- [36] J. Heintzenberg. "Particle size distribution and optical properties of Arctic haze (Ny-Alesund, Svalbard)." In: *Tellus* 32.3 (1980), pp. 251–260. ISSN: 00402826. DOI: 10.3402/tellusa.v32i3.10580.
- [37] R. W. Fenn and H. K. Weickmann. "Some results of aerosol measurements". In: *Geofisica Pura e Applicata* 42.1 (1959), pp. 53–61. ISSN: 00334553. DOI: 10.1007/BF02113389.
- [38] Robert W Fenn. "Measurements of the concentration and size distribution of particles in the Arctic air of Greenland". In: *Journal of Geophysical Research* 65.10 (1960), pp. 3371–3376. ISSN: 0148-0227. DOI: 10.1029/jz065i010p03371.
- [39] Jozef M. Pacyna et al. "Long-range transport of trace elements to Ny Ålesund, Spitsbergen". In: *Atmospheric Environment* 19.6 (1985), pp. 857–865. ISSN: 00046981. DOI: 10.1016/0004-6981(85)90231-8.
- [40] M. Possanzini, V. Di Palo, and P. Masia. "Evaluation of a denuder method for ambient no2 measurements at ppb levels". In: *International Journal of Environmental Analytical Chemistry* 49.3 (1992), pp. 139–147. ISSN: 10290397. DOI: 10.1080/03067319208027565.
- [41] Trond Iversen and Einar Joranger. "Arctic air pollution and large scale atmospheric flows". In: *Atmospheric Environment (1967)* 19.12 (1985), pp. 2099–2108. ISSN: 00046981. DOI: 10.1016/0004-6981(85)90117-9.
- [42] M. Oehme and B. Ottar. "The long range transport of polychlorinated hydrocarbons to the Arctic". In: *Geophysical Research Letters* 11.11 (1984), pp. 1133–1136. ISSN: 19448007. DOI: 10.1029/GL011i011p01133.
- [43] Jozef M. Pacyna. "The origin of Arctic air pollutants: lessons learned and future research". In: *Science of the Total Environment* 160-161.C (1995), pp. 39–53. ISSN: 00489697. DOI: 10.1016/0048-9697(95)04343-Y.

- [44] Jianqiong Zhan et al. "Effects of ship emissions on summertime aerosols at Ny-Alesund in the Arctic". In: *Atmospheric Pollution Research* 5.3 (2014), pp. 500–510. ISSN: 13091042. DOI: 10.5094/APR.2014.059.
- [45] J. A. Fisher et al. "Sources, distribution, and acidity of sulfate-ammonium aerosol in the Arctic in winter-spring". In: *Atmospheric Environment* 45.39 (2011), pp. 7301–7318. ISSN: 13522310. DOI: 10.1016/j.atmosenv.2011.08.030. URL: <http://dx.doi.org/10.1016/j.atmosenv.2011.08.030>.
- [46] K. E. Yttri et al. "Quantifying black carbon from biomass burning by means of levoglucosan - A one-year time series at the Arctic observatory Zeppelin". In: *Atmospheric Chemistry and Physics* 14.12 (2014), pp. 6427–6442. ISSN: 16807324. DOI: 10.5194/acp-14-6427-2014.
- [47] A. Stohl et al. "Arctic smoke – record high air pollution levels in the European Arctic due to agricultural fires in Eastern Europe". In: *Atmospheric Chemistry and Physics Discussions* 6.5 (2006), pp. 9655–9722. ISSN: 1680-7324. DOI: 10.5194/acpd-6-9655-2006.
- [48] A. M.K. Hansen et al. "Organosulfates and organic acids in Arctic aerosols: Speciation, annual variation and concentration levels". In: *Atmospheric Chemistry and Physics* 14.15 (2014), pp. 7807–7823. ISSN: 16807324. DOI: 10.5194/acp-14-7807-2014.
- [49] David Cappelletti et al. "Environmental changes in the Arctic: an Italian perspective". In: *Rendiconti Lincei* 27.1 (2016), pp. 1–6. ISSN: 17200776. DOI: 10.1007/s12210-016-0555-1.
- [50] R. Zangrando et al. "Molecular markers of biomass burning in Arctic aerosols". In: *Environmental Science and Technology* 47.15 (2013), pp. 8565–8574. ISSN: 0013936X. DOI: 10.1021/es400125r.
- [51] F. Giardi et al. "Size distribution and ion composition of aerosol collected at Ny-Ålesund in the spring-summer field campaign 2013". In: *Rendiconti Lincei* 27 (2016), pp. 47–58. ISSN: 17200776. DOI: 10.1007/s12210-016-0529-3.
- [52] A. Bazzano et al. "Source assessment of atmospheric lead measured at Ny-Ålesund, Svalbard". In: *Atmospheric Environment* 113 (2015), pp. 20–26. ISSN: 18732844. DOI: 10.1016/j.atmosenv.2015.04.053.
- [53] Andrea Bazzano et al. "Elemental and lead isotopic composition of atmospheric particulate measured in the Arctic region (Ny-Ålesund, Svalbard Islands)". In: *Rendiconti Lincei* 27.1 (2016), pp. 73–84. ISSN: 17200776. DOI: 10.1007/s12210-016-0507-9.
- [54] R. Udisti et al. "Sulfate source apportionment in the Ny-Ålesund (Svalbard Islands) Arctic aerosol". In: *Rendiconti Lincei* 27 (2016), pp. 85–94. ISSN: 17200776. DOI: 10.1007/s12210-016-0517-7.
- [55] Silvia Becagli et al. "Biogenic Aerosol in the Arctic from Eight Years of MSA Data from Ny Ålesund (Svalbard Islands) and Thule (Greenland)". In: *atmosphere* 10.349 (2019), pp. 1–12.
- [56] E. Conca et al. "Source identification and temporal evolution of trace elements in PM10 collected near to Ny-Ålesund (Norwegian Arctic)". In: *Atmospheric Environment* 203.January (2019), pp. 153–165. ISSN: 18732844. DOI: 10.1016/j.atmosenv.2019.02.001. URL: <https://doi.org/10.1016/j.atmosenv.2019.02.001>.

- [57] C. Alves, C. Pio, and A. Duarte. "The organic composition of air particulate matter from rural and urban Portuguese areas". In: *Physics and Chemistry of the Earth, Part B: Hydrology, Oceans and Atmosphere* 24.6 (1999), pp. 705–709. ISSN: 14641909. DOI: 10.1016/S1464-1909(99)00069-6.
- [58] K. F. Boon, Lore Kiefert, and Grant H. Ctainsh. "Organic matter content of rural dusts in Australia". In: *Atmospheric Environment* 32.16 (1998), pp. 2817–2823. ISSN: 13522310. DOI: 10.1016/S1352-2310(97)00475-5.
- [59] L. M. Hildemann et al. "Contribution of primary aerosol emissions from vegetation-derived sources to fine particle concentrations in Los Angeles". In: *Journal of Geophysical Research Atmospheres* 101.14 (1996), pp. 19541–19549. ISSN: 01480227. DOI: 10.1029/95jd02136.
- [60] W. F. Rogge et al. "Quantification of urban organic aerosols at a molecular level: Identification, abundance and seasonal variation". In: *Atmospheric Environment Part A, General Topics* 27.8 (1993), pp. 1309–1330. ISSN: 09601686. DOI: 10.1016/0960-1686(93)90257-Y.
- [61] E. Barbaro et al. "Particle size distribution of inorganic and organic ions in coastal and inland Antarctic aerosol". In: *Environmental Science and Pollution Research* 24.3 (2017), pp. 2724–2733. ISSN: 16147499. DOI: 10.1007/s11356-016-8042-x. URL: <http://dx.doi.org/10.1007/s11356-016-8042-x>.
- [62] K. Hara et al. "Fractionation of inorganic nitrates in winter Arctic troposphere: Coarse aerosol particles containing inorganic nitrates". In: *Journal of Geophysical Research: Atmospheres* 104.D19 (1999), pp. 23671–23679. ISSN: 21698996. DOI: 10.1029/1998JD900348.
- [63] Patrice Nadeau, Dimitrios Berk, and Richard J. Munz. "Ammonium chloride aerosol nucleation and growth in a cross-flow impinging jet reactor". In: *Aerosol Science and Technology* 37.1 (2003), pp. 82–95. ISSN: 02786826. DOI: 10.1080/02786820300896.
- [64] R. A. Braun et al. "Impact of Wildfire Emissions on Chloride and Bromide Depletion in Marine Aerosol Particles". In: *Environmental Science and Technology* 51.16 (2017), pp. 9013–9021. ISSN: 15205851. DOI: 10.1021/acs.est.7b02039.
- [65] X. Tang et al. "Water-soluble organic carbon (WSOC) and its temperature-resolved carbon fractions in atmospheric aerosols in Beijing". In: *Atmospheric Research* 181 (2016), pp. 200–210. ISSN: 01698095. DOI: 10.1016/j.atmosres.2016.06.019. URL: <http://dx.doi.org/10.1016/j.atmosres.2016.06.019>.
- [66] M. Claeys et al. "Formation of Secondary Organic Aerosols Through Photooxidation of Isoprene". In: *Science* 303.5661 (2004), pp. 1173–1176. ISSN: 00368075. DOI: 10.1126/science.1092805.
- [67] K. Kawamura and F. Sakaguchi. "Molecular distributions of water soluble dicarboxylic acids in marine aerosols over the Pacific Ocean including tropics". In: *Journal of Geophysical Research* 104.D3 (1999), pp. 3501–3509.
- [68] V. Librando and G. Tringali. "Atmospheric fate of OH initiated oxidation of terpenes. Reaction mechanism of α -pinene degradation and secondary organic aerosol formation". In: *Journal of Environmental Management* 75.3 (2005), pp. 275–282. ISSN: 03014797. DOI: 10.1016/j.jenvman.2005.01.001.

- [69] M. Kanakidou et al. "Human-activity-enhanced formation of organic aerosols by biogenic hydrocarbon oxidation". In: *Journal of Geophysical Research* 105.D7 (2000), pp. 9243–9254. ISSN: 0148-0227. DOI: 10.1029/1999JD901148.
- [70] F. Fehsenfeld, J. Calvert, and R. Fall. "Emissions of volatile organic compounds from vegetation and the implications for atmospheric chemistry". In: *Global Biogeochemical Cycles* 6.4 (1992), pp. 389–430. URL: <http://www.agu.org/pubs/crossref/1992.../92GB02125.shtml>.
- [71] I. G. Kavouras, N. Mihalopoulos, and E.G. Stephanou. "Formation of atmospheric particles from organic acids produced by forests". In: *Nature* 372.3 (1998), pp. 683–686. ISSN: 0028-0836. DOI: 10.1038/27179. URL: <http://www.nature.com/nature/journal/v395/n6703/abs/395683a0.html>.
- [72] M. Feltracco et al. "Photo-oxidation products of α -pinene in coarse, fine and ultrafine aerosol: A new high sensitive HPLC-MS/MS method". In: *Atmospheric Environment* 180.March (2018), pp. 149–155. ISSN: 13522310. DOI: 10.1016/j.atmosenv.2018.02.052. URL: <http://linkinghub.elsevier.com/retrieve/pii/S1352231018301377>.
- [73] J. T. V. Matos, Regina M B O Duarte, and Armando C. Duarte. "Challenges in the identification and characterization of free amino acids and proteinaceous compounds in atmospheric aerosols: A critical review". In: *TrAC - Trends in Analytical Chemistry* 75 (2016), pp. 97–107. ISSN: 18793142. DOI: 10.1016/j.trac.2015.08.004. URL: <http://dx.doi.org/10.1016/j.trac.2015.08.004>.
- [74] M. Kuznetsova, C. Lee, and J. Aller. "Characterization of the proteinaceous matter in marine aerosols". In: *Marine Chemistry* 96 (2005), pp. 359–377. DOI: 10.1016/j.marchem.2005.03.007.
- [75] M. Feltracco et al. "Free and combined L- and D-amino acids in Arctic aerosol". In: *Chemosphere* 220 (2019), pp. 412–421. ISSN: 0045-6535. DOI: 10.1016/j.chemosphere.2018.12.147. URL: <https://doi.org/10.1016/j.chemosphere.2018.12.147>.
- [76] E. Barbaro et al. "D- and L-amino acids in Antarctic lakes: Assessment of a very sensitive HPLC-MS method". In: *Analytical and Bioanalytical Chemistry* 406.22 (2014), pp. 5259–5270. ISSN: 16182650. DOI: 10.1007/s00216-014-7961-y.
- [77] P. M. Medeiros et al. "Sugars as source indicators of biogenic organic carbon in aerosols collected above the Howland Experimental Forest, Maine". In: *Atmospheric Environment* 40.9 (2006), pp. 1694–1705. ISSN: 13522310. DOI: 10.1016/j.atmosenv.2005.11.001.
- [78] B. R. T. Simoneit et al. "Sugars - Dominant water-soluble organic compounds in soils and characterization as tracers in atmospheric particulate matter". In: *Environmental Science and Technology* 38.22 (2004), pp. 5939–5949. ISSN: 0013936X. DOI: 10.1021/es0403099.
- [79] B. R. T. Simoneit. *Biomass burning - A review of organic tracers for smoke from incomplete combustion*. Vol. 17. 3. 2002, pp. 129–162. ISBN: 5417372064. DOI: 10.1016/S0883-2927(01)00061-0.
- [80] E. Barbaro et al. "Sugars in Antarctic aerosol". In: *Atmospheric Environment* 118 (2015), pp. 135–144. ISSN: 18732844. DOI: 10.1016/j.atmosenv.2015.07.047. URL: <http://dx.doi.org/10.1016/j.atmosenv.2015.07.047>.

- [81] K. M. Shakya, Patrick Louchouart, and Robert J. Griffin. "Lignin-derived phenols in Houston aerosols: Implications for natural background sources". In: *Environmental Science and Technology* 45.19 (2011), pp. 8268–8275. ISSN: 0013936X. DOI: 10.1021/es201668y.
- [82] R. Tignat-Perrier et al. "Global airborne microbial communities controlled by surrounding landscapes and wind conditions". In: *Scientific Reports* 9.1 (2019), pp. 1–11. ISSN: 20452322. DOI: 10.1038/s41598-019-51073-4.
- [83] N. Lang-Yona et al. "Links between airborne microbiome, meteorology, and chemical composition in northwestern Turkey". In: *Science of the Total Environment* 725 (2020). ISSN: 18791026. DOI: 10.1016/j.scitotenv.2020.138227.
- [84] A. Dommergue et al. "Methods to Investigate the Global Atmospheric Microbiome". In: *Frontiers in Microbiology* 10.February (2019), pp. 1–12. ISSN: 1664-302X. DOI: 10.3389/fmicb.2019.00243. URL: <https://www.frontiersin.org/article/10.3389/fmicb.2019.00243/full>.
- [85] M. Feltracco et al. "Interannual variability of sugars in Arctic aerosol: Biomass burning and biogenic inputs". In: *Science of the Total Environment* 706 (2020), p. 136089. ISSN: 18791026. DOI: 10.1016/j.scitotenv.2019.136089. URL: <https://doi.org/10.1016/j.scitotenv.2019.136089>.
- [86] M. Feltracco et al. "Year-round measurements of size-segregated low molecular weight organic acids in Arctic aerosol". In: *Science of the Total Environment* (2021), p. 142954. ISSN: 0048-9697. DOI: 10.1016/j.scitotenv.2020.142954. URL: <https://doi.org/10.1016/j.scitotenv.2020.142954>.
- [87] H. Timonen et al. "Size distributions, sources and source areas of water-soluble organic carbon in urban background air". In: *Atmospheric Chemistry and Physics* 8.18 (2008), pp. 5635–5647. ISSN: 16807324. DOI: 10.5194/acp-8-5635-2008.
- [88] J. R. Laing et al. "Long-term particle measurements in Finnish Arctic: Part I - Chemical composition and trace metal solubility". In: *Atmospheric Environment* 88 (2014), pp. 275–284. ISSN: 18732844. DOI: 10.1016/j.atmosenv.2014.03.002. URL: <http://dx.doi.org/10.1016/j.atmosenv.2014.03.002>.
- [89] J. Zhao et al. "Characterization of water-soluble inorganic ions in size-segregated aerosols in coastal city, Xiamen". In: *Atmospheric Research* 99.3-4 (2011), pp. 546–562. ISSN: 01698095. DOI: 10.1016/j.atmosres.2010.12.017.
- [90] H. Wang and D. Shooter. "Water soluble ions of atmospheric aerosols in three New Zealand cities: Seasonal changes and sources". In: *Atmospheric Environment* 35.34 (2001), pp. 6031–6040. ISSN: 13522310. DOI: 10.1016/S1352-2310(01)00437-X.
- [91] S. Becagli et al. "Relationships linking primary production, sea ice melting, and biogenic aerosol in the Arctic". In: *Atmospheric Environment* 136 (2016), pp. 1–15. ISSN: 18732844. DOI: 10.1016/j.atmosenv.2016.04.002. URL: <http://dx.doi.org/10.1016/j.atmosenv.2016.04.002>.
- [92] H. Geng et al. "Single-particle characterization of summertime Arctic aerosols collected at Ny-Ålesund, Svalbard". In: *Environmental Science and Technology* 44.7 (2010), pp. 2348–2353. ISSN: 0013936X. DOI: 10.1021/es903268j.

- [93] K. Kawamura et al. "Size distributions of dicarboxylic acids and inorganic ions in atmospheric aerosols collected during polar sunrise in the Canadian high Arctic". In: *Journal of Geophysical Research Atmospheres* 112.10 (2007). ISSN: 01480227. DOI: 10.1029/2006JD008244.
- [94] A. Saiz-Lopez and C. S. Boxe. "A mechanism for biologically-induced iodine emissions from sea-ice". In: *Atmospheric Chemistry and Physics Discussions* 8.1 (2008), pp. 2953–2976. ISSN: 1680-7375. DOI: 10.5194/acpd-8-2953-2008.
- [95] A. Saiz-Lopez and Roland Von Glasow. "Reactive halogen chemistry in the troposphere". In: *Chemical Society Reviews* 41.19 (2012), pp. 6448–6472. ISSN: 03060012. DOI: 10.1039/c2cs35208g.
- [96] A. Saiz-Lopez et al. "Boundary layer halogens in coastal Antarctica". In: *Science* 317.5836 (2007), pp. 348–351. ISSN: 00368075. DOI: 10.1126/science.1141408.
- [97] J. W. Halfacre et al. "Temporal and spatial characteristics of ozone depletion events from measurements in the Arctic". In: *Atmospheric Chemistry and Physics* 14.10 (2014), pp. 4875–4894. ISSN: 16807324. DOI: 10.5194/acp-14-4875-2014.
- [98] A. Spolaor et al. "Diurnal cycle of iodine, bromine, and mercury concentrations in Svalbard surface snow". In: *Atmospheric Chemistry and Physics* 19.20 (2019), pp. 13325–13339. ISSN: 16807324. DOI: 10.5194/acp-19-13325-2019.
- [99] K. Kim et al. "Production of Molecular Iodine and Tri-iodide in the Frozen Solution of Iodide: Implication for Polar Atmosphere". In: *Environmental Science and Technology* 50.3 (2016), pp. 1280–1287. ISSN: 15205851. DOI: 10.1021/acs.est.5b05148.
- [100] A.R.W. Raso et al. "Active molecular iodine photochemistry in the Arctic". In: *Proceedings of the National Academy of Sciences of the United States of America* 114.38 (2017), pp. 10053–10058. ISSN: 10916490. DOI: 10.1073/pnas.1702803114.
- [101] P. K. Quinn et al. "Arctic haze: Current trends and knowledge gaps". In: *Tellus, Series B: Chemical and Physical Meteorology* 59.1 (2007), pp. 99–114. ISSN: 02806509. DOI: 10.1111/j.1600-0889.2006.00238.x.
- [102] J. Sciare et al. "Long-term measurements of carbonaceous aerosols in the Eastern Mediterranean: Evidence of long-range transport of biomass burning". In: *Atmospheric Chemistry and Physics* 8.18 (2008), pp. 5551–5563. ISSN: 16807324. DOI: 10.5194/acp-8-5551-2008.
- [103] N. Meskhidze and A. Nenes. "Phytoplankton and Cloudiness in the Southern Ocean". In: *Science* 314 (2016), pp. 1419–1423. DOI: 10.1007/s10162-016-0558-8.
- [104] W. C. Keene et al. "Sea-salt corrections and interpretation of constituent ratios in marine precipitation". In: *Journal of Geophysical Research* 91.D6 (1986), p. 6647. ISSN: 0148-0227. DOI: 10.1029/jd091id06p06647.
- [105] M. Legrand et al. "Boreal fire records in Northern Hemisphere ice cores: A review". In: *Climate of the Past* 12.10 (2016), pp. 2033–2059. ISSN: 18149332. DOI: 10.5194/cp-12-2033-2016.
- [106] C. D. O'Dowd et al. "Biogenically driven organic contribution to marine aerosol". In: *Nature* 431.7009 (2004), pp. 676–680. ISSN: 00280836. DOI: 10.1038/nature02959.

- [107] H. Zhuang et al. "Formation of nitrate and non-sea-salt sulfate on coarse particles". In: *Atmospheric Environment* 33.26 (1999), pp. 4223–4233. ISSN: 13522310. DOI: 10.1016/S1352-2310(99)00186-7.
- [108] H.M. ten Brink. "Reactive uptake of HNO₃ and H₂SO₄ in sea-salt (NaCl) particles". In: *Journal of Aerosol Science* 29 (1998), pp. 57–64.
- [109] P. De Caritat et al. "Chemical composition of arctic snow: Concentration levels and regional distribution of major elements". In: *Science of the Total Environment* 336.1-3 (2005), pp. 183–199. ISSN: 00489697. DOI: 10.1016/j.scitotenv.2004.05.031.
- [110] A. Spolaor et al. "Canadian arctic sea ice reconstructed from bromine in the Greenland NEEM ice core". In: *Scientific Reports* 6.May (2016), pp. 1–8. ISSN: 20452322. DOI: 10.1038/srep33925.
- [111] C. A. Cuevas et al. "Rapid increase in atmospheric iodine levels in the North Atlantic since the mid-20th century". In: *Nature Communications* 9.1 (2018), pp. 1–6. ISSN: 20411723. DOI: 10.1038/s41467-018-03756-1. URL: <http://dx.doi.org/10.1038/s41467-018-03756-1>.
- [112] C. Horvat et al. "The frequency and extent of sub-ice phytoplankton blooms in the Arctic Ocean". In: *Science Advances* 3.3 (2017). ISSN: 23752548. DOI: 10.1126/sciadv.1601191.
- [113] K. Kawamura and I. R. Kaplan. "Motor Exhaust Emissions as a Primary Source for Dicarboxylic Acids in Los Angeles Ambient Air". In: *Environmental Science and Technology* 21.1 (1987), pp. 105–110. ISSN: 15205851. DOI: 10.1021/es00155a014.
- [114] M. Narukawa et al. "Distribution of dicarboxylic acids and carbon isotopic compositions in aerosols from 1997 Indonesian forest fires". In: *Geophysical Research Letters* 26.20 (1999), pp. 3101–3104.
- [115] E. O. Edney et al. "Impact of aerosol liquid water on secondary organic aerosol yields of irradiated toluene/propylene/NO(x)/(NH₄)₂SO₄/air mixtures". In: *Atmospheric Environment* 34.23 (2000), pp. 3907–3919. ISSN: 13522310. DOI: 10.1016/S1352-2310(00)00174-6.
- [116] M. Kalberer et al. "Aerosol formation in the cyclohexene-ozone system". In: *Environmental Science and Technology* 34.23 (2000), pp. 4894–4901. ISSN: 0013936X. DOI: 10.1021/es001180f.
- [117] P. Fu et al. "Isoprene, Monoterpene, and Sesquiterpene Oxidation Products in the High Arctic Aerosols during Late Winter to Early Summer". In: *Environmental Science and Technology* 43.11 (2009), pp. 4022–4028. DOI: 10.1021/es803669a.
- [118] Y. Rudich, Neil M. Donahue, and Thomas F. Mentel. "Aging of Organic Aerosol: Bridging the Gap Between Laboratory and Field Studies". In: *Annual Review of Physical Chemistry* 58.1 (2007), pp. 321–352. ISSN: 0066-426X. DOI: 10.1146/annurev.physchem.58.032806.104432. URL: <http://www.annualreviews.org/doi/10.1146/annurev.physchem.58.032806.104432>.
- [119] P. Fu et al. "Seasonal variations of sugars in atmospheric particulate matter from Gosan, Jeju Island: Significant contributions of airborne pollen and Asian dust in spring". In: *Atmospheric Environment* 55 (2012), pp. 234–239. ISSN: 13522310. DOI: 10.1016/j.atmosenv.2012.02.061. URL: <http://dx.doi.org/10.1016/j.atmosenv.2012.02.061>.

- [120] K. E. Yttri, C Dye, and G Kiss. "Ambient aerosol concentrations of sugars and sugar-alcohols at four different sites in Norway". In: *Atmospheric Chemistry and Physics Discussions* 7.2 (2007), pp. 5769–5803. ISSN: 1680-7367, 1680-7367. DOI: 10.5194/acpd-7-5769-2007.
- [121] J. Chen et al. "Long-term observations of saccharides in remote marine aerosols from the western North Pacific: A comparison between 1990-1993 and 2006-2009 periods". In: *Atmospheric Environment* 67 (2013), pp. 448–458. ISSN: 13522310. DOI: 10.1016/j.atmosenv.2012.11.014. URL: <http://dx.doi.org/10.1016/j.atmosenv.2012.11.014>.
- [122] Man Nin Chan et al. "Hygroscopicity of water-soluble organic compounds in atmospheric aerosols: Amino acids and biomass burning derived organic species". In: *Environmental Science and Technology* 39.6 (2005), pp. 1555–1562. ISSN: 0013936X. DOI: 10.1021/es0495841.
- [123] D. R. Oros and B. R. T. Simoneit. "Identification and emission factors of molecular tracers in organic aerosols from biomass burning Part 2. Deciduous trees". In: 16 (2001).
- [124] D. R. Oros and B. R. T. Simoneit. *Identification and emission factors of molecular tracers in organic aerosols from biomass burning Part 1. Temperate climate conifers*. Vol. 16. 2001. ISBN: 5417372064.
- [125] D. R. Oros et al. "Identification and emission factors of molecular tracers in organic aerosols from biomass burning: Part 3. Grasses". In: *Applied Geochemistry* 21.6 (2006), pp. 919–940. ISSN: 08832927. DOI: 10.1016/j.apgeochem.2006.01.008.
- [126] I. Fattori et al. "Chemical composition and physical features of summer aerosol at Terra Nova Bay and Dome C, Antarctica". In: *Journal of Environmental Monitoring* 7.12 (2005), pp. 1265–1274. ISSN: 14640325. DOI: 10.1039/b507327h.
- [127] R. Zangrando et al. "Levoglucosan and phenols in Antarctic marine, coastal and plateau aerosols". In: *Science of the Total Environment* 544 (2016), pp. 606–616. ISSN: 18791026. DOI: 10.1016/j.scitotenv.2015.11.166. URL: <http://dx.doi.org/10.1016/j.scitotenv.2015.11.166>.
- [128] G. Wang et al. "Molecular composition and size distribution of sugars, sugar-alcohols and carboxylic acids in airborne particles during a severe urban haze event caused by wheat straw burning". In: *Atmospheric Environment* 45.15 (2011), pp. 2473–2479. ISSN: 13522310. DOI: 10.1016/j.atmosenv.2011.02.045. URL: <http://dx.doi.org/10.1016/j.atmosenv.2011.02.045>.
- [129] R. Zangrando et al. "Free phenolic compounds in waters of the Ross Sea". In: *Science of the Total Environment* 650 (2019), pp. 2117–2128. ISSN: 18791026. DOI: 10.1016/j.scitotenv.2018.09.360. URL: <https://doi.org/10.1016/j.scitotenv.2018.09.360>.
- [130] M. Rico et al. "Variability of the phenolic profile in the diatom *Phaeodactylum tricorutum* growing under copper and iron stress". In: *Limnology and Oceanography* 58.1 (2013), pp. 144–152. ISSN: 00243590. DOI: 10.4319/lo.2013.58.1.0144.
- [131] Rita Traversi et al. *Arctic haze in a climate changing world: the 2010-2020 trend (HAZECLIC)*. Jan. 2021. DOI: 10.5281/zenodo.4293826. URL: <https://doi.org/10.5281/zenodo.4293826>.

Appendix A

Journal author rights

I wish to express my appreciation at being granted permission from Elsevier to reproduce here the following articles.

Please note that, as first author of these Elsevier articles, I retain the right to include them in this thesis (not for commercial use). Elsevier apply this right to all authors who publish their article as either a subscription article or an open access article. In all cases Elsevier requires to include a full acknowledgement and, if appropriate, a link to the final published version hosted on Science Direct. Each article include the complete list of authors and the full bibliographic references.

References of each published article were not reported again in the bibliography of this thesis. For more information on this and on other retained rights, please visit *this page*.

Published and submitted papers

Here are reported the following articles:

- "Free and combined L- and D-amino acids in Arctic aerosol". Supplementary data to this article can be found online *here*
- "Interannual variability of sugars in Arctic aerosol: Biomass burning and biogenic inputs". Supplementary data to this article can be found online *here*
- "Year-round measurements of size-segregated low molecular weight organic acids in Arctic aerosol". Supplementary data to this article can be found online *here*
- "Airborne bacteria and particulate chemistry capture phytoplankton bloom dynamics in an Arctic Fjord" (*submitted*).



Free and combined L- and D-amino acids in Arctic aerosol

Matteo Feltracco^{a, b, *}, Elena Barbaro^b, Torben Kirchgeorg^a, Andrea Spolaor^b, Clara Turetta^b, Roberta Zangrando^b, Carlo Barbante^{a, b}, Andrea Gambaro^{a, b}

^a Department of Environmental Sciences, Informatics and Statistics, Ca' Foscari University of Venice, Via Torino 155, 30172, Venice, Italy

^b Institute for the Dynamics of Environmental Processes CNR, Via Torino 155, 30172, Venice, Italy

HIGHLIGHTS

- The article provides information about the presence of amino acids in the Arctic aerosol.
- The study identifies mainly the phytoplanktonic bloom and biomass burning as sources.
- For the first time free and combined L- and D-amino acids were studied in Arctic aerosol.

GRAPHICAL ABSTRACT



ARTICLE INFO

Article history:

Received 31 October 2018

Received in revised form

19 December 2018

Accepted 20 December 2018

Available online 21 December 2018

Handling Editor: R. Ebinghaus

Keywords:

Arctic

Bio aerosol

Amino acids

Algae bloom

Biomass burning

ABSTRACT

Aerosol samples were collected with a high-volume cascade impactor with a 10 day sampling frequency at the Gruvebadet observatory, close to Ny-Ålesund (Svalbard Islands). A total of 42 filters were analyzed for free and combined amino acids, as they are key components of bio-aerosol. This article provides the first investigation of free and combined L- and D-amino acids in Arctic atmospheric particulate matter. The main aim of this study was to determine how these compounds are distributed in size-segregated aerosols after short-range and long-range atmospheric transport and understand the possible sources of amino acids. The total load of free amino acids ranged from 2.0 to 10.8 pmol m⁻³, while combined amino acids ranged from 5.5 to 18.0 pmol m⁻³. At these levels amino compounds could play a role in the chemistry of cloud condensation nuclei and fine particles, for example by influencing their buffering capacity and basicity. Free and combined amino acids were mainly found in the fine aerosol fraction (<0.49 μm) and their concentrations could be affected by several sources, the most important of which were biological primary production and biomass burning.

© 2018 Elsevier Ltd. All rights reserved.

1. Introduction

Organic nitrogen compounds (ONCs) contribute to the nutrient budgets of ecosystems and influence atmospheric chemistry and

* Corresponding author. Ca' Foscari University of Venice, Via Torino 155, 30172, Venice, Italy.

E-mail address: matteo.feltracco@unive.it (M. Feltracco).

air quality (Cornell et al., 2001; McGregor and Anastasio, 2001; Weathers et al., 2000). The most investigated ONCs in the atmosphere are amino compounds (i.e. amino acids and alkyl amines) due to their potential roles in ecological processes and plant nutrition (Zhang and Anastasio, 2003). Amino compounds could affect the atmospheric water cycle since they are involved in cloud condensation nuclei and cloud formation due to their surface-active properties (Saxena, 1983), thus altering the atmospheric radiation balance and the scavenging of air pollutants (Chan et al.,

2005; McGregor and Anastasio, 2001).

Amino acids are usually separated into free amino acids (FAAs), combined amino acids (CAAs) and total amino acids (TAAs). CAAs is the difference between TAAs and FAAs. TAAs are particularly bioavailable (Chan et al., 2005; De Haan et al., 2009; Leck and Bigg, 1999; Mandalakis et al., 2011; Miguel et al., 1999; Mikhailov et al., 2003) and therefore may also contribute to the nitrogen and carbon budgets through atmospheric deposition (Cornell et al., 2001, 2003). Atmospheric deposition of amino acids can be also a source of nutrients to marine ecosystems (Wedyan and Preston, 2008). Most amino acids contain an asymmetric centre, and the analysis of their L- or D-enantiomers is often carried out in several research fields, such as food chemistry (Friedman, 1991), geochronology (Fitznar et al., 1999) and extraterrestrial exploration (Cronin and Pizzarello, 1999). A substantial number of studies have confirmed the presence of amino acids in urban and sub-urban aerosol (Barbaro et al., 2011; Chen and Hildemann, 2009; Di Filippo et al., 2014; Menetrez et al., 2009; Samy et al., 2013), rural aerosol (Mace et al., 2003a; Samy et al., 2011; Yang et al., 2004; Zhang and Anastasio, 2003) and marine aerosol (Mace et al., 2003b; Mandalakis et al., 2011; Matsumoto and Uematsu, 2005; Wedyan and Preston, 2008).

Amino acids are present as dissolved combined amino acids (proteins and peptides) (Ge et al., 2011; Kuznetsova et al., 2005), dissolved free amino acids (Milne and Zika, 1993; Mopper and Zika, 1987) and particulate amino acids from solid microorganisms and debris particles inside the liquid aerosol phase (Kuznetsova et al., 2005).

FAAs have been studied in both Arctic and the Antarctic aerosol. In Arctic aerosol sampled from the 19th April to 14th September 2010, amino acids were detected with a mean concentration of 1.1 pmol m^{-3} without any differentiation between L- and D- or combined amino acids (Scalabrin et al., 2012). In Antarctica, free amino acids have been investigated at the coastal site of Mario Zucchelli Station (MZS) where a mean concentration of 11 pmol m^{-3} was found, on the high plateau at Dome C an average concentration of 0.8 pmol m^{-3} was reported.

Due to their long distance from anthropogenic and continental emission sources, Polar Regions are excellent natural laboratories for conducting studies on the behavior, evolution and fate of biogenic aerosol.

CAAs derive from bacteria, fungi, house dust mites, multiple pollens, animal and fragments of animals, insects and plants (Di Filippo et al., 2014). In addition, proteinaceous matter is a major source of organic nitrogen in surface seawater. It is found as part of the dissolved organic matter of planktonic and bacterial origin and as particulate organic matter in microorganisms (Hansell and Carlson, 2014; Kuznetsova et al., 2005). Many proteins present in aerosol particles are strong allergens and there is an increasing concern on the contribution of proteinaceous materials on the allergenic influence of aerosols and their possible effects on human health.

The main aims of this study were 1) to investigate the occurrence and concentration levels of L- and D- FAAs and CAAs in atmospheric aerosol in Ny Ålesund (Svalbard Islands) during the 2015 spring campaign (4th April – 13th June); 2) to determine how these compounds are distributed in size-segregated aerosols; and 3) to investigate the possible emission sources. To confirm the amino acid sources, other specific tracers were also investigated. Levoglucosan was used as a biomass burning marker (Iinuma et al., 2007; Oros et al., 2006; Oros and Simoneit, 2001; Zangrando et al., 2013) while methanesulfonic acid (MSA) was used as an algal bloom marker (Quinn et al., 2007, 2002). Non-sea salt sulfate (nss-SO_4^{2-}) was used to distinguish between sources. The data acquired will provide an improved understanding of the fate FAAs

and CAAs in the Arctic area and should assist in foreseeing their role in atmospheric processes. To the best of our knowledge, we have determined for the first time free and combined L- and D-amino acids in Arctic aerosol.

2. Experimental

2.1. Aerosol sampling

Svalbard is Norway's northernmost region, and the archipelago is one of the northernmost land-areas in the world. The archipelago is confined between the West Spitsbergen Current and the northern-most remnant of the Gulf Stream, that moves relatively warm water northwards along the west coast while the East Spitsbergen Current brings cold water and sea ice southwestwards from east of the Spitsbergen and eastern islands (Harland, 1998). For these reasons, the Svalbard region is particularly interesting in regard to climate change because is located at the extreme northern limit of the ocean currents and air masses that transfer heat poleward through the North Atlantic.

Seven aerosol samples were collected from 4th April to 13th June 2015 at the Gruvebadet atmospheric laboratory, close to Ny-Ålesund (Svalbard Islands, $78^\circ 54' 59.99'' \text{ N } 11^\circ 55' 59.99'' \text{ E}$). A sampling resolution of 10 days was adopted, following the results and the protocols of previous campaigns (Scalabrin et al., 2012; Turetta et al., 2016). This sampling time is necessary to collect enough sample so we can determine and quantify molecular species at pico-molar atmospheric concentrations (Barbaro et al., 2017b, 2016, 2015b). The sampling campaign was performed using a five-stage high-volume cascade impactor Model TE-235 equipped with a TE-6070 PM_{10} size-selective head (Tisch Environmental Inc., Village of Cleves, OH) operating at a flow rate of $68 \text{ m}^3 \text{ h}^{-1}$. The aerosols were collected on slotted quartz fiber filters (QFF) with 10 parallel perforated slots (FilterLab, Spain) plus a back-up filter. The description of the slotted QFF is reported elsewhere (Turetta et al., 2016). This sampler allows the collection of airborne particles in five size classes with aerodynamic diameter ranges of $10\text{--}7.2 \mu\text{m}$ (S1), $7.2\text{--}3.0 \mu\text{m}$ (S2), $3.0\text{--}1.5 \mu\text{m}$ (S3), $1.5\text{--}0.95 \mu\text{m}$ (S4), $0.95\text{--}0.49 \mu\text{m}$ (S5) and $<0.49 \mu\text{m}$ (B).

2.2. Aerosol samples processing for FAAs analysis

Reagents and standards solutions used in this study are reported in the [Supplementary Material](#). The description of the sampling area, sample collection and treatment are reported in three previous studies (Scalabrin et al., 2012; Turetta et al., 2016; Zangrando et al., 2013). Briefly, each half filter was spiked with a mixed solution of 8 labelled FAAs (reagents and standards solutions see [Supplementary Material](#)) as an internal standard (500 absolute ng for slotted filters and 1500 absolute ng for back-up filters) and were then extracted twice for 15 min with ultrapure water in an ultrasonic bath. The slotted filters were extracted with 9 mL followed by 1 mL of ultrapure water, whilst the back-up filters were extracted with 25 mL followed by 5 mL of ultrapure water. The unified extracts were then filtered through a $0.45 \mu\text{m}$, $\varnothing 25 \text{ mm}$ polytetrafluoroethylene (PTFE) filter (Whatman, Maidstone, Kent, UK) before analysis. To avoid any contamination from laboratory air particles, samples were handled inside an ISO 5 clean room under a laminar flow bench (class 100). Field blank filters were also taken and treated using the same procedure. All reported values are blank-corrected. The method detection limits (MDL) and method quantification limits (MQL) of the analytical procedure were determined as three and ten times the standard deviation of the average value of the field blank.

2.3. CAAs analysis

A hydrolysis step is necessary to release FAAs from proteinaceous material or other polypeptides contained in the aqueous extracts obtained during sample processing (Section 2.2). In a 1.5 mL vial, 500 μ L of each sample extract was mixed with 500 μ L of 12 M HCl and 5 μ L of ascorbic acid at a concentration of 1 ng μ L⁻¹ (5 ng absolute) to avoid oxidation of the amino acids. The vial was flushed with a stream of nitrogen before sealing and placed in a heat-block at 110 °C for 24 h (Fountoulakis and Lahm, 1998; Matos et al., 2016; Wedyan and Preston, 2008) with a Liebig prototype glass condenser used to condense compounds in the vapor (gas) phase back down to the liquid phase under boiling conditions through heat exchange with the environment (Fig. S1 – Supplementary Material shows the Liebig prototypes placed in the heat-block). The hydrolysis products were freeze-dried to eliminate traces of HCl, which can damage the chromatographic column. The dry residues were subsequently dissolved in 500 μ L of ultrapure water and diluted 1:10 before analysis for TAAs. The extracts of the field blank filters were also hydrolyzed so all TAA concentrations could be blank corrected. The concentrations of the CAAs were calculated as the difference between the TAA and FAA concentrations.

2.4. Instrumental analysis

The instrumental method for the determination of L- and D-amino acids applied in this study was previously described in detail by Barbaro et al. (2015a,b). Briefly, an Agilent 1100 Series HPLC System (Waldbronn, Germany) equipped with a binary pump, vacuum degasser, and autosampler was coupled to an API 4000 Triple Quadrupole Mass Spectrometer (Applied Biosystem/MDS SCIEX, Concord, Ontario, Canada) through a positive electrospray ion source (TurboV). Chromatographic separation was performed using a 2.1 \times 250 mm Astec CHIROBIOTIC™ TAG column (Advanced Separation Technologies Inc., USA) with a chiral stationary phase based on teicoplanin aglycone. The column temperature was maintained at 25 °C, and flow rate was 150 μ L min⁻¹. Elution was achieved by a linear gradient using as mobile phase 0.1% formic acid (A) and methanol containing 0.1% formic acid (B). At the beginning, an isocratic step with 30% eluent B was used for 10 min. The linear gradient started with 30% eluent B and reached 100% over 2 min. To wash the column, 100% of eluent B was maintained for 5 min, a followed by final equilibration step of 12 min, the time necessary to wash and equilibrate the column. The total run time was 30 min. The injection volume was 10 μ L for Ala, Asp, Glu, Gln, Leu, Ile, Met, Val, Asn and Gly due to their relatively high concentration in the aerosol samples, while others amino acids were injected with a volume of 100 μ L to enhance the quantification limit. The mass spectrometer operated in multiple reaction monitoring (MRM) mode. Two transitions were considered for each analyte: the most intense one was applied for quantification, while the second was used to confirm the presence of amino acids.

2.5. Levoglucosan, MSA and nss-SO₄²⁻

Levoglucosan, methanesulfonate (MSA) and non-sea salt sulfate (nss-SO₄²⁻) were used as specific markers for biomass burning, and phytoplankton blooms and were used in comparison with the concentration of FAAs to confirm potential emission sources. Determination and quantification of these compounds were performed using an ion chromatograph (Thermo Scientific™ Dionex™ ICS-5000, Waltham, US) coupled to a single quadrupole mass spectrometer (MSQ Plus™, Thermo Scientific™, Bremen, Germany). The analytical performance of the methods was described

by Barbaro et al. (2017a, 2015a). Briefly, the separation of levoglucosan was performed using a CarboPac MA1™ analytical column (Thermo Scientific, 2 mm \times 250 mm) equipped with an AminoTrap column (2 \times 50 mm). The sodium hydroxide eluent gradient at a flow rate of 0.25 mL min⁻¹ was as follows: 20 mM (0–23 min), 100 mM (23–43 min, column cleaning), 20 mM (43–53 min, equilibration). The injection volume was 50 μ L and the determination of levoglucosan was performed in selected ion monitoring (SIM) using 161 as mass to charge ratio for [M-H]⁻. Quantification was performed using labelled ¹³C₆-levoglucosan as the internal standard.

MSA and nss-SO₄²⁻ determination and quantification were achieved using an anionic exchange column (Dionex Ion Pac AS11 2 \times 250 mm) and a guard column (Dionex Ion Pac AG11 2 \times 50 mm). The sodium hydroxide gradient at a flow rate of 0.25 mL min⁻¹ was as follows: 0–3.5 min gradient from 0.5 to 5 mM; 3.5–5 min gradient from 5 to 10 mM; 5–25 min gradient from 10 to 38 mM; 25–30 min, column cleaning with 38 mM; 30–35 min; equilibration at 0.5 mM. The injection volume was 100 μ L. Mass to charge ratios of [M-H]⁻ used for SIM determination were 95 and 97 for MSA and sulfate, respectively. Quantification was achieved using an external calibration curve. The nss-SO₄²⁻ fraction was evaluated as the difference between the sulfate concentration and the sea salt contribution, that was calculated using the SO₄²⁻ to Na⁺ ratio in seawater (0.253).

2.6. Quality control

The analytical procedure for FAAs was previously validated (Barbaro et al., 2015b) by calculating the trueness, repeatability and efficiency (yield %) of the sample treatment process as described by Bliessner (2006). The average yield for each amino acid was 61%, all L- and D-amino acids determined in this work were found to have an analytical error ranging from -13% to +9%. The repeatability was determined as the relative standard deviation of the analytical results for 5 spiked filters and was always below 10%.

To check the hydrolysis efficiency during the quantification of CAAs, the procedure was validated by calculating trueness, precision and recovery for the analysis of 210 ng of Human Serum Albumin (HSA) after internal standardization with 200 ng of each isotopically labelled amino acid. To calculate the concentration of hydrolyzed FAAs from HSA, the amino acid sequence of human serum albumin reported by Meloun et al. (1975) was used. The molecule of this protein consists of a single polypeptide chain and contains 585 amino acid residues: 62 Ala, 24 Arg, 53 Asp, 35 Cys, 82 Glu, 12 Gly, 16 Hys, 61 Leu, 8 Ile, 59 Lys, 6 Met, 31 Phe, 24 Pro, 24 Ser, 28 Thr, 1 Trp, 18 Tyr, 41 Val. The molecular weight of the protein calculated from its amino acid composition is 66500 amu. Quantification was carried out using response factors between the target substances and their corresponding internal standard to correct instrumental signal fluctuations. Trueness, precision and recovery have been also calculated for FAAs by performing the hydrolysis technique achieved with CAAs procedure to consider the FAAs racemization that could be possible at 110 °C for 24 h. In fact, Kaiser and Benner (2005) showed how it is possible to use hydrolysis conditions that avoid a wide range of stereochemical inversions of amino acids, with the production of substantial amounts of D-enantiomers from the corresponding L-enantiomers during the hydrolysis process. Furthermore, it is known that racemization of FAAs was substantially lower during liquid-phase hydrolysis compared to microwave vapor-phase hydrolysis (Csapó et al., 1998; Liardon et al., 1981; Manning, 1990). To evaluate the extraction yield and to estimate the procedural extraction efficiency, the isotopically labelled amino acids were added after PTFE filtration. Table 1 shows the validation values just described for FAAs and

Table 1
Average errors (%) and CV%, recovery (%) and CV%, blank (ng) and CV% for FAAs and CAAs hydrolysis.

Analyte	IS	FAAs			CAAs		
		Error%; (CV%)	Recovery%; (CV%)	Blank (ng)	Error%; (CV%)	Recovery%; (CV%)	Blank (ng)
L-Ala	Ala*	−2 (8)	107; (8)	0.63	1; (2)	92; (7)	0.50
D-Ala	Ala*	4 (7)	105; (4)	0.06	−	−	0.02
L-Arg	Arg*	4; (3)	100; (6)	2.13	−9; (3)	91; (3)	0.68
D-Arg	Arg*	−6 (5)	106; (8)	0.01	−	−	0.01
L-Asp/L-Asn	Asp*	−7; (3)	105; (9)	3.13	3; (2)	95; (6)	0.89
D-Asp/D-Asn	Asp*	−2.; (5)	104; (3)	0.88	−	−	0.83
L-Glu/L-Gln	Glu*	−3.; (6)	106; (5)	7.11	−9; (2)	98; (3)	1.28
Gly	Ala*	5; (2)	104; (1)	0.51	6; (5)	106; (4)	0.02
L-Hyp	Pro*	7; (2)	98; (5)	0.42	−	−	1.03
D-Hyp	Pro*	6; (0)	99; (1)	0.01	−	−	0.01
L/D-Hys	Arg*	10; (3)	98; (5)	1.79	7; (0)	100; (3)	0.24
L-Leu/Ile	Leu*	−3; (2)	93; (5)	8.56	−6; (1)	91; (2)	0.99
D-Leu/Ile	Leu*	9; (2)	104; (8)	0.08	−	−	0.01
L/D-Orn	Arg*	10; (2)	105; (9)	3.31	−	−	0.15
L-Phe	Phe*	7; (7)	100; (5)	2.03	−8; (3)	90; (4)	0.65
D-Phe	Phe*	8; (4)	100; (4)	0.13	−	−	0.05
L-Pro	Pro*	8; (2)	100; (6)	0.64	9; (1)	105; (9)	0.63
L/D-Ser	Arg*	4; (8)	94; (9)	2.73	9; (8)	107; (2)	1.02
L-Thr	Arg*	7; (1)	97; (6)	1.19	7; (10)	104; (4)	0.26
D-Thr	Arg*	8; (4)	99; (2)	0.15	−	−	0.03
L-Val	Val*	1; (3)	94; (4)	2.95	−10; (3)	90; (8)	0.73
D-Val	Val*	10; (1)	103; (5)	0.04	−	−	0.01

hydrolyzed FAAs from HSA. The precision was evaluated and values of coefficient-of-variation% (CV%) were always below 10%. The mean recovery (%) of the procedure was equal to 100% and the error % was always below $\pm 10\%$ for each amino acid. In accordance with the literature values, D-Glu, L-/D-Met, L-/D-Trp and L-/D-Tyr are not shown in Table 1 due to the insufficient validation values. D-Glu and L-Asp peaks were covered by huge instrumental interferences, which made peak integration impossible. It is also well known that L-/D-Met has a half-life of less than 2.5 h in atmosphere since it is destroyed by ozone (McGregor and Anastasio, 2001) and the hydrolysis conditions may have accelerated this degradation process. L-/D-Trp and L-/D-Tyr are almost completely decomposed in our hydrolysis method (Csapó et al., 1997, 1995).

2.7. Back trajectory calculation and statistical methods

24 h back trajectories (BT), with a new trajectory starting every 3 h, were calculated at 100 m a.s.l. to evaluate the contribution of short-range transport, while 120 h back trajectories were calculated every 6 h at 500 m a.s.l. to evaluate the long-range transport, which corresponds to the elevation of the Zeppelin Mountain, the highest neighboring mountain to the sampling site (Fig. S2a and 2b – Supplementary Material). The NOAA HYSPLIT trajectory model from the NOAA ARL was applied, using the GDAS one-degree meteorological database (<https://www.ready.noaa.gov/archives.php>). Five runs were computed for every sampling day and the trajectories were “mean-clustered aggregated”, considering the total spatial variance. The BTs were overlapped with the oceanic chlorophyll-a concentrations from the Moderate Resolution Imaging Spectroradiometer (MODIS - NASA). The MODIS chlorophyll-a data product provides an estimate of the near-surface concentration of chlorophyll-a using an empirical relationship derived from in-situ measurements of chlorophyll-a and remote sensing reflectance (Rrs) in the blue-to-green region of the visible spectrum.

For statistical analysis, the concentration values below the limit of detection (LOD) were substituted with a value of 1/2 MDL. Factor analysis (FCA) with varimax rotation was performed on the auto scaled data matrix using Statistica 10.0 (StatSoft, Inc., 2007).

3. Results and discussion

3.1. FAAs concentration and particle size distribution

The total mean concentration of FAAs in PM₁₀ (calculated as the sum of all the stages) was 6.1 ± 3.4 pmol m^{−3} and ranged from 2.0 to 10.8 pmol m^{−3}. Samples collected during the first two periods have the highest concentrations, with total FAAs concentrations twice as high as those collected from 24th April – 13th June (Fig. 1). The mean value of the total dataset is almost six times higher than those obtained during the 2010 sampling campaign (Scalabrin et al., 2012; Turetta et al., 2016) at the same sampling site of Gruebadet (mean value of 1.1 pmol m^{−3}). The concentrations found in this campaign were comparable with the values determined by Barbaro et al. (2015b) at the coastal Mario Zucchelli Station, Antarctica, with a total mean of FAAs of 11 pmol m^{−3}. Those results showed how marine sources and their chemical composition can radically alter the amino acids concentration in atmosphere. In general, the highest amino acid concentrations were detected in the back-up filters (<0.49 μm) and in the S5 (0.95–0.49 μm), accounting for 37% and 31% of the total sum of FAAs (Fig. 2 - FAAs), respectively.

Gly (59%, average concentration of 3.6 ± 0.7 pmol m^{−3}), D-Ala (10%, 0.6 ± 0.2 pmol m^{−3}) and D-Asp (9%, 0.5 ± 0.2 pmol m^{−3}) together accounted for 78% of the total amino acid content (Fig. 3, FAAs). These compounds were mainly distributed below 0.95 μm (Fig. S3a). The particle size distribution of Gly is consistent with previous studies (Matsumoto and Uematsu, 2005; Scalabrin et al., 2012; Turetta et al., 2016; Zhang and Anastasio, 2003). Gly was suggested as an indicator of long-range atmospheric transport (Barbaro et al., 2015b, 2011; Milne and Zika, 1993) because it is the most stable FAA with a half-life of 19 days (McGregor and Anastasio, 2001).

The relative abundance of D-Ala and D-Asp agree with Wedyan and Preston (2008), where these compounds had the greatest relative contribution of D-FAAs in Atlantic Ocean aerosol. D-Asp is characteristic of soil humic substances: Kimber et al. (1990) and Dittmar et al. (2001) show that it is the most abundant D-FAAs in Russian Arctic river water.

The FAAs L-Ala (4%), L-Hyp (3%) and L-/D-Ser (3%) had individual

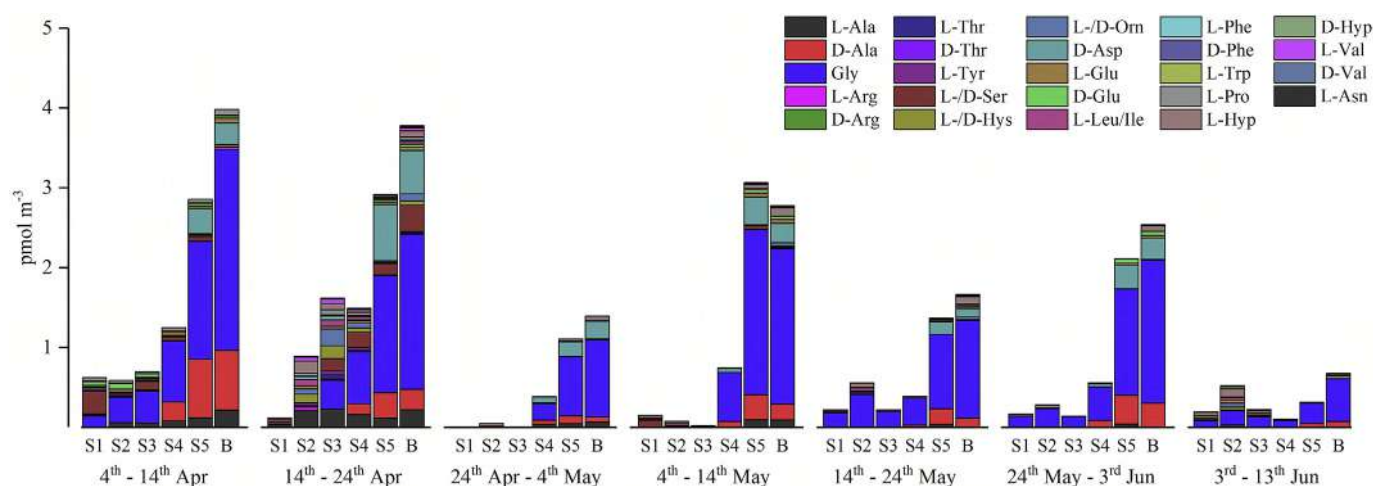


Fig. 1. FAAs concentration and distribution in the six stages for each sampling period.

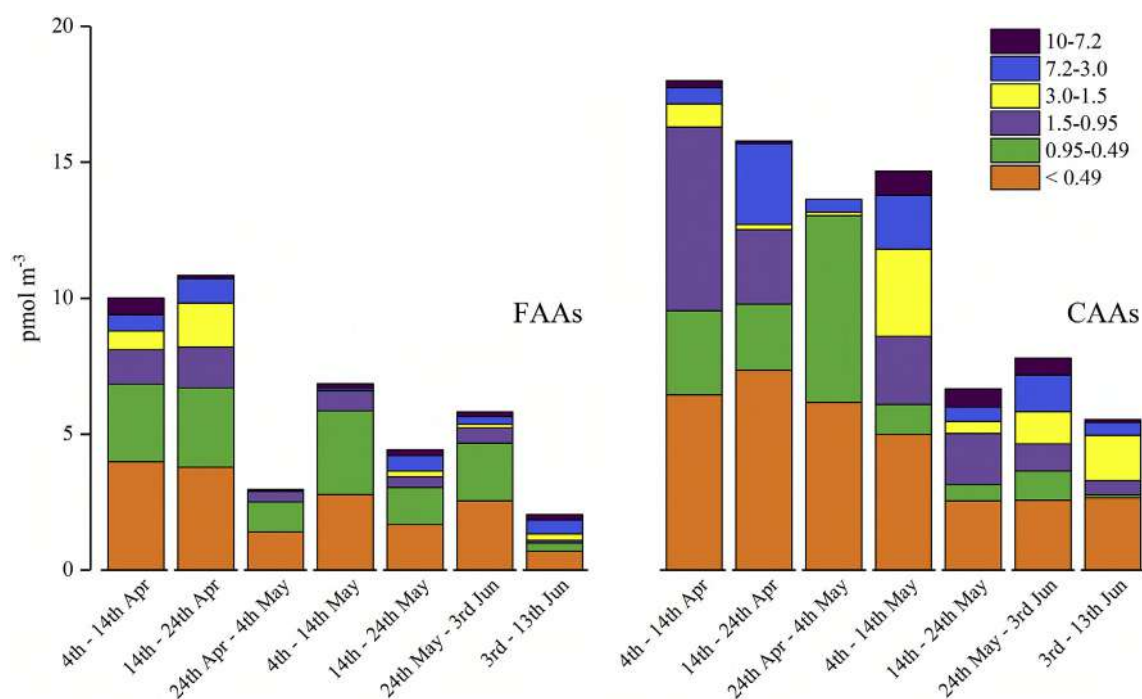


Fig. 2. FAAs and CAAs size distributions in the six stages.

concentrations of around 0.3 pmol m^{-3} . L-Ala and D-Ala are mainly found in fine particles, but L-Ala is strongly enriched in the coarse particles in the second sampling period (Fig. S3a). A possible explanation for this enrichment may be local sea-spray emissions due to wind speeds of up to 13 m s^{-1} . The occurrence of L-Ala in sea water is due to its synthesis by the enzyme aspartate decarboxylase used in the metabolic processes of prokaryote diatoms (Bromke, 2013; Park et al., 2018).

L- and D-Ser represent only 3% of the total FAAs load and has an average concentration of $0.1 \pm 0.2 \text{ pmol m}^{-3}$. It is only present in three samples and its size distribution is very variable (Fig. S3a). Ser could derive from oxidative reactions that transform CAAs and other potential FAA precursors into Ser (Samy et al., 2013). L-Hyp, as well as Ser, has a variable distribution but is present from 14th April to the end of sampling campaign. The remaining compounds (L-Arg, L-Thr, D-Thr, L-Tyr, D-Phe, L-Trp, L-Hyp, D-Val and L-Asn)

represent 12%.

The first sampling period from 4th to 14th April 2015 showed the second highest concentrations of the whole sampling period, with a mean value of $10.0 \pm 0.6 \text{ pmol m}^{-3}$. Several sources were investigated but the most plausible is biomass burning. Some researchers (Chan et al., 2005; Mace et al., 2003a) have reported the combustion of biomass as a possible source of FAAs because they are part of the WSOC fraction. The BT shown in Fig. S2a originate from areas neighboring Siberia and Northern Russia, suggesting that the FAAs load in this sample might originate from a biomass burning event. In effect, a series of wildfires began on the 12th April and were completely extinguished on the 13th April (see: firms-modaps.eosdis.nasa.gov/map). One of the most important biomass burning tracers, levoglucosan (Iinuma et al., 2007; Oros et al., 2006; Oros and Simoneit, 2001), was used to support our hypothesis. Fig. 4 shows how levoglucosan had the highest concentration

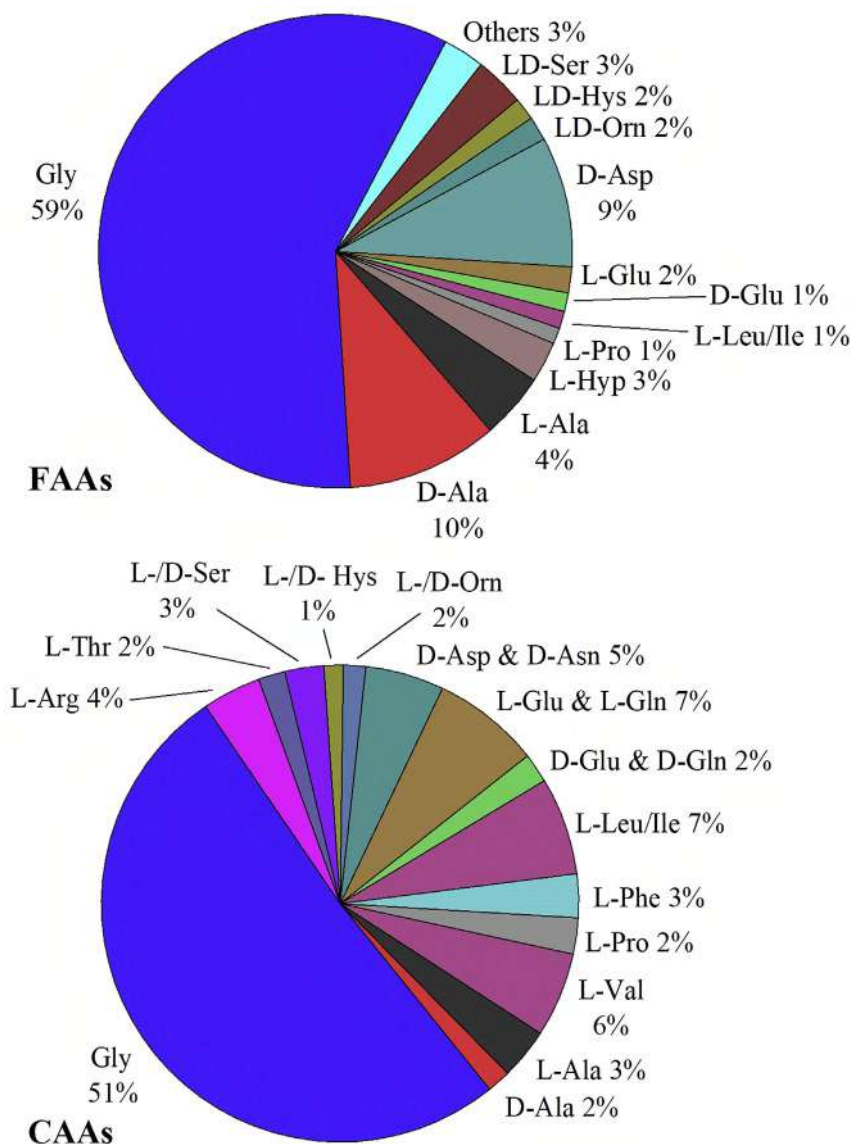


Fig. 3. Mean relative abundances of FAAs and CAAs in all samples. "Others" in FAAs pie referred to L-Arg, L-Thr, D-Thr, L-Tyr, D-Phe, L-Trp, L-Hyp, D-Val and L-Asn.

values in the first and second samples, supporting that it was released from the Northern Russian wildfires. Another possible tracer of biomass burning is nss-SO_4^{2-} because it has likely a combustion source (Quinn et al., 2007; Sciare et al., 2008) as well as resulting from emissions from phytoplanktonic blooms (Meskhidze and Nenes, 2016; Müller et al., 2009; Vignati et al., 2010; Yoon et al., 2007). In our samples, nss-SO_4^{2-} showed the highest concentrations in the first sampling period similar to levoglucosan and further reinforces the confirmation of a biomass burning source. Levoglucosan and nss-SO_4^{2-} , are considered long-range atmospheric transport tracers, are were distributed mainly in the fine fraction ($<0.49 \mu\text{m}$), together with the FAAs.

In the first sample, FAAs were also distributed in the coarse particles, suggesting local sources or a particle growth process during long-range transport. Due to their hygroscopicity (Chan et al., 2005), amino acids and proteinaceous material can potentially affect the hygroscopic growth and cloud formation activity of aerosols (Mandalakis et al., 2010).

The highest FAAs concentration was observed in the second sampling period, from 14th to 24th April, with a total concentration

$10.8 \pm 0.5 \text{ pmol m}^{-3}$. The elevated load of FAAs in this period may originate from phytoplanktonic/bacterial rich sea spray (Matsumoto and Uematsu, 2005), in this period, the BT changed direction towards the Greenland Sea and coincided with a large decrease in levoglucosan. Fig. 4 reports also the MSA concentration, considered a reliable marker of phytoplanktonic emissions and derives from the photolysis of DMS (Quinn et al., 2007, 2002), its value increased from 60.9 to $154.0 \text{ pmol m}^{-3}$ between the first and second sample. The samples collected after 24th April show a positive correlation between FAAs and MSA ($R^2 = 0.84$, p-value 0.02) and nss-SO_4^{2-} ($R^2 = 0.49$, and 0.30). For the period after 4th May, R^2 changes to 0.82 and 0.99 (p-value 0.09 and 0.0005) for MSA and nss-SO_4^{2-} , respectively. These values suggest an algae bloom input of FAAs from the 24th April to 13th June, supported by 24 h BT calculated at 100 m a.s.l. (Fig. S2b) which always originate from a marine area of either the Greenland Sea (West), Barents Sea (East) or Arctic Sea (North). Park et al. (2018) recorded and analyzed the atmospheric dimethyl sulfide (DMS) in Ny Ålesund during phytoplankton bloom periods in 2015. DMS is mostly produced by marine phytoplankton and is the most abundant form of biogenic

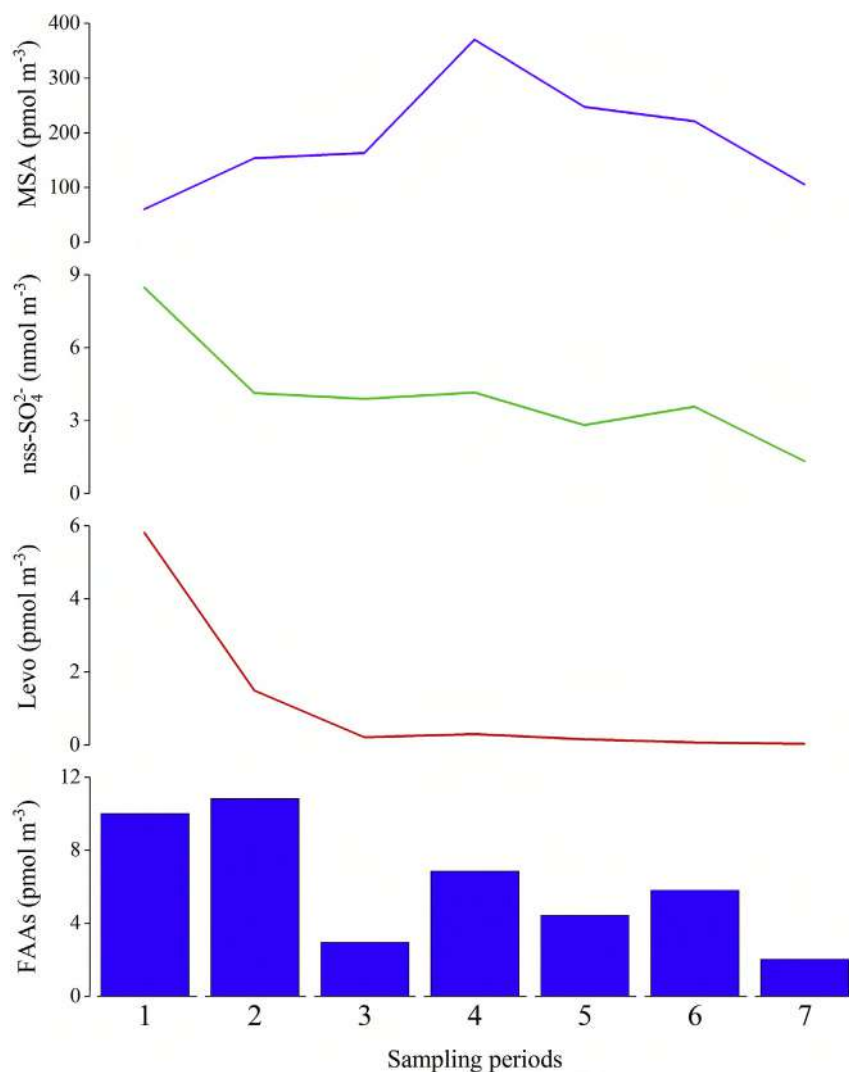


Fig. 4. Trend concentration comparison between FAAs, levoglucosan, nss-SO_4^{2-} and MSA.

sulfur released from the sea (Stefels et al., 2007). This study observed a concentration enhance of DMS from 14th to 20th April (the higher value was about $0.3 \mu\text{g L}^{-1}$).

Park et al. (2018) also reported strong emissions of DMS during May due to the typical of the late spring and summer phytoplankton blooms, suggesting algae bloom as a possible source for FAAs from 24th April to 13th June. To support this hypothesis, the correlation between PM_{10} FAAs, MSA and nss-SO_4^{2-} was investigated and described above.

3.2. CAAs concentrations and particle-size distribution

The mean concentration of CAAs in PM_{10} (as a sum of all stages) was $11.7 \pm 5.0 \text{ pmol m}^{-3}$ and ranged from 5.5 to 18.0 pmol m^{-3} (Fig. 5). The concentrations are around 2 times higher than those of FAAs in the same samples. This is the first reported occurrence of CAAs in the Arctic area. Previous studies reported mean concentrations of $719 \pm 326 \text{ pmol m}^{-3}$ in the eastern Mediterranean (Mandalakis et al., 2011) and $2050 \pm 730 \text{ pmol m}^{-3}$ in Northern California (Zhang and Anastasio, 2003). The lower concentrations of CAAs in Arctic aerosol suggest why the Arctic is a key-area for their study, because the concentrations are not heavily affected by local emissions from forests, house dust mites, insects, etc.

The highest combined amino acid concentrations were detected in the back-up filters ($<0.49 \mu\text{m}$), S5 ($0.95\text{--}0.49 \mu\text{m}$) and S4 ($1.5\text{--}0.95 \mu\text{m}$) accounting for 40%, 19% and 18% of the total sum of CAAs (Fig. 2), respectively.

Combined Gly, L-Leu/Ile, L-Glu & L-Gln, L-Arg and D-Asp & D-Asn accounted for 74% of the total CAAs content (Fig. 3, CAAs). L-/D-Ser and L-Val consisted of up to 10% of the total CAAs concentration. Gly is the most abundant CAA (51%) and has an average concentration of $6.0 \pm 1.1 \text{ pmol m}^{-3}$, about three times higher than total FAAs. Gly is the most abundant compound accounting for approximately one third of the total of CAAs as it plays a central role in the molecular structure of collagen, and Gly accounts for one third of the sequence (Lodish et al., 2008). The relative abundance of Gly is in accordance with previous studies on marine aerosol over the Eastern Mediterranean and urban aerosol in Beijing, China (Mandalakis et al., 2011; Ren et al., 2018). There is a strong difference between the occurrence of proteinaceous Gly and free Gly: combined Gly is found also in the coarse fraction (Fig. S3b), while free Gly is found in aerosol below $1.5 \mu\text{m}$. Other sources of proteinaceous material of Gly in aerosol may be marine bacteria for coarse particles (Kuznetsova et al., 2005) and viruses for fine particles (Matos et al., 2016).

Another relevant CAA in terms of its relative abundance is L-Leu/

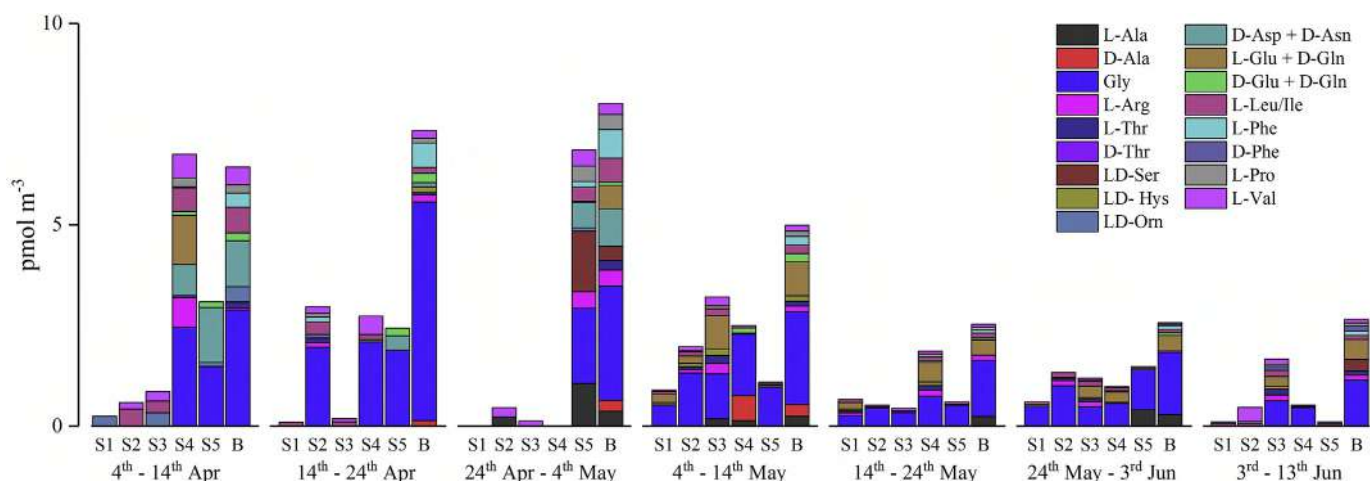


Fig. 5. CAAs concentrations and distribution in the six stages for each sampling period.

Ile (7%), with an average concentration of $0.8 \pm 0.1 \text{ pmol m}^{-3}$. The concentration of combined L-Leu/Ile is almost 10 times higher than free L-Leu/Ile. Fig. S3b shows that L-Leu/Ile is mainly distributed in the coarse fraction but was rarely quantifiable. The strong enrichment in terms of concentration between free and combined L-Leu/Ile was also found by Mandalakis et al. (2010) at a coastal site 70 km east of Heraklion (Crete, Greece) where an enrichment factor of 12 was reported.

L-Glu and L-Gln account for 7% with an average concentration of $1.3 \pm 0.3 \text{ pmol m}^{-3}$. Glu and Gln were quantified together, because Gln was transformed in Glu during hydrolysis.

L-Arg accounts for 5% of the total, with an average concentration of $0.5 \pm 0.1 \text{ pmol m}^{-3}$, its distribution is extremely variable throughout the sampling period. Proteinaceous Arg was the main CAA in aerosol samples from rural areas in Germany and Virginia (USA) (Gorzelska et al., 1992; Scheller, 2001) in concomitance with precipitation, though no correlation was found between combined Arg and precipitation during the sampling period.

The sum of D-Asp and D-Asn account for 4% of the total, with an average concentration of $0.6 \pm 0.3 \text{ pmol m}^{-3}$. These two CAAs were determined together due to the transformation of Asn into Asp during the hydrolysis process. Combined D-Asp and D-Asn were found only in particles with a diameter above $1.5 \mu\text{m}$ and were detected only from 4th April to 4th May.

L-/D-Ser represent 5% of the CAAs, with an average concentration of $0.9 \pm 0.5 \text{ pmol m}^{-3}$. This CAA is found only in fine particles ($<0.95 \mu\text{m}$), indicating that it may originate from long range atmospheric transport. No clear tendencies can be detected with the other CAAs.

The highest CAA concentrations were observed from 4th April to 14th May, but no relationships were found with levoglucosan, MSA or nss-SO_4^{2-} . It may be possible that the negative trend of CAAs during the sampling period was caused by an increase in photochemical reactions because proteins and peptides are decomposed by UV radiation and photooxidant agents to give a complex series of simpler products (Milne and Zika, 1993; Mopper and Zika, 1987). The Fig. S4a shows the temporal trend of solar shortwave radiation. The radiometer measures the IR radiation with a pyranometer spectral response from 305 to 2800 nm. The radiation increases during the sampling period follows the increase of sunlight, while the radiation drops are due to cloud cover and precipitations. Fig. S4b in Supplementary Material shows that the correlation between CAAs and shortwave radiation trend seems to be negative, but further investigations are necessary.

The presence of CAAs in the fine aerosol ($<0.95 \mu\text{m}$) suggests a slight contribution from pollen and terrestrial primary biological aerosol particles that usually are found in coarse particles, but it is also possible that those particles were broken up into fine particles (Abe et al., 2016).

3.3. Factor analysis

To identify the origins of free and combined amino acids, factor analysis (FCA) was performed. In FCA, levoglucosan, MSA nss-SO_4^{2-} , plus other specific and known tracers, were included to confirm the different aerosol sources.

Table S1 in Supplementary material shows the factor loadings matrix obtained by the FCA analysis applied for the period from 4th to 24th April to distinguish the marine and biomass burning sources. Four factors (F) explain 80% of the total variance. High values of factor loadings were found in F1 (total variance of 29%) for MSA, free D-Val and 3 CAAs (combined Gly, LD-Hys and L-Phe), suggesting a marine source for these amino acids for the sampling period from 4th to 24th April. In F2 (total variance of 25%), factor loadings were high for 8 FAAs, while F3 (16% total variance) has high factor loadings for 6 CAAs. F2 and F3 factors explain how FAAs and CAAs might have different sources and the definition of a specific source is too speculative and further investigations are necessary.

The main result of this FCA is the high loading values in F4 (10%). This factor linked the compounds with a biomass burning source, because levoglucosan and nss-SO_4^{2-} were present. In this factor free Gly and D-Ala also have high loadings and these compounds are the most abundant FAAs in these two samples (Fig. S3a). Thus, the biomass burning source for the first two samples hypothesized in Section 3.1 may be confirmed.

FCA was also performed from 24th April to 13th June (Table S2, Supplementary Material) to identify the marine source and five factors explain 75% of the total variance. FAAs are split between F1 (32%), F3 (11%) and F4 (8%), while CAAs are present in F2 (16%) and F5 (8%). Thus, FCA again shows a possible source difference between FAAs and CAAs (Table S2).

Higher factor loadings of 4 FAAs (including Gly and D-Ala, the most concentrated FAAs), MSA and nss-SO_4^{2-} , were obtained in the first factor (F1) confirming the marine biogenic source for the period after 24th April, as already discussed in Section 3.1. In this FCA CAAs are not present in the third factor (F3) while F2, F4 and F5 show high factor loadings for some specific FAAs.

4. Conclusions

This is the first time that L- and D- FAAs and CAAs have been studied in Arctic aerosol. Aerosol samples were collected at the Gruevbadet observatory (Svalbard Islands) from 4th April to 13th June 2015. These samples provide information on concentration trends along the sampling period, size distribution and possible source apportionment. The presence of amino acids in the atmosphere can be an indicator of biological material as well biomass burning, as confirmed by FcA. CAAs concentrations were 2 times higher than FAAs. Gly was the most abundant amino acid in both FAAs and CAAs. Free Gly is found in aerosol below 1.5 µm and is generally considered as an indicator of long-lived aerosols, because has a very low photochemical reactivity, while combined Gly is found also in the coarse fraction. Other amino acids show trends and distributions differences.

Back-trajectories analysis, MSA, nss-SO_4^{2-} and FcA were used to describe the geographic origin of the air masses and to explain how biomass burning events and phytoplankton blooms may influenced the FAAs concentration. Long range atmospheric transport of biomass burning particles from neighboring areas in Siberia and the North Russia was identified as a possible source for the period from 4th to 14th April and local phytoplankton blooms affected FAAs concentration from 14th April to 13th June. FcA even defined two apparently different sources for FAAs and CAAs. Overall, the results clearly indicate that there are significant concentrations of airborne amino acid compounds, but compared to non-polar areas, the concentrations are up to one order of magnitude lower.

Acknowledgements

The scientific activity in Ny-Ålesund was carried out in the framework of the Italian Consiglio Nazionale delle Ricerche (CNR) Polar Program. The logistic support of the National Research Council – Department of Earth Systems Science and Environmental Technologies (CNR-DTA) is gratefully acknowledged. We would like to thank all our colleagues at the CNR Dirigibile Italia Arctic Station who worked and helped us during the field campaign. The authors are also grateful for meteorological data from the Climate Change Tower Integrated Project (CCT-IP) of the National Research Council (<http://www.isac.cnr.it/~radiclim/CCTower/>). We acknowledge the help of ELGA LabWater in providing the PURELAB Pulse and PURELAB Flex which produced the ultrapure water used in these experiments. The authors gratefully acknowledge the NOAA Air Resources Laboratory (ARL) for the provision of the HYSPLIT transport and dispersion model and READY website (<http://www.ready.noaa.gov>) used in this publication. We would also like to thank Dr. Warren Raymond Lee Cairns for the revision of our manuscript.

Appendix A. Supplementary data

Supplementary data to this article can be found online at <https://doi.org/10.1016/j.chemosphere.2018.12.147>.

References

- Abe, R.Y., Akutsu, Y., Kagemoto, H., 2016. Protein amino acids as markers for biological sources in urban aerosols. *Environ. Chem. Lett.* 14, 155–161. <https://doi.org/10.1007/s10311-015-0536-0>.
- Barbaro, E., Kirchgeorg, T., Zangrando, R., Vecchiato, M., Piazza, R., Barbante, C., Gambaro, A., 2015a. Sugars in antarctic aerosol. *Atmos. Environ.* 118, 135–144. <https://doi.org/10.1016/j.atmosenv.2015.07.047>.
- Barbaro, E., Padoan, S., Kirchgeorg, T., Zangrando, R., Toscano, G., Barbante, C., Gambaro, A., 2017a. Particle size distribution of inorganic and organic ions in coastal and inland Antarctic aerosol. *Environ. Sci. Pollut. Res.* 24, 2724–2733. <https://doi.org/10.1007/s11356-016-8042-x>.
- Barbaro, E., Zangrando, R., Kirchgeorg, T., Bazzano, A., Illuminati, S., Annibaldi, A., Rella, S., Truzzi, C., Grotti, M., Ceccarini, A., Malatesta, C., Scarponi, G., Gambaro, A., 2016. An integrated study of the chemical composition of Antarctic aerosol to investigate natural and anthropogenic sources. *Environ. Chem.* 13, 867–876. <https://doi.org/10.1071/EN16056>.
- Barbaro, E., Zangrando, R., Moret, I., Barbante, C., Cescon, P., Gambaro, A., 2011. Free amino acids in atmospheric particulate matter of Venice, Italy. *Atmos. Environ.* 45, 5050–5057. <https://doi.org/10.1016/j.atmosenv.2011.01.068>.
- Barbaro, E., Zangrando, R., Padoan, S., Karroca, O., Toscano, G., Cairns, W.R.L., Barbante, C., Gambaro, A., 2017b. Aerosol and snow transfer processes: an investigation on the behavior of water-soluble organic compounds and ionic species. *Chemosphere* 183, 132–138. <https://doi.org/10.1016/j.chemosphere.2017.05.098>.
- Barbaro, E., Zangrando, R., Vecchiato, M., Piazza, R., Cairns, W.R.L., Capodaglio, G., Barbante, C., Gambaro, A., 2015b. Free amino acids in Antarctic aerosol: potential markers for the evolution and fate of marine aerosol, pp. 5457–5469. <https://doi.org/10.5194/acp-15-5457-2015>.
- Bliesner, D.M., 2006. Validating chromatographic methods: a practical guide. *Brochure* 1–297.
- Bromke, M.A., 2013. Amino acid biosynthesis pathways in diatoms. *Metabolites* 3, 294–311. <https://doi.org/10.3390/metabo3020294>.
- Chan, M.N., Choi, M.Y., Ng, N.L., Chan, C.K., 2005. Hygroscopicity of water-soluble organic compounds in atmospheric aerosols: amino acids and biomass burning derived organic species. *Environ. Sci. Technol.* 39, 1555–1562. <https://doi.org/10.1021/es049584i>.
- Chen, Q., Hildemann, L.M., 2009. Size-resolved concentrations of particulate matter and bioaerosols inside versus outside of homes. *Aerosol Sci. Technol.* 43, 699–713. <https://doi.org/10.1080/02786820902882726>.
- Cornell, S., Mace, K., Coepicus, S., Duce, R., Huebert, B., Jickells, T., Zhuang, L., 2001. Organic nitrogen in Hawaiian rain and aerosol ON m which makes up roughly one third of the total nitrogen in aerosol N m-3). The inorganic nitrogen as nitrate) is predominantly found in coarse-mode rainwater rainwater. *References: J. Geophys. Res.* 106, 7973–7983. <https://doi.org/10.1029/2000JD900655>.
- Cornell, S.E., Jickells, T.D., Cape, J.N., Rowland, A.P., Duce, R.A., 2003. Organic nitrogen deposition on land and coastal environments: a review of methods and data. *Atmos. Environ.* 37, 2173–2191. [https://doi.org/10.1016/S1352-2310\(03\)00133-X](https://doi.org/10.1016/S1352-2310(03)00133-X).
- Cronin, J.R., Pizzarello, S., 1999. Amino acid enantiomer excesses in meteorites: origin and significance. *Adv. Space Res.* 23, 293–299. [https://doi.org/10.1016/S0273-1177\(99\)00050-2](https://doi.org/10.1016/S0273-1177(99)00050-2).
- Csapó, J., Csapó-Kiss, Z., Csapó, J., 1998. Use of amino acids and their racemisation for age determination in archaeometry. *TrAC - Trends Anal. Chem.* 17, 140–148. [https://doi.org/10.1016/S0165-9936\(97\)00126-X](https://doi.org/10.1016/S0165-9936(97)00126-X).
- Csapó, J., Csapó-Kiss, Z., Stefler, J., Martin, T.G., Nemethy, S., 1995. Influence of mastitis on D-amino acid content of milk. *J. Dairy Sci.* 78, 2375–2381. [https://doi.org/10.3168/jds.S0022-0302\(95\)76865-5](https://doi.org/10.3168/jds.S0022-0302(95)76865-5).
- Csapó, J., Csapó-Kiss, Z., Wágner, L., Tólos, T., Martin, T.G., Folestad, S., Tivesten, A., Némethy, S., 1997. Hydrolysis of proteins performed at high temperatures and for short times with reduced racemization, in order to determine the enantiomers of D- and L-amino acids. *Anal. Chim. Acta* 339, 99–107. [https://doi.org/10.1016/S0003-2670\(96\)00452-7](https://doi.org/10.1016/S0003-2670(96)00452-7).
- De Haan, D.O., Corrigan, A.L., Smith, K.W., Stroik, D.R., Turley, J.J., Lee, F.E., Tolbert, M.A., Jimenez, J.L., Cordova, K.E., Ferrell, G.R., 2009. Secondary organic aerosol-forming reactions of glyoxal with amino acids secondary organic aerosol-forming reactions of glyoxal with amino acids, 43, 2818–2824. <https://doi.org/10.1021/es803534f>.
- Di Filippo, P., Pomata, D., Riccardi, C., Buiarelli, F., Gallo, V., Quaranta, A., 2014. Free and combined amino acids in size-segregated atmospheric aerosol samples. *Atmos. Environ.* 98, 179–189. <https://doi.org/10.1016/j.atmosenv.2014.08.069>.
- Dittmar, T., Fitznar, H.P., Kattner, G., 2001. Origin and biogeochemical cycling of organic nitrogen in the eastern Arctic Ocean as evident from D- and L-amino acids. *Geochim. Cosmochim. Acta* 65, 4103–4114.
- Fitznar, H.P., Lobbes, M., Kattner, G., 1999. Determination of enantiomeric amino acids with high-performance liquid chromatography and pre-column derivatization with o-phthalaldehyde and N-isobutyrylcysteine in seawater and fossil samples (mollusks). *J. Chromatogr. A* 832, 123–132.
- Fountoulakis, M., Lahm, H.-W., 1998. Hydrolysis and amino acid composition analysis of proteins. *J. Chromatogr. A* 826, 109–134. [https://doi.org/10.1016/S0021-9673\(98\)00721-3](https://doi.org/10.1016/S0021-9673(98)00721-3).
- Friedman, M., 1991. Formation, nutritional value, and safety of D-amino acids. *Nutr. Toxicol. Consequences Food Process* 289, 447–481. https://doi.org/10.1007/978-1-4899-2626-5_31.
- Ge, X., Wexler, A.S., Clegg, S.L., 2011. Atmospheric amines - Part I. A review. *Atmos. Environ.* 45, 524–546. <https://doi.org/10.1016/j.atmosenv.2010.10.012>.
- Gorzelska, K., Galloway, J.N., Watterson, K., Keene, W.C., 1992. Water-soluble primary amine compounds in rural continental precipitation. *Atmos. Environ. Part A, Gen. Top.* 26, 1005–1018. [https://doi.org/10.1016/0960-1686\(92\)90032-G](https://doi.org/10.1016/0960-1686(92)90032-G).
- Hansell, D.A., Carlson, C.A., 2014. Biogeochemistry of Marine Dissolved Organic Matter. *Acad. Press. Elsevier, USA*. <https://doi.org/10.1016/B978-0-12-405940-5.09990-8>.
- Inuma, Y., Brüggemann, E., Gnauk, T., Müller, K., Andreae, M.O., Helas, G., Parmar, R., Herrmann, H., 2007. Source characterization of biomass burning particles: the combustion of selected European conifers, African hardwood, savanna grass, and German and Indonesian peat. *J. Geophys. Res. Atmos.* 112. <https://doi.org/10.1029/2006JD007120>.

- Kaiser, K., Benner, R., 2005. Hydrolysis-induced racemization of amino acids. *Limnol Oceanogr. Methods* 3, 318–325. <https://doi.org/10.4319/lom.2005.3.318>.
- Kimber, R.W.L., Nannipieri, P., Ceccanti, B., 1990. The degree of racemization of amino acids released by hydrolysis of humic-protein complexes: implications for age assessment. *Soil Biol. Biochem.* 22, 181–185. [https://doi.org/10.1016/0038-0717\(90\)90084-D](https://doi.org/10.1016/0038-0717(90)90084-D).
- Kuznetsova, M., Lee, C., Aller, J., 2005. Characterization of the proteinaceous matter in marine aerosols. *Mar. Chem.* 96, 359–377. <https://doi.org/10.1016/j.marchem.2005.03.007>.
- Leck, C., Bigg, E.K., 1999. Aerosol production over remote marine areas—A new route. *Geophys. Res. Lett.* 26, 3577–3580. <https://doi.org/10.1029/1999GL010807>.
- Liardon, R., Ledermann, S., Ott, U., 1981. Determination of D-amino acids by deuterium labelling and selected ion monitoring. *J. Chromatogr. A* 203, 385–395. [https://doi.org/10.1016/S0021-9673\(00\)80309-X](https://doi.org/10.1016/S0021-9673(00)80309-X).
- Lodish, H., Berk, A., Kaiser, C.A., Krieger, M., Scott, M.P., Bretscher, A., Ploegh, H., Matsudaira, P., 2008. *Molecular Cell Biology*.
- Mace, K.A., Artaxo, P., Duce, R.A., 2003a. Water-soluble organic nitrogen in Amazon Basin aerosols during the dry (biomass burning) and wet seasons. *J. Geophys. Res.* 108, 4512. <https://doi.org/10.1029/2003JD003557>.
- Mace, K.A., Kubilay, N., Duce, R.A., 2003b. Organic nitrogen in rain and aerosol in the eastern Mediterranean atmosphere: an association with atmospheric dust. *J. Geophys. Res.* 108, 4320. <https://doi.org/10.1029/2002JD002997>.
- Mandalakis, M., Apostolaki, M., Stephanou, E.G., 2010. Trace analysis of free and combined amino acids in atmospheric aerosols by gas chromatography-mass spectrometry. *J. Chromatogr. A* 1217, 143–150. <https://doi.org/10.1016/j.chroma.2009.11.021>.
- Mandalakis, M., Apostolaki, M., Tziaras, T., Polymenakou, P., Stephanou, E.G., 2011. Free and combined amino acids in marine background atmospheric aerosols over the Eastern Mediterranean. *Atmos. Environ.* 45, 1003–1009. <https://doi.org/10.1016/j.atmosenv.2010.10.046>.
- Manning, J.M., 1990. Determination of D- and L-amino acid residues in peptides. Use of tritiated hydrochloric acid to correct for racemization during acid hydrolysis. *J. Am. Chem. Soc.* 95, 7449–7454.
- Matos, J.T.V., Duarte, R.M.B.O., Duarte, A.C., 2016. Challenges in the identification and characterization of free amino acids and proteinaceous compounds in atmospheric aerosols: a critical review. *TrAC - Trends Anal. Chem.* 75, 97–107. <https://doi.org/10.1016/j.trac.2015.08.004>.
- Matsumoto, K., Uematsu, M., 2005. Free amino acids in marine aerosols over the western North Pacific Ocean. *Atmos. Environ.* 39, 2163–2170. <https://doi.org/10.1016/j.atmosenv.2004.12.022>.
- McGregor, K.G., Anastasio, C., 2001. Chemistry of fog waters in California's Central Valley: 2. Photochemical transformations of amino acids and alkyl amines. *Atmos. Environ.* 35, 1091–1104. [https://doi.org/10.1016/S1352-2310\(00\)00282-X](https://doi.org/10.1016/S1352-2310(00)00282-X).
- Meloun, B., Morávek, L., Kostka, V., 1975. Complete amino acid sequence of human serum albumin. *FEBS Lett.* 58, 134–137.
- Menetrez, M.Y., Foarde, K.K., Esch, R.K., Schwartz, T.D., Dean, T.R., Hays, M.D., Cho, S.H., Betancourt, D.A., Moore, S.A., 2009. An evaluation of indoor and outdoor biological particulate matter. *Atmos. Environ.* 43, 5476–5483. <https://doi.org/10.1016/j.atmosenv.2009.07.027>.
- Meskhidze, N., Nenes, A., 2016. Phytoplankton and cloudiness in the southern ocean. *Science* 314, 1419–1423. <https://doi.org/10.1007/s10162-016-0558-8> (80-).
- Miguel, A.G., Cass, G.R., Glovsky, M.M., Weiss, J., 1999. Allergens in paved road dust and airborne particles. *Environ. Sci. Technol.* 33, 4159–4168. <https://doi.org/10.1021/es9904890>.
- Mikhailov, E., Vlasenko, S., Niessner, R., Pöschl, U., 2003. Interaction of aerosol particles composed of protein and salts with water vapor: hygroscopic growth and microstructural rearrangement. *Atmos. Chem. Phys. Discuss.* 3, 4755–4832. <https://doi.org/10.5194/acpd-3-4755-2003>.
- Milne, P.J., Zika, R.G., 1993. Amino acid nitrogen in atmospheric aerosols: occurrence, sources and photochemical modification. *J. Atmos. Chem.* 16, 361–398. <https://doi.org/10.1007/BF01032631>.
- Mopper, K., Zika, R.G., 1987. Free amino acids in marine rains: evidence for oxidation and potential role in nitrogen cycling. *Nature* 325, 246–249.
- Müller, C., Iinuma, Y., Karstensen, J., Pinxteren, D. Van, Lehmann, S., Gnauk, T., Herrmann, H., 2009. Seasonal Variation of Aliphatic Amines at the Cape Verde Islands 4318.
- Oros, D.R., Abas, M.R. bin, Omar, N.Y.M.J., Rahman, N.A., Simoneit, B.R.T., 2006. Identification and emission factors of molecular tracers in organic aerosols from biomass burning: Part 3. Grasses. *Appl. Geochem.* 21, 919–940. <https://doi.org/10.1016/j.apgeochem.2006.01.008>.
- Oros, D.R., Simoneit, B.R.T., 2001. Identifications and emission factors of molecular tracers in organic aerosols from biomass burning Part 2. Deciduous Trees 16.
- Park, K.T., Lee, K., Kim, T.W., Yoon, Y.J., Jang, E.H., Jang, S., Lee, B.Y., Hermansen, O., 2018. Atmospheric DMS in the Arctic ocean and its relation to phytoplankton biomass. *Global Biogeochem. Cycles* 32, 351–359. <https://doi.org/10.1002/2017GB005805>.
- Quinn, P.K., Miller, T.L., Bates, T.S., Ogren, J.A., Andrews, E., Shaw, G.E., 2002. A 3-year record of simultaneously measured aerosol chemical and optical properties at Barrow, Alaska. *J. Geophys. Res. Atmos.* 107. <https://doi.org/10.1029/2001JD001248>. AAC 8-1–AAC 8-15.
- Quinn, P.K., Shaw, G., Andrews, E., Dutton, E.G., Ruoho-Airola, T., Gong, S.L., 2007. Arctic haze: Current trends and knowledge gaps. *Tellus Ser. B Chem. Phys. Meteorol.* 59, 99–114. <https://doi.org/10.1111/j.1600-0889.2006.00238.x>.
- Ren, L., Bai, H., Yu, X., Wu, F., Yue, S., Ren, H., Li, L., Lai, S., Sun, Y., Wang, Z., Fu, P., 2018. Molecular composition and seasonal variation of amino acids in urban aerosols from Beijing, China. *Atmos. Res.* 203, 28–35. <https://doi.org/10.1016/j.atmosres.2017.11.032>.
- Samy, S., Robinson, J., Hays, M.D., 2011. An advanced LC-MS (Q-TOF) technique for the detection of amino acids in atmospheric aerosols. *Anal. Bioanal. Chem.* 401, 3103–3113. <https://doi.org/10.1007/s00216-011-5238-2>.
- Samy, S., Robinson, J., Rumsey, I.C., Walker, J.T., Hays, M.D., 2013. Speciation and trends of organic nitrogen in southeastern U.S. fine particulate matter (PM_{2.5}). *J. Geophys. Res. Atmos.* 118, 1996–2006. <https://doi.org/10.1029/2012JD017868>.
- Saxena, V.K., 1983. Evidence of the biogenic nuclei involvement in antarctic coastal clouds. *J. Phys. Chem.* 87, 4130–4134. <https://doi.org/10.1021/j100244a029>.
- Scalabrin, E., Zangrando, R., Barbaro, E., Kehrwald, N.M., Gabrieli, J., Barbante, C., Gambaro, A., 2012. Amino acids in Arctic aerosols. *Atmos. Chem. Phys.* 8, 5551–5563. <https://doi.org/10.5194/acp-8-5551-2008>.
- Scheller, E., 2001. Amino acids in dew - origin and seasonal variation. *Atmos. Environ.* 35, 2179–2192. [https://doi.org/10.1016/S1352-2310\(00\)00477-5](https://doi.org/10.1016/S1352-2310(00)00477-5).
- Sciare, J., Oikonomou, K., Favez, O., Markaki, Z., Liakakou, E., Cachier, H., Mihalopoulos, N., 2008. Long-term measurements of carbonaceous aerosols in the eastern Mediterranean: evidence of long-range transport of biomass burning. *Atmos. Chem. Phys. Discuss.* 8, 6949–6982. <https://doi.org/10.5194/acpd-8-6949-2008>.
- Stefels, J., Steinke, M., Turner, S., Malin, G., Belviso, S., 2007. Environmental constraints on the production and removal of the climatically active gas dimethylsulphide (DMS) and implications for ecosystem modelling. *Phaeocystis Major Link Biogeochem. Cycl. Clim. Elem.* 245–275. https://doi.org/10.1007/978-1-4020-6214-8_18.
- Turetta, C., Zangrando, R., Barbaro, E., Gabrieli, J., Scalabrin, E., Zennaro, P., Gambaro, A., Toscano, G., Barbante, C., 2016. Water-soluble trace, rare earth elements and organic compounds in Arctic aerosol. *Rend. Lincei* 27, 95–103. <https://doi.org/10.1007/s12210-016-0518-6>.
- Vignati, E., Facchini, M.C., Rinaldi, M., Scannell, C., Ceburnis, D., Sciare, J., Kanakidou, M., Myriokefalitakis, S., Dentener, F., O'Dowd, C.D., 2010. Global scale emission and distribution of sea-spray aerosol: sea-salt and organic enrichment. *Atmos. Environ.* 44, 670–677. <https://doi.org/10.1016/j.atmosenv.2009.11.013>.
- Weathers, K.C., Lovett, G.M., Likens, G.E., Caraco, N.F.M., 2000. Cloudwater inputs of nitrogen to forest ecosystem in southern Chile: forms, fluxes, and sources. *Ecosystems* 3, 590–595. <https://doi.org/10.1007/s100210000051>.
- Wedyan, M.A., Preston, M.R., 2008. The coupling of surface seawater organic nitrogen and the marine aerosol as inferred from enantiomer-specific amino acid analysis. *Atmos. Environ.* 42, 8698–8705. <https://doi.org/10.1016/j.atmosenv.2008.04.038>.
- Yang, H., Xu, J., Wu, W.S., Wan, C.H., Yu, J.Z., 2004. Chemical characterization of water-soluble organic aerosols at Jeju Island collected during ACE-Asia. *Environ. Chem.* 1, 13–17. <https://doi.org/10.1071/EN04006>.
- Yoon, Y.J., Ceburnis, D., Cavalli, F., Jourdan, O., Putaud, J.P., Facchini, M.C., Decesari, S., Fuzzi, S., Sellegri, K., Jennings, S.G., O'Dowd, C.D., 2007. Seasonal characteristics of the physicochemical properties of North Atlantic marine atmospheric aerosols. *J. Geophys. Res. Atmos.* 112, 1–14. <https://doi.org/10.1029/2005JD007044>.
- Zangrando, R., Barbaro, E., Zennaro, P., Rossi, S., Kehrwald, N.M., Gabrieli, J., Barbante, C., Gambaro, A., 2013. Molecular markers of biomass burning in Arctic aerosols. *Environ. Sci. Technol.* 47, 8565–8574. <https://doi.org/10.1021/es400125v>.
- Zhang, Q., Anastasio, C., 2003. Free and combined amino compounds in atmospheric fine particles (PM 2.5) and fog waters from Northern California, 37, 2247–2258. [https://doi.org/10.1016/S1352-2310\(03\)00127-4](https://doi.org/10.1016/S1352-2310(03)00127-4).



Interannual variability of sugars in Arctic aerosol: Biomass burning and biogenic inputs

Matteo Feltracco^{a,*}, Elena Barbaro^b, Silvia Tedeschi^a, Andrea Spolaor^b, Clara Turetta^b, Marco Vecchiato^b, Elisa Morabito^a, Roberta Zangrando^b, Carlo Barbante^{a,b}, Andrea Gambaro^{a,b}

^a Department of Environmental Sciences, Informatics and Statistics, Ca'Foscari University of Venice, Via Torino 155, 30172 Venice, Italy

^b Institute of Polar Sciences CNR, Via Torino 155, 30172 Venice, Italy

HIGHLIGHTS

- For the first time a broad class of sugars were studied in Svalbard aerosol.
- The study provides information about the sources and transport of sugars in Arctic.
- The study identifies biomass burning and local terrestrial/sea input as sources.

GRAPHICAL ABSTRACT



ARTICLE INFO

Article history:

Received 11 October 2019

Received in revised form 9 December 2019

Accepted 10 December 2019

Available online xxxx

Editor: Pingqing Fu

Keywords:

Arctic

Bioaerosol

PBAPs

Sugars

ABSTRACT

The concentrations and particle-size distribution of sugars in Arctic aerosol samples were studied to investigate their potential sources and transport. Sugars are constituents of the water-soluble organic compounds (WSOC) fraction in aerosol particles where some saccharides are used as tracers of Primary Biological Aerosol Particles (PBAPs). Monosaccharides (arabinose, fructose, galactose, glucose, mannose, ribose, xylose), disaccharides (sucrose, lactose, maltose, lactulose), alcohol-sugars (erythritol, mannitol, ribitol, sorbitol, xylitol, maltitol, galactitol) and anhydroglucosans (levoglucosan, mannosan and galactosan) were quantified in aerosol samples collected during three different sampling campaigns (spring and summer 2013, spring 2014 and 2015). The mean total concentrations of sugars were 0.4 ± 0.3 , 0.6 ± 0.5 and 0.5 ± 0.6 ng m^{-3} for 2013, 2014 and 2015 spring campaigns, while the mean concentration increased to 3 ± 3 ng m^{-3} in the summer of 2013. This work identified a reproducibility in the sugars trend during spring, while the summer data in 2013 allowed to us to demonstrate strong local inputs when the ground was free of snow and ice. Furthermore, the study aims to show that the two specific ratios of sorbitol & galactitol to arabinose were diagnostic for the type of biomass that was burnt. This study demonstrates that not only is long-range atmospheric transport significant. But depending on seasonality, local inputs can also play an important role in the chemical composition of sugars in Arctic aerosol.

© 2019 Elsevier B.V. All rights reserved.

1. Introduction

The chemical characterization of Arctic aerosol has been studied in several investigations, either focused on ions (Giardi et al., 2016;

* Corresponding author at: University of Venice, Via Torino 155, 30172 Venice, Italy.
E-mail address: matteo.feltracco@unive.it (M. Feltracco).

Udisti et al., 2016), trace elements (Barbante et al., 2017; Bazzano et al., 2016; Turetta et al., 2016), or organic compounds (Becagli et al., 2016; Feltracco et al., 2019; Stohl et al., 2006a; Yttri et al., 2014; Zangrando et al., 2013). The presence and concentration of some atmospheric markers give us some useful information about origin of aerosol and atmospheric long-range transport processes. The investigation of sources and emission of particles is crucial, to better understanding their impact in the Arctic environment.

Primary Biological Aerosol Particles (PBAPs) (sugars, amino acids, phenolic compounds, etc) are gaining attention in the Svalbard Archipelago because they can act directly as cloud condensation nuclei (CCN) and ice nuclei (IN) (Haga et al., 2013; Morris et al., 2013; Pummer et al., 2012). The presence of PBAPs have been also associated with precipitation (Huffman et al., 2013; Prenni et al., 2009).

Primary saccharides, can originate from several animals, plants and microorganisms, while alcohol-sugars are released by bacteria, airborne fungal spores and lichens (Bauer et al., 2008; Elbert et al., 2007; Medeiros et al., 2006). Glucose, for example, is the most abundant carbohydrate in vascular plants (Cowie and Hedges, 1984) and sucrose has a key role in plant flowering (Bialeski, 1995). Recent studies have reported that sucrose is the dominant component of airborne pollen granules (Fu et al., 2012; Pacini, 2000; Yttri et al., 2007). Alcohol-sugars are present in bacteria and lichens, which can produce and accumulate these compounds to overcome osmotic stress (Medeiros et al., 2006). Arabitol is an univocal atmospheric tracer of fungal spores and lichens, while mannitol is present in lichen, fungal spores, algae, and higher plants (Bauer et al., 2008; Ila Gosselin et al., 2016). Sugars can also be derived from soil resuspension phenomena (Li et al., 2015; Simoneit et al., 2004) and are also found in airborne marine organic particles generated by sea spray (Hawkins and Russell, 2010). Anhydrosugars like levoglucosan and its isomers (mannosan and galactosan) can originate from biomass burning (Barbaro et al., 2015; Iinuma et al., 2007; Medeiros et al., 2006; Oros et al., 2006; Oros and Simoneit, 2001; Simoneit et al., 2004). The presence of individual anhydrosugars in aerosol generated from biomass burning events can be used to identify specific types of biomass. Thus, the ratio of levoglucosan to mannosan (L/M) has recently been used to discriminate between the predominance of coniferous or deciduous wood combustion (Engling et al., 2009; Fabbri et al., 2009; Oliveira et al., 2007; Pio et al., 2008; Ward et al., 2006).

Several studies have investigated sugars in atmospheric aerosol samples collected in urban areas (Jia and Fraser, 2011; Pashynska et al., 2002; Pietrogrande et al., 2017, 2014), forests (Graham et al., 2003; Yttri et al., 2007), while little information is available from remote marine regions (Chen et al., 2013; Fu et al., 2013; P.Q. Fu et al., 2009) and polar areas, such as Antarctica (Barbaro et al., 2015).

The main objective of this study is to investigate the size distribution of sugars, as climatically relevant components of the Arctic environment, in order to understand the origin, sources and transport processes of these compounds. This is the first study in which alcohol-sugars, monosaccharides and di-saccharides have been determined in Svalbard aerosol, enhancing previous campaigns (2010) that were focused mainly on biomass burning tracers (Turetta et al., 2016; Zangrando et al., 2013).

The sugar composition of Arctic aerosol was evaluated in 2013 (from 13th April to 9th September), 2014 (2th April–29th June) and 2015 (14th April to 13th June) at Ny Ålesund (Svalbard Island - 78°55'03"N, 11°53'39"E). The particle-size distribution of these compounds allowed us to evaluate the origin and the transport processes. The three sampling campaigns were conducted during the spring and were aimed at evaluating possible inter-annual trends. The sampling campaign of 2013 gave us the opportunity to evaluate the impact of ice-free areas after exposure during the summer.

2. Experimental

2.1. Sampling collection, processing and instrumental analysis

Arctic sampling campaigns were conducted in 2013, 2014 and 2015 at the Gruebadet Observatory, close to Ny Ålesund, Svalbard (78°55'03"N, 11°53'39"E, 50 m a.s.l.). Each sample has a sampling time of between 1 and 10 days, with the aim of identifying specific events, while maintaining the protocols used in previous studies (Feltracco et al., 2019; Scalabrin et al., 2012; Turetta et al., 2016). Samples were collected with a PM10 high volume air sampler (TE-6070) at a flow rate of 68 m³ h⁻¹ equipped with a five stage high volume cascade impactor (TE-235, Tisch Environmental Inc., Cleves, OH) provided with a high volume back up 8" × 10" Quartz Fiber Filter (QFF) and 5.625" × 5.375" slotted QFF (FILTERLAB, Barcelona, Spain) to collect aerosol particles in the following size ranges: 10.0–7.2 μm (S1), 7.2–3.0 μm (S2), 3.0–1.5 μm (S3), 1.5–0.95 μm (S4), 0.95–0.49 μm (S5), < 0.49 μm (B). In order to test contamination, field blank samples were collected by positioning filters in the impactor plates with the sampler turned off. Filters were pre-combusted (400 °C, 4 h) before sampling and stored afterwards at -20 °C enfolded in aluminium foil. After sampling, our previously described (Barbaro et al., 2015; Zangrando et al., 2013) pre-analytical protocol was followed. Briefly, the samples were processed inside an ISO5 clean room under a laminar flow bench (class 100) to minimize the contaminations. The filters were removed from their aluminium cover, cut in a half and fragmented into small pieces using steel tweezers and placed in a 15 or 50 mL conical flask. A mixed standard of labelled ¹³C₆-levoglucosan and ¹³C₆-glucose (48 and 47 ng, respectively), was used as an internal standard, and was added to each half filter. The sample was then extracted twice, with 9 mL and then 1 mL of ultrapure water in an ultrasonic bath if it was a slotted filter. Meanwhile, back-up filters, were extracted with 25 mL then 5 mL of ultrapure water. The combined extracts were then filtered through a 0.45 μm, Ø13 mm PTFE filter before analysis. Field blank filters were handled using the same procedure. The method detection limits (MDL) and method quantification limits (MQL) of the analytical procedure were determined as three and ten times the standard deviation of the average concentration of the field blank. Real sample values were blank corrected and only those above MQL were considered. Details of utilized materials are reported in the Supplementary Material.

Determination and quantification of anhydrosugars, alcohol-sugars, monosaccharides and di-saccharides were performed using an ion chromatograph (Thermo Scientific™ Dionex™ ICS-5000, Waltham, US) coupled to a single quadrupole mass spectrometer (MSQ Plus™, Thermo Scientific™, Bremen, Germany). In this study, the instrumental method used was that developed by Barbaro et al. (2015) and is reported in the Supplementary Material.

2.2. Air mass trajectory analysis

To investigate the source regions of air masses arriving in Ny Ålesund, backward trajectories (BTs) were calculated using HYSPLIT4 and the GDAS one-degree meteorological database (Draxler, 1997, 1998, 1999; Stein et al., 2015). Seven days back trajectories were calculated every 12 h at 500 m a.s.l. to evaluate long-range transport, which corresponds to the elevation of the Zeppelin Mountain, the highest mountain neighbouring the sampling site. The daily trajectories obtained were subjected to frequency displaying, by considering the residence time.

3. Results

Three different spring seasons and one summer season were compared by considering the mean PM₁₀ concentrations of target compounds (anhydrosugars, saccharides, alcohol-sugar and arabitol +

mannitol) (Fig. 1). The PM₁₀ concentration was obtained by summing the values obtained from each sampling stage (6 filters with different particle diameter range). During the 2013 campaign, aerosol samples were collected from the 13th of April to 9th of September and the mean concentration of sugars was $2 \pm 2 \text{ ng m}^{-3}$. The sampling campaign performed in 2013 showed a trend in sugar concentrations over the spring and summer, the two different seasons can be distinguished after considering the snow cover. We have defined spring as the sampling period between 10th April and 28th May, summer was defined as from 28th May to 9th September, the period when coastal snow cover was absent. The period between the 10th April – 28th May was characterized by a total mean sugar concentration of $0.4 \pm 0.3 \text{ ng m}^{-3}$, and the major compounds were arabinose (32% of the total), maltitol (20%), levoglucosan (16%) and sorbitol + galactiol (11%) (sorbitol and galactiol were quantified together, as reported by Barbaro et al. (2015)). The highest concentrations of sugars were found in the summer with a mean total concentration of $3 \pm 3 \text{ ng m}^{-3}$, the most abundant compounds were arabinose (45%), arabitol (23%) and mannitol (20%).

The 2014 campaign started on the 2nd of April and ended the 29th of June. The mean total concentration of sugars was $0.6 \pm 0.5 \text{ ng m}^{-3}$. The

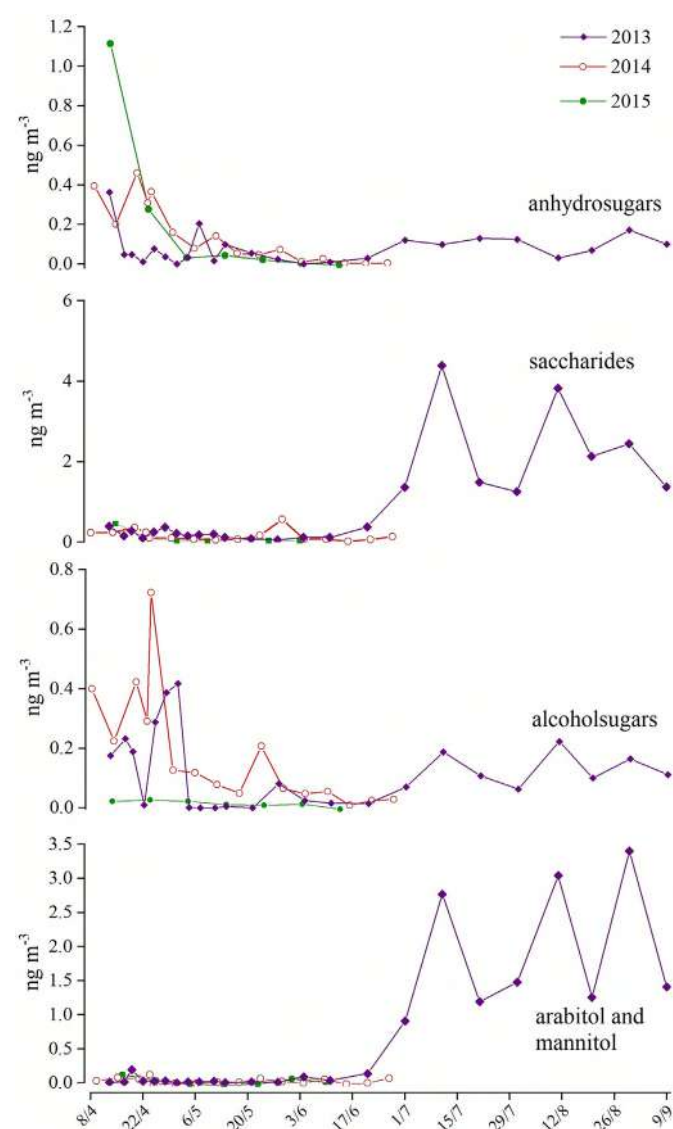


Fig. 1. PM₁₀ concentration overlap of 2013, 2014 and 2015. On the top biomass burning tracers are reported, below saccharides, alcohol-sugar and on the bottom arabitol and mannitol.

major compounds were sorbitol + galactiol (28%), levoglucosan (20%) and glucose (12%). The relative abundances are dissimilar to 2013 mainly because the 2014 sampling campaign ended in early summer. Anhydrosugars and alcohol-sugars showed a concentration maximum in April (Fig. 1).

The 2015 campaign started on the 4th of April and ended on the 13th of June. The mean total concentration of sugar was $0.5 \pm 0.6 \text{ ng m}^{-3}$. The major compounds were levoglucosan (35%), sorbitol + galactiol (29%) and glucose (8%). The period from 4th to 24th April was highly affected by levoglucosan, mannosan and galactosan (Fig. 1): in April 2015 anhydrosugars had relatively higher concentration values than those from the 2013 and 2014 campaigns. Sorbitol & galactiol (47%) and glucose (14%) were the most abundant compounds between the 24th April and 13th June 2015.

4. Discussion

4.1. Biomass burning particles in Arctic aerosol

4.1.1. Fire in 2013, 2014 and 2015 spring seasons

To evaluate the presence of biomass burning particles we studied the concentration trends of levoglucosan, mannosan and galactosan. These anhydrosugars are specific tracers for biomass fire events since they are emitted during cellulose combustion at temperatures $>300 \text{ }^\circ\text{C}$ (Simoneit, 2002).

The mean concentrations of anhydrosugars in PM₁₀ observed in Arctic aerosol during the spring (April–May) of 2013, 2014 and 2015 were 0.08 ± 0.01 , 0.1 ± 0.1 , and $0.2 \pm 0.4 \text{ ng m}^{-3}$. Levoglucosan, mannosan and galactosan were mostly present in fine particles (below of $0.95 \mu\text{m}$) (Fig. S1–S3), suggesting long range atmospheric transport (LRAT). These concentration values are consistent with levoglucosan concentrations previously found in Arctic remote areas (Feltracco et al., 2019; Fu et al., 2013; P. Fu et al., 2009; Stohl et al., 2006b; von Schneidmeyer et al., 2009; Yttri et al., 2014; Zangrando et al., 2013). Moreover, the anhydrosugars concentrations are similar to values found in Antarctic marine and coastal aerosol and an order of magnitude greater than those in Antarctic plateau aerosol (Barbaro et al., 2015; Zangrando et al., 2016b).

Fig. 2 shows the box-plot diagram of levoglucosan, mannosan and galactosan concentrations in PM₁₀ fractions for spring of 2013, 2014 and 2015 and the summer of 2013. The trend reports an inter-annual increase in the spring of 2013, 2014 and 2015 and an intra-annual increase from spring to summer 2013.

To better understand the different classes of combustion sources during the sampling we studied the L/M ratio (Fabbri et al., 2009). For example, L/M ratios were found to be high for hardwoods (angiosperms) (14–15) and low (3–5) for softwoods (gymnosperms) in Austria (Schmidl et al., 2008). In Belgrade aerosols, L/M ratio were very low in September (1.5–3.0) and increased in October (range 2.5–16.7) (Zangrando et al., 2016a). In the spring of 2013 and of 2014, L/M values in the Arctic samples are spread (Fig. 2), indicating a poorly defined smoke source (mean $\gg 10$). This is also confirmed by BTs (Fig. 3) and the FIRMS map: in spring 2013 and 2014 trajectories frequency overlap with fires from the North-East of Russia and the North of Canada. These two macro-areas are mainly characterized by deciduous and evergreen needleleaf trees, respectively (see: unep-wcmc.org), resulting in a mix of softwood and hardwood combustion products reaching our sampling site. Fig. 2 shows that in the spring of 2013 and 2014, L/M ratios sometimes exceeded 40, suggesting crop or rice straw burning from household heating (Yan et al., 2014).

The 2015 anhydrosugars trend was previously investigated by Feltracco et al. (2019) to demonstrate the possible correlation between free amino acids to biomass burning events. North Western Russian wildfire events were suggested as possible sources of biomass burning tracers, principally in the first period. The mean L/M ratio for 2015

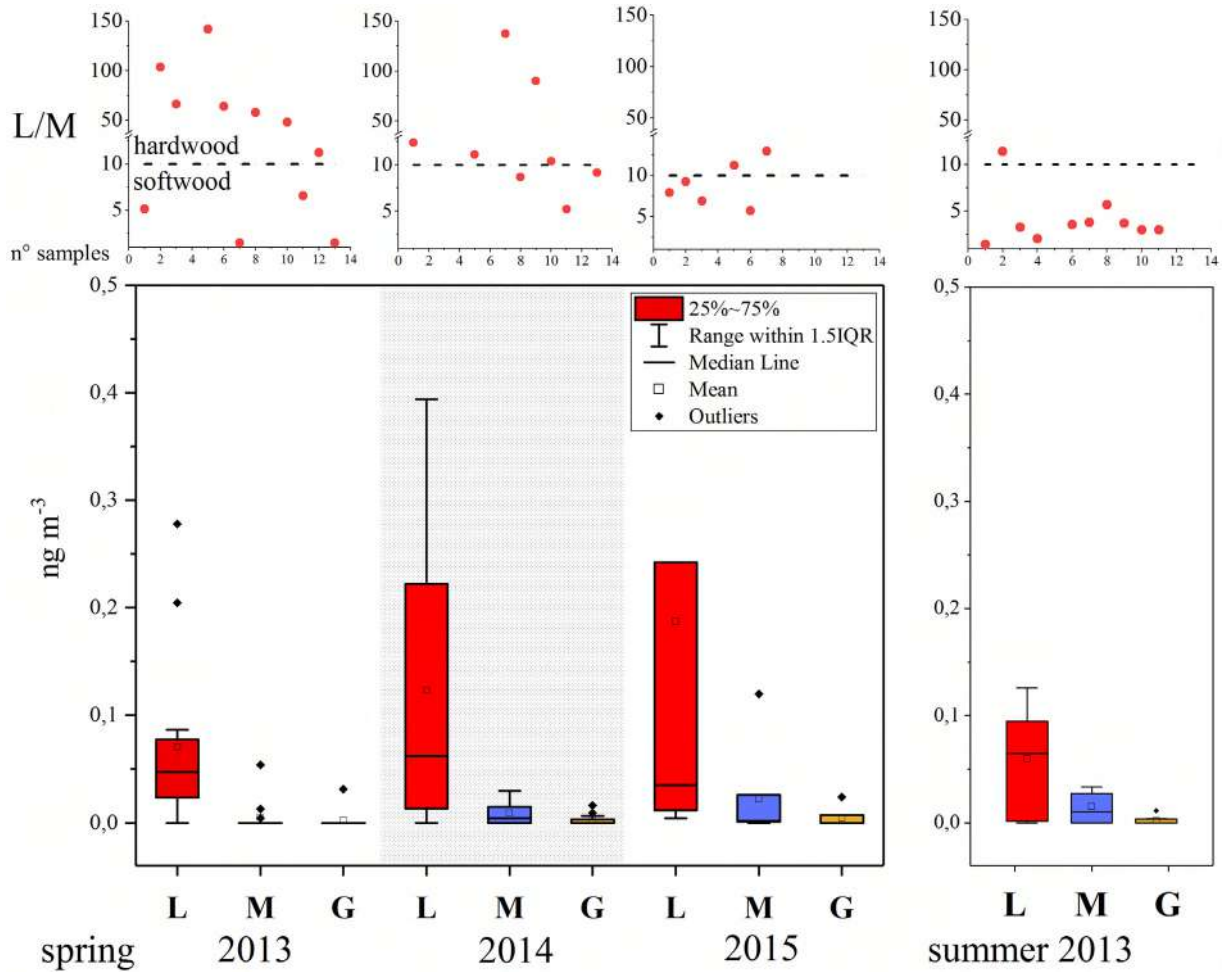


Fig. 2. Boxplot of levoglucosan (L), mannosan (M) and galactosan (G) PM₁₀ concentrations in spring 2013, 2014 and 2015 and summer 2013. On the top, the ratio of L/M for each sample is reported.

was 10 ± 5 suggesting a combination of burned hardwood and softwood as sources.

4.1.2. Fire in summer 2013 and local combustion event investigation in 2014

The particle size distribution of anhydrosugars during the 2013 campaign changed between spring and summer (Fig. S1). Anhydrosugars

were mainly distributed in the fine fraction (87%) during spring, suggesting that particles from biomass burning sources underwent LRAT. The percentage of fine particles decreased to 62% from June to the end of summer probably due to a relative increase in contributions from local sources. Such smoke particle distributions may also be the result of resuspension of local soil particles into the air during summer together with the smoke particles (Lee et al., 2008). The seasonal decrease

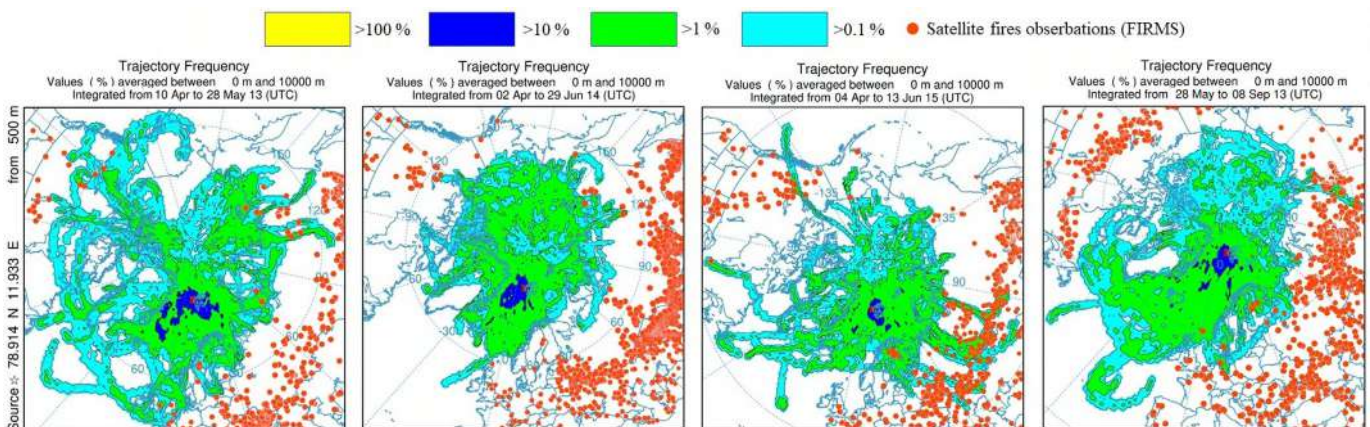


Fig. 3. Back trajectories of spring 2013, 2014 and 2015 and summer 2013 overlapped with Fire Information for Resource Management System (FIRMS) from Visible Infrared Imaging Radiometer Suite (VIIRS).

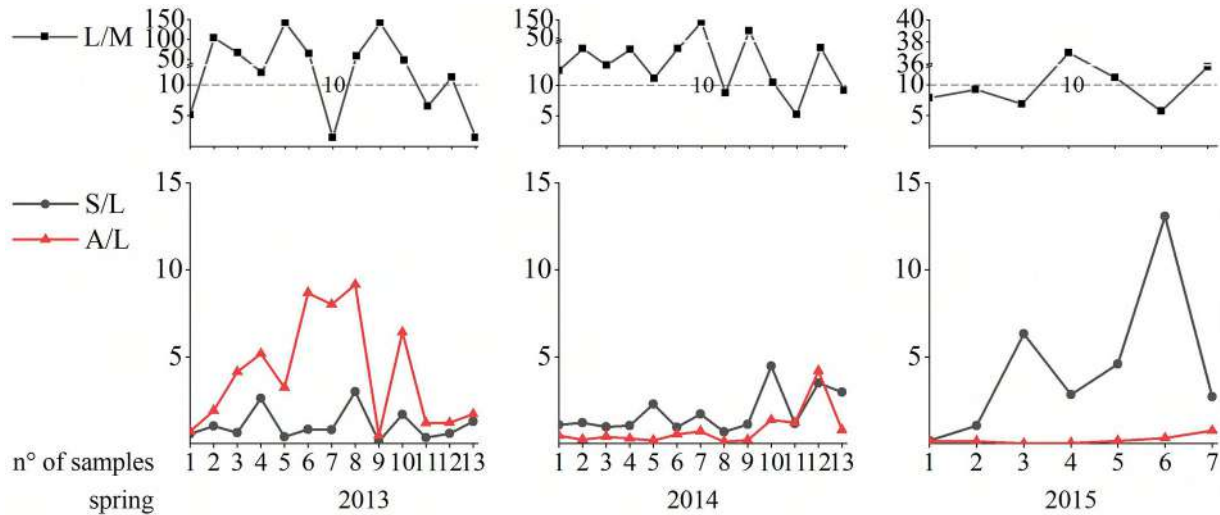


Fig. 4. S/L and A/L trend ratios related to spring 2013, 2014 and 2015. On the top, L/M is reported.

of biomass burning tracers from spring to summer that we observed was also reported by other studies conducted at Zeppelin station, Ny Ålesund (Eleftheriadis et al., 2009; Yttri et al., 2014).

During the 2014 campaign, a “controlled fire” event occurred close to the storage building in Ny Ålesund (North-East from the sampling site, 1.5 km distance). To evaluate the possible local contribution, the

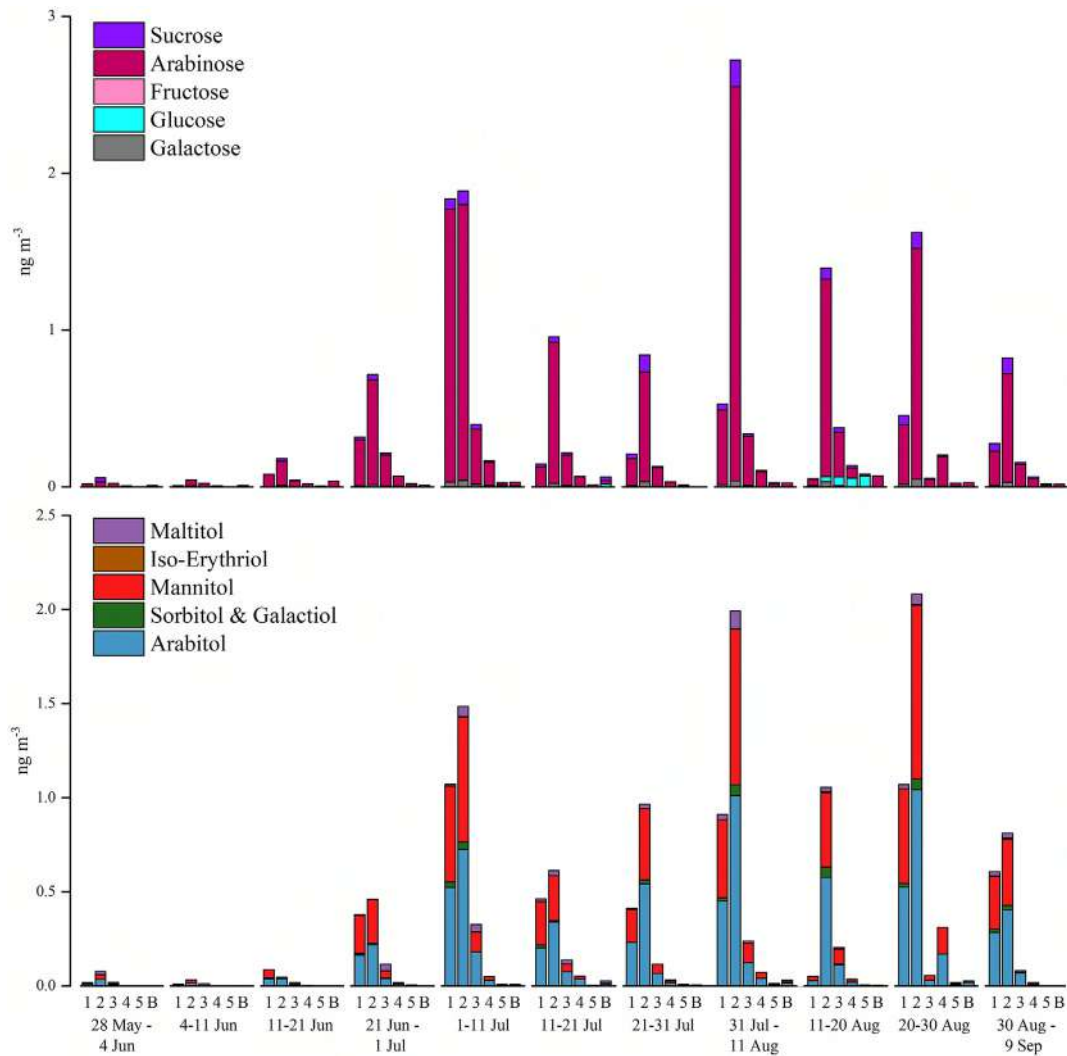


Fig. 5. Particle-size distribution of saccharides (on top) and alcohol-sugars (bottom) in summer 2013.

sampling period was reduced to 3 days from 20th to 23rd April 2014. The concentration trend does not seem to be affected by this fire event because no increase in coarse particles or total PM₁₀ were found (0.3 ng m⁻³ PM₁₀ constant concentration during pre-combustion, combustion and post-combustion period) probably due to adverse winds for short-range transport (Fig. S4). A similar process was previously recognized in Ny Ålesund, which could constitute a local source of contamination for the nearby area, which is strongly dependant on the direction of the prevailing winds (Vecchiato et al., 2018). The 1-day sampling from 23rd to 24th April was carried out to test for possible post-combustion contamination, but we found the same levoglucosan concentration (0.3 ng m⁻³) and no increase in the coarse particles, the wind roses for that period exclude any local fire influence.

4.1.3. Can other sugars be suggested as innovative biomass burning tracers?

A great number of recognisable organic compounds can be emitted during combustion of biomass (Simoneit, 2002). The dominant organic components of smoke particulate matter are monosaccharides originating from the thermal breakdown of cellulose and phenolic compounds from the thermal degradation of lignin. Table 2 shows how levoglucosan, a key tracer of biomass burning, is highly correlated with glucose, iso-erythritol, arabinose and sorbitol & galactitol. The correlation value changes depending on season and year.

A high correlation of erythritol with anhydrosugars can be due to soil biota resuspended into the atmosphere during the biomass burning period (Tsai et al., 2013). On the other hand, arabinose is an important constituent of cell wall polysaccharides, such as the pectic component rhamnogalacturonan and the cellulose binding compound glucuronarabinoxylans (softwood) (Burget et al., 2003), while sorbitol & galactitol are usually found only in *Rosaceae* and *Celestraceae* (hardwood) tree families (Loescher, 1987). In particular, sorbitol was found in relatively high concentrations in leaf smoke samples, suggesting it is a tracers for leaf burning (deciduous matrix) in ambient PM samples (Schmidl et al., 2008). These two sugars were also used to identify the biomass burning source in previous studies (Scaramboni et al., 2015; Urban et al., 2014). Here we propose the arabinose to levoglucosan (A/L) and sorbitol & galactitol to levoglucosan (S/L) ratios, according to their high correlation, as diagnostic ratios to strengthen L/M

correlations. In spring of 2013, 2014 and 2015 A/L and S/L mean ratios are similar and < 4, suggesting a comparable softwood and hardwood contribution, confirmed by the L/M results (Fig. 4). In summer 2013, it was not possible to observe these values, due to the exposure of local ice-free areas that created a ratio-contamination. In fact, primary saccharides (arabinose, sucrose, etc) and saccharides polyols (sorbitol, arabitol, etc) are candidate tracers for surface soil dust (Simoneit et al., 2004) and are discussed next. For these reasons, these ratios should be used only in ice or snow-covered polar areas to avoid the contribution of local contamination.

4.2. Local inputs

The increase in the sugar content, especially for saccharides and alcohol-sugar (including arabitol and mannitol) (Fig. 1) in summer 2013 reflected sugar production in the ecosystem, with major synthesis of primary sugars in the summer. No local inputs can be distinguished for 2014 and 2015, as no data were available for summer in those years. As already explained in Section 4.1, these periods were mainly affected by biomass burning LRAT.

Fig. 5 shows the trend for saccharides (i.e. arabinose, glucose, fructose, galactose and sucrose) and alcohol-sugars (i.e. maltitol, arabitol, mannitol, isoerythriol, sorbitol & galactitol) from 28th May to 9th September 2013. These sugars are mainly distributed in coarse particles, indicating a mainly local input (Jaenicke, 1980). Although accumulation processes are possible, the coarse mode is generated mainly by mechanical processes (Schumann, 2012), because of the different formation pathways, coarse mode particles are clearly separated from smaller particles with respect to their chemical composition.

The prevalent presence of arabinose, arabitol and mannitol in coarse particles (2 ± 1 , 0.8 ± 0.6 and 0.7 ± 0.6 ng m⁻³, respectively) denotes a local biogenic source, most likely due to soil resuspension from local snow-free areas and sea-spray (Barbaro et al., 2015; Hawkins and Russell, 2010; Medeiros et al., 2006; Park et al., 2019; Simoneit, 2002).

Arabinose metabolism is well known in bacteria (Lee et al., 1986) and in filamentous fungi (Chiang and Knight, 1961; VanKuyk et al., 2001). In addition to what we have already explained, most organisms convert arabinose to xylulose-5-phosphate, though different pathways

Table 1
Average PM₁₀ concentrations of each class of sugars in the aerosol collected at Gruevbadet. In brackets, the percentage of each sugar relative to each size class.

	Anhydrosugars	Saccharides	Alcohol-sugars
April–May 2013	0.08 ng m ⁻³ Levoglucosan (90%) Mannosan (7%) Galactosan (3%)	0.2 ng m ⁻³ Arabinose (71%) Galactose (13%) Glucose (8%) Sucrose (4%) Mannose (3%) Ribose, Fructose, Xylose (<1%)	0.2 ng m ⁻³ Maltitol (52%) Sorbitol & Galactitol (29%) Arabitol (14%) Mannitol (4%) Iso-erythritol, Xylitol, Ribitol (<1%)
April–June 2014	0.1 ng m ⁻³ Levoglucosan (91%) Mannosan (7%) Galactosan (2%)	0.2 ng m ⁻³ Glucose (28%) Arabinose (21%) Fructose (20%) Sucrose (15%) Galactose (14%) Ribose, Mannose, Xylose (<2%)	0.2 ng m ⁻³ Sorbitol & Galactitol (76%) Mannitol (13%) Arabitol (5%) Iso-erythritol (5%) Maltitol, Xylitol, Ribitol (<1%)
April–June 2015	0.2 ng m ⁻³ Levoglucosan (88%) Mannosan (10%) Galactosan (2%)	0.1 ng m ⁻³ Glucose (37%) Arabinose (25%) Sucrose (14%) Fructose (10%) Xylose (9%) Galactose (3%) Ribose, Mannose (<2%)	0.2 ng m ⁻³ Sorbitol & Galactitol (73%) Arabitol (10%) Mannitol (9%) Iso-erythritol (6%) Maltitol, Xylitol, Ribitol (<2%)
June–September 2013	0.08 ng m ⁻³ Levoglucosan (77%) Mannosan (20%) Galactosan (3%)	1.7 ng m ⁻³ Arabinose (88%) Sucrose (7%) Galactose (2%) Ribose, Mannose, Fructose, Glucose (<3%)	1.5 ng m ⁻³ Arabitol (51%) Mannitol (42%) Maltitol (4%) Sorbitol & Galactitol (2%) Iso-erythritol, Xylitol, Ribitol (<1%)

Table 2
Correlation matrix for the analysed sugars. Each box reports the values of spring and summer 2013 (2013¹ and 2013², respectively), 2014 and 2015. The table shows only the significant correlations with *p*-value<0.10.

	2013 ¹	2013 ²	2014	2015	Levogluco- saccharan	Mannosan	Galactosan	Sorbitol & Galactol	Mannitol	Iso-erythritol	Galactose	Glucose	Fructose	Arabinose
Levogluco- saccharan	-	-	-	-	-	-	-	-	-	-	-	-	-	-
Mannosan	0.5681	0.7228	0.7071	-	0.9257	-	-	-	-	-	-	-	-	-
Galactosan	0.5840	0.8107	0.9957	-	0.6368	0.5498	-	-	-	-	-	-	-	-
Sorbitol & Galactol	0.4991	0.6688	0.3172	0.9613	0.6440	0.2727	0.9236	0.3660	0.6242	0.8385	0.1947	0.5053	-	-
Mannitol	0.9362	0.5952	0.9463	0.4433	0.8916	0.3166	0.6811	0.6009	0.2185	0.4322	0.3208	-	-	-
Iso-erythritol	0.3589	0.8586	0.4425	0.6982	0.4284	0.4154	0.3120	0.2297	0.7107	-	-	-	-	-
Galactose	0.9603	0.8238	-	-	-	-	-	0.5115	-	-	-	-	-	-
Glucose	0.5482	0.5788	-	-	0.8379	0.8624	-	0.8966	0.2563	0.9029	0.2161	0.9086	0.1988	0.2230
Fructose	0.4851	0.1821	0.9494	0.9406	0.2093	0.8624	-	0.8821	0.1957	0.8821	0.2704	0.6735	0.2202	-
Arabinose	0.9476	0.3056	-	0.3545	0.3739	-	-	0.5973	-	-	-	-	-	-
Sucrose	0.7487	0.4584	-	0.8942	0.8517	-	-	0.3985	0.9090	-	0.2134	0.3743	-	0.1890
	0.2077	0.5483	-	0.6822	0.7421	0.6049	-	0.8827	-	-	-	-	-	0.8900
	0.1888	0.5846	-	0.5988	0.6049	-	-	0.3600	-	-	-	-	-	0.4639
	0.6123	0.2029	-	0.2230	-	-	-	-	-	-	-	-	-	-
	0.9338	0.7683	0.9682	0.7210	0.9700	0.7083	0.9576	0.5880	-	-	-	-	-	-
	0.4264	0.3731	0.4667	0.3393	0.4979	-	0.4446	0.3600	-	-	-	-	-	-

are used by different organisms (Witteveen et al., 1989). A significant difference between bacteria and fungi is the way in which they convert xylose to xylulose. Bacteria usually use an isomerase, whereas fungi reduce xylose to xylitol which is subsequently oxidized to xylulose (Jeffries, 1985). Several pathways have been described for L-arabinose breakdown. The pathway described for *Penicillium chrysogenum* by Chiang and Knight (1961) includes a reduction to L-arabitol and oxidation to xylulose. Therefore, the presence of arabinose and arabitol can indicate bacterial or fungal activity.

Arabinose, arabitol and mannitol showed high correlations between their concentrations in the summer of 2013 (Table 2), implying a common source. This may confirm bacterial and fungal summer activity in the Svalbard Archipelago (Bauer et al., 2008). Mannitol has a potential cryoprotectant role (Weinstein et al., 1997) in fungal spores, and has been found at high levels in maritime Antarctic soil due to the high production of mannitol under low-temperature conditions (Robinson, 2001). In addition, mannitol is also a common sugar alcohol in plants; it is particularly abundant in algae and has been detected in 70 higher plant families (Burshtein et al., 2011; Loescher, 1987). This suggests that mannitol may not be a specific biomarker for bacteria and fungi and indicates that it may also have a marine primary production source (Park et al., 2019).

Sucrose represents the 7% of the total load of saccharides (Table 1) and is highly correlated with arabitol and mannitol. This saccharide is present mainly in the coarse mode and is a key component of pollen grain (Yttri et al., 2007). Pollens were found in twenty species of tundra plants with flowers (Yao et al., 2013) collected in Ny-Ålesund. Sucrose was found to increase in concentration in afternoon in mid-latitude forests (Zhu et al., 2016), coinciding with the flowering time of the vegetation. The confirmed presence of spores in the Arctic tundra and their trend to grow faster in dry, mild or warm conditions suggests that sucrose has a possible local source.

5. Conclusions

We have applied two sensitive HPAEC-MS methods developed by Barbaro et al. (2015) to determine monosaccharides, disaccharides, alcohol-sugars and anhydrosugars in Arctic aerosol samples. As such, this study presents the first results on the sugar composition and concentrations in Svalbard aerosol.

We verified with BTs how anhydrosugars derive mainly from Russian wildfires and how iso-erythritol could be derived from biomass burning. We have even proposed the new diagnostic ratios of S/L and A/L ratio in order to strengthen L/M. Furthermore, the 2013 campaign showed how the level of anhydrosugars decreased in fine particles in the summer season.

Arabinose, arabitol and mannitol were associated primarily with coarse aerosols in summer, suggesting local transport, while these compounds do not show significant differences in spring. The 2013 campaign showed a clear difference between spring and summer, with a strong concentration increase in arabinose, arabitol and mannitol due to the exposure of the ground during summer around Ny Ålesund.

Declaration of competing interest

The authors declare that they have no known competing financial interests or personal relationships that could have appeared to influence the work reported in this paper.

Acknowledgements

The scientific activity in Ny-Ålesund was carried out in the framework of the National Research Council of Italy (CNR) polar program. Logistical support of the CNR - Department of Earth System Science and Environmental Technologies (DTA) is gratefully acknowledged. We want to thank all colleagues at the CNR Dirigibile Italia Arctic Station

who worked during the field campaign. The authors are also grateful for meteorological data from the Climate Change Tower Integrated Project (CCT-IP) of the National Research Council. We acknowledge the help of ELGA LabWater which provides the ultrapure water used in these experiments. The authors gratefully acknowledge the NOAA Air Resources Laboratory (ARL) for the provision of the HYSPLIT transport and dispersion model and READY website (<http://www.ready.noaa.gov>) used in this publication. We would also like to thank Dr. Warren Raymond Lee Cairns for the revision of our manuscript.

Appendix A. Supplementary data

Supplementary data to this article can be found online at <https://doi.org/10.1016/j.scitotenv.2019.136089>.

References

- Barbante, C., Spolaor, A., Cairns, W.R., Boutron, C., 2017. Man's footprint on the Arctic environment as revealed by analysis of ice and snow. *Earth-Science Rev* 168, 218–231. <https://doi.org/10.1016/j.earscirev.2017.02.010>.
- Barbaro, E., Kirchgorg, T., Zangrando, R., Vecchiato, M., Piazza, R., Barbante, C., Gambaro, A., 2015. Sugars in Antarctic aerosol. *Atmos. Environ.* 118, 135–144. <https://doi.org/10.1016/j.atmosenv.2015.07.047>.
- Bauer, H., Claeys, M., Vermeylen, R., Schueller, E., Weinke, G., Berger, A., Puxbaum, H., 2008. Arabinol and mannitol as tracers for the quantification of airborne fungal spores. *Atmos. Environ.* 42, 588–593. <https://doi.org/10.1016/j.atmosenv.2007.10.013>.
- Bazzano, A., Cappelletti, D., Udisti, R., Grotti, M., 2016. Long-range transport of atmospheric lead reaching Ny-Ålesund: inter-annual and seasonal variations of potential source areas. *Atmos. Environ.* 139, 11–19. <https://doi.org/10.1016/j.atmosenv.2016.05.026>.
- Becagli, S., Lazzara, L., Marchese, C., Dayan, U., Ascanius, S.E., Cacciani, M., Caiazza, L., Di Biagio, C., Di Iorio, T., di Sarra, A., Eriksen, P., Fani, F., Giardi, F., Meloni, D., Muscari, G., Pace, G., Severi, M., Traversi, R., Udisti, R., 2016. Relationships linking primary production, sea ice melting, and biogenic aerosol in the Arctic. *Atmos. Environ.* 136, 1–15. <https://doi.org/10.1016/j.atmosenv.2016.04.002>.
- Bielecki, R.L., 1995. Onset of phloem export from senescent petals of daylily. *Plant Physiol.* 109, 557–565. <https://doi.org/10.1104/pp.109.2.557>.
- Burget, E.G., Verma, R., Møhlhøj, M., Reiter, W.-D., 2003. The biosynthesis of L-arabinose in plants: molecular cloning and characterization of a Golgi-localized UDP-D-xylose 4-epimerase encoded by the MUR4 gene of *Arabidopsis*. *Plant Cell* 15, 523–531. <https://doi.org/10.1105/tpc.008425>.
- Burshtein, N., Lang-Yona, N., Rudich, Y., 2011. Ergosterol, arabinol and mannitol as tracers for biogenic aerosols in the eastern Mediterranean. *Atmos. Chem. Phys.* 11, 829–839. <https://doi.org/10.5194/acp-11-829-2011>.
- Chen, J., Kawamura, K., Liu, C.Q., Fu, P., 2013. Long-term observations of saccharides in remote marine aerosols from the western North Pacific: a comparison between 1990–1993 and 2006–2009 periods. *Atmos. Environ.* 67, 448–458. <https://doi.org/10.1016/j.atmosenv.2012.11.014>.
- Chiang, C., Knight, S.G., 1961. L-Arabinose metabolism by cell-free extracts of *Penicillium chrysogenum*. *Biochim. Biophys. Acta* 46, 271–278. [https://doi.org/10.1016/0006-3002\(61\)90750-8](https://doi.org/10.1016/0006-3002(61)90750-8).
- Cowie, G.L., Hedges, J.L., 1984. Carbohydrate sources in a coastal marine environment. *Geochim. Cosmochim. Acta* 48, 2075–2087. [https://doi.org/10.1016/0016-7037\(84\)90388-0](https://doi.org/10.1016/0016-7037(84)90388-0).
- Draxler, R.R., 1997. Description of the Hysplit_4 Modeling System. NOAA Tech. Memo (ERL ARL-224).
- Draxler, R.R., 1998. An overview of the HYSPLIT_4 modelling system for trajectories, dispersion and deposition. *Aust. Meteorol. Mag.* 47, 295–308.
- Draxler, R.R., 1999. Hysplit_4 user's guide. NOAA Tech. Memo. ERL ARL-230.
- Elbert, W., Taylor, P.E., Andreae, M.O., Pöschl, U., 2007. Contribution of fungi to primary biogenic aerosols in the atmosphere: wet and dry discharged spores, carbohydrates, and inorganic ions. *Atmos. Chem. Phys.* 7, 4569–4588. <https://doi.org/10.5194/acp-7-4569-2007>.
- Eleftheriadis, K., Vratolis, S., Nyeki, S., 2009. Aerosol black carbon in the European Arctic: Measurements at Zeppelin station, Ny-Ålesund, Svalbard from 1998–2007. *Geophys. Res. Lett.* 36, 1–5. <https://doi.org/10.1029/2008GL035741>.
- Engling, G., Lee, J.J., Tsai, Y.W., Lung, S.C.C., Chou, C.K.K., Chan, C.Y., 2009. Size-resolved anhydrosugar composition in smoke aerosol from controlled field burning of rice straw. *Aerosol Sci. Technol.* 43, 662–672. <https://doi.org/10.1080/02786820902825113>.
- Fabbri, D., Torri, C., Simoneit, B.R.T., Marynowski, L., Rushdi, A.I., Fabiańska, M.J., 2009. Levoglucosan and other cellulose and lignin markers in emissions from burning of Miocene lignites. *Atmos. Environ.* 43, 2286–2295. <https://doi.org/10.1016/j.atmosenv.2009.01.030>.
- Feltracco, M., Barbaro, E., Kirchgorg, T., Spolaor, A., Turetta, C., Zangrando, R., Barbante, C., Gambaro, A., 2019. Free and combined L- and D-amino acids in Arctic aerosol. *Chemosphere* 220, 412–421. <https://doi.org/10.1016/j.chemosphere.2018.12.147>.
- Fu, P., Kawamura, K., Barrie, L.A., 2009a. Photochemical and other sources of organic compounds in the Canadian High Arctic aerosol pollution during winter - spring. *Environ. Sci. Technol.* 43, 286–292.
- Fu, P.Q., Kawamura, K., Pochanart, P., Tanimoto, H., Kanaya, Y., Wang, Z.F., 2009b. Summertime contributions of isoprene, monoterpenes, and sesquiterpene oxidation to the formation of secondary organic aerosol in the troposphere over Mt. Tai, Central East China during. *Atmos. Chem. Phys. Discuss.* 9, 16941–16972. <https://doi.org/10.5194/acpd-9-16941-2009>.
- Fu, P., Kawamura, K., Kobayashi, M., Simoneit, B.R.T., 2012. Seasonal variations of sugars in atmospheric particulate matter from Gosan, Jeju Island: significant contributions of airborne pollen and Asian dust in spring. *Atmos. Environ.* 55, 234–239. <https://doi.org/10.1016/j.atmosenv.2012.02.061>.
- Fu, P., Kawamura, K., Chen, J., Charrière, B., Sempéré, R., 2013. Organic molecular composition of marine aerosols over the Arctic Ocean in summer: contributions of primary emission and secondary aerosol formation. *Biogeosciences* 10, 653–667. <https://doi.org/10.5194/bg-10-653-2013>.
- Giardi, F., Becagli, S., Traversi, R., Frosini, D., Severi, M., Caiazza, L., Ancillotti, C., Cappelletti, D., Moroni, B., Grotti, M., Bazzano, A., Lupi, A., Mazzola, M., Vitale, V., Abollino, O., Ferrero, L., Bolzacchini, E., Viola, A., Udisti, R., 2016. Size distribution and ion composition of aerosol collected at Ny-Ålesund in the spring-summer field campaign 2013. *Rend. Lincei* 27, 47–58. <https://doi.org/10.1007/s12210-016-0529-3>.
- Graham, B., Guyon, P., Taylor, P.E., Artaxo, P., Maenhaut, W., Glovsky, M.M., Flagan, R.C., Andreae, M.O., 2003. Organic compounds present in the natural Amazonian aerosol: characterization by gas chromatography-mass spectrometry. *J. Geophys. Res. Atmos.* 108. <https://doi.org/10.1029/2003JD003990> n/a-n/a.
- Haga, D.I., Iannone, R., Wheeler, M.J., Mason, R., Polishchuk, E.A., Fetch, T., Van Der Kamp, B.J., McKendry, I.G., Bertram, A.K., 2013. Ice nucleation properties of rust and bunt fungal spores and their transport to high altitudes, where they can cause heterogeneous freezing. *J. Geophys. Res. Atmos.* 118, 7260–7272. <https://doi.org/10.1002/jgrd.50556>.
- Hawkins, L.N., Russell, L.M., 2010. Polysaccharides, proteins, and phytoplankton fragments: four chemically distinct types of marine primary organic aerosol classified by single particle spectromicroscopy. *Adv. Meteorol.* 2010, 1–14. <https://doi.org/10.1155/2010/612132>.
- Huffman, J.A., Prenni, A.J., DeMott, P.J., Pöhlker, C., Mason, R.H., Robinson, N.H., Fröhlich-Nowoisky, J., Tobo, J., Després, V.R., Garcia, E., Gochis, D.J., Harris, E., Müller-German, L., Ruzene, C., Schmer, B., Sinha, B., Day, D.A., Andreae, M.O., Jimenez, J.L., Gallagher, M., Kreidenweis, S.M., Bertram, A.K., Pöschl, U., 2013. High concentrations of biological aerosol particles and ice nuclei during and after rain. *Atmos. Chem. Phys.* 13, 6151–6164. <https://doi.org/10.5194/acp-13-6151-2013>.
- Iinuma, Y., Brüggemann, E., Gnauk, T., Müller, K., Andreae, M.O., Helas, G., Parmar, R., Herrmann, H., 2007. Source characterization of biomass burning particles: the combustion of selected European conifers, African hardwood, savanna grass, and German and Indonesian peat. *J. Geophys. Res. Atmos.* 112. <https://doi.org/10.1029/2006JD007120>.
- Ila Gosselin, M., Rathnayake, C.M., Crawford, I., Pöhlker, C., Fröhlich-Nowoisky, J., Schmer, B., Després, V.R., Engling, G., Gallagher, M., Stone, E., Pöschl, U., Alex Huffman, J., 2016. Fluorescent bioaerosol particle, molecular tracer, and fungal spore concentrations during dry and rainy periods in a semi-arid forest. *Atmos. Chem. Phys.* 16, 15165–15184. <https://doi.org/10.5194/acp-16-15165-2016>.
- Jaenicke, R., 1980. Atmospheric aerosol and global climate. *J. Aerosol Sci.* 11, 577–588.
- Jeffries, T.W., 1985. Emerging technology for fermenting D-xylose. *Trends Biotechnol.* 3, 208–212.
- Jia, Y., Fraser, M., 2011. Characterization of saccharides in size-fractionated ambient particulate matter and aerosol sources: the contribution of primary biological aerosol particles (PBAPs) and soil to ambient particulate matter. *Environ. Sci. Technol.* 45, 930–936. <https://doi.org/10.1021/es103104e>.
- Lee, N., Gielow, W., Martin, R., Hamilton, E., Fowler, A., 1986. The organization of the arabad operon of *Escherichia coli*. *Gene* 47, 231–244. [https://doi.org/10.1016/0378-1119\(86\)90067-3](https://doi.org/10.1016/0378-1119(86)90067-3).
- Lee, J.J., Engling, G., Candice Lung, S.C., Lee, K.Y., 2008. Particle size characteristics of levoglucosan in ambient aerosols from rice straw burning. *Atmos. Environ.* 42, 8300–8308. <https://doi.org/10.1016/j.atmosenv.2008.07.047>.
- Li, Z., Chen, Y., Li, W., Deng, H., Fang, G., 2015. Organic tracers of primary biological aerosol particles at subtropical Okinawa Island in the western North Pacific Rim. *J. Geophys. Res. Atmos.* 120, 5504–5523. <https://doi.org/10.1002/2015JD023618>. Received.
- Loescher, W.H., 1987. Physiology and Metabolism of Sugar Alcohols in Higher Plants. 70, pp. 553–557. <https://doi.org/10.1111/j.1399-3054.1987.tb02857.x>.
- Medeiros, P.M., Conte, M.H., Weber, J.C., Simoneit, B.R.T., 2006. Sugars as source indicators of biogenic organic carbon in aerosols collected above the Howland Experimental Forest, Maine. *Atmos. Environ.* 40, 1694–1705. <https://doi.org/10.1016/j.atmosenv.2005.11.001>.
- Morris, C.E., Sands, D.C., Glaux, C., Samsatly, J., Asaad, S., Moukamel, A.R., Gonçalves, F.L.T., Bigg, E.K., 2013. Urediospores of rust fungi are ice nucleation active at >−10 °C and harbor ice nucleation active bacteria. *Atmos. Chem. Phys.* 13, 4223–4233. <https://doi.org/10.5194/acp-13-4223-2013>.
- Oliveira, C., Pio, C., Alves, C., Evtuygina, M., Santos, P., Gonçalves, V., Nunes, T., Silvestre, A.J.D., Palmgren, F., Wählin, P., Harrad, S., 2007. Seasonal distribution of polar organic compounds in the urban atmosphere of two large cities from the North and South of Europe. *Atmos. Environ.* 41, 5555–5570. <https://doi.org/10.1016/j.atmosenv.2007.03.001>.
- Oros, D.R., Simoneit, B.R.T., 2001. Identification and emission factors of molecular tracers in organic aerosols from biomass burning part 2. *Deciduous Trees*. 16.
- Oros, D.R., Abas, M.R. bin, Omar, N.Y.M.J., Rahman, N.A., Simoneit, B.R.T., 2006. Identification and emission factors of molecular tracers in organic aerosols from biomass burning: part 3. *Grasses*. *Appl. Geochem.* 21, 919–940. <https://doi.org/10.1016/j.apgeochem.2006.01.008>.
- Pacini, E., 2000. From anther and pollen ripening to pollen presentation. *Plant Syst. Evol.* 222, 19–43. <https://doi.org/10.1007/BF00984094>.

- Park, J., Dall'Osto, M., Park, K., Kim, J.-H., Park, J., Park, K.-T., Hwang, C.Y., Jang, G.I., Gim, Y., Kang, S., Park, S., Jin, Y.K., Yum, S.S., Simó, R., Yoon, Y.J., 2019. Arctic primary aerosol production strongly influenced by riverine organic matter. *Environ. Sci. Technol.* 53, 8621–8630. <https://doi.org/10.1021/acs.est.9b03399>.
- Pashynska, V., Vermeulen, R., Vas, G., Maenhaut, W., Claeys, M., 2002. Development of a gas chromatographic/ion trap mass spectrometric method for the determination of levoglucosan and saccharidic compounds in atmospheric aerosols. Application to urban aerosols. *J. Mass Spectrom.* 37, 1249–1257. <https://doi.org/10.1002/jms.391>.
- Pietrogrande, M.C., Bacco, D., Visentin, M., Ferrari, S., Casali, P., 2014. Polar organic marker compounds in atmospheric aerosol in the Po Valley during the Supersito campaigns - part 2: seasonal variations of sugars. *Atmos. Environ.* 97, 215–225. <https://doi.org/10.1016/j.atmosenv.2014.07.056>.
- Pietrogrande, M.C., Barbaro, E., Bove, M.C., Clauser, G., Colombi, C., Corbella, L., Cuccia, E., Dalla Torre, S., Decesari, S., Fermo, P., Gambaro, A., Gianelle, V., Ielpo, P., Larcher, R., Lazzari, P., Massabò, D., Melchionna, G., Nardin, T., Paglione, M., Perrino, C., Prati, P., Visentin, M., Zanca, N., Zangrando, R., 2017. Results of an interlaboratory comparison of analytical methods for quantification of anhydrosugars and biosugars in atmospheric aerosol. *Chemosphere* 184, 269–277. <https://doi.org/10.1016/j.chemosphere.2017.05.131>.
- Pio, C.A., Legrand, M., Alves, C.A., Oliveira, T., Afonso, J., Caseiro, A., Puxbaum, H., Sanchez-Ochoa, A., Gelencsér, A., 2008. Chemical composition of atmospheric aerosols during the 2003 summer intense forest fire period. *Atmos. Environ.* 42, 7530–7543. <https://doi.org/10.1016/j.atmosenv.2008.05.032>.
- Prentiss, A.J., Petters, M.D., Kreidenweis, S.M., Heald, C.L., Martin, S.T., Artaxo, P., Garland, R.M., Wollny, A.G., Pöschl, U., 2009. Relative roles of biogenic emissions and saharan dust as ice nuclei in the amazon basin. *Nat. Geosci.* 2, 402–405. <https://doi.org/10.1038/ngeo517>.
- Pummer, B.G., Bauer, H., Bernardi, J., Bleicher, S., Grothe, H., 2012. Suspendable macromolecules are responsible for ice nucleation activity of birch and conifer pollen. *Atmos. Chem. Phys.* 12, 2541–2550. <https://doi.org/10.5194/acp-12-2541-2012>.
- Scalabrin, E., Zangrando, R., Barbaro, E., Kehrwald, N.M., Gabrieli, J., Barbante, C., Gambaro, A., 2012. Amino acids in Arctic aerosols. *Atmos. Chem. Phys.* 12, 10453–10463. <https://doi.org/10.5194/acp-12-10453-2012>.
- Scaramboni, C., Urban, R.C., Lima-Souza, M., Nogueira, R.F.P., Cardoso, A.A., Allen, A.G., Campos, M.L.A.M., 2015. Total sugars in atmospheric aerosols: an alternative tracer for biomass burning. *Atmos. Environ.* 100, 185–192. <https://doi.org/10.1016/j.atmosenv.2014.11.003>.
- Schmidl, C., Marr, L.L., Caseiro, A., Kotianová, P., Berner, A., Bauer, H., Kasper-Giebl, A., Puxbaum, H., 2008. Chemical characterisation of fine particle emissions from wood stove combustion of common woods growing in mid-European alpine regions. *Atmos. Environ.* 42, 126–141. <https://doi.org/10.1016/j.atmosenv.2007.09.028>.
- Schumann, U., 2012. Atmospheric Physics. <https://doi.org/10.1007/978-3-642-29190-6>.
- Simoneit, B.R.T., 2002. Biomass burning - a review of organic tracers for smoke from incomplete combustion. *Appl. Geochem.* [https://doi.org/10.1016/S0883-2927\(01\)00061-0](https://doi.org/10.1016/S0883-2927(01)00061-0).
- Simoneit, B.R.T., Elias, V.O., Kobayashi, M., Kawamura, K., Rushdi, A.I., Medeiros, P.M., Rogge, W.F., Didyk, B.M., 2004. Sugars-dominant water-soluble organic compounds in soils and characterization as tracers in atmospheric particulate matter. *Environ. Sci. Technol.* 38, 5939–5949. <https://doi.org/10.1021/es0403099>.
- Stein, A.F., Draxler, R.R., Rolph, G.D., Stunder, B.J.B., Cohen, M.D., Ngan, F., 2015. NOAA's hybrid atmospheric transport and dispersion modeling system. *Bull. Am. Meteorol. Soc.* 96, 2059–2077. <https://doi.org/10.1175/BAMS-D-14-00110.1>.
- Stohl, A., Andrews, E., Burkhardt, J.F., Forster, C., Herber, A., Hoch, S.W., Kowal, D., Lunder, C., Mefford, T., Ogren, J.A., Sharma, S., Spichtinger, N., Stebel, K., Stone, R., Ström, J., Tørseth, K., Wehrli, C., Yttri, K.E., 2006a. Pan-Arctic enhancements of light absorbing aerosol concentrations due to North American boreal forest fires during summer 2004. *J. Geophys. Res.* Atmos. 111. <https://doi.org/10.1029/2006JD007216>.
- Stohl, A., Berg, T., Burkhardt, J.F., Fjæraa, aM, Forster, C., Herber, A., Hov, Ø., Lunder, C., McMillan, W.W., Oltmans, S., Shiobara, M., Simpson, D., Solberg, S., Stebel, K., Ström, J., Tørseth, K., Treffeisen, R., Virkkunen, K., Yttri, K.E., 2006b. Arctic smoke - record high air pollution levels in the European Arctic due to agricultural fires in Eastern Europe. *Atmos. Chem. Phys. Discuss.* 6, 9655–9722. <https://doi.org/10.5194/acpd-6-9655-2006>.
- Tsai, Y.I., Sopajaree, K., Chotruksa, A., Wu, H.C., Kuo, S.C., 2013. Source indicators of biomass burning associated with inorganic salts and carboxylates in dry season ambient aerosol in Chiang Mai Basin, Thailand. *Atmos. Environ.* 78, 93–104. <https://doi.org/10.1016/j.atmosenv.2012.09.040>.
- Turetta, C., Zangrando, R., Barbaro, E., Gabrieli, J., Scalabrin, E., Zennaro, P., Gambaro, A., Toscano, G., Barbante, C., 2016. Water-soluble trace, rare earth elements and organic compounds in Arctic aerosol. *Rend. Lincei* 27, 95–103. <https://doi.org/10.1007/s12210-016-0518-6>.
- Udisti, R., Bazzano, A., Becagli, S., Bolzacchini, E., Caiazza, L., Cappelletti, D., Ferrero, L., Frosini, D., Giardi, F., Grotti, M., Lupi, A., Malandrino, M., Mazzola, M., Moroni, B., Severi, M., Traversi, R., Viola, A., Vitale, V., 2016. Sulfate source apportionment in the Ny-Ålesund (Svalbard Islands) Arctic aerosol. *Rend. Lincei* 27, 85–94. <https://doi.org/10.1007/s12210-016-0517-7>.
- Urban, R.C., Alves, C.A., Allen, A.G., Cardoso, A.A., Queiroz, M.E.C., Campos, M.L.A.M., 2014. Sugar markers in aerosol particles from an agro-industrial region in Brazil. *Atmos. Environ.* 90, 106–112. <https://doi.org/10.1016/j.atmosenv.2014.03.034>.
- VanKuyk, P.A., De Groot, M.J.L., Ruijter, G.J.G., De Vries, R.P., Visser, J., 2001. The *Aspergillus Niger* D-xylulose kinase gene is co-expressed with genes encoding arabinan degrading enzymes, and is essential for growth on D-xylulose and L-arabinose. *Eur. J. Biochem.* 268, 5414–5423. <https://doi.org/10.1046/j.0014-2956.2001.02482.x>.
- Vecchiato, M., Barbaro, E., Spolaor, A., Burgay, F., Barbante, C., Piazza, R., Gambaro, A., 2018. Fragrances and PAHs in snow and seawater of Ny-Ålesund (Svalbard): local and long-range contamination. *Environ. Pollut.* 242, 1740–1747. <https://doi.org/10.1016/j.envpol.2018.07.095>.
- von Schneidmesser, E., Schauer, J.J., Hagler, G.S.W., Bergin, M.H., 2009. Concentrations and sources of carbonaceous aerosol in the atmosphere of summit, Greenland. *Atmos. Environ.* 43, 4155–4162. <https://doi.org/10.1016/j.atmosenv.2009.05.043>.
- Ward, T.J., Hamilton, R.F., Dixon, R.W., Paulsen, M., Simpson, C.D., 2006. Characterization and evaluation of smoke tracers in PM: results from the 2003 Montana wildfire season. *Atmos. Environ.* 40, 7005–7017. <https://doi.org/10.1016/j.atmosenv.2006.06.034>.
- Witteveen, C.F., Busink, R., Van De Vondervoort, P., C. D., K. S., Visser, J., 1989. L-Arabinose and D-xylulose catabolism in *Aspergillus niger*. *J. Gen. Microbiol.* 135, 2163–2171.
- Yan, C., Zheng, M., Sullivan, A.P., Bosch, C., Desyaterik, Y., Andersson, A., Li, X., Guo, X., Zhou, T., Gustafsson, Ö., Collett, J.L., 2014. Chemical characteristics and light-absorbing property of water-soluble organic carbon in Beijing: biomass burning contributions. *Atmos. Environ.* 121, 4–12. <https://doi.org/10.1016/j.atmosenv.2015.05.005>.
- Yao, Y., Zhao, Q., Bera, S., Li, X., Li, C., 2013. Pollen morphology of selected tundra plants from the high Arctic of Ny-Ålesund, Svalbard. *Adv. Polar Sci.* 23, 103–115. <https://doi.org/10.3724/sp.j.1085.2012.00103>.
- Yttri, K.E., Dye, C., Kiss, G., 2007. Ambient aerosol concentrations of sugars and sugar-alcohols at four different sites in Norway. *Atmos. Chem. Phys. Discuss.* 7, 5769–5803. <https://doi.org/10.5194/acpd-7-5769-2007>.
- Yttri, K.E., Lund Myhre, C., Eckhardt, S., Fiebig, M., Dye, C., Hirdman, D., Ström, J., Klimont, Z., Stohl, A., 2014. Quantifying black carbon from biomass burning by means of levoglucosan - a one-year time series at the Arctic observatory Zeppelin. *Atmos. Chem. Phys.* 14, 6427–6442. <https://doi.org/10.5194/acp-14-6427-2014>.
- Zangrando, R., Barbaro, E., Zennaro, P., Rossi, S., Kehrwald, N.M., Gabrieli, J., Barbante, C., Gambaro, A., 2013. Molecular markers of biomass burning in Arctic aerosols. *Environ. Sci. Technol.* 47, 8565–8574. <https://doi.org/10.1021/es400125r>.
- Zangrando, R., Barbaro, E., Kirchgöreg, T., Vecchiato, M., Scalabrin, E., Radaelli, M., Đorđević, D., Barbante, C., Gambaro, A., 2016a. Five primary sources of organic aerosols in the urban atmosphere of Belgrade (Serbia). *Sci. Total Environ.* 571, 1441–1453. <https://doi.org/10.1016/j.scitotenv.2016.06.188>.
- Zangrando, R., Barbaro, E., Vecchiato, M., Kehrwald, N.M., Barbante, C., Gambaro, A., 2016b. Levoglucosan and phenols in Antarctic marine, coastal and plateau aerosols. *Sci. Total Environ.* 544, 606–616. <https://doi.org/10.1016/j.scitotenv.2015.11.166>.
- Zhu, C., Kawamura, K., Fukuda, Y., Mochida, M., Iwamoto, Y., 2016. Fungal spores overwhelm biogenic organic aerosols in a midlatitudinal forest. *Atmos. Chem. Phys.* 16, 7497–7506. <https://doi.org/10.5194/acp-16-7497-2016>.



Contents lists available at ScienceDirect

Science of the Total Environment

journal homepage: www.elsevier.com/locate/scitotenv

Year-round measurements of size-segregated low molecular weight organic acids in Arctic aerosol



Matteo Feltracco^{a,*}, Elena Barbaro^{b,a}, Andrea Spolaor^{b,a}, Marco Vecchiato^b, Alice Callegaro^b, François Burgay^{a,c}, Massimiliano Vardè^{b,d}, Niccolò Maffezzoli^a, Federico Dallo^b, Federico Scoto^e, Roberta Zangrando^b, Carlo Barbante^{a,b}, Andrea Gambaro^{a,b}

^a Department of Environmental Sciences, Informatics and Statistics, Ca' Foscari University of Venice, Via Torino 155, 30172 Venice, Italy

^b Institute of Polar Sciences - National Research Council of Italy (ISP-CNR), Via Torino 155, 30172 Venice, Italy

^c Laboratory of Environmental Chemistry, Paul Scherrer Institute, 5232 Villigen, Switzerland

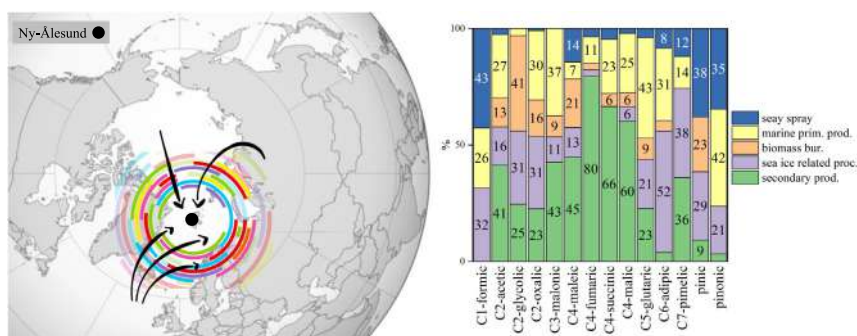
^d Department of Chemical and Pharmaceutical Sciences, University of Ferrara, via L. Borsari 46, Ferrara 44121, Italy

^e Institute of Atmospheric Sciences and Climate, National Research Council of Italy (ISAC-CNR), SP Lecce-Monteroni Km 1.2, 73100 Lecce, Italy

HIGHLIGHTS

- A year-round record of organic acids was studied in Arctic aerosols.
- The study investigates sources and seasonal trend of particulate organic acids.
- The study provides an overview of the change of sources throughout the seasons.
- PMF defines five sources for low molecular weight organic acids.

GRAPHICAL ABSTRACT



ARTICLE INFO

Article history:

Received 7 August 2020

Received in revised form 7 October 2020

Accepted 9 October 2020

Available online 14 October 2020

Editor: Pingqing Fu

Keywords:

Arctic
Aerosol
Organic acids
Ions
PMF

ABSTRACT

Organic acids in aerosols Earth's atmosphere are ubiquitous and they have been extensively studied across urban, rural and polar environments. However, little is known about their properties, transport, source and seasonal variations in the Svalbard Archipelago. Here, we present the annual trend of organic acids in the aerosol collected at Ny-Ålesund and consider their size-distributions to infer their possible sources and relative contributions. A series of carboxylic acids were detected with a predominance of C2-oxalic acid. Pinic acid and cis-pinonic acid were studied in order to better understand the oxidative and gas-to-particle processes occurred in the Arctic atmosphere. Since the water-soluble organic fraction is mainly composed by organic acids and ions, we investigated how the seasonal variation leads to different atmospheric transport mechanisms, focusing on the chemical variations between the polar night and boreal summer. Using major ions, levoglucosan and MSA, the Positive Matrix Factorization (PMF) identified five different possible sources: a) sea spray; b) marine primary production; c) biomass burning; d) sea ice related process and e) secondary products.

© 2020 Elsevier B.V. All rights reserved.

1. Introduction

Svalbard is a region of the Arctic undergoing rapid climate change, with warming occurring at a faster rate than the global average (Maturilli et al., 2015). In winter, due to cyclonic storms associated

* Corresponding author.

E-mail address: matteo.feltracco@unive.it (M. Feltracco).

with anomalous warming events (Rinke et al., 2017), atmospheric circulation patterns concentrate into the Svalbard Archipelago an increasing flux of pollutants sourced from Central Europe, Scandinavia and Northern Russia (Kozak et al., 2013). This has a large impact on atmospheric aerosol sources and sinks as well as on cloud property distribution in the Svalbard region (Tunved et al., 2013). Atmospheric aerosols play an important role in regulating climate (Fu et al., 2015), because they can interfere with solar radiation by scattering and absorption, influencing the radiation energy balance of the earth system (Haywood and Boucher, 2000; Haywood and Shine, 1995). Furthermore, aerosol particles can act as cloud condensation nuclei (CCN), leading to the formation of a larger number of water droplets that increase the clouds reflectivity.

The sources determination of such particles is crucial to better interpret their impact on Arctic environment. During summer and autumn, the transport from mid-latitudes decreases due to weaker vertical stratification and an enhanced of wet scavenging in-route (Garrett et al., 2010). In winter, the Arctic air mass can cover a larger area: its mean position in January shows that the large end of the mass is anchored in Eurasia while the narrow end projects into North America (Kawamura et al., 1996; Tunved et al., 2013). In fact, biomass burning aerosols originating from Russia and Siberia are an important component of spring-time Arctic aerosols (Feltracco et al., 2020; Warneke et al., 2009) and eastern European agricultural fires improve the air pollution levels in the European Arctic (Stohl et al., 2006).

Recently, research on Arctic aerosols has been focusing on major ions (Feltracco et al., 2019; Geng et al., 2010; Giardi et al., 2016; Udisti et al., 2016), anhydrosugars (Feltracco et al., 2020; Fu et al., 2009a; Zangrando et al., 2013), amino acids (Feltracco et al., 2019; Scalabrin et al., 2012), black carbon (BC) (Eleftheriadis et al., 2009; Stohl, 2006), and to a lesser extent to secondary organic aerosol (SOA) deriving from organic pollutants and biogenic volatile organic compounds (i.e. carboxylic acids) (Fu et al., 2013a; Narukawa et al., 2002, 2003). Some studies detected short-chain organic acids in the Arctic atmosphere in both size-segregated and PM₁₀ aerosols (Fu et al., 2009a; Kawamura et al., 1996; Kerminen et al., 1999). Carboxylic acids (CAs) have different emission sources in the atmosphere, although these they have not been well constrained yet. CAs can be produced by photochemical reactions of oxidation of anthropogenic organic pollutants (Mochida et al., 2007). Once emitted in the atmosphere, CA precursors undergo oxidation or photochemical reactions (Kawamura et al., 1996). The aerosol concentration of carboxylic acids can be also influenced by primary sources, such as biomass burning (Falkovich et al., 2005) and marine emissions (Rinaldi et al., 2011). The quantification of each source contribution is unknown yet. Pinic acid and cis-pinonic acid derive from the photo-oxidation of α -pinene, the most important monoterpene released by biogenic sources, particularly conifers (Guenther et al., 1995). These acids were mainly studied in rural and urban aerosols (Feltracco et al., 2018; Fu et al., 2009c; Haque et al., 2016; Parshintsev et al., 2010).

Here, we evaluate and describe for the first time the all-year around seasonal variations in Svalbard aerosol of the following organic acids: C1-formic, C2-oxalic, C2-acetic, C2-glycolic, C3-malonic, C4-succinic, hC4-malic, cis-usC4-maleic, trans-usC4-fumaric, C5-glutaric, C6-adipic, C7-pimelic, pinic and pinonic acids. The samples were collected with a time resolution from 6 to 10 days at Gruevbadet Laboratory, close to Ny Ålesund (Svalbard Island - 78°55'03"N, 11°53'39"E) from 26th February 2018 to 26th February 2019, with a technical stop during September 2018. Particles were collected in six different fractions (10.0–7.2 μm (S1), 7.2–3.0 μm (S2), 3.0–1.5 μm (S3), 1.5–0.95 μm (S4), 0.95–0.49 μm (S5), <0.49 μm (B)). The main aim of this paper is to define a source apportionment of CAs using the size distributions and a chemometric approach. Positive Matrix Factorization (PMF) was performed using a dataset composed of CAs, major ions, methanesulfonate (MSA) and levoglucosan. Major ions and in particular Na⁺, Cl⁻, and Mg²⁺ are used to define the sea spray contribution (Raes et al., 2002), MSA is

commonly considered a marker of marine primary production (Gondwe et al., 2003), while levoglucosan is the specific tracers of biomass burning (Simoneit et al., 1999). This paper wants to define the different source contributions to CAs in Arctic aerosols across a full year period.

2. Experimental

2.1. Sampling collection, processing and instrumental analysis

A multi-stage Andersen impactor (TE-6000 series, Tisch Environmental Inc.) was used to collect aerosol samples on six pre-combusted (4 h at 400 °C in a muffle furnace) quartz fiber filters. The sampler accumulated particles with a cut-off diameters of 10.0 μm , 7.2 μm , 3.0 μm , 1.5 μm , and 0.95 μm on slotted filters and <0.49 μm on backup filter. The frequency of sampling varied from 6 to 10 days, for a total air volume of 9000 or 15000 m³ per sample. Field blanks were obtained using the same filters installed on the sampler with the air pump switched off. Both samples and blanks were wrapped in a double layer of aluminium foil and stored at -20 °C until analysis. Carboxylic acids and major ions are determined using the Barbaro et al. (2017) pre-analytical procedure, already applied to investigate these species in Antarctica. Briefly, the samples preparation consists of an extraction of a quarter of sample in ultrasonic bath with 7 mL and 15 mL of ultrapure water for slotted and back-up filters, respectively.

The anion analysis (Cl⁻, NO₃⁻, Br⁻, I⁻, SO₄²⁻, MSA and CAs) was performed using an IC (Thermo Scientific™ Dionex™ ICS-5000, Waltham, US) equipped with an anionic exchange column (Dionex IonPac AS11 2 × 250 mm) and a guard column (Dionex Ion Pac AG11 2 × 50 mm) coupled to a single quadrupole mass spectrometer (MSQ Plus™, Thermo Scientific™, Bremen, Germany). Cationic species (Li⁺, Na⁺, Mg²⁺, Ca²⁺, K⁺, NH₄⁺) were determined using a capillary IC (Thermo Scientific Dionex ICS-5000), equipped with a capillary cation exchange column (Dionex IonPac CS19-4 μm , 0.4 × 250 mm), a guard column (Dionex IonPac CG19-4 μm , 0.4 × 50 mm) connected with a conductivity detector (Barbaro et al., 2017).

Pinic and cis-pinonic acid were differently extracted using half filter that was spiked with the isotopically labelled vanillin ¹³C₆ (500 absolute ng for slotted filters and 1500 absolute ng for back-up filters) and then extracted twice for 15 min with ultrapure water in an ultrasonic bath. The slotted filters were extracted with 9 mL followed by 1 mL of ultrapure water, while the back-up filters were extracted with 25 mL followed by 5 mL of ultrapure water. All the extracts were filtered through a 0.45 μm , Ø13mm polytetrafluoroethylene (PTFE) filter (Whatman, Maidstone, Kent, UK) before analysis.

The instrumental method, described in details in the Supplementary Material, were performed with an Agilent 1100 Series HPLC System (Waldbronn, Germany) coupled to an API 4000 Triple Quadrupole Mass Spectrometer (Applied Biosystem/MDS SCIEX, Concord, Ontario, Canada), using the same procedure reported by Feltracco et al. (2018). All reagents and standards solutions used in this study are reported in the Supplementary Information.

2.2. Atmospheric circulation and PMF

To understand the general transport pattern of air masses recorded at the sampling site, we conducted a 7-days backward trajectories analysis, by starting a trajectory every 6 h at 500 m a.s.l. using the Hybrid Single-Particle Lagrangian Integrated Trajectory (HYSPPLIT) model (Draxler, 1998). This method has been widely used to understand the transport and origins of air pollutants (Ding et al., 2013; Stohl et al., 2003). Based on the backward particle release simulation, the cluster aggregation was displayed for each month (Fig. S3).

To characterize the source of short-chain organic acids, the PMF method was applied (Paatero and Tapper, 1994). PMF is a factor analysis method that utilizes non-negativity constraints for the analysis of

environmental data and associated error estimates. The goal of PMF is to identify the number of factors/sources, their chemical profiles, and the amount of mass, associated with each factor/source, that contributed to measured PM concentrations. The model uses data for all concentration and uncertainty values for all j species and i days. Data confidence can be maintained by adjusting the uncertainties for real observations. This allows the user to downgrade the importance of these data in the least squares fit. PMF is more thoroughly described in previous publications (Lee et al., 1999; Paatero and Tapper, 1994; Viana et al., 2008). For the current analysis, the U.S. EPA version of PMF was used (EPA PMF 5.0), which is based on the multilinear engine ME-2 developed by Paatero (1999). The application of PMF depends on uncertainties for each of the measured data values. The uncertainty estimation provides a useful tool to decrease the weight of missing and below detection limits data in the solution. In this work, the widely adopted procedure suggested by Polissar et al. (1998) was used for the measurement data and the associated uncertainties as the input data. The input dataset has been composed with the concentrations of all detected chemical species ($n = 26$) in PM₁₀ samples ($n = 46$), obtained by the sum of six different size ranges. The values below the detection limits (MDL) were substituted by half of MDL. As uncertainty, we used the relative standard deviations of the procedural method reported in our previous paper (Barbaro et al., 2017). The uncertainty of values under MDL was 5/6 MDL. Uncertainties in the PMF results have been obtained using the bootstrap method. We also add extra modelling uncertainty of 5% which is applied to all species. This value encompasses various errors that are not considered measurement or analytical errors. The PM₁₀ mass was not included as total variable in the datasets (not available) and the source apportionment was conducted to the sum of the all species analysed. The determination of the factors optimal number was achieved by considering the parameters IM (maximum individual column mean), and IS (maximum individual column standard deviation), obtained from the scaled residual matrix, together with Q-values (goodness of fit parameter) (Lee et al., 1999; Viana et al., 2008).

3. Results and discussion

3.1. Concentrations and size-distribution of organic acids

The main result of this paper is to give an all-year round trend from March 2018 to March 2019 of carboxylic, pinonic and pinic acids composition of Arctic atmospheric aerosol. To better understand and support the annual trend observed, we compared the 2018–19 data with our unpublished data collected during three spring and summer campaigns. These sampling collections were performed from 13th April to 9th September 2013, from 2nd April to 29th June 2014, and from 14th April to 13th June 2015. Table 1 shows the mean PM₁₀ concentrations of CAs on a seasonal basis for every sampling campaign.

CAs and pinonic and pinic acids concentrations are very variable through the years (Fig. S1), mainly due to their diversified sources and the chemical transformation they undergo during the long-range atmospheric transport. C2-oxalic acid was always the most abundant CA detected (accounts for 31–53% of the total CA concentration) with a very similar concentration throughout all campaigns (from 4 to 7 ng m⁻³). C3-malonic and C1-formic acids were the second and third most abundant compounds (respectively 7–30% and 4–23% of the total CAs). Some short-chain CAs are well known as “end products” of photochemical oxidation of organic precursors or other carboxylic acids with atmospheric oxidants (Kawamura and Sakaguchi, 1999). Indeed, C4-succinic acid can be degraded to C3-malonic acid by decarboxylation reactions activated by OH radicals (Fu et al., 2013b). This explains why C3-malonic acid are one of the most concentrated CA. Other CAs, including the long-chain compounds, always accounted for less than 10%. Similar relative abundances, but with lower concentrations, were found by Kawamura et al. (1995, 1996) in the very first study of CAs in 1987–1988 campaign at the Alert site (Canadian Arctic), suggesting a uniform CAs spatial

Table 1
Seasonal averages of PM₁₀ (ng m⁻³) organic acids concentrations during the 2013, 2014, 2015 and 2018–19 campaigns. Winter samplings are reported as either “Feb-Mar” or “Dec-Feb”.

	C1-formic	C2-acetic	C2-glycolic	C2-oxalic	C3-malonic	C4-fumaric	C4-maleic	C4-malic	C4-succinic	C5-glutaric	C6-adipic	C7-pimelic	Pinonic a.	Pinic a.
2013	4 ± 3	4 ± 2	0.7 ± 0.3	5 ± 3	1 ± 1	0.02 ± 0.02	0.2 ± 0.2	0.6 ± 0.3	0.8 ± 0.4	0.3 ± 0.2	0.1 ± 0.1	0.01 ± 0.02	0.2 ± 0.2	0.2 ± 0.2
Summer	3 ± 1	1.2 ± 0.3	0.6 ± 0.1	3 ± 1	1.0 ± 0.5	0.01 ± 0.02	0.08 ± 0.03	0.7 ± 0.4	0.7 ± 0.3	0.3 ± 0.1	0.02 ± 0.02	0.02 ± 0.02	0.08 ± 0.04	0.04 ± 0.04
2014	1 ± 1	0.8 ± 0.3	0.5 ± 0.3	4 ± 2	0.8 ± 0.4	0.04 ± 0.03	0.05 ± 0.03	0.4 ± 0.3	0.2 ± 0.1	0.06 ± 0.04	0.03 ± 0.02	<0.006	0.2 ± 0.1	0.1 ± 0.1
2015	1 ± 1	1 ± 1	0.6 ± 0.7	7 ± 3	6 ± 2	0.03 ± 0.02	0.07 ± 0.04	0.9 ± 0.4	1.4 ± 0.5	0.3 ± 0.2	0.1 ± 0.1	0.05 ± 0.03	0.3 ± 0.2	0.1 ± 0.1
Feb-Mar	2 ± 2	1 ± 1	0.8 ± 0.3	8 ± 3	0.7 ± 0.2	0.03 ± 0.02	0.4 ± 0.2	0.4 ± 0.1	0.2 ± 0.1	0.1 ± 0.1	0.5 ± 0.3	0.04 ± 0.02	0.05 ± 0.03	0.2 ± 0.1
2018	1 ± 1	0.6 ± 0.4	0.4 ± 0.4	6 ± 3	0.8 ± 0.5	0.05 ± 0.04	0.1 ± 0.1	0.5 ± 0.3	0.2 ± 0.1	0.1 ± 0.1	0.02 ± 0.1	0.02 ± 0.01	0.07 ± 0.04	0.1 ± 0.1
Spring	1 ± 1	1 ± 1	1 ± 1	6 ± 2	2 ± 1	0.1 ± 0.1	0.3 ± 0.2	1 ± 1	0.9 ± 0.4	0.4 ± 0.3	0.3 ± 0.2	0.05 ± 0.04	0.07 ± 0.05	0.1 ± 0.1
Summer	1 ± 1	1 ± 1	1 ± 1	6 ± 2	2 ± 1	0.1 ± 0.1	0.3 ± 0.2	1 ± 1	0.9 ± 0.4	0.4 ± 0.3	0.3 ± 0.2	0.05 ± 0.04	0.07 ± 0.05	0.1 ± 0.1
Autumn	0.1 ± 0.1	0.1 ± 0.1	0.2 ± 0.1	1 ± 1	0.08 ± 0.03	<0.001	0.1 ± 0.1	0.04 ± 0.02	0.04 ± 0.05	0.03 ± 0.01	0.07 ± 0.03	0.01 ± 0.01	0.01 ± 0.02	0.1 ± 0.1
Dec-Feb	1 ± 1	0.3 ± 0.3	0.8 ± 0.4	2 ± 1	0.2 ± 0.1	<0.003	0.2 ± 0.1	0.08 ± 0.04	0.06 ± 0.02	0.03 ± 0.01	0.06 ± 0.02	<0.004	0.03 ± 0.01	0.2 ± 0.1

distribution in Arctic aerosols. Here we found a peak value of oxalic acid in March 2018 (during polar sunrise) of $8 \pm 3 \text{ ng m}^{-3}$ (Fig. S1), while Kawamura et al. (1995, 1996) found a concentration peak of 40 ng m^{-3} in March 1988. Furthermore, the average concentration of CAs at Ny-Ålesund shown in Table 1 are similar to those studied in the coastal site of MZS, Antarctica (Barbaro et al., 2017) and one order of magnitude lower than those reported in urban aerosols from central Alaska (Deshmukh et al., 2018) and Eastern Italian Alps (Barbaro et al., 2020), probably due to the difference in the sources distances. These species were probably emitted in the middle latitude and then undergo a long-range atmospheric transport to arrive in the Arctic region. This speculation is then confirmed by our results about the sources, reported in Section 3.4.

Pinonic and pinic acids always accounted for a marginal contribution to the total CA concentration (up to 3%, together). Several studies describe pinonic acid as a first generation product, produced by the photo-oxidation of α -pinene (Jimenez et al., 2009), while pinic acid derives from pinonic acid through further oxidation processes (Feltracco et al., 2018; Librando and Tringali, 2005). Both acids can be further degraded due to the long-range transport, which in turn explains the low concentration values found in Ny-Ålesund (pinonic acid $0.01\text{--}0.3 \text{ ng m}^{-3}$, pinic acid $0.04\text{--}0.2 \text{ ng m}^{-3}$, Table 1). These concentrations were similar to those found at another Ny-Ålesund sampling site (Zeppelin Station) and Station Nord (Greenland) (Hansen et al., 2014) and up to 3 order of magnitude lower for pinonic and pinic acid than those reported in the Canadian High Arctic (Fu et al., 2009b) and Eastern Italian Alps (Barbaro et al., 2020). Short-chained C1 and C2 acids showed major peaks from March to June in all the selected years (Fig. S1), although other peaks appeared in late summer in 2013 and 2018. A similar trend concentration was reported by Kawamura et al. (1996) in a one-year observation in 1988 at Alert.

C2-oxalic acid drove the annual concentration of CAs in the 2018–19 campaign, representing the 50% of all the studied compounds, and peaked in summer (Figs. 1 and S1). Short chain CAs (C1 and C2, although we detected a minor contribution for C4-maleic and C6-adipic) also showed an enrichment in winter 2018, that included the polar sunrise occurred at Ny-Ålesund on Feb 18th (Fig. S1). Pinonic and pinic acids have a reverse trend: pinonic acid peaked in summer, while pinic acid showed its major concentration in the two winter periods.

The trend of pinonic acid might be explained by the increase of the photo oxidative capacity of the summer atmosphere that constantly produces cis-pinonic acid from the precursor, being a first-generation product (Barbaro et al., 2019; Feltracco et al., 2018; Jimenez et al., 2009). The low concentration detected after polar sunrise for pinic acid suggests a further degradation due to the increase of photo oxidation processes in the atmosphere (Müller et al., 2012).

Fig. 1 also shows the aerosol particle-size distribution. Such distribution of all low molecular weight organic acids was uniform through the year and all species were mainly distributed in the fine fraction ($<0.95 \mu\text{m}$). The only exceptions are represented by C1-formic, peaking in spring, C4-fumaric peaking in summer and C6-adipic peaking in winter 2018. All these species presented a sporadic presence in coarse particles (57% - 85% of the total PM_{10}).

3.2. Source apportionment approach

To identify the sources of the low molecular weight organic acids sources using specific and known markers, a PMF was performed, by including in the CAs dataset also major ions, MSA and levoglucosan. Na^+ , Cl^- , and Mg^{2+} are originated by sea spray; conversely, Ca^{2+} , K^+ , and SO_4^{2-} have relevant contributions from other sources, especially crustal aerosol and anthropic/biogenic emissions (also using nss-SO_4^{2-} , calculated as $[\text{SO}_4^{2-}] - 0.253 \times [\text{Na}^+]$) (Fisher et al., 2011; Giardi et al., 2016). MSA is originated by the atmospheric oxidation of dimethyl sulphide (DMS), emitted by phytoplankton (Gondwe et al., 2003), while levoglucosan is a specific indicator for biomass burning emissions (Simoneit et al., 1999).

The source apportionment approach gave a reasonable solution with five factors. The comparison of aerosol concentrations reconstructed by the PMF and those real measured showed that the PMF can reconstruct the observed PM_{10} concentrations (as sum of six size intervals), with a slope of 0.98 and an R^2 of 0.88. The profile of each factor is shown in Fig. 2, in terms of concentrations (bars) and in terms of relative concentrations (black points), while the temporal trend of each factor is shown in Fig. 3.

The first factor (F1) describes 47% of the total PM_{10} concentration, and it is mainly characterized by saline ions and a non-negligible contribution from C1-formic, pinic and pinonic acids (Fig. 2). The presence of

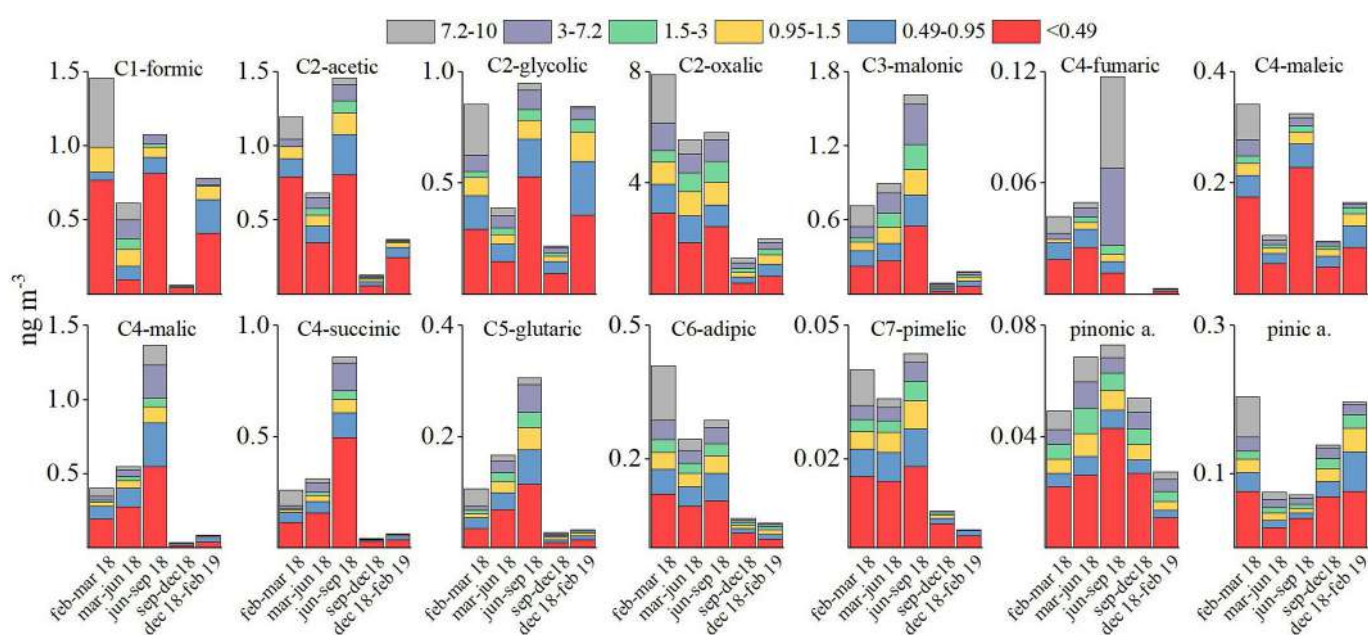


Fig. 1. Average concentrations of carboxylic acids, pinonic and pinic acids, relative particle size-distribution (μm) and seasonal variation of Arctic aerosol.

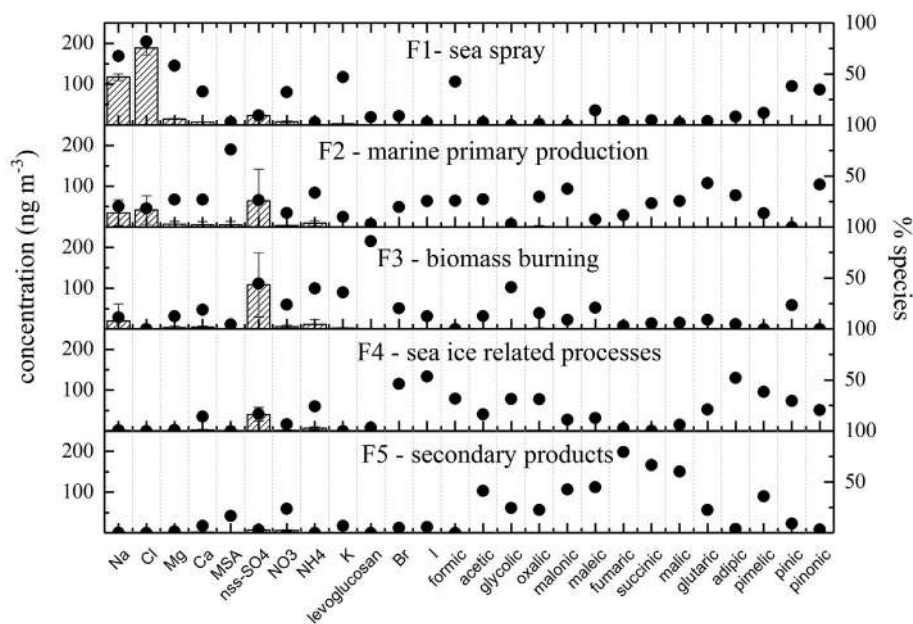


Fig. 2. Source profiles obtained with the PMF. The bars identify the species in ng m^{-3} that mainly characterize each factor profile. Error bars were obtained with bootstrap method. The black points describe the species in terms of relative concentrations.

Na^+ and Cl^- , that are recognized as specific tracers of sea salt aerosol (Gong, 2003; O'Dowd et al., 1997; Perrino et al., 2009; Raes et al., 2002), suggests that this factor represents the sea spray component.

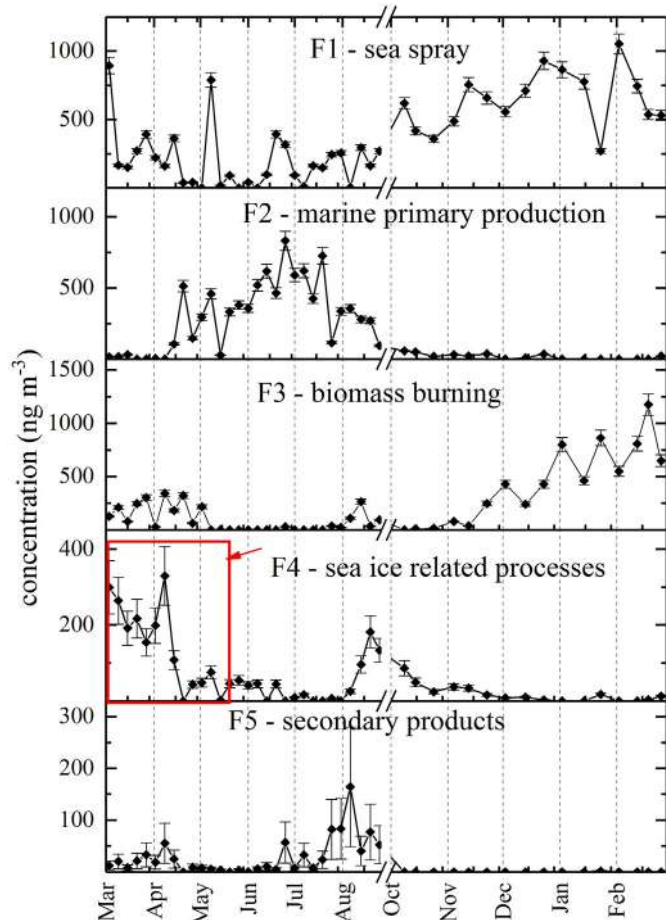


Fig. 3. Factor contributions estimated by PMF during the sampling period.

To confirm this, Na^+ and Cl^- were mainly distributed in the coarse fraction ($D > 0.95 \mu\text{m}$) during all-year around, and especially in the particles with diameters above $3 \mu\text{m}$. The contribution of C1-formic, pinic and pinonic acids in F1 could be due to the gas-to-particles conversion in the sea-salt particles that further transported these organic acids (Arlander et al., 1990; Baboukas et al., 2000; Feltracco et al., 2018; Paulot et al., 2011). Furthermore, these acids can also have a common origin: the photo-oxidation of natural hydrocarbons (isoprene and terpenes) emitted from the forest (Kavouras et al., 1998).

The second factor (F2), mainly loaded with MSA, NH_4^+ , C3-malonic, C5-glutaric and pinonic acids, describes 23% of the simulated PM_{10} concentration (Fig. 2). Other compounds were also present, including CAs, nss-SO_4^{2-} , Br^- , I^- , etc. MSA is the main products of DMS, emitted during algal bloom (Gondwe et al., 2003), and this suggest that the marine primary production is represented by the F2. The presence of several compounds in F2 indicates the high complexity of the marine input, with the phytoplankton-associated compounds being the most relevant ones. Thus, greater emission of marine derived organic matter in the Arctic activates the sea/air exchange of seawater lipid components, which are enriched in a microlayer of seawater surface (Kawamura et al., 1996; Marty et al., 1979). The presence of CAs may be primarily controlled by biological activity conditions (Kawamura et al., 1996). It should be noted that surface seawater contains a large amount of water soluble organic compounds, ranging from small organic acids, sugars to large molecular weight proteins, which can be emitted into the atmosphere in remote oceans (Facchini et al., 2008; Fu et al., 2013a; Hawkins and Russell, 2010; Leck and Bigg, 2005). This could explain the presence of pinonic acid in this factor. The presence of Br^- may be attributed to the presence of organo-bromine-synthesizing algae (Sturges, 1990), while I^- is related to marine biological production (Cuevas et al., 2018) directly related to Arctic sea ice thinning (Horvat et al., 2017).

The third factor (F3) is characterized by levoglucosan, nss-SO_4^{2-} , NH_4^+ , K^+ and C2-glycolic acid, representing the biomass burning contribution (Fig. 2). It described 20% of the simulated PM_{10} concentration. Oxidation of SO_2 pollution, either in the gas phase or by heterogeneous processes in sea-salt aerosols or cloud droplets, is considered to be the source of most of the nss-SO_4^{2-} found in aerosols and precipitation in remote marine regions (Keene et al., 1986). The contribution of NH_4^+ and K^+ suggests their anthropogenic contribution (Hegg et al., 1988). The

K^+ load is certainly due to the presence of $nss-K^+$ (calculated as $[K^+] - 0.037 \times [Na^+]$), considered as a tracer for biomass burning (Andreae, 1983; Legrand et al., 2016; Zhao et al., 2016). C2-glycolic acid can be produced by biomass burning and fossil fuel combustion (Ervens and Volkamer, 2010; Volkamer et al., 2001) explaining its presence in F3, and also from the gas phase oxidation of volatile organic compounds (VOCs) (Myriokefalitakis et al., 2011).

The fourth factor (F4, 7%) is loaded with Br^- , I^- and C6-adipic and C7-pimelic acids, with a slight contribution by other CAs (Fig. 2). The high relative concentration of bromine and iodine suggests a sea-ice contribution (Sturges and Barrie, 1988). The connection between bromine emissions and sea ice extent has been recently suggested. Spolaor et al. (2016) hypothesised that Br^- deposition in Arctic regions and its subsequent preservation in ice cores could be used as a tracer for changes in sea ice cover. Springtime photochemical recycling of BrO is observed over first-year sea ice (FYSI) and heterogeneous and photochemical recycling of bromine that involved the FYSI is called “bromine explosion” and is associated with marginal sea ice regions (Frieß et al., 2004). The extent of Br^- explosions is well known from satellite measurements (Frieß et al., 2011), which show the increase of BrO in the springtime in the Arctic atmosphere. Iodine can be released by the snow-pack with the photo oxidation of iodide in ice with the resulting production of I_3^- and evaporable molecular iodine I_2 and, the emission of an iodine photo-fragments following the heterogeneous photoreduction of iodate in ice (Gálvez et al., 2016; Kim et al., 2016). The long chain CAs presents in F4 may be controlled by atmospheric oxidation of precursor fatty acids in the microlayer (Kawamura et al., 1996) or by an emission probably linked the sub-ice algal populations.

The fifth factor (F5) describes the 3% of the total concentration estimated by PMF, and it loads with the majority of the CAs, excluding C1-formic, C6-adipic, pinic and pinonic acids. A huge contribution (>60%) was given by C4-fumaric, succinic and malic acids (Fig. 2). We assume that F5 represents the secondary photo oxidation products. Photochemical oxidation of aromatic hydrocarbons such as benzene and toluene predominantly produces C4-maleic acid, which can be further isomerized to result in trans-C4-fumaric acid during long-range transport (Kawamura and Sakaguchi, 1999). This explains the lower relative concentration of C4-maleic acid in the Factor 5. Succinic acid is likely an oxidation product of gaseous aliphatic acids, which are in part produced by photo-induced oxidations of fatty acids (Kawamura and Gagosian, 1987) and other precursors such as n-alkanes, aldehydes and ketocarboxylic acids (Kawamura et al., 1996). Furthermore, C4-malic acid is an intermediate of the production of C3-malonic acid by the photochemical oxidation of succinic acid (Kawamura and Ikushima, 1993).

The C3-malonic/C4-succinic acids ratio can be used as an indicator of enhanced photo-chemical production of diacids (Kawamura and Ikushima, 1993), as C4-succinic acid can be degraded to C3-malonic acid by decarboxylation reactions activated by OH radicals. The mean C3/C4 ratio calculated in the Arctic sampling campaign was 6 ± 3 in winter, 6 ± 3 in spring, 4 ± 1 in summer, and 8 ± 2 in autumn for coarse particles and had a lower constant value (2 ± 1) during all-year around for fine particles. The higher ratio in coarse particles suggests a not-defined local source of C3-malonic acid and likely excludes a degradation process from C4 to C3, due to the lower surface area of coarse particles. Conversely, the fine fraction that contained these species underwent long range transport processes, where photochemical degradation occurred.

Cis-usC4-maleic (M) can also isomerize due to solar radiation to trans-usC4-fumaric (F). The ratio F/M in mid-March showed the highest value in PM_{10} (2.4), suggesting a long-range conversion of unsaturated diacids in the Arctic atmosphere during polar sunrise in spring, while F/M in coarse aerosol increased to 3.9 in August suggesting a gradual isomerization due to the low available surface area in such fraction. The ratio decreased in winter to 0.02 ± 0.01 , due to the absence of sunlight that triggers the photo-chemical reaction.

3.3. Temporal variations of each identified factor

The temporal variations in the concentrations of each identified factor are shown in Fig. 3. The “sea-spray” factor (F1) shows the higher concentration from October 2018 to March 2019. In general, sea salt aerosol emissions from the ocean maximizes in September and October in the Arctic region as a result of more frequent cyclonic system. Sea salt emissions from sea-ice due to blowing snow reach their maximum in December (Huang and Jaeglé, 2017). The source of sea salt from frost flower emissions maximize from December to March with a smaller influence compared to sea salt aerosol from sea spray and blowing snow (Huang and Jaeglé, 2017; Yang et al., 2010).

The “marine primary production” (F2) factor shows the clear late-spring and summer phytoplanktonic bloom, well detected by MSA. In mid-August, the concentrations of MSA drastically decreased, probably due to the change of the marine optical properties because of the increase of turbid waters originating from glacial outflow (Hop, 2002). The resulting turbidity controls the depth of the euphotic zone as well as the spectral composition of penetrating radiation (Svendsen et al., 2002; Urbanski et al., 1980) which directly influences phytoplankton composition and primary production (Piwosz et al., 2009).

The “biomass burning factor” (F3) allows to distinguish three events. From March to end of April 2018, F3 shows an increase of biomass burning particles (Fig. 3). This input is confirmed in spring, where back trajectories (Fig. S3) indicate possible forest fires from Northern Europe and Siberia, as already confirmed in the same period in 2013, 2014 and 2015 (Feltracco et al., 2020). These particles can have a very long lifetimes in spring and also in winter, due to the Arctic Haze phenomenon, that results in the transport of particulates to the Arctic and the trapping of the pollutant haze for up to 30 days (Quinn et al., 2007; Stohl et al., 2006). In mid-August 2018 we found the second biomass burning event: back trajectories in August clearly overlapped Northern Russia where in July 27 wildfires covered 8682 ha (nasa.gov). These events certainly affected the Arctic atmosphere during that period. The winter 2018–2019 season showed an enhanced F3 contribution, suggesting a strong intrusion of biomass burning particles from Northern Russia, confirmed by back trajectories showed in Fig. S3. The increased wintertime influence of biomass burning air masses was also detected in some previous works (Quinn et al., 2007; Yttri et al., 2007, 2014).

The “sea-ice related process” factor (F4), driven by Br^- and I^- , showed the highest concentration in spring and in late summer (Fig. 3). The bromine enrichment resulting from sea ice events, described in Section 3.2, was calculated as $Br_{enr} = Br/(Na \times 0.006)$ using the mass ratios of Br and Na and the average sea water Br/Na mass ratio (Millero et al., 2008). Here, we found the highest PM_{10} values of Br_{enr} from 9th March to 2nd May 2018 (Fig. S2), associated to FYSI-related springtime bromine processes (Spolaor et al., 2016). In addition, iodine followed the temporal trend of bromine during all the sampling period (Fig. S4). Since the presence of I^- could be partially related to marine biological production (Cuevas et al., 2018), the high load in late summer of I^- is may due to the sub-ice biological productivity, related to Arctic sea ice thinning (Horvat et al., 2017). No studied so far have clearly state if CAs can derive by emission from FYSI or sub-ice biological productivity and further investigation are necessary to better understand these phenomena. The summer peak of this factor is probably due to the emission of marine derived organic matter in the Arctic not connected with MSA, that activates a late-summer the sea/air exchange of seawater lipid components, which are enriched in a microlayer of seawater surface (Kawamura et al., 1996; Marty et al., 1979). The lipid components are further oxidised to produce long-chain CAs.

The “secondary products” factor (F5) shows a non-negligible first contribute from March to mid-April 2018, but the main concentration peak occurred from mid-July to the end of August (Fig. 3). Considering the size distribution, we can suppose that the presence of CAs appeared

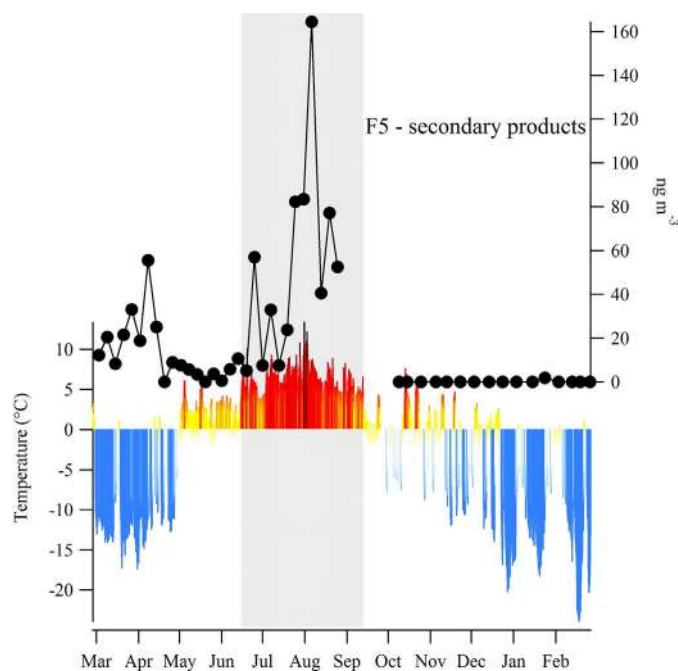


Fig. 4. Comparison of Factor 5 and temperature during the sampling period.

at the time of Arctic sunrise these acids are significantly produced in the Arctic atmosphere by photo-induced reactions. On the other hand, the presence of summer peak may be explained by three considerations: 1) some studies have suggested that soil emission is an important source of organic acids, including CAs, where production from terrestrial vegetation is low (Paulot et al., 2011). 2) The secondary products peak may also be the results of the rise in temperature. Some studies demonstrated how, on an annual basis, the formation of carboxylic acids can directly depend on temperature (Granby et al., 1997). Fig. 4 shows the temporal trend of F5, overlapped with air temperature (Maturilli, 2020). The 31st of July the temperature reached its maximum at 13.5 °C. This increase may have enhanced the photochemical transformation of organic precursors to carboxylic acids. 3) An undefined biomass burning event may have also been a possible source of secondary products during this period (Ervens and Volkamer, 2010;

Volkamer et al., 2001) since an overlap between the F5 peak and the biomass burning factor peak is observed (Fig. 3).

3.4. Source contributions of CAs

The five factors related to the described sources were modelled on PM₁₀ during the 2018–2019 campaign. Fig. 5 shows the relative percentage contribution on the sources of each CAs. According to the data reported, C1-formic, pinic and pinonic acids contributed to 35–43% in the sea spray factor (F1), while the marine primary production factor (F2) was present significantly for most of the target compounds, with C3-malonic acid (37%) and C5-glutaric acid (43%) as main contributors. The biomass burning contribution (F3) was predominant for C2-glycolic acid (41%) with a contribution <23% for C4-maleic and pinic acid. F4, related to sea ice chemistry, was significant for shorter (C1, C2, C3) and longer acids (C5, C6, C7) including pinic and pinonic acids. The middle-chain did not show any relevant contribution. The last factor, related to marine primary production, affected all the CAs with a slight contribution for C6-adipic acid.

4. Conclusions

Aerosols were collected with a multi-stage cascade impactor at Ny-Ålesund, Svalbard Island, considering one-year of sampling, from March 2018 to March 2019. The main purpose of the study was to investigate the sources and the seasonal trend of particulate low molecular weight organic acids, using major ions as ancillary data. The size distribution of low molecular weight organic acids was uniform throughout the year and these species were mainly distributed in the fine fraction, although C1-formic in spring, C4-fumaric in summer and C6-adipic in winter 2018 presented an occasional presence in coarse particles. On the basis of the available dataset of chemical species, five different sources were suggested on the basis of the PMF results: 1) sea spray, 2) marine primary production, 3) biomass burning, 4) sea ice related process and 5) secondary products. Furthermore, this approach gave us an overview of the change of sources throughout the seasons, depending on various climate phenomena and atmospheric processes.

The presence of C1-formic, pinic and pinonic acids in the sea spray factor suggests a gas-to-particles conversion in the sea-salt particles. This factor reached its maximum in winter. The factor 2, named as “marine primary production”, shows the spring and summer concentration

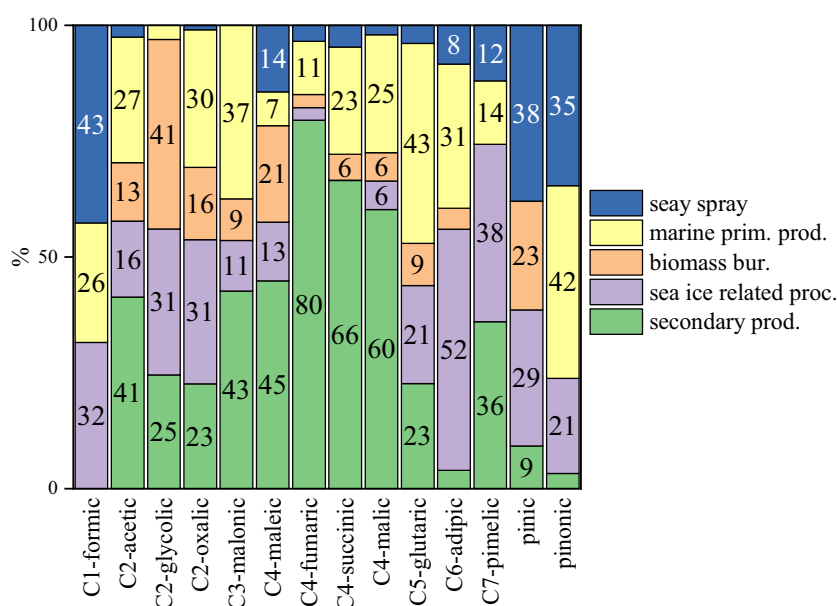


Fig. 5. Relative percentage contribution on factors for each CAs.

increase. The presence of several organic acids in this factor indicates the high complexity of marine inputs, with the algae bloom as main source. The “biomass burning” factor had an important load in March and April and winter, with also an event detected in mid-August 2018. Here we found C2-glycolic showed a strong contribution. Factor 4, nominated as “sea-ice related process” was significant for shorter (C1, C2, C3) and longer acids (C5, C6, C7) including pinic and pinonic acids with a strong contribution in March and April 2018. The peak of F4 in late summer was probably due to sub-ice biological productivity or sea/air exchange of lipid components. The “secondary products” factor identified the majority of CAs, due to their well known secondary organic aerosol origin. F5 peaked during polar sunrise and in late summer.

CRedit authorship contribution statement

Matteo Feltracco: Conceptualization, Investigation, Formal analysis, Data curation, Writing - original draft, Writing - review & editing. **Elena Barbaro:** Conceptualization, Investigation, Formal analysis, Data curation, Writing - original draft, Writing - review & editing. **Andrea Spolaor:** Conceptualization, Data curation. **Marco Vecchiato:** Investigation. **Alice Callegaro:** Investigation. **François Burgay:** Investigation. **Massimiliano Vardè:** Investigation. **Niccolò Maffezzoli:** Investigation. **Federico Dallo:** Investigation. **Federico Scoto:** Investigation. **Roberta Zangrando:** Investigation. **Carlo Barbante:** Validation, Supervision. **Andrea Gambaro:** Validation, Supervision.

Declaration of competing interest

The authors declare that they have no known competing financial interests or personal relationships that could have appeared to influence the work reported in this paper.

Acknowledgements

This project has received funding from the European Union's Horizon 2020 research and innovation programme under grant agreement no. 689443, project iCUPE (Integrative and Comprehensive Understanding on Polar Environments). It is a result of the multi and interdisciplinary research activities based at the Arctic Station Dirigibile Italia managed and coordinated by Institute of Polar Sciences of the National Research Council of Italy.

Appendix A. Supplementary data

Supplementary data to this article can be found online at <https://doi.org/10.1016/j.scitotenv.2020.142954>.

References

- Andreae, M.O., 1983. Soot carbon and excess fine potassium: long-range transport of combustion-derived aerosols. *Science* 220, 10–13.
- Arlander, D.W., Cronn, D.R., Farmer, J.C., Menzia, F.A., Westberg, H.H., 1990. Gaseous oxygenated hydrocarbons in the remote marine troposphere. *J. Geophys. Res.* 95. <https://doi.org/10.1029/jd095id10p16391>.
- Baboukas, E.D., Kanakidou, M., Mihalopoulos, N., 2000. Carboxylic acids in gas and particulate phase above the Atlantic Ocean. *J. Geophys. Res. Atmos.* 105, 14459–14471. <https://doi.org/10.1029/1999JD900977>.
- Barbaro, E., Padoan, S., Kirchgeorg, T., Zangrando, R., Toscano, G., Barbante, C., Gambaro, A., 2017. Particle size distribution of inorganic and organic ions in coastal and inland Antarctic aerosol. *Environ. Sci. Pollut. Res.* 24, 2724–2733. <https://doi.org/10.1007/s11356-016-8042-x>.
- Barbaro, E., Feltracco, M., Cesari, D., Padoan, S., Zangrando, R., Contini, D., Barbante, C., Gambaro, A., 2019. Characterization of the water soluble fraction in ultrafine, fine, and coarse atmospheric aerosol. *Sci. Total Environ.* 658, 1423–1439. <https://doi.org/10.1016/j.scitotenv.2018.12.298>.
- Barbaro, E., Morabito, E., Gregoris, E., Feltracco, M., Gabrieli, J., Vardè, M., Cairns, W.R.L., Dallo, F., De Blasi, F., Zangrando, R., Barbante, C., Gambaro, A., 2020. Col Margherita Observatory: a background site in the Eastern Italian Alps for investigating the chemical composition of atmospheric aerosols. *Atmos. Environ.* 221. <https://doi.org/10.1016/j.atmosenv.2019.117071>.

- Cuevas, C.A., Maffezzoli, N., Corella, J.P., Spolaor, A., Vallelonga, P., Kjær, H.A., Simonsen, M., Winstrup, M., Vinther, B., Horvat, C., Fernandez, R.P., Kinnison, D., Lamarque, J.F., Barbante, C., Saiz-Lopez, A., 2018. Rapid increase in atmospheric iodine levels in the North Atlantic since the mid-20th century. *Nat. Commun.* 9, 1–6. <https://doi.org/10.1038/s41467-018-03756-1>.
- Deshmukh, D.K., Mozammel Haque, M., Kawamura, K., Kim, Y., 2018. Dicarboxylic acids, oxocarboxylic acids and α -dicarbonyls in fine aerosols over central Alaska: implications for sources and atmospheric processes. *Atmos. Res.* 202, 128–139. <https://doi.org/10.1016/j.atmosres.2017.11.003>.
- Ding, A., Wang, T., Fu, C., 2013. Transport characteristics and origins of carbon monoxide and ozone in Hong Kong, South China. *J. Geophys. Res. Atmos.* 118, 9475–9488. <https://doi.org/10.1002/jgrd.50714>.
- Draxler, R.R., 1998. An overview of the HYSPLIT_4 modelling system for trajectories, dispersion and deposition. *Aust. Meteorol. Mag.* 47, 295–308.
- Eleftheriadis, K., Vratolis, S., Nyeki, S., 2009. Aerosol black carbon in the European Arctic: measurements at zeppelin station, Ny-Ålesund, Svalbard from 1998–2007. *Geophys. Res. Lett.* 36, 1–5. <https://doi.org/10.1029/2008GL035741>.
- Ervens, B., Volkamer, R., 2010. Glyoxal processing by aerosol multiphase chemistry: towards a kinetic modeling framework of secondary organic aerosol formation in aqueous particles. *Atmos. Chem. Phys.* 10, 8219–8244. <https://doi.org/10.5194/acp-10-8219-2010>.
- Facchini, M.C., Rinaldi, M., Decesari, S., Carbone, C., Finessi, E., Mircea, M., Fuzzi, S., Ceburnis, D., Flanagan, R., Nilsson, E.D., de Leeuw, G., Martino, M., Woeltjen, J., O'Dowd, C.D., 2008. Primary submicron marine aerosol dominated by insoluble organic colloids and aggregates. *Geophys. Res. Lett.* 35, 1–6. <https://doi.org/10.1029/2008GL034210>.
- Falkovich, A.H., Graber, E.R., Schkolnik, G., Rudich, Y., Maenhaut, W., Artaxo, P., 2005. Low molecular weight organic acids in aerosol particles from Rondônia, Brazil, during the biomass-burning, transition and wet periods. *Atmos. Chem. Phys.* 5, 781–797. <https://doi.org/10.5194/acp-5-781-2005>.
- Feltracco, M., Barbaro, E., Contini, D., Zangrando, R., Toscano, G., Battistel, D., Barbante, C., Gambaro, A., 2018. Photo-oxidation products of α -pinene in coarse, fine and ultrafine aerosol: a new high sensitive HPLC-MS/MS method. *Atmos. Environ.* 180, 149–155. <https://doi.org/10.1016/j.atmosenv.2018.02.052>.
- Feltracco, M., Barbaro, E., Kirchgeorg, T., Spolaor, A., Turetta, C., Zangrando, R., Barbante, C., Gambaro, A., 2019. Free and combined L- and D-amino acids in Arctic aerosol. *Chemosphere* 220, 412–421. <https://doi.org/10.1016/j.chemosphere.2018.12.147>.
- Feltracco, M., Barbaro, E., Tedeschi, S., Spolaor, A., Turetta, C., Vecchiato, M., Morabito, E., Zangrando, R., Barbante, C., Gambaro, A., 2020. Interannual variability of sugars in Arctic aerosol: biomass burning and biogenic inputs. *Sci. Total Environ.* 706, 136089. <https://doi.org/10.1016/j.scitotenv.2019.136089>.
- Fisher, J.A., Jacob, D.J., Wang, Q., Bahreini, R., Carouge, C.C., Cubison, M.J., Dibb, J.E., Diehl, T., Jimenez, J.L., Leubensperger, E.M., Lu, Z., Meinders, M.B.J., Pye, H.O.T., Quinn, P.K., Sharma, S., Streets, D.G., van Donkelaar, A., Yantosca, R.M., 2011. Sources, distribution, and acidity of sulfate-ammonium aerosol in the Arctic in winter-spring. *Atmos. Environ.* 45, 7301–7318. <https://doi.org/10.1016/j.atmosenv.2011.08.030>.
- Frieß, U., Hollwedel, J., König-Langlo, G., Wagner, T., Platt, U., 2004. Dynamics and chemistry of tropospheric bromine explosion events in the Antarctic coastal region. *J. Geophys. Res. D Atmos.* 109, 1–15. <https://doi.org/10.1029/2003jd004133>.
- Frieß, U., Sihler, H., Sander, R., Phler, D., Yilmaz, S., Platt, U., 2011. The vertical distribution of BrO and aerosols in the Arctic: measurements by active and passive differential optical absorption spectroscopy. *J. Geophys. Res. Atmos.* 116, 1–19. <https://doi.org/10.1029/2011JD015938>.
- Fu, P., Kawamura, K., Barrie, L.A., 2009a. Photochemical and other sources of organic compounds in the Canadian High Arctic aerosol pollution during winter - spring. *Environ. Sci. Technol.* 43, 286–292.
- Fu, P., Kawamura, K., Chen, J., Barrie, L.A., 2009b. Isoprene, monoterpene, and sesquiterpene oxidation products in the High Arctic aerosols during late winter to early summer. *Environ. Sci. Technol.* 43, 4022–4028. <https://doi.org/10.1021/es803669a>.
- Fu, P., Kawamura, K., Pochanart, P., Tanimoto, H., Kanaya, Y., Wang, Z.F., 2009c. Summer-time contributions of isoprene, monoterpenes, and sesquiterpene oxidation to the formation of secondary organic aerosol in the troposphere over Mt. Tai, Central East China during. *Atmos. Chem. Phys. Discuss* 9, 16941–16972. <https://doi.org/10.5194/acpd-9-16941-2009>.
- Fu, P., Kawamura, K., Chen, J., Charrière, B., Sempéré, R., 2013a. Organic molecular composition of marine aerosols over the Arctic Ocean in summer: contributions of primary emission and secondary aerosol formation. *Biogeosciences* 10, 653–667. <https://doi.org/10.5194/bg-10-653-2013>.
- Fu, P., Kawamura, K., Usukura, K., Miura, K., 2013b. Dicarboxylic acids, ketocarboxylic acids and glyoxal in the marine aerosols collected during a round-the-world cruise. *Mar. Chem.* 148, 22–32. <https://doi.org/10.1016/j.marchem.2012.11.002>.
- Fu, P., Kawamura, K., Chen, J., Qin, M., Ren, L., Sun, Y., Wang, Z., Barrie, L.A., Tachibana, E., Ding, A., Yamashita, Y., 2015. Fluorescent water-soluble organic aerosols in the High Arctic atmosphere. *Sci. Rep.* 5, 1–8. <https://doi.org/10.1038/srep09845>.
- Gálvez, Ó., Teresa Baeza-Romero, M., Sanz, M., Saiz-Lopez, A., 2016. Photolysis of frozen iodate salts as a source of active iodine in the polar environment. *Atmos. Chem. Phys.* 16, 12703–12713. <https://doi.org/10.5194/acp-16-12703-2016>.
- Garrett, T.J., Zhao, C., Novelli, P.C., 2010. Assessing the relative contributions of transport efficiency and scavenging to seasonal variability in Arctic aerosol. *Tellus Ser. B Chem. Phys. Meteorol.* 62, 190–196. <https://doi.org/10.1111/j.1600-0889.2010.00453.x>.
- Geng, H., Ryu, J., Jung, H.J., Chung, H., Ahn, K.H.O., Ro, C.U.N., 2010. Single-particle characterization of summertime arctic aerosols collected at Ny-Ålesund, Svalbard. *Environ. Sci. Technol.* 44, 2348–2353. <https://doi.org/10.1021/es903268j>.
- Giardi, F., Becagli, S., Traversi, R., Frosini, D., Severi, M., Caiazzo, L., Ancillotti, C., Cappelletti, D., Moroni, B., Grotti, M., Bazzano, A., Lupi, A., Mazzola, M., Vitale, V., Abollino, O.,

- Ferrero, L., Bolzacchini, E., Viola, A., Udisti, R., 2016. Size distribution and ion composition of aerosol collected at Ny-Ålesund in the spring-summer field campaign 2013. *Rend. Lincei* 27, 47–58. <https://doi.org/10.1007/s12210-016-0529-3>.
- Gondwe, M., Krol, M., Gieskes, W., Klaassen, W., de Baar, H., 2003. The contribution of ocean-leaving DMS to the global atmospheric burdens of DMS, MSA, SO₂, and NSS SO₄ =. *Glob. Biogeochem. Cycles* 17. <https://doi.org/10.1029/2002gb001937> n/a-n/a.
- Gong, S.L., 2003. A parameterization of sea-salt aerosol source function for sub- and super-micron particles. *Glob. Biogeochem. Cycles* 17. <https://doi.org/10.1029/2003gb002079> n/a-n/a.
- Granby, K., Egeløv, A.H., Nielsen, T., Lohse, C., 1997. Carboxylic acids: seasonal variation and relation to chemical and meteorological parameters. *J. Atmos. Chem.* 28, 195–207. <https://doi.org/10.1023/A:1005877419395>.
- Guenther, A., Hewitt, C., Erickson, D., 1995. A global model of natural volatile organic compound emissions. *J. Geophys. Res.* 100, 8873–8892.
- Hansen, A.M.K., Kristensen, K., Nguyen, Q.T., Zare, A., Cozzi, F., Nøjgaard, J.K., Skov, H., Brandt, J., Christensen, J.H., Ström, J., Tunved, P., Krejci, R., Glasius, M., 2014. Organosulfates and organic acids in Arctic aerosols: speciation, annual variation and concentration levels. *Atmos. Chem. Phys.* 14, 7807–7823. <https://doi.org/10.5194/acp-14-7807-2014>.
- Haque, M.M., Kawamura, K., Kim, Y., 2016. Seasonal variations of biogenic secondary organic aerosol tracers in ambient aerosols from Alaska. *Atmos. Environ.* 130, 95–104. <https://doi.org/10.1016/j.atmosenv.2015.09.075>.
- Hawkins, L.N., Russell, L.M., 2010. Polysaccharides, proteins, and phytoplankton fragments: four chemically distinct types of marine primary organic aerosol classified by single particle spectromicroscopy. *Adv. Meteorol.* 2010, 1–14. <https://doi.org/10.1155/2010/612132>.
- Haywood, J., Boucher, O., 2000. Estimates of the direct and indirect radiative forcing due to tropospheric aerosols: a review. *Rev. Geophys.* 38, 513–543. <https://doi.org/10.1029/1999RG000078>.
- Haywood, J.M., Shine, K.P., 1995. The effect of anthropogenic sulfate and soot aerosol on the clear sky planetary radiation budget. *Geophys. Res. Lett.* 22, 603–606. <https://doi.org/10.1029/95GL00075>.
- Hegg, D.A., Radke, F.L., Hobbs, P.V., 1988. Ammonia emission from biomass burning. *Geophys. Res. Lett.* 15, 335–337.
- Hop, H., 2002. The marine ecosystem of Kongsfjorden, Svalbard. *Polar Res* 21, 167–208. <https://doi.org/10.1016/j.polar.2016.11.001>.
- Horvat, C., Jones, D.R., Iams, S., Schroeder, D., Flocco, D., Feltham, D., 2017. The frequency and extent of sub-ice phytoplankton blooms in the Arctic Ocean. *Sci. Adv.* 3. <https://doi.org/10.1126/sciadv.1601191>.
- Huang, J., Jaeglé, L., 2017. Wintertime enhancements of sea salt aerosol in polar regions consistent with a sea ice source from blowing snow. *Atmos. Chem. Phys.* 17, 3699–3712. <https://doi.org/10.5194/acp-17-3699-2017>.
- Jimenez, J.L., Canagaratna, M.R., Donahue, N.M., Prevot, A.S.H., Zhang, Q., Kroll, J.H., DeCarlo, P.F., Allan, J.D., Coe, H., Ng, N.L., Aiken, A.C., Docherty, K.S., Ulbrich, I.M., Grieshop, A.P., Robinson, A.L., Duplissy, J., Smith, J.D., Wilson, K.R., Lanz, V.A., Hueglin, C., Sun, Y.L., Tian, J., Laaksonen, A., Raatikainen, T., Rautiainen, J., Vaattovaara, P., Ehn, M., Kulmala, M., Tomlinson, J.M., Collins, D.R., Cubison, M.J., Dunlea, J., Huffman, J.A., Onasch, T.B., Alfarra, M.R., Williams, P.I., Bower, K., Kondo, Y., Schneider, J., Drewnick, F., Borrmann, S., Weimer, S., Demerjian, K., Salcedo, D., Cottrell, L., Griffin, R., Takami, A., Miyoshi, T., Hatakeyama, S., Shimojo, A., Sun, J.Y., Zhang, Y.M., Dzepina, K., Kimmel, J.R., Sueper, D., Jayne, J.T., Herndon, S.C., Trimborn, A.M., Williams, L.R., Wood, E.C., Middlebrook, A.M., Kolb, C.E., Baltensperger, U., Worsnop, D.R., 2009. Evolution of organic aerosols in the atmosphere. *Science* (80-) 326, 1525–1529. <https://doi.org/10.1126/science.1180353>.
- Kavouras, I.G., Mihalopoulos, N., Stephanou, E.G., 1998. Formation of atmospheric particles from organic acids produced by forests. *Nature* 372, 683–686. <https://doi.org/10.1038/27179>.
- Kawamura, K., Gagosian, B., 1987. Implications of ω-oxocarboxylic acids in the remote marine atmosphere for photo-oxidation of unsaturated fatty acids. *Lett. to Nat.* 325, 330–332.
- Kawamura, K., Ikushima, K., 1993. Seasonal changes in the distribution of dicarboxylic acids in the urban atmosphere. *Environ. Sci. Technol.* 27, 2227–2235. <https://doi.org/10.1021/es00047a033>.
- Kawamura, K., Sakaguchi, F., 1999. Molecular distributions of water soluble dicarboxylic acids in marine aerosols over the Pacific Ocean including tropics. *J. Geophys. Res.* 104, 3501–3509.
- Kawamura, K., Kasukabe, H., Yasui, O., Barrie, L.A., 1995. Production of dicarboxylic acids in the Arctic atmosphere at polar sunrise. *Geophys. Res. Lett.* 22, 1253–1256. <https://doi.org/10.1029/95GL00880>.
- Kawamura, K., Kasukabe, H., Barrie, L.A., 1996. Source and reaction pathways of dicarboxylic acids, ketoacids and dicarboxyls in Arctic aerosols: one year of observations. *Atmos. Environ.* 30, 1709–1722. [https://doi.org/10.1016/1352-2310\(95\)00395-9](https://doi.org/10.1016/1352-2310(95)00395-9).
- Keene, W.C., Pszenny, A.A.P., Galloway, J.N., Hawley, M.E., 1986. Sea-salt corrections and interpretation of constituent ratios in marine precipitation. *J. Geophys. Res.* 91, 6647. <https://doi.org/10.1029/jd091i06p06647>.
- Kerminen, V.M., Teinilä, K., Hillamo, R., Mäkelä, T., 1999. Size-segregated chemistry of particulate dicarboxylic acids in the Arctic atmosphere. *Atmos. Environ.* 33, 2089–2100. [https://doi.org/10.1016/S1352-2310\(98\)00350-1](https://doi.org/10.1016/S1352-2310(98)00350-1).
- Kim, K., Yabushita, A., Okumura, M., Saiz-Lopez, A., Cuevas, C.A., Blaszcak-Boxe, C.S., Min, D.W., Yoon, H. II, Choi, W., 2016. Production of molecular iodine and tri-iodide in the frozen solution of iodide: implication for polar atmosphere. *Environ. Sci. Technol.* 50, 1280–1287. <https://doi.org/10.1021/acs.est.5b05148>.
- Kozak, K., Polkowska, Z., Ruman, M., Koział, K., Namieśnik, J., 2013. Analytical studies on the environmental state of the Svalbard Archipelago provide a critical source of information about anthropogenic global impact. *TrAC - Trends Anal. Chem.* 50, 107–126. <https://doi.org/10.1016/j.trac.2013.04.016>.
- Leck, C., Bigg, E.K., 2005. Biogenic particles in the surface microlayer and overlying atmosphere in the central Arctic Ocean during summer. *Tellus Ser. B Chem. Phys. Meteorol.* 57, 305–316. <https://doi.org/10.1111/j.1600-0889.2005.00148.x>.
- Lee, E., Chan, C.K., Paatero, P., 1999. Application of positive matrix factorization in source apportionment of particulate pollutants in Hong Kong. *Atmos. Environ.* 33, 3201–3212. [https://doi.org/10.1016/S1352-2310\(99\)00113-2](https://doi.org/10.1016/S1352-2310(99)00113-2).
- Legrand, M., McConnell, J., Fischer, H., Wolff, E.W., Preunkert, S., Arienzo, M., Chellman, N., Leuenberger, D., Maselli, O., Place, P., Sigl, M., Schüpbach, S., Flannigan, M., 2016. Boreal fire records in Northern Hemisphere ice cores: a review. *Clim. Past* 12, 2033–2059. <https://doi.org/10.5194/cp-12-2033-2016>.
- Librando, V., Tringali, G., 2005. Atmospheric fate of OH initiated oxidation of terpenes. Reaction mechanism of α-pinene degradation and secondary organic aerosol formation. *J. Environ. Manag.* 75, 275–282. <https://doi.org/10.1016/j.jenvman.2005.01.001>.
- Marty, J.C., Salot, A., Buat-Ménard, P., Chesselet, R., Hunter, K.A., 1979. Relationship between the lipid compositions of marine aerosols, the sea surface microlayer, and subsurface water. *J. Geophys. Res.* 84, 5707. <https://doi.org/10.1029/jc084ic09p05707>.
- Maturilli, M., 2020. Continuous meteorological observations at station Ny-Ålesund (2011–08 et seq). Alfred Wegener Institute - Research Unit Potsdam, PANGAEA. <https://doi.pangaea.de/10.1594/PANGAEA.914979>.
- Maturilli, M., Herber, A., König-langlo, G., 2015. Surface radiation climatology for Ny-Ålesund, Svalbard (78.9°N), basic observations for trend detection corresponding author: short- and longwave radiation are operated since august 1992 in the frame of the baseline since August 1993. The long-te. *Theor Appl Clim.* 120, 331–339. <https://doi.org/10.1594/PANGAEA.150000>.
- Millero, F.J., Feistel, R., Wright, D.G., McDougall, T.J., 2008. The composition of standard seawater and the definition of the reference-composition salinity scale. *Deep. Res. Part I Oceanogr. Res. Pap.* 55, 50–72. <https://doi.org/10.1016/j.jdsr.2007.10.001>.
- Mochida, M., Umamoto, N., Kawamura, K., Lim, H.J., Turpin, B.J., 2007. Bimodal size distributions of various organic acids and fatty acids in the marine atmosphere: influence of anthropogenic aerosols, Asian dusts, and sea spray off the coast of East Asia. *J. Geophys. Res. Atmos.* 112, 1–13. <https://doi.org/10.1029/2006JD007773>.
- Müller, L., Reinnig, M.C., Naumann, K.H., Saathoff, H., Mentel, T.F., Donahue, N.M., Hoffmann, T., 2012. Formation of 3-methyl-1,2,3-butanetricarboxylic acid via gas phase oxidation of pinonic acid - a mass spectrometric study of SOA aging. *Atmos. Chem. Phys.* 12, 1483–1496. <https://doi.org/10.5194/acp-12-1483-2012>.
- Myriokefalitakis, S., Tsigaridis, K., Mihalopoulos, N., Sciare, J., Nenes, A., Kawamura, K., Segers, A., Kanakidou, M., 2011. In-cloud oxalate formation in the global troposphere: a 3-D modeling study. *Atmos. Chem. Phys.* 11, 5761–5782. <https://doi.org/10.5194/acp-11-5761-2011>.
- Narukawa, M., Kawamura, K., Li, S.M., Bottenheim, J.W., 2002. Dicarboxylic acids in the Arctic aerosols and snowpacks collected during ALERT 2000. *Atmos. Environ.* 36, 2491–2499. [https://doi.org/10.1016/S1352-2310\(02\)00126-7](https://doi.org/10.1016/S1352-2310(02)00126-7).
- Narukawa, M., Kawamura, K., Anlauf, K.G., Barrie, L.A., 2003. Fine and coarse modes of dicarboxylic acids in the Arctic aerosols collected during the polar sunrise experiment 1997. *J. Geophys. Res. D Atmos.* 108, 1–9. <https://doi.org/10.1029/2003jd003646>.
- O'Dowd, C.D., Smith, M.H., Consterdine, I.E., Lowe, J.A., 1997. Marine aerosol, sea-salt, and the marine sulphur cycle: a short review. *Atmos. Environ.* 31, 73–80. [https://doi.org/10.1016/S1352-2310\(96\)00106-9](https://doi.org/10.1016/S1352-2310(96)00106-9).
- Paatero, P., 1999. The multilinear engine—a table-driven, least squares program for solving multilinear problems, including the n-way parallel factor analysis model. *J. Comput. Graph. Stat.* 8, 854–888. <https://doi.org/10.1080/10618600.1999.10474853>.
- Paatero, P., Tapper, U., 1994. Positive matrix factorization: a non-negative factor model with optimal utilization of error estimates of data values. *Environmetrics* 5, 111–126. <https://doi.org/10.1002/env.3170050203>.
- Parshintsev, J., Hyötyläinen, T., Hartonen, K., Kulmala, M., Riekkola, M.L., 2010. Solid-phase extraction of organic compounds in atmospheric aerosol particles collected with the particle-into-liquid sampler and analysis by liquid chromatography-mass spectrometry. *Talanta* 80, 1170–1176. <https://doi.org/10.1016/j.talanta.2009.09.004>.
- Paulot, F., Wunch, D., Crouse, J.D., Toon, G.C., Millet, D.B., Decarlo, P.F., Vigouroux, C., Deutscher, N.M., Abad, G.G., Notholt, J., Warneke, T., Hannigan, J.W., Warneke, C., De Gouw, J.A., Dunlea, E.J., De Mazière, M., Griffith, D.W.T., Bernath, P., Jimenez, J.L., Wennberg, P.O., 2011. Importance of secondary sources in the atmospheric budgets of formic and acetic acids. *Atmos. Chem. Phys.* 11, 1989–2013. <https://doi.org/10.5194/acp-11-1989-2011>.
- Perrino, C., Canepari, S., Catrambone, M., Dalla Torre, S., Rantica, E., Sargolini, T., 2009. Influence of natural events on the concentration and composition of atmospheric particulate matter. *Atmos. Environ.* 43, 4766–4779. <https://doi.org/10.1016/j.atmosenv.2008.06.035>.
- Piwoz, K., Walkusz, W., Hapter, R., Wieczorek, P., Hop, H., Wiktor, J., 2009. Comparison of productivity and phytoplankton in a warm (Kongsfjord) and a cold (Hornsund) Spitsbergen fjord in mid-summer 2002. *Polar Biol.* 32, 549–559. <https://doi.org/10.1007/s00300-008-0549-2>.
- Polissar, A.V., Hopke, P.K., Paatero, P., Malm, W.C., Sisler, J.F., 1998. Atmospheric aerosol over Alaska 2. Elemental composition and sources. *J. Geophys. Res. Atmos.* 103, 19045–19057. <https://doi.org/10.1029/98JD01212>.
- Quinn, P.K., Shaw, G., Andrews, E., Dutton, E.G., Ruoho-Airola, T., Gong, S.L., 2007. Arctic haze: current trends and knowledge gaps. *Tellus Ser. B Chem. Phys. Meteorol.* 59, 99–114. <https://doi.org/10.1111/j.1600-0889.2006.00238.x>.
- Raes, F., Dingenen, R. Van, Elisabetta, V., Wilson, J., Putaud, J.P., Seinfeld, J.H., Adams, P., 2002. Formation and cycling of aerosols in the global troposphere. *Dev. Environ. Sci.* 24, 519–563. [https://doi.org/10.1016/S1474-8177\(02\)80021-3](https://doi.org/10.1016/S1474-8177(02)80021-3).
- Rinaldi, M., Decesari, S., Carbone, C., Finessi, E., Fuzzi, S., Ceburnis, D., O'Dowd, C.D., Sciare, J., Burrows, J.P., Vrekoussis, M., Ervens, B., Tsigaridis, K., Facchini, M.C., 2011. Evidence

- of a natural marine source of oxalic acid and a possible link to glyoxal. *J. Geophys. Res. Atmos.* 116, 1–12. <https://doi.org/10.1029/2011JD015659>.
- Rinke, A., Maturilli, M., Graham, R.M., Matthes, H., Handorf, D., Cohen, L., Hudson, S.R., Moore, J.C., 2017. Extreme cyclone events in the Arctic: wintertime variability and trends. *Environ. Res. Lett.* 12. <https://doi.org/10.1088/1748-9326/aa7def>.
- Scalabrin, E., Zangrando, R., Barbaro, E., Kehrwald, N.M., Gabrieli, J., Barbante, C., Gambaro, A., 2012. Amino acids in Arctic aerosols. *Atmos. Chem. Phys.* 12, 10453–10463. <https://doi.org/10.5194/acp-12-10453-2012>.
- Simoneit, B.R.T., Schauer, J.J., Nolte, C.G., Oros, D.R., Elias, V.O., Fraser, M.P., Rogge, W.F., Cass, G.R., 1999. Levoglucosan, a tracer for cellulose in biomass burning and atmospheric particles. *Atmos. Environ.* 33, 173–183.
- Spolaor, A., Vallenga, P., Turetta, C., Maffezzoli, N., Cozzi, G., Gabrieli, J., Barbante, C., Goto-Azuma, K., Saiz-Lopez, A., Cuevas, C.A., Dahl-Jensen, D., 2016. Canadian arctic sea ice reconstructed from bromine in the Greenland NEMM ice core. *Sci. Rep.* 6, 1–8. <https://doi.org/10.1038/srep33925>.
- Stohl, A., 2006. Characteristics of atmospheric transport into the Arctic troposphere. *J. Geophys. Res. Atmos.* 111, 1–17. <https://doi.org/10.1029/2005JD006888>.
- Stohl, A., Forster, C., Eckhardt, S., Spichtinger, N., Huntrieser, H., Heland, J., Schlager, H., Wilhelm, S., Arnold, F., Cooper, O., 2003. A backward modeling study of intercontinental pollution transport using aircraft measurements. *J. Geophys. Res. Atmos.* 108. <https://doi.org/10.1029/2002jd002862>.
- Stohl, A., Berg, T., Burkhardt, J.F., Fjæraa, a.M., Forster, C., Herber, A., Hov, Ø., Lunder, C., McMillan, W.W., Oltmans, S., Shiobara, M., Simpson, D., Solberg, S., Stebel, K., Ström, J., Tørseth, K., Treffeisen, R., Virkkunen, K., Yttri, K.E., 2006. Arctic smoke – record high air pollution levels in the European Arctic due to agricultural fires in Eastern Europe. *Atmos. Chem. Phys. Discuss* 6, 9655–9722. <https://doi.org/10.5194/acpd-6-9655-2006>.
- Sturges, W.T., 1990. Excess particulate and gaseous bromine at a remote coastal location. *Atmos. Environ. Part A, Gen. Top.* 24, 167–171. [https://doi.org/10.1016/0960-1686\(90\)90452-S](https://doi.org/10.1016/0960-1686(90)90452-S).
- Sturges, W.T., Barrie, L.A., 1988. Chlorine, bromine and iodine in arctic aerosols. *Atmos. Environ.* 22, 1179–1194. [https://doi.org/10.1016/0004-6981\(88\)90349-6](https://doi.org/10.1016/0004-6981(88)90349-6).
- Svendsen, H., Beszczynska-Møller, A., Hagen, J.O., Lefauconnier, B., Tverberg, V., Gerland, S., Ørbæk, J.B., Bischof, K., Papucci, C., Zajaczkowski, M., Azzolini, R., Bruland, O., Wiencke, C., Winther, J.G., Dallmann, W., 2002. The physical environment of Kongsfjorden-Krossfjorden, and Arctic fjord system in Svalbard. *Polar Res.* 21, 133–166. <https://doi.org/10.1111/j.1751-8369.2002.tb00072.x>.
- Tunved, P., Ström, J., Krejci, R., 2013. Arctic aerosol life cycle: linking aerosol size distributions observed between 2000 and 2010 with air mass transport and precipitation at Zeppelin station, Ny-Ålesund, Svalbard. *Atmos. Chem. Phys.* 13, 3643–3660. <https://doi.org/10.5194/acp-13-3643-2013>.
- Udisti, R., Bazzano, A., Becagli, S., Bolzacchini, E., Caiazza, L., Cappelletti, D., Ferrero, L., Frosini, D., Giardi, F., Grotti, M., Lupi, A., Malandrino, M., Mazzola, M., Moroni, B., Severi, M., Traversi, R., Viola, A., Vitale, V., 2016. Sulfate source apportionment in the Ny-Ålesund (Svalbard Islands) Arctic aerosol. *Rend. Lincei* 27, 85–94. <https://doi.org/10.1007/s12210-016-0517-7>.
- Urbanski, J., Neugebauer, E., Spacjer, R., Faikowska, L., 1980. Physico-chemical characteristic of the waters of Hornsund Fjord on south-west Spitsbergen (Svalbard Archipelago) in the summer season 1979. *Polish Polar Res* 1, 43–51.
- Viana, M., Kuhlbusch, T.A.J., Querol, X., Alastuey, A., Harrison, R.M., Hopke, P.K., Winiwarter, W., Vallius, M., Szidat, S., Prévôt, A.S.H., Hueglin, C., Bloemen, H., Wählin, P., Vecchi, R., Miranda, A.I., Kasper-Giebl, A., Maenhaut, W., Hitznerberger, R., 2008. Source apportionment of particulate matter in Europe: a review of methods and results. *J. Aerosol Sci.* 39, 827–849. <https://doi.org/10.1016/j.jaerosci.2008.05.007>.
- Volkamer, R., Platt, U., Wirtz, K., 2001. Primary and secondary glyoxal formation from aromatics: experimental evidence for the bicycloalkyl - radical pathway from benzene, toluene, and p-xylene. *J. Phys. Chem. A* 105, 7865–7874. <https://doi.org/10.1021/jp010152w>.
- Warneke, C., Bahreini, R., Brioude, J., Brock, C.A., De Gouw, J.A., Fahey, D.W., Froyd, K.D., Holloway, J.S., Middlebrook, A., Miller, L., Montzka, S., Murphy, D.M., Peischl, J., Ryerson, T.B., Schwarz, J.P., Spademan, J.R., Veres, P., 2009. Biomass burning in Siberia and Kazakhstan as an important source for haze over the Alaskan Arctic in April 2008. *Geophys. Res. Lett.* 36. <https://doi.org/10.1029/2008GL036194>.
- Yang, X., Pyle, J.A., Cox, R.A., Theys, N., Van Roozendaal, M., 2010. Snow-sourced bromine and its implications for polar tropospheric ozone. *Atmos. Chem. Phys.* 10, 7763–7773. <https://doi.org/10.5194/acp-10-7763-2010>.
- Yttri, K.E., Dye, C., Kiss, G., 2007. Ambient aerosol concentrations of sugars and sugar-alcohols at four different sites in Norway. *Atmos. Chem. Phys. Discuss* 7, 5769–5803. <https://doi.org/10.5194/acpd-7-5769-2007>.
- Yttri, K.E., Lund Myhre, C., Eckhardt, S., Fiebig, M., Dye, C., Hirdman, D., Ström, J., Klimont, Z., Stohl, A., 2014. Quantifying black carbon from biomass burning by means of levoglucosan - a one-year time series at the Arctic observatory zeppelin. *Atmos. Chem. Phys.* 14, 6427–6442. <https://doi.org/10.5194/acp-14-6427-2014>.
- Zangrando, R., Barbaro, E., Zennaro, P., Rossi, S., Kehrwald, N.M., Gabrieli, J., Barbante, C., Gambaro, A., 2013. Molecular markers of biomass burning in Arctic aerosols. *Environ. Sci. Technol.* 47, 8565–8574. <https://doi.org/10.1021/es400125r>.
- Zhao, Y., Zhang, Y., Fu, P., Ho, S.S.H., Ho, K.F., Liu, F., Zou, S., Wang, S., Lai, S., 2016. Non-polar organic compounds in marine aerosols over the northern South China Sea: influence of continental outflow. *Chemosphere* 153, 332–339. <https://doi.org/10.1016/j.chemosphere.2016.03.069>.

Atmospheric Environment

Airborne bacteria and particulate chemistry capture phytoplankton bloom dynamics in an Arctic Fjord --Manuscript Draft--

Manuscript Number:	
Article Type:	Research Paper
Keywords:	Arctic; Amino acids; Atmospheric microorganisms; air-to-sea exchanges; marine plankton bloom
Corresponding Author:	Elena Barbaro, PhD CNR Mestre Venice, ITALY
First Author:	Matteo Feltracco
Order of Authors:	Matteo Feltracco Elena Barbaro Clara J. M. Hoppe Klara K. E. Wolf Andrea Spolaor Rose Layton Christoph Keuschnig Carlo Barbante Andrea Gambaro Catherine Larose
Abstract:	<p>Primary biological aerosol particles and microorganisms are ubiquitous in the atmosphere. Investigations of airborne chemical markers and microbial communities are critical for identifying sources, transport and transformation processes of aerosols. One potential major source of airborne chemical compounds and microbial communities (e.g. L- and D-amino acids, Flavobacteria) could be related to phytoplankton blooms that occur during the spring season in Arctic fjord systems. Here, we conducted a field study in a polar environment to investigate the particle-size distribution of water-soluble compounds (major ions, carboxylic acids and free L- and D-amino acids) and airborne bacterial communities in aerosol samples. The sampling was conducted with a 6 day sampling frequency at the Gruvebadet observatory, close to Ny-Ålesund (Svalbard Islands). Glycine, D-amino acids and C4- organic acids increased during the exponential phase of a marine bloom that occurred in Kongsfjorden and started to drop at the beginning of the post-bloom phase. On the other hand, Polaribacter together with free L-amino acid overlapped with the Chlorophyll a peak and the subsequent decline, and thus might constitute a useful marker for the post-bloom phase.</p>
Suggested Reviewers:	<p>Ki-Tae Park Korea Polar Research Institute ktpark@kopri.re.kr Expert of marine primary production tracers in the aerosols</p> <p>Kimberly Prather UC Riverside: University of California Riverside kprather@ucsd.edu Expert of atmospheric aerosol particles characterization</p> <p>Yu-Zhong Zhang Shandong University zhangyz@sdu.edu.cn Expert of Bacterioplankton, Polynucleobacter and Alpha-Proteobacteria</p>

Highlights

- Chemical and biological data were used to study Kongsfjorden dynamics
- D-amino acids could serve as indicators of developing marine blooms
- Polaribacter and L-amino acids as useful markers for the post-bloom phase

Abstract

Primary biological aerosol particles and microorganisms are ubiquitous in the atmosphere. Investigations of airborne chemical markers and microbial communities are critical for identifying sources, transport and transformation processes of aerosols. One potential major source of airborne chemical compounds and microbial communities (e.g. L- and D-amino acids, Flavobacteria) could be related to phytoplankton blooms that occur during the spring season in Arctic fjord systems. Here, we conducted a field study in a polar environment to investigate the particle-size distribution of water-soluble compounds (major ions, carboxylic acids and free L- and D-amino acids) and airborne bacterial communities in aerosol samples. The sampling was conducted with a 6 day sampling frequency at the Gruvebadet observatory, close to Ny-Ålesund (Svalbard Islands). Glycine, D-amino acids and C₄- organic acids increased during the exponential phase of a marine bloom that occurred in Kongsfjorden and started to drop at the beginning of the post-bloom phase. On the other hand, Polaribacter together with free L-amino acid overlapped with the Chlorophyll a peak and the subsequent decline, and thus might constitute a useful marker for the post-bloom phase.

1. Introduction

Aerosols in the summer Arctic atmosphere are mainly derived from the biologically active waters of the adjacent seas (Bigg and Leck, 2001; Keith Bigg et al., 2004; Leck and Persson, 1996), with the highest contribution of marine input being measured in summer (Bigg and Leck, 2008; Gao et al., 2012). These bioaerosols are mostly composed of organic compounds derived from marine microorganisms, bacteria or vegetal material, implicating the production of multi-fraction particles in the atmosphere. Bioaerosols and in particular Primary Biological Aerosol Particles (PBAPs) are gaining attention in the Svalbard Archipelago, because they can act directly as cloud condensation nuclei (CCN) and ice nuclei (IN) (Beck et

al., 2020; Leck and Svensson, 2015; Orellana et al., 2011). The composition of PBAPs is to date not fully resolved but coupling microbiological analyses and chemical tracers should lead to knowledge gains. The presence and concentration of atmospheric biomarkers provide useful information on the origin of aerosols and short- and long-range atmospheric transport (LRAT) processes.

To the best of our knowledge, the possible common sources and emission processes of free amino acids (FAAs), carboxylic acids (CAs), major anions and cations, chlorophyll *a* (Chl *a*) and microorganisms that might be released during phytoplankton blooms has never been investigated in Arctic aerosol samples. While FAAs, CAs, major ions and Chl *a* have been studied in the Arctic aerosol (Feltracco et al., 2021, 2020, 2019; Geng et al., 2010; Giardi et al., 2016; Mashayekhy Rad et al., 2019; Quinn et al., 2015; Zangrando et al., 2013), there are only a few studies measuring bacterial community composition in marine air, and even fewer over polar waters (Li et al., 2017; Orellana et al., 2011; Tignat-Perrier et al., 2020, 2019). The primary source of airborne FAAs is the proteinaceous material associated with bacteria, phytoplankton, terrestrial dust and biological degradation (Dittmar et al., 2001; Ge et al., 2011). FAAs can also have other sources such as biomass burning emissions (Chan et al., 2005; Feltracco et al., 2019). Moreover, the aerosol concentration of CAs can be influenced by primary sources, such as marine emissions (Rinaldi et al., 2011) and biomass burning (Falkovich et al., 2005). CAs can be also produced by photochemical reactions of oxidation of anthropogenic organic pollutants and once emitted to the atmosphere, CA precursors undergo oxidation or other photochemical reactions (Kawamura et al., 1996). Major ions in the aerosol were usually investigated to define the sea spray contribution, because Na^+ , Cl^- , and Mg^{2+} are the main components of seawater (Hamacher-Barth et al., 2016; Salter et al., 2016). Conversely, Ca^{2+} , K^+ , and SO_4^{2-} have relevant contributions from other sources, especially crustal aerosol and anthropic emissions by long-range atmospheric transport from continental regions (Fisher et al., 2011; Giardi et al., 2016). Finally, methanesulfonic acid (MSA) has been considered a marker of marine primary production (Beck et al., 2020). MSA originates from photochemical oxidation of dimethyl sulfide (DMS), which is a result of microbiological transformation of dimethylsulfoniopropionate (DMSP) produced and released by phytoplankton (Stefels et al., 2007).

The main pigment of photosynthesis, Chl *a*, is the most widely used proxy for marine phytoplankton biomass. Even though this is a potentially problematic simplification due to

strong variability in the carbon to Chl *a* ratio of phytoplankton due to taxonomic differences as well as photoacclimatory processes, it is the most useful proxy for overall spatial and temporal patterns that can even be derived from satellite products (Behrenfeld et al., 2008). Chl *a* has also been used to explore influences of oceanic biological activity on sea salt aerosol (SSA) properties. Positive correlations between satellite-derived Chl *a* and the organic fraction of SSA were observed in the northeast Atlantic (O'Dowd et al., 2004). It has been suggested that bacteria and other primary biological particles can be released into the atmosphere from the sea-surface micro-layer by bubble bursting in breaking waves, a process that occurs both during wave-breaking at the coasts, and in whitecaps on wind-driven waves in the open ocean (Blanchard, 1989). Non-wind induced potential production mechanisms for bubbles formations are also possible (Norris et al., 2011). In spring, biological primary productivity is initiated in surface waters and both algal and bacterial abundance increases in so called "blooms", which should lead to increased biomass for aerosolization. This has been shown to occur experimentally in a mesocosm nutrient enrichment study (Michaud et al., 2018), but has yet to be observed in the field.

The main objective of this study was to investigate the potential common sources of chemical markers and microorganisms in different size-segregated aerosol particles collected weekly at the Gruvebadet Observatory, close to Ny-Ålesund, Svalbard from end of February to beginning of June 2018. This is the first investigation that combined chemical and biological data in order to evaluate and predict changes in Kongsfjorden dynamics using aerosol samples.

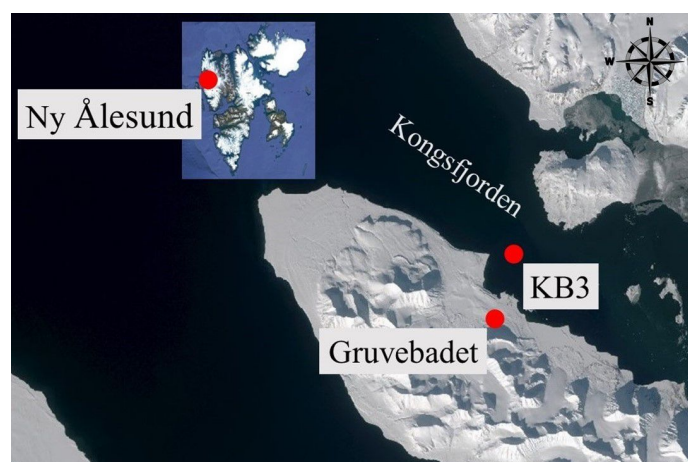


FIGURE 1: Map of the Brøgger peninsula and Kongsfjorden. The red dots indicate Ny-Ålesund, Gruvebadet Laboratory and the KB3 marine sampling site. Image courtesy of the Norwegian Polar Institute.

2. Experimental

2.1 Site description and sample collection

The Svalbard Archipelago is one of the northernmost land-areas in the world and is situated in a climatically and oceanographically complex area. This Arctic region is considered among the most sensitive to climate change, with warming occurring considerably faster than the global average due to several positive feedback mechanisms (Maturilli M. et al., 2019). Svalbard is also influenced by the warm waters of the West Spitzbergen Current and the cold Arctic waters of the Spitsbergen Polar Current. Kongsfjorden is a fjord located on the west Spitsbergen coast and is positioned right at the interface of High Arctic and Atlantic influences (Bischof et al., 2019).

Sixteen aerosol samples were collected from 26th February to 1st June 2018 at the Gruvebadet atmospheric laboratory (Svalbard Islands, 78°55'03"N, 11°53'39"E, 50 m a.s.l.), close to Ny-Ålesund and 1.4 km far from the Kongsfjorden (Figure 1). Kongsfjorden is a 26-km-long and 3–8-km-wide fjord on the westcoast of Spitsbergen, with maximum depth of about 400 m (Hop et al., 2016). The fjord is influenced by both Arctic and Atlantic water masses, and by tidal glaciers, which contribute freshwater influx through melting and calving (Tverberg et al., 2019). Marine sampling was conducted with a resolution of 2 to 6 days in April and May 2018 in the deeper part of the fjord at station KB3 (78°56'50"N, 11°57'04"E).

A multi-stage Andersen impactor (TE-6000 series, Tisch Environmental Inc.) was used to collect aerosol samples on six pre-combusted (4 h at 400°C in a muffle furnace) quartz fiber filters. The sampler accumulated particles with cut-off diameters of 10.0 μm , 7.2 μm , 3.0 μm , 1.5 μm , and 0.95 μm on slotted filters and <0.49 μm on backup filter. The frequency of sampling was 6 days with a mean total air volume of 9000 m³ per sample. Field blanks were obtained using filters installed on the sampler for 5 minutes with the air pump switched off. Samples and blanks were wrapped in a double layer of aluminium foil and stored at -20°C until analysis.

2.2 Chemical analysis

Chemical and microbial analysis were carried out on the same aerosol samples. Each sample was cut in four parts: one half was used to determine free amino acids, a quarter of the filter was processed for major ions and small organic acids, an eighth of the filter was used for

microbial analysis and the last part was archived.

To avoid any contamination from laboratory air particles, samples were handled inside an ISO 5 clean room under a laminar flow bench (class 100). Field blank filters were also taken and treated using the same procedure. All reported values are blank-corrected. The method detection limits (MDL) and method quantification limits (MQL) of the analytical procedure were determined as three and ten times the standard deviation of the average value of the field blank.

For major ions and organic acids, the pre-analytical procedure was based on that described by Barbaro et al. (2017) for Antarctic samples. Briefly, sample preparation consisted of the extraction of a quarter of a filter (different diameters were analysed separately) in an ultrasonic bath with 7 mL and 15 mL of ultra-pure water (18.2 M σ cm, 0.01 TOC) for slotted and back-up filters, respectively.

The anion analysis was performed using an ion chromatography system (IC, Thermo Scientific™ Dionex™ ICS-5000, Waltham, US) equipped with an anionic exchange column (Dionex IonPac AS11 2×250 mm) and a guard column (Dionex Ion Pac AG11 2×50 mm), coupled to a single quadrupole mass spectrometer (MSQ Plus™, Thermo Scientific™, Bremen, Germany). Cationic species were determined using a capillary IC (Thermo Scientific Dionex ICS-5000), equipped with a capillary cation exchange column (Dionex IonPac CS19-4 μ m, 0.4×250mm) and a guard column (Dionex IonPac CG19-4 μ m, 0.4×50 mm), then connected with a conductivity detector. Details regarding the analytical method are reported by Barbaro et al., (2017).

For free amino acids (FAAs), each half filter was spiked with a mixed solution of 8 labelled FAAs as an internal standard (0.5 absolute μ g for slotted filters and 1.5 absolute μ g for back-up filters) and were then extracted twice for 15 min with ultrapure water in an ultrasonic bath. The slotted filters were extracted with 9 mL followed by 1 mL of ultrapure water, whilst the back-up filters were extracted with 25 mL followed by 5mL of ultrapure water. The instrumental method was performed using an Agilent 1100 Series HPLC System (Waldbronn, Germany) coupled to an API 4000 Triple Quadrupole Mass Spectrometer (Applied Biosystem/MDS SCIEX, Concord, Ontario, Canada). Sample analysis methods of FAAs are described in detail by Barbaro et al. (2015, 2014). Reagents, standards solutions and details on instrumental analysis are reported in the Supplementary Information.

2.3 Microbial analysis - DNA extraction

DNA was extracted from samples and blanks using the protocol outlined in Dommergue et al. (2019) specifically developed for atmospheric samples collected onto quartz filters. Briefly, an eighth of each filter was chopped up into small pieces directly into the PowerBead tubes provided in the DNeasy PowerWater kit. The PowerBead tubes (containing sample and lysis solution) were then heated at 65°C for one hour after a 10-min vortex treatment at maximum speed (2500 rpm). The mixture was then centrifuged for 4 minutes at 1000 rcf to separate the filter debris from the lysate using a pipette. The DNeasy PowerWater protocol was then applied to the lysate. DNA was then stored at -20°C.

2.4 Real-Time qPCR analyses: 16S rRNA gene qPCR

Bacterial cell abundance was approximated through the quantification of the 16S rRNA gene using qPCR analysis, with the following primers that target the V3 region (180 bp): Eub 338f 5'-ACTCCTACGGGAGGCAGCAG-3' as the forward primer and Eub 518r 5'-ATTACCG CGGCTGCTGG-3' as the reverse primer (Fierer et al., 2005) on a Corbett Rotor-Gene 6000 real-time PCR cycler. The SensiFast SYBR No-Rox kit (Bioline) was used and the final 20 µL reaction mix contained 10 µL of SYBR master mix, 2µL of DNA 1 µL of each primer (10 µM) and 6 µL ultra-pure water. The qPCR program was: 95°C for 2 min, 35 cycles of 5sec at 95°C and 20 sec at 60°C, followed by a final denaturation step from 55°C to 95°C with increments of 1°C min⁻¹. PCR products obtained from DNA from a pure culture of E.coli were inserted in a plasmid (pCRTM2.1-TOPO vector, Invitrogen) and subsequent PCR using M13 primers resulted in amplicons containing the targeted sequence and flanking regions which was used as standards after quantification by a Qubit assay (InvitrogenTM). Each run included standards in a range of 101-107 copies/reaction as well as non-template controls (ultra-pure water) to check for contamination. Runs with no amplification in the no-template-control and values > 0.98 and between 0.9 and 1.1 for R² and efficiency respectively from the standard curves were used for further analysis.

2.5 MiSeq Illumina 16S rRNA gene sequencing

Platinum Taq Polymerase (ThermoFisher Scientific) was used to amplify the V3-V4 region of the 16S rRNA gene with primers published by Klindworth et al. 2013 (Klindworth et al.,

2013). The PCR program used was: 95°C for 3 minutes, 35 cycles of 95°C for 30 seconds, 55°C for 30 seconds and 72°C for 30 seconds, followed by a final step of 72°C for 5 minutes. Library preparation including PCR clean-up, index PCR, index PCR clean-up, normalization and pooling were carried out following the Illumina library preparation protocol ("16S Metagenomic Sequencing Library Preparation"). The final library pool was loaded on a V2 flow cell for 2×250 bp paired-end sequencing on an Illumina MiSeq platform.

2.6 Read quality filtering and Taxonomic annotation

The tools `fastx_quality_stats` and `fastq_quality_boxplot_graph` of the FASTX-Toolkit (http://hannonlab.cshl.edu/fastx_toolkit/) were used to visualize the base quality of reads 1 and reads 2. PANDAseq (Masella et al., 2012) was used to merge forward and reverse reads using the RDP algorithm for assembly with a minimum and maximum length of the resulting sequence of 410 bp and 500 bp respectively, a minimum and maximum overlap length of 20 bp and 100 bp respectively as well as a quality threshold of 0.6. The resulting sequences were stripped of their primers and annotated by RDP Classifier (Wang et al., 2007) with an assignment confidence cutoff of 0.6. Samples were blank corrected using the `decontam` package in R (Davis et al., 2018).

2.7 Sequence analyses

The total number of samples were 114, including field blanks. To reduce the possible interferences on the statistical analyses and to simplify the dataset we pooled the fractions into two categories, fine and coarse based on the cut-off diameter of $0.95 \mu\text{m}$. We calculated coarse mode as sum of the stages 1, 2, 3 and 4, and fine particles as sum of stage 5 and 6. All statistical analyses were conducted using R (v3.4.1; R Core Team 2013) in RStudio (v1.0.153; RStudio Team, 2020). Taxonomic data was analyzed using the R package 'phyloseq' (v1.20.0; McMurdie & Holmes, 2013) and plots were generated using the R package 'ggplot2' (v2.2.1; Wickham, 2016). Overlaps in taxonomy was analysed using presence-absence analysis and visualized with Venn diagrams (<http://bioinformatics.psb.ugent.be/webtools/Venn/>). Diversity statistics, including rarefaction curves (Figure S1) and richness and diversity estimations (Table S2) were calculated for each sample using the `vegan` R package. Relative abundances were calculated for each sample at the genus and class levels and stacked barplots were generated. PCoA analysis was conducted on Bray-Curtis transformed relative abundance

matrices and tested for significance using permutational multivariate analysis of variance (Figure S2). Adonis tests were used to test for significant differences in the bacterial communities among seasons and between fine and coarse particles, followed by fold-change in abundance analysis to identify the genera likely to be the major contributors to the difference between the groups using the R package 'DESeq2' (Love et al., 2014). The relationship between the chemical and taxonomic data was evaluated using co-inertia analysis in R. Briefly, chemical data was log transformed and Z normalized (Tromas et al., 2017), while taxa tables were Hellinger transformed. The significance of the co-inertia was tested using a permutation test (1000 permutations). Linear correlations between chemical parameters and OTUs were also calculated.

2.8 Chl *a* analysis

Discrete samples from 10, 25 and 50 m water depth were collected by single 10 L Niskin hauls. Samples for determination of discrete Chlorophyll *a* (Chl *a*) were gently (max. 200 mBar) filtered onto precombusted GF/F filters (Whatman), immediately placed into 6 mL 90% acetone, homogenized using a cell mill (Precellys) and extracted at -20°C over night. Chl *a* concentrations were determined on a fluorometer (Trilogy, Turner Designs), using an acidification step (1M HCl) (Knap et al., 1996). Depth-resolved fluorescence-derived Chl *a* concentrations [$\mu\text{g L}^{-1}$] were collected with a XR-620 CTD from RBR Ltd, equipped with a fluorescence sensor, from board the research vessel Jean Flo'c'h. Values were corrected based on discrete Chl *a* samples ($n = 39$; $R^2 = 0.81$). An underestimation of surface Chl *a* concentrations due to fluorescence quenching by high actinic irradiances was corrected following Xing et al. (2012) (Xing et al., 2012). In short, maximal Chl *a* concentrations measured in the optically derived turbulent mixed layer depths (MLD) were projected to the surface. Depth-integrated Chl *a* concentrations (0-100 m) were calculated via numerical integration using the trapezoidal rule. In cases where CTD profiles did not reach full 100 m, the average of last 5 m was projected down to 100 m.

3. Results

3.1 Water soluble compounds concentrations and size-distribution

The most abundant water-soluble compounds detected in the particulate matter (PM_{10}) (calculated as sum of the six fractions sampled) were SO_4^{2-} (46%), Cl^- (21%) and Na^+ (16%) with

mean PM₁₀ concentration of 333 ± 172 , 155 ± 147 and 118 ± 86 ng m⁻³, respectively (Figure 2 and S3). Mg²⁺ (19 ± 13 ng m⁻³), Ca²⁺ (20 ± 8 ng m⁻³), NH₄⁺ (36 ± 17 ng m⁻³), and NO₃⁻ (22 ± 14 ng m⁻³) contributed less than 13% of the total compounds in the PM₁₀. MSA, K⁺, Br⁻ and I⁻ made up only a small fraction of the PM₁₀ aerosol concentration (~1% each, 9 ± 9 , 4 ± 3 , 1.5 ± 0.9 and 0.3 ± 0.2 ng m⁻³). All the major ions had a constant particle size distribution during the sampling period with Cl⁻, Na⁺, Mg²⁺ and NO₃⁻ mainly distributed above 0.95 μm (representing the 76 to 96% of the total PM₁₀). Na⁺ and Cl⁻ are recognized as specific tracers of sea salt aerosol (Gong, 2003; O'Dowd et al., 1997; Perrino et al., 2009; Raes et al., 2002). The main formation pathway of NO₃⁻ was likely the interaction of nitric acid or other reactive nitrogen compounds with sea-salt particles in the Arctic atmosphere (Friedman et al., 2009; Geng et al., 2010b). Nss-SO₄²⁻ (calculated as $[\text{SO}_4^{2-}] - 0.253 \times [\text{Na}^+]$) represented the 91% of total SO₄²⁻ and showed the highest concentration in April (427 ± 148 ng m⁻³), being two times greater than those of March and May. This suggests an extra input of sulphate coming from LRAT because fine particles represent 61% of the total PM₁₀. NH₄⁺ showed a similar trend in spring with the strongest presence in fine particles (71% of the total PM₁₀). The summer decline of ammonium coincided with nutrient drawdown in the water column (Feltracco et al., 2021). Significant concentration peaks of Na⁺, Cl⁻ and Mg²⁺ were detected the 8th of March, probably due to bubble bursting events associated with strong winds. These species were highly distributed in coarse particles (91, 99 and 87% of the PM₁₀). Calcium showed a similar concentration during all sampling period and the coarse fraction represented the 64% of the total PM₁₀ concentration. Nss-Ca²⁺ (calculated as $\text{tot}[\text{Ca}^{2+}] - 0.038 \times [\text{Na}^+]$) dominated the total concentration of Ca²⁺. The important content of nss-Ca²⁺ is plausibly associated with soil-related particles (Timonen et al., 2008; Virkkula et al., 2006). MSA showed a clear increase in late-spring and summer. In fact, the highest MSA concentrations were determined in May with a concentration of 18 ± 10 ng m⁻³. MSA, NH₄⁺, Br⁻ and I⁻ were also mainly present in the fine fraction (>50%). Again, these compounds showed a non-negligible presence in the coarsest fraction in April (18-30%) (Table S1).

The CAs loads represented 1% of the total analysed compounds. During all the sampling period, C2-oxalic acid represented the most abundant CA (59%, 6 ± 3 ng m⁻³) (Figure S3). The C1-C3 carboxylic acids accounted for 88% of total CAs: C1-formic (10%), C2-acetic (7%), C2-oxalic (59%), C3-malonic (7%) and C2-glycolic (5%) The particle size of these compounds was very variable. In general, C1-formic and C2-oxalic acids showed a bimodal distribution

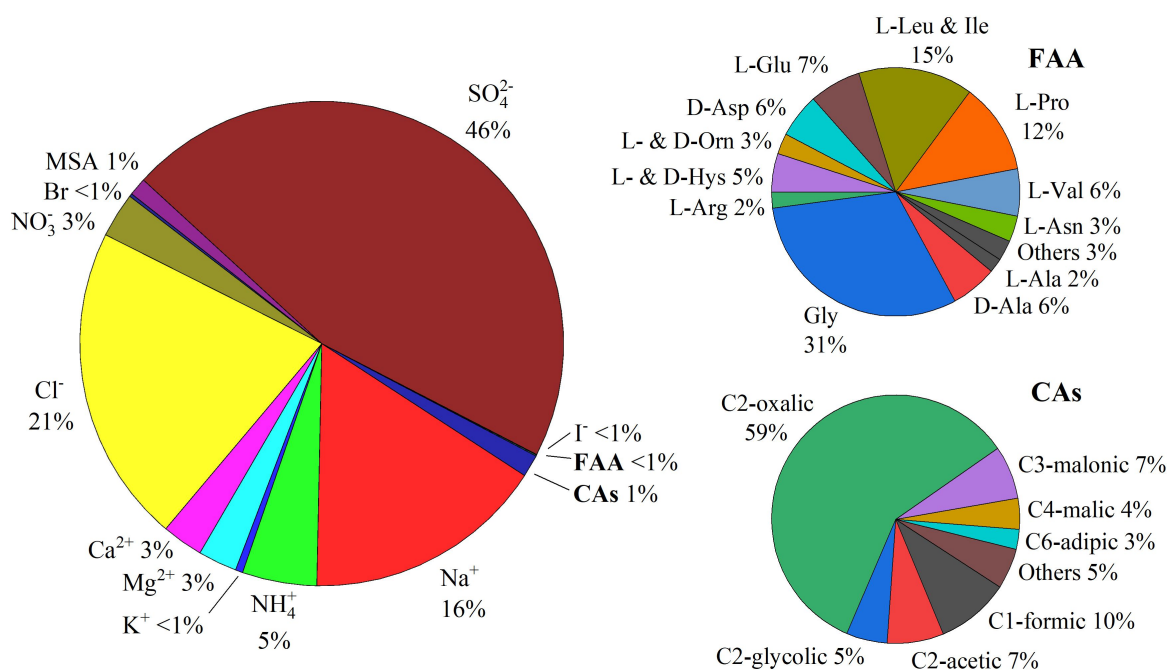


FIGURE 2: Relative % of major ions, FAAs and CAs.

in accumulation and coarse fractions, with exception in May for C1-formic acid that was distributed only in coarse fraction. C2-acetic and C2-glycolic acid had a constant particle size distribution, mainly distributed in fine particles (51-74%), although a non-negligible presence of these CAs was found in the coarsest fraction in April (15-30%). C1 and C2 carboxylic acids showed a clear decreasing trend from March to May. Other CAs percentage contribution in coarse and fine particles are reported in Table S1. In our previous work (Feltracco et al., 2021), we found that CAs can derive from five different possible sources: sea spray, marine primary production, biomass burning, sea ice related process and secondary products. Sources strongly depended on the season and, during spring, CAs concentration is mainly influenced by sea ice related processes and marine primary production.

The total FAAs in PM₁₀ represented less than 1% of the target compounds (Figure 2). Gly, the most stable amino acid in atmosphere (McGregor and Anastasio, 2001), was the most abundant FAA (31%, $0.2 \pm 0.1 \text{ ng m}^{-3}$), followed by L-Leu & Ile (15%) and L-Pro (12%). Gly, D-Ala and D-Asp increased their concentrations similarly in mid-April, while a very important presence of L-Leu & Ile, L-Pro, L-Glu, L-Val, L-Asn, L- & D-Hys and L- & D-Orn from 2nd to 8th May was found (Figure 3 and S3). FAAs also had a variable particle size distribution, with Gly equally distributed among the fractions during the sampling, while the L-amino acids previously described were constantly distributed in coarse particles (78 – 100%,

Table S1). The fractions of other minor FAAs varied depending on the sampling period. Feltracco et al., (2019) identified biological material and biomass burning as a main source for FAAs. Here, L-amino acids, excluding L-Arg, correlated with marine salts ($0.4 < R^2 < 0.8$, $p < 0.01$), while CAs co-varied with iodide and bromine ($0.5 < R^2 < 0.8$, $p < 0.01$).

Changes in phytoplankton biomass were followed by measuring Chl *a* concentration in Kongsfjorden water samples from April 10th to May 22nd, covering the entire spring bloom from a pre- to a post-bloom state. Despite being more variable during the pre- and post-bloom phases, POC:Chl *a* ratios were relatively stable during the main bloom when phototrophic biomass dominated, thus allowing the use of Chl *a* as a proxy for phytoplankton biomass despite potential effects of photoacclimation (Hoppe et al., unpublished results). Depth-integrated biomass inventories strongly increased from the end of April onwards, while the peak of the bloom was observed on May 11th (Figure 3), followed by a post-bloom state characterised by nutrient limitation and decreasing Chl *a* concentrations. A shallow coastal monitoring station near Ny-Ålesund confirms low Chl *a* fluorescence before mid April, as well as the collapse of the bloom at the end of May (Fischer et al., 2019). While no DMSP samples were collected in this study, previous co-located sampling of Chl *a* and DMSP in Kongsfjorden indicated linear relationships between both compounds ($R^2 = 0.8-0.9$; Hoppe et al., unpublished results). As reported in Figure 3, the bloom corresponded to the first peak of MSA in the air samples from 2nd to 8th of May. This overlap is equally followed by all the sea salt particles (Na^+ , Cl^- , Mg^{2+} , Ca^{2+} and partially NO_3^- and K^+) and all the L-amino acids detected. Gly, D-Ala, D-Asp, NH_4^+ peaked in the phase of exponential biomass accumulation and dropped during the post-bloom phase. Bacterial cell abundance estimates in the aerosol also dropped during the exponential increase in biomass (Figure S6, supplementary material).

3.2 Microbial communities in coarse vs fine particles

Based on Adonis and permanova analysis, there is a significant difference in aerosol community composition between coarse and fine fractions (Table S3, $p = 0.01$), however particle size explains less than 7% of the variability. Based on Venn diagram analysis, 41 OTUs were unique to the fine fractions, 277 OTUs were unique to the coarse fractions and 323 were shared (Figure 4). There were no clear taxonomic differences in unique genera, however, all

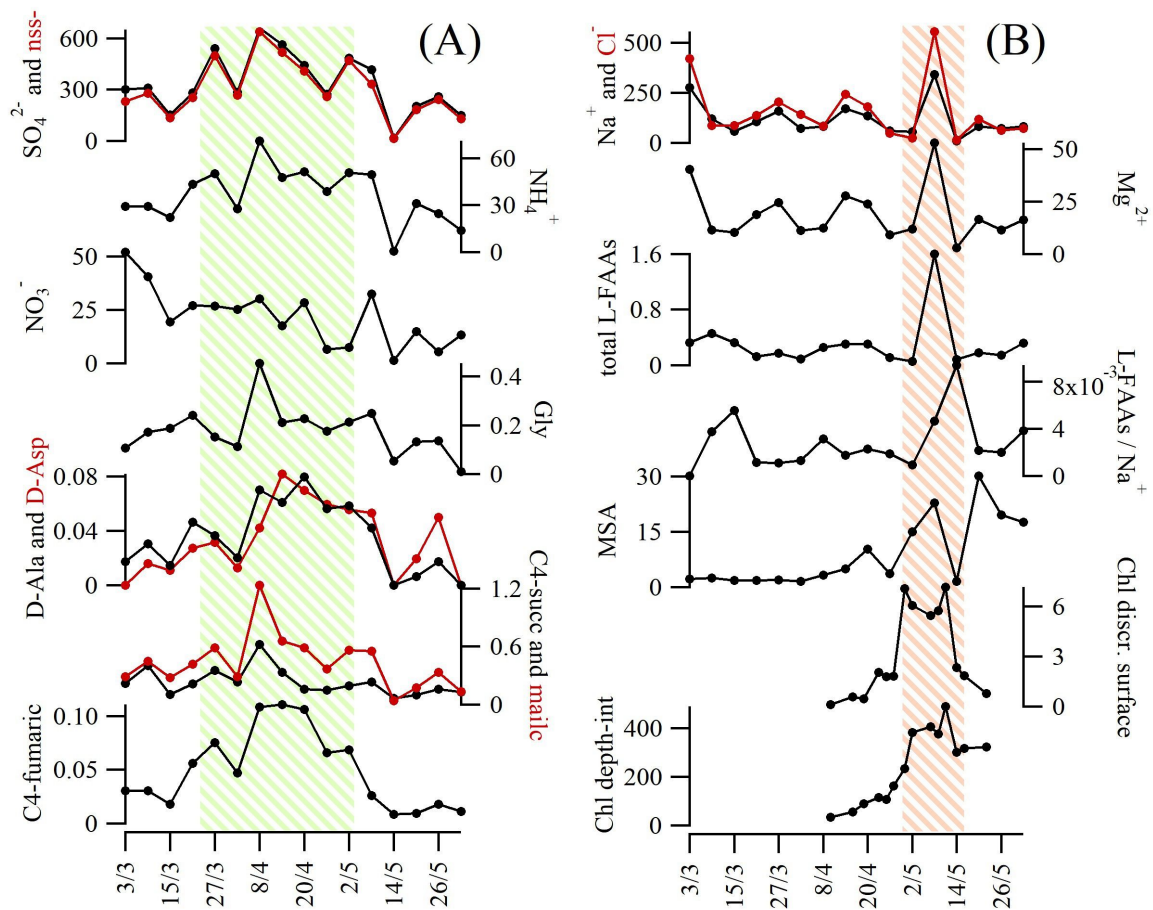


FIGURE 3: Target compounds PM₁₀ concentration trend (ng m⁻³). L-FAAs/Na⁺ is dimensionless. "Chl depth-int" represents the 0-100 m depth-integrated standing stocks (mg Chl *a* m⁻²) and "Chl discr. surface" represents the 10 m surface discrete concentrations (μg Chl *a* L⁻¹). The graphs in column A represents the compounds derived from the exponential bloom (green-shaded), while column B represents the post-bloom phase (orange-shaded).

detected Euryarchaeota were unique to the coarse fraction. Deseq2 analysis found 17 genera that were significant in driving the differences observed between fractions, and all were more abundant in the coarse fraction, with 5 found only in the coarse fraction including *Morganella*, *Pseudophaeobacter*, *Granulicatella*, *Fronidhabitans* and *Ilumatobacter*.



FIGURE 4: Comparisons of microbial communities between coarse and fine fractions. The Venn diagram represents the amount of unique and shared OTUs across fractions, while the stacked histogram represents the relative abundance of OTUs at the Class level in each of the samples over time.

3.3 Temporal variability in microbial aerosol communities

Microbial aerosol community structure and diversity varied significantly over time. Based on adonis and permanova analysis, samples collected in March and April were significantly different from those collected in May ($p=0.003$ for both comparisons, although no differences were detected between March and April (Table S3). Both months had higher Shannon and Observed species indices as compared to May (Figure 5, March vs May, $p=0.0013$, April vs May, $p=0.0017$, Pairwise Wilcoxon test, adjustment method, Holm).

Samples from May had a higher relative abundance in *Betaproteobacteria* and a lower relative abundance in *Gammaproteobacteria* (Figure 5) relative to those from March and April. Based on Deseq2 analysis, 6 taxa were significantly more abundant in May relative to March:

Rugamonas (Oxalobacteraceae, Betaproteobacteria), unclassified Oxalobacteraceae, unclassified Betaproteobacteria, *Butyrivibrio* and *Roseburia* (Lachnospiraceae, Clostridia) and *Selenomonas* (Veillonellaceae, Negativicutes) (Table S5). The same genera were also significantly more abundant in May relative to April, with the addition of *Janthinobacterium* (Oxalobacteraceae, Betaproteobacteria) and *Polaribacter* (Flavobacteria) (Table S5). SIMPER analysis showed that, among the 10 genera that contributed the most to seasonal differences in taxonomy, *Oxalobacteraceae* (Betaproteobacteria), *Polaribacter* and *Actinobacteria* were more abundant in May, while *Gammaproteobacteria* were more abundant in March and April (Table S6).

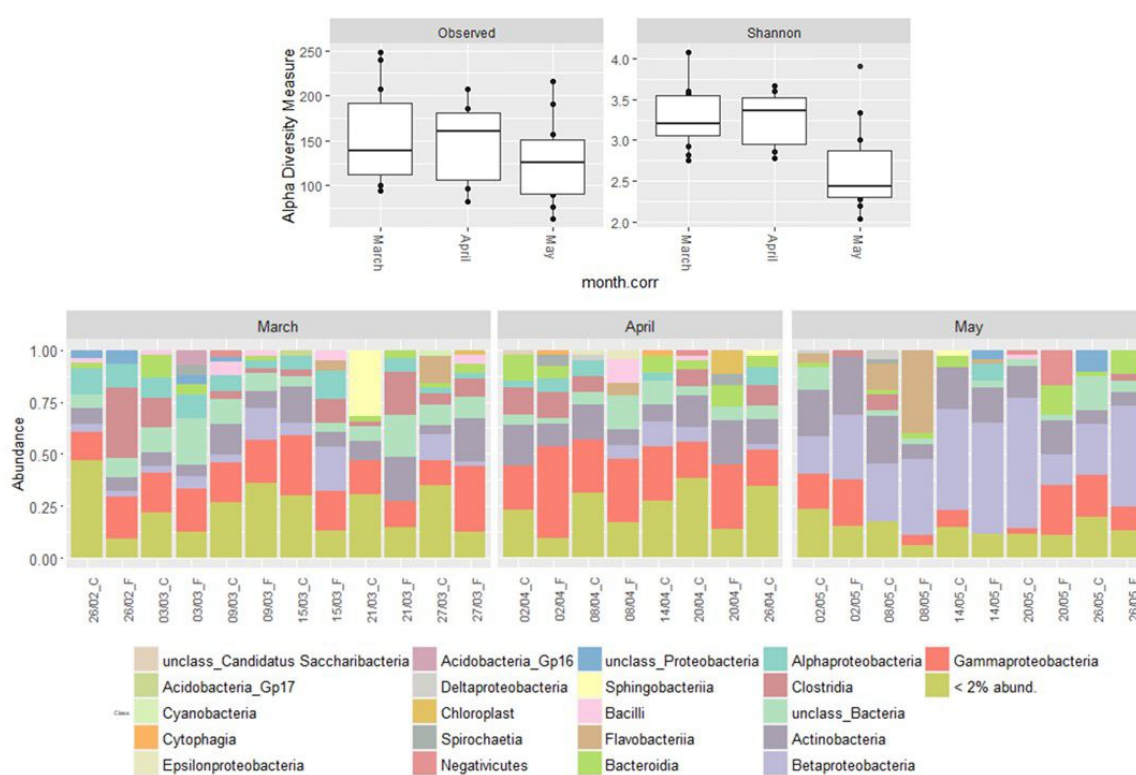


FIGURE 5: Changes in biodiversity and community structure of air samples over time.

3.4 Correlations among chemical and biological datasets in aerosol

Based on co-inertia analysis, bacterial and chemical data from aerosol samples co-varied significantly (0.49, simulated p-value on 999 replicates: 0.001). The main chemical axes of the co-inertia analysis (arrows, Figure S4) were represented by marine salts and nitrate (Na^+ , Cl^- , Ca^{2+}), MSA, C4-carboxylic acids (malic, succinic and fumaric) and D-amino acids, Br^- and I^-

(Figure S4). VIF analysis showed that parameters with the most significant impact on the co-structure were D-Ala, MSA, Br⁻, C1-formic acid, cell count estimations and NO₃⁻ (VIF parameters: 1.71, 1.69, 2.10, 1.65, 2.23, 1.85). OTUs associated with marine salts included taxa from Gammaproteobacteria (*Azomonas*, *Kluyvera*, *Lysobacter*, *Salinimonas*) Deltaproteobacteria (unclassified Deltaproteobacteria, *Geothermobacter*), Alphaproteobacteria (*Pseudopelagicola*), Actinobacteria (*Ilumatobacter*), Planctomycetes (*Gimesia*). MSA-associated OTUs included Betaproteobacteria, specifically Oxalobacteraceae (unclass., *Janthinobacterium*, *Rugamonas*), Alphaproteobacteria (*Alsobacter*), Actinobacteria (uncl. Micrococceae, *Zhihengliuella*), Bacteroides (Bacteroidia). D-amino-acid associated OTUs included Gammaproteobacteria (Enterobacteriales: *Ewingella*, *Plesiomonas*, *Biostraticola*), Firmicutes (Clostridia (*Clostridium* XIVb, *Mobilitalea*), Bacilli (*Lactovum* and *Pilibacter*)) and Actinobacteria (Propionibacteriaceae and Corynebacteriaceae). The Br⁻/I⁻ axis (including C1-C3 organic acids) co-varied with Gammaproteobacteria (unclassified Oceanospirillales, *Amphritea*, *Neptuniibacter*), and Alphaproteobacteria (unclassified Streptococcaceae).

4. Discussion

4.1 Origin of airborne microorganisms

Airborne microorganisms in the planetary boundary layer (PBL) are aerosolized from their surrounding ecosystems (generally those within a 50 km radius) and variations in their community composition have been shown to be determined by a number of factors, including the diversity and evenness of the surrounding landscapes and wind direction variability over time (Tignat-Perrier et al., 2019). The sampling site at Gruebadet Atmospheric Laboratory (Ny-Ålesund) was surrounded by snow-covered tundra and mountains during the sampling period and within 1.2 kms of Kongsfjorden, which was not covered by sea-ice in spring 2018. Potential sources for the sampled airborne microbial communities therefore include long-range atmospheric transport (LRAT), snow-covered landscapes and marine environment. To better identify the short- or long-range atmospheric transport, the differences between coarse ($D > 0.95 \mu\text{m}$) and fine fractions ($D < 0.95 \mu\text{m}$) were studied. In order for organisms to undergo LRAT, they must first enter the free troposphere from the PBL, a selective process that is in part size-dependent (Els et al., 2019b, 2019a; Poschl et al., 2010).

Based on the comparisons between coarse and fine fractions (Figure 4), the coarse fraction had a higher amount of unique genera. Although the communities were significantly

different, particle size only explained 7% of the variability. Given the higher diversity in coarse particles, we hypothesize that the contribution from LRAT to our airborne communities was minimal and that most of the microorganisms were sourced locally. Tignat-Perrier et al. (2019), also suggested that LRAT would have a minimal impact on PBL communities in a global study on the aerobiome using a similar sampling set-up as described here. In addition, the free troposphere community is generally dominated by globally omnipresent thermophilic, resistant, spore-forming Bacilli, generalistic Planctomycetes and yeast formers (Els et al., 2019a), which we were unable to identify in the fine fraction of our samples.

The most likely source of bacteria in our aerosol samples is the marine environment. Although these surfaces emit less organisms than terrestrial ones, the snow-covered mountains and tundra are predicted to emit even less (Burrows et al., 2009b, 2009a; Tignat-Perrier et al., 2019). In addition, the dominant wind direction was from the fjord, and rarely from the terrestrial environment (Figure S5). Aerosolization of microorganisms from the marine environment can occur through bubble bursting, breaking waves and sea-spray and a recent study suggested that certain taxa such as Actinobacteria and Gammaproteobacteria are preferentially aerosolized (Michaud et al., 2018). Gammaproteobacteria dominated in our air samples in March and April, while Betaproteobacteria dominated in May, which suggests that processes other than preferential aerosolization determined airborne microbial structure. Co-inertia analysis also showed that the chemical and biological data sets covaried significantly, and the major drivers were related to marine sources, such as Na^+ , Cl^- , Br^- and MSA, which supports the hypothesis of a similar source in our atmospheric samples.

4.2 Impact of phytoplankton blooms on atmospheric bacterial community structure and chemistry

A typical phytoplankton spring bloom was observed over the sampling period (Figure 3) (Hegseth et al., 2019). Previous research in Svalbard has shown that fjords are biologically active even during the polar night (Berge et al., 2015; Kvernvik et al., 2018), while as early as March phototrophic activities strongly increase with the return of the sun (Iversen and Seuthe, 2011). Phytoplankton mass accumulations, i.e. blooms generally occur in April-May (Hegseth et al., 2019). Bloom intensity and composition varies over time, with associated changes in biogeochemical responses, such as CO_2 and inorganic nutrient (nitrogen, phosphorus and silicon) assimilation. Congruently, NO_3^- strongly decreased during

the main phase of the bloom and was completely depleted by mid-May (data not shown). Photosynthetic activity leads to the production and release of organic molecules, not exclusively but especially under macronutrient limitation (Kragh and Søndergaard, 2009), that serves as chemo-attractants for other microorganisms, especially bacteria. In Arctic waters, the bacterial taxa that are generally associated with phytoplankton blooms are members of the classes Flavobacteriia, Alphaproteobacteria (specifically Rhodobacteraceae), and Gammaproteobacteria (Buchan et al., 2014). As the bloom evolves, changes in both the types of organic molecules released and the associated microorganisms occur. In the early bloom stage, phytoplankton produces and releases a variety of soluble low molecular weight organic molecules including carbohydrates, sugar alcohols, amino/organic acids (Buchan et al., 2014) that initially attract Gammaproteobacteria, which have shown to be dominant in pre-bloom stages (Zhou et al., 2018). As the bloom evolves, a shift towards the release of more high molecular weight organic molecules such as cellulose, chitin, and pectin (Kirchman, 2002) occurs that drives the succession pattern in the microbial community to one in which Alphaproteobacteria and Flavobacteria dominate during the peak, stationary and decline phases (Pinhassi et al., 2004; Teeling et al., 2016; Zhou et al., 2018). Zhou et al. (2018), also reported the appearance of Betaproteobacteria and Deltaproteobacteria during the post-bloom stage.

The similarities to our aerosol samples are striking. Gammaproteobacteria, including members of the *Alteromonas* and *Pseudomonas* group, were dominant in our March-April pre-bloom air samples and were correlated to marine chemistry and LMW organic acids (Br⁻, and C1-C3 organic acids). The airborne community shifted in May, with a dominance of Betaproteobacteria including the rare marine genus *Janthinobacterium* and *Polaribacter* (Flavobacteria). Interestingly, this shift occurred in conjunction with an observed shift in the species composition of marine plankton from diatoms to *Phaeocystis* in our water samples (C. Hoppe pers. comm.). Bloom events of *Janthinobacterium* in the ocean, similar to those detected in our air samples over the course of our field study, have only been reported once (Alonso-Sáez et al., 2014), and it is hypothesized that these organisms are able to break down complex organic matter (Huston and Deming, 2002). Airborne *Polaribacter* peaked during the post-bloom and declining phase of the bloom. In the open ocean, transient blooms of rare Flavobacteria populations have been found associated with phytoplankton blooms (Teeling et al., 2012).

Roseobacter, a genus within the Rhodobacteraceae family in the Alphaproteobacteria, are

often associated to phytoplankton and serve as a model for microbial-plankton interactions (Buchan et al., 2014). Despite their reported dominance in Arctic marine waters (Alonso-Sáez et al., 2014; Bowman et al., 2012; Manganelli et al., 2009; Williams et al., 2013; Zeng et al., 2013), we were unable to detect this genus in our data set, but unclassified Rhodobacteraceae were shown to be significant in driving seasonal changes in microbial community structure based on simpler analysis. A year-long study on marine microbiology of the Arctic ocean conducted along the coast of Svalbard was also unable to detect *Roseobacter* (Wilson et al., 2017) and attributed this, in part, to primer mismatches, but our primers cover 84% of the *Roseobacter* sequences identified in the SILVA database. It is also possible that this genus has a low aerosolization potential. Michaud et al. (2018) reported that some Alphaproteobacteria were underrepresented in sea spray aerosol emissions.

Data on bacterial diversity and abundance also support the hypothesis of marine biological activity driving airborne community structure. We observed a decrease in phylogenetic diversity from March to May in our air samples, which mirrors observations carried out in a year-long study on bacterial diversity in Svalbard coastal waters. Wilson et al. (2017) found distinct seasonal fluctuations in marine bacterial communities with high richness in the autumn and winter months and low richness in late spring and summer, similar to previously published results on polar marine ecosystems (Ghiglione et al., 2012; Grzymiski et al., 2012; Ladau et al., 2013; Murray et al., 1998; Murray and Grzymiski, 2007). Bacterial abundance in our air samples also varied throughout the season and decreased during the exponential growth phase of the bloom (Figure S6). This has also been reported in the marine environment, with a decrease in microbial abundance that might be related to bacterial predation or competition (Buchan et al., 2014). An alternative hypothesis is that as the bloom progresses, bacteria undergo life-style changes, from free-living to particle attached, which might impact their aerosolization. In a study on the partitioning of microbial communities between suspended and sinking particles in polar marine waters, suspended particles were shown to be enriched in Bacteroidetes (including Flavobacteriales), Planctomycetes, Euryarchaeota (Cenarchaeales), and Deltaproteobacteria, amongst others (Duret et al., 2019). Sinking particles were generally more enriched in Gammaproteobacteria, Alphaproteobacteria (Rhodobacterales and Rhizobiales), Firmicutes (Bacillales, Gemellales and Lactobacillales) and Actinobacteria (Actinomycetales) and might be less prone to aerosolization (Duret et al., 2019).

Phytoplankton blooms occur rapidly over the course of several weeks, and the lifespan of individual algal cells within is short (Teeling et al., 2016, Hegseth et al. 2019). As the bloom is progressively more nutrient limited and finally collapses, high molecular weight organic molecules, including proteins, nucleic acids, polysaccharides and lipids, are released, and the decaying phytoplankton form aggregates such that are further mineralized by particle-associated bacteria (Buchan et al., 2014). These aggregates will either sink (Emil Ruff et al., 2014), or can be further released to the atmosphere by sea-spray where they can influence atmospheric chemistry. This phenomenon can explain the increase in C5, C6 and C7 acid concentrations at the end of May: these CA trends (Figure 3 and S3) may be primarily controlled by atmospheric oxidation of precursor fatty acids, whose sea emission should be enhanced during phases of higher biological activity (Kawamura et al., 1996). Phytoplankton, especially the genus *Phaeocystis* which dominated the second half of the bloom in Kongsfjorden from the second week of May onwards, also produce large amounts of the organic sulphur compound dimethylsulphoniopropionate (DMSP) that is metabolized to dimethyl sulphide (DMS), which can undergo photo-oxidation to MSA in the atmosphere (Saltzman et al., 1983). The highest MSA concentrations in our air samples, exclusively formed by photo-oxidation of DMS, emitted by phytoplankton, were determined in the beginning of May during the peak of phytoplankton biomass, supporting the hypothesis that atmospheric data can capture fjord bloom dynamics.

4.3 D- and L-amino acids, and Flavobacteria as markers for different stages in phytoplankton blooms

Amino acids exist in two forms, L- and D- enantiomers, with L-amino acids being almost exclusively incorporated into proteins. D-amino acids are produced by biotic racemization (Hernández and Cava, 2016) by bacteria, algae, and archaea and constitute a significant fraction of the dissolved organic matter content of oceans (Xu et al., 2017). D-amino acids exist in either combined, or free forms, with algal and bacterial peptidoglycan as the most common combined form (Xu et al., 2017; Yokoyama et al., 2003). In the present study, we investigated the free fraction of amino acids. During the sampling period, Gly, together with D-Ala and D-Asp, had a very similar trend with nss-SO_4^{2-} and NH_4^+ as well as C4-organic acids such as succinic, malic and fumaric acids, suggesting a similar source for these molecules (see the

correlation matrix in Table S2). The concentration peaks of these molecules were measured in atmospheric samples during the exponential phase of the algal bloom (Figure 3A). The main source of free amino acids in the environment is through the degradation of peptidoglycan, but microorganisms are also able to actively release them. Marine microalgae were shown to be among the most significant producers, with high levels of free D-amino acids measured in their cells (Yokoyama et al., 2003). While D-Ala was shown to be produced by all strains tested, D-Arg was only found in marine algae strains, further supporting a marine source for this amino acid. Possible roles for D-amino acids in microorganisms include a N-source, structural molecules for peptidoglycan walls of chloroplasts and bacteria or as a pool of molecules that can be converted to their L-enantiomer form for further use (Aliashkevich et al., 2018). L-Ala and L-Arg are both central metabolites in C4 photosynthesis (Schlüter et al., 2019), and it could be that the D-forms of these amino acids might be conserved as a storage pool for later use during CO₂ fixation. Reinfelder et al. (2000), suggested that C4 photosynthesis might be a dominant process in marine diatoms. In C4 photosynthesis, C4 organic acids, especially C4-malic acid, play a critical role in CO₂ fixation and uptake (Ludwig, 2016) and serve as organic carbon storage molecules (Reinfelder et al., 2004). We posit that, D-amino acids can serve as markers of biological marine production and that they correspond to the pre- and exponential phase of algal blooms.

A strong enrichment in L-amino acids in the coarse fraction was identified on the 8th of May, suggesting a local source. The same enrichment was also observed in Na⁺, Cl⁻, Mg²⁺, Ca²⁺ and partially by NO₃⁻ and K⁺ and this suggests a local event of bubble bursting. This peak is consistent with the post-bloom stage, during which phytoplankton releases proteins, amongst other molecules. The total L-FAAs (calculated as sum of all L-amino acids detected) well overlapped with the Chl *a* trend (Figure 3B) and can predict the change in the atmospheric microbiome occurred in May. Based on these results, we suggest that L-amino acids should be studied further as markers of the declining phases of phytoplankton blooms. In fact, some amino acids such as L-Glu, L-Leu and L-Ile and L-Val that are generally concentrated in diatom cell plasma and show strong depletion with an increasing state of decomposition (Zhang et al., 2015). To minimize the contribution of the bubble bursting event occurred during the stationary phase, we also normalized the total L-FAAs with the Na⁺ concentration, emphasizing only the bloom input. As reported in Figure 3B, the ratio L-FAA/Na⁺ started to increase the 8th of May and showed its higher value the 14th of May,

overlapping with the Chl *a* trend. This would suggest that the local phytoplankton bloom is the main source of L-FAAs.

Another marker might be *Polaribacter*, which correlates with the chlorophyll peak. A *Polaribacter* (Flavobacteria) bloom was also observed earlier in the season and might be linked to unmeasured microbial activity in the fjord, but longer time series need to be collected to validate this. If these markers are validated, they can then be further exploited in other archives, such as snow and ice cores.

5. Conclusions

Atmospheric biological and chemical sampling is an underexploited tool that could help monitor and predict changes in fjord dynamics. This is the first applied study that allows to associate chemical markers with biological analysis to clearly correlate them and to define sources of these tracers. This is a mandatory step towards using specific tracers in environmental or paleoclimatic studies. Gly, D-Ala and D-Asp and some C₄- organic acids increased during the exponential phase of marine bloom and started to drop at the beginning of the post-bloom phase. D-amino acids in microorganisms can act as N-sources and be converted to their L-enantiomer form for further use. Thus, D-amino acids could serve as indicators of developing marine blooms and be used to predict biological activity in marine ecosystems. On the other hand, *Polaribacter* together with free L-amino acids might constitute a useful marker for the post-bloom phase and decline of algal blooms, even considering the good overlap with the Chl *a* temporal distribution. A future perspective is to use L-amino acids as markers for bloom decline in other types of archives such as ice cores. Further research including year-round atmospheric monitoring coupled to marine sampling should be carried out to test these hypotheses.

Supplementary data

Supplementary data to this article can be found online *here*.

References

- Aliashkevich, A., Alvarez, L., Cava, F., 2018. New insights into the mechanisms and biological roles of D-amino acids in complex eco-systems. *Front. Microbiol.* 9, 1–11. <https://doi.org/10.3389/fmicb.2018.00683>
- Alonso-Sáez, L., Zeder, M., Harding, T., Pernthaler, J., Lovejoy, C., Bertilsson, S., Pedrós-Alió, C., 2014. Winter bloom of a rare betaproteobacterium in the Arctic Ocean. *Front. Microbiol.* 5, 1–9. <https://doi.org/10.3389/fmicb.2014.00425>
- Barbaro, E., Padoan, S., Kirchgeorg, T., Zangrando, R., Toscano, G., Barbante, C., Gambaro, A., 2017. Particle size distribution of inorganic and organic ions in coastal and inland Antarctic aerosol. *Environ. Sci. Pollut. Res.* 24, 2724–2733. <https://doi.org/10.1007/s11356-016-8042-x>
- Barbaro, E., Zangrando, R., Vecchiato, M., Piazza, R., Cairns, W.R.L., Capodaglio, G., Barbante, C., Gambaro, A., 2015. Free amino acids in Antarctic aerosol: potential markers for the evolution and fate of marine aerosol 5457–5469. <https://doi.org/10.5194/acp-15-5457-2015>
- Barbaro, E., Zangrando, R., Vecchiato, M., Turetta, C., Barbante, C., Gambaro, A., 2014. D- and L-amino acids in Antarctic lakes: Assessment of a very sensitive HPLC-MS method. *Anal. Bioanal. Chem.* 406, 5259–5270. <https://doi.org/10.1007/s00216-014-7961-y>
- Beck, L.J., Sarnela, N., Junninen, H., Hoppe, C.J.M., Garmash, O., Bianchi, F., Riva, M., Rose, C., Peräkylä, O., Wimmer, D., Kausiala, O., Jokinen, T., Ahonen, L., Mikkilä, J., Hakala, J., He, X., Kontkanen, J., Wolf, K.K.E., Cappelletti, D., Mazzola, M., Traversi, R., Petroselli, C., Viola, A.P., Vitale, V., Lange, R., Massling, A., Nøjgaard, J.K., Krejci, R., Karlsson, L., Zieger, P., Jang, S., Lee, K., Vakkari, V., Lampilahti, J., Thakur, R.C., Leino, K., Kangasluoma, J., Duplissy, E., Siivola, E., Marbouti, M., Tham, Y.J., Saiz-Lopez, A., Petäjä, T., Ehn, M., Worsnop, D.R., Skov, H., Kulmala, M., Kerminen, V., Sipilä, M., 2020. Differing mechanisms of new particle formation at two Arctic sites. *Geophys. Res. Lett.* in press. <https://doi.org/10.1029/2020gl091334>
- Behrenfeld, M.J., Halsey, K.H., Milligan, A.J., 2008. Evolved physiological responses of phytoplankton to their integrated growth environment. *Philos. Trans. R. Soc. B Biol. Sci.* 363, 2687–2703. <https://doi.org/10.1098/rstb.2008.0019>
- Berge, J., Daase, M., Renaud, P.E., Ambrose, W.G., Darnis, G., Last, K.S., Leu, E., Cohen, J.H., Johnsen, G., Moline, M.A., Cottier, F., Varpe, O., Shunatova, N., Bałazy, P., Morata, N., Massabuau, J.C., Falk-Petersen, S., Kosobokova, K., Hoppe, C.J.M., Węślawski, J.M., Kukliński, P., Legeżyńska, J., Nikishina, D., Cusa, M., Kędra, M., Włodarska-Kowalczyk, M., Vogedes, D., Camus, L., Tran, D., Michaud, E., Gabrielsen, T.M., Granovitch, A., Gonchar, A., Krapp, R., Callesen, T.A., 2015. Unexpected levels of biological activity during the polar night offer new perspectives on a warming arctic. *Curr. Biol.* 25, 2555–2561. <https://doi.org/10.1016/j.cub.2015.08.024>

- Bigg, E.K., Leck, C., 2008. The composition of fragments of bubbles bursting at the ocean surface. *J. Geophys. Res. Atmos.* 113, 1–7. <https://doi.org/10.1029/2007JD009078>
- Bigg, E.K., Leck, C., 2001. Cloud-active particles over the central Arctic Ocean. *J. Geophys. Res. Atmos.* 106, 32155–32166. <https://doi.org/10.1029/1999JD901152>
- Bischof, K., Convey, P., Duarte, P., Gattuso, J.-P., Granberg, M., Hop, H., Hoppe, C., Jiménez, C., Lisitsyn, L., Martinez, B., Roleda, M.Y., Thor, P., Wiktor, J.M., Gabrielsen, G.W., 2019. Kongsfjorden as Harbinger of the Future Arctic: Knowns, Unknowns and Research Priorities 537–562. https://doi.org/10.1007/978-3-319-46425-1_14
- Blanchard, D.C., 1989. The ejection of drops from the sea and their enrichment with bacteria and other materials: A review. *Estuaries* 12, 127–137. <https://doi.org/10.2307/1351816>
- Bowman, J.S., Rasmussen, S., Blom, N., Deming, J.W., Rysgaard, S., Sicheritz-Ponten, T., 2012. Microbial community structure of Arctic multiyear sea ice and surface seawater by 454 sequencing of the 16S RNA gene. *ISME J.* 6, 11–20. <https://doi.org/10.1038/ismej.2011.76>
- Buchan, A., LeClerc, G.R., Gulvik, C.A., González, J.M., 2014. Master recyclers: features and functions of bacteria associated with phytoplankton blooms. *Nat. Rev. Microbiol.* 12, 686–698. <https://doi.org/10.1038/nrmicro3326>
- Burrows, S.M., Butler, T., Jöckel, P., Tost, H., Kerkweg, A., Pöschl, U., Lawrence, M.G., 2009a. Bacteria in the global atmosphere – Part 2: Modelling of emissions and transport between different ecosystems. *Atmos. Chem. Phys. Discuss.* 9, 10829–10881. <https://doi.org/10.5194/acpd-9-10829-2009>
- Burrows, S.M., Elbert, W., Lawrence, M.G., Pöschl, U., 2009b. Bacteria in the global atmosphere - Part 1: Review and synthesis of literature data for different ecosystems. *Atmos. Chem. Phys.* 9, 9263–9280. <https://doi.org/10.5194/acp-9-9263-2009>
- Chan, M.N., Choi, M.Y., Ng, N.L., Chan, C.K., 2005. Hygroscopicity of water-soluble organic compounds in atmospheric aerosols: Amino acids and biomass burning derived organic species. *Environ. Sci. Technol.* 39, 1555–1562. <https://doi.org/10.1021/es049584l>
- Davis, N.M., Proctor, D.M., Holmes, S.P., Relman, D.A., Callahan, B.J., 2018. Simple statistical identification and removal of contaminant sequences in marker-gene and metagenomics data. *Microbiome* 6, 1–14. <https://doi.org/10.1186/s40168-018-0605-2>
- Dittmar, T., Fitznar, H.P., Kattner, G., 2001. Origin and biogeochemical cycling of organic nitrogen in the eastern Arctic Ocean as evident from D- and L-amino acids. *Geochim. Cosmochim. Acta* 65, 4103–4114.
- Dommergue, A., Amato, P., Tignat-Perrier, R., Magand, O., Thollot, A., Joly, M., Bouvier, L., Sellegri, K., Vogel, T., Sonke, J.E.,

- Jaffrezo, J.-L., Andrade, M., Moreno, I., Labuschagne, C., Martin, L., Zhang, Q., Larose, C., 2019. Methods to Investigate the Global Atmospheric Microbiome. *Front. Microbiol.* 10, 1–12. <https://doi.org/10.3389/fmicb.2019.00243>
- Duret, M.T., Lampitt, R.S., Lam, P., 2019. Prokaryotic niche partitioning between suspended and sinking marine particles. *Environ. Microbiol. Rep.* 11, 386–400. <https://doi.org/10.1111/1758-2229.12692>
- Els, N., Baumann-Stanzer, K., Larose, C., Vogel, T.M., Sattler, B., 2019a. Beyond the planetary boundary layer: Bacterial and fungal vertical biogeography at Mount Sonnblick, Austria. *Geo Geogr. Environ.* 6. <https://doi.org/10.1002/geo2.69>
- Els, N., Larose, C., Baumann-Stanzer, K., Tignat-Perrier, R., Keuschnig, C., Vogel, T.M., Sattler, B., 2019b. Microbial composition in seasonal time series of free tropospheric air and precipitation reveals community separation, *Aerobiologia*. Springer Netherlands. <https://doi.org/10.1007/s10453-019-09606-x>
- Emil Ruff, S., Probandt, D., Zinkann, A.C., Iversen, M.H., Klaas, C., Würzberg, L., Krombholz, N., Wolf-Gladrow, D., Amann, R., Knittel, K., 2014. Indications for algae-degrading benthic microbial communities in deep-sea sediments along the Antarctic Polar Front. *Deep. Res. Part II Top. Stud. Oceanogr.* 108, 6–16. <https://doi.org/10.1016/j.dsr2.2014.05.011>
- Falkovich, A.H., Graber, E.R., Schkolnik, G., Rudich, Y., Maenhaut, W., Artaxo, P., 2005. Low molecular weight organic acids in aerosol particles from Rondônia, Brazil, during the biomass-burning, transition and wet periods. *Atmos. Chem. Phys.* 5, 781–797. <https://doi.org/10.5194/acp-5-781-2005>
- Feltracco, M., Barbaro, E., Kirchgeorg, T., Spolaor, A., Turetta, C., Zangrando, R., Barbante, C., Gambaro, A., 2019. Free and combined L- and D-amino acids in Arctic aerosol. *Chemosphere* 220, 412–421. <https://doi.org/10.1016/j.chemosphere.2018.12.147>
- Feltracco, M., Barbaro, E., Spolaor, A., Vecchiato, M., Callegaro, A., Burgay, F., Vardè, M., Maffezzoli, N., Dallo, F., Scoto, F., Zangrando, R., Barbante, C., Gambaro, A., 2021. Year-round measurements of size-segregated low molecular weight organic acids in Arctic aerosol. *Sci. Total Environ.* 763, 10. <https://doi.org/10.1016/j.scitotenv.2020.142954>
- Feltracco, M., Barbaro, E., Tedeschi, S., Spolaor, A., Turetta, C., Vecchiato, M., Morabito, E., Zangrando, R., Barbante, C., Gambaro, A., 2020. Interannual variability of sugars in Arctic aerosol: Biomass burning and biogenic inputs. *Sci. Total Environ.* 706, 136089. <https://doi.org/10.1016/j.scitotenv.2019.136089>
- Fierer, N., Jackson, J.A., Vilgalys, R., Jackson, R.B., 2005. Assessment of soil microbial community structure by use of taxon-specific quantitative PCR assays. *Appl. Environ. Microbiol.* 71, 4117–4120. <https://doi.org/10.1128/AEM.71.7.4117-4120.2005>
- Friedman, B., Herich, H., Kammermann, L., Gross, D.S., Arneth, A., Holst, T., Cziczo, D.J., 2009. Subarctic atmospheric aerosol composition: 1. Ambient aerosol characterization. *J. Geophys. Res. Atmos.* 114, 1–11. <https://doi.org/10.1029/2009JD011772>

- Gao, Q., Leck, C., Rauschenberg, C., Matrai, P.A., 2012. On the chemical dynamics of extracellular polysaccharides in the high Arctic surface microlayer. *Ocean Sci.* 8, 401–418. <https://doi.org/10.5194/os-8-401-2012>
- Ge, X., Wexler, A.S., Clegg, S.L., 2011. Atmospheric amines - Part I. A review. *Atmos. Environ.* 45, 524–546. <https://doi.org/10.1016/j.atmosenv.2010.10.012>
- Geng, H., Ryu, J., Jung, H.J., Chung, H., Ahn, K.H.O., Ro, C.U.N., 2010. Single-particle characterization of summertime arctic aerosols collected at Ny-Ålesund, Svalbard. *Environ. Sci. Technol.* 44, 2348–2353. <https://doi.org/10.1021/es903268j>
- Ghiglione, J.F., Galand, P.E., Pommier, T., Pedrós-Alió, C., Maas, E.W., Bakker, K., Bertilson, S., Kirchman, D.L., Lovejoy, C., Yager, P.L., Murray, A.E., 2012. Pole-to-pole biogeography of surface and deep marine bacterial communities. *Proc. Natl. Acad. Sci. U. S. A.* 109, 17633–17638. <https://doi.org/10.1073/pnas.1208160109>
- Giardi, F., Becagli, S., Traversi, R., Frosini, D., Severi, M., Caiazza, L., Ancillotti, C., Cappelletti, D., Moroni, B., Grotti, M., Bazzano, A., Lupi, A., Mazzola, M., Vitale, V., Abollino, O., Ferrero, L., Bolzacchini, E., Viola, A., Udisti, R., 2016. Size distribution and ion composition of aerosol collected at Ny-Ålesund in the spring-summer field campaign 2013. *Rend. Lincei* 27, 47–58. <https://doi.org/10.1007/s12210-016-0529-3>
- Gong, S.L., 2003. A parameterization of sea-salt aerosol source function for sub- and super-micron particles. *Global Biogeochem. Cycles* 17, n/a-n/a. <https://doi.org/10.1029/2003gb002079>
- Grzymiski, J.J., Riesenfeld, C.S., Williams, T.J., Dussaq, A.M., Ducklow, H., Erickson, M., Cavicchioli, R., Murray, A.E., 2012. A metagenomic assessment of winter and summer bacterioplankton from Antarctica Peninsula coastal surface waters. *ISME J.* 6, 1901–1915. <https://doi.org/10.1038/ismej.2012.31>
- Hamacher-Barth, E., Leck, C., Jansson, K., 2016. Size-resolved morphological properties of the high Arctic summer aerosol during ASCOS-2008. *Atmos. Chem. Phys.* 16, 6577–6593. <https://doi.org/10.5194/acp-16-6577-2016>
- Hegseth, E.N., Assmy, P., Wiktor, J.M., Wiktor, J., Kristiansen, S., Leu, E., Tverberg, V., Gabrielsen, T.M., Skogseth, R., Cottier, F., 2019. Phytoplankton Seasonal Dynamics in Kongsfjorden, Svalbard and the Adjacent Shelf. https://doi.org/10.1007/978-3-319-46425-1_6
- Hernández, S.B., Cava, F., 2016. Environmental roles of microbial amino acid racemases. *Environ. Microbiol.* 18, 1673–1685. <https://doi.org/10.1111/1462-2920.13072>
- Huston, A.L., Deming, J.W., 2002. Relationships between microbial extracellular enzymatic activity and suspended and sinking particulate organic matter: Seasonal transformations in the North Water. *Deep. Res. Part II Top. Stud. Oceanogr.* 49, 5211–5225. [https://doi.org/10.1016/S0967-0645\(02\)00186-8](https://doi.org/10.1016/S0967-0645(02)00186-8)

- Iversen, K.R., Seuthe, L., 2011. Seasonal microbial processes in a high-latitude fjord (Kongsfjorden, Svalbard): I. Heterotrophic bacteria, picoplankton and nanoflagellates. *Polar Biol.* 34, 731–749. <https://doi.org/10.1007/s00300-010-0929-2>
- Kawamura, K., Kasukabe, H., Barrie, L.A., 1996. Source and reaction pathways of dicarboxylic acids, ketoacids and dicarbonyls in arctic aerosols: One year of observations. *Atmos. Environ.* 30, 1709–1722. [https://doi.org/10.1016/1352-2310\(95\)00395-9](https://doi.org/10.1016/1352-2310(95)00395-9)
- Keith Bigg, E., Leck, C., Tranvik, L., 2004. Particulates of the surface microlayer of open water in the central Arctic Ocean in summer. *Mar. Chem.* 91, 131–141. <https://doi.org/10.1016/j.marchem.2004.06.005>
- Kirchman, D.L., 2002. The ecology of Cytophaga-Flavobacteria in aquatic environments. *FEMS Microbiol. Ecol.* 39, 91–100. [https://doi.org/10.1016/S0168-6496\(01\)00206-9](https://doi.org/10.1016/S0168-6496(01)00206-9)
- Klindworth, A., Pruesse, E., Schweer, T., Peplies, J., Quast, C., Horn, M., Glöckner, F.O., 2013. Evaluation of general 16S ribosomal RNA gene PCR primers for classical and next-generation sequencing-based diversity studies. *Nucleic Acids Res.* 41, 1–11. <https://doi.org/10.1093/nar/gks808>
- Kragh, T., Søndergaard, M., 2009. Production and decomposition of new DOC by marine plankton communities: Carbohydrates, refractory components and nutrient limitation. *Biogeochemistry* 96, 177–187. <https://doi.org/10.1007/s10533-009-9357-1>
- Kvernvik, A.C., Hoppe, C.J.M., Lawrenz, E., Prášil, O., Greenacre, M., Wiktor, J.M., Leu, E., 2018. Fast reactivation of photosynthesis in arctic phytoplankton during the polar night¹. *J. Phycol.* 54, 461–470. <https://doi.org/10.1111/jpy.12750>
- Ladau, J., Sharpton, T.J., Finucane, M.M., Jospin, G., Kembel, S.W., O'Dwyer, J., Koepfel, A.F., Green, J.L., Pollard, K.S., 2013. Global marine bacterial diversity peaks at high latitudes in winter. *ISME J.* 7, 1669–1677. <https://doi.org/10.1038/ismej.2013.37>
- Leck, C., Persson, C., 1996. The central Arctic Ocean as a source of dimethyl sulfide Seasonal variability in relation to biological activity. *Tellus, Ser. B Chem. Phys. Meteorol.* 48, 156–177. <https://doi.org/10.3402/tellusb.v48i2.15834>
- Leck, C., Svensson, E., 2015. Importance of aerosol composition and mixing state for cloud droplet activation over the Arctic pack ice in summer. *Atmos. Chem. Phys.* 15, 2545–2568. <https://doi.org/10.5194/acp-15-2545-2015>
- Li, M., Yu, X., Kang, H., Xie, Z., Zhang, P., 2017. Concentrations and size distributions of bacteria-containing particles over oceans from China to the Arctic ocean. *Atmosphere (Basel)*. 8. <https://doi.org/10.3390/atmos8050082>
- Love, M.I., Huber, W., Anders, S., 2014. Moderated estimation of fold change and dispersion for RNA-seq data with DESeq2. *Genome Biol.* 15, 550. <https://doi.org/10.1186/s13059-014-0550-8>
- Ludwig, M., 2016. The roles of organic acids in C4 photosynthesis. *Front. Plant Sci.* 7, 1–11. <https://doi.org/10.3389/fpls.2016.00647>
- Manganelli, M., Malfatti, F., Samo, T.J., Mitchell, B.G., Wang, H., Azam, F., 2009. Major role of microbes in carbon fluxes during

- austral winter in the southern Drake Passage. *PLoS One* 4, 1–11. <https://doi.org/10.1371/journal.pone.0006941>
- Masella, A.P., Bartram, A.K., Truszkowski, J.M., Brown, D.G., Neufeld, J.D., 2012. PANDAseq: PAired-eND Assembler for Illumina sequences. *BMC Bioinformatics* 13, 1–7. [https://doi.org/10.1016/s0739-5930\(09\)79285-2](https://doi.org/10.1016/s0739-5930(09)79285-2)
- Mashayekhy Rad, F., Zurita, J., Gilles, P., Rutgeerts, L.A.J., Nilsson, U., Ilag, L.L., Leck, C., 2019. Measurements of Atmospheric Proteinaceous Aerosol in the Arctic Using a Selective UHPLC/ESI-MS/MS Strategy. *J. Am. Soc. Mass Spectrom.* 30, 161–173. <https://doi.org/10.1007/s13361-018-2009-8>
- Maturilli M., I., H.-B., R., N., M., R., K., E., 2019. The Atmosphere Above Ny-Ålesund: Climate and Global Warming, Ozone and Surface UV Radiation, in: Hop H., Wiencke C. (Eds) *The Ecosystem of Kongsfjorden, Svalbard.* https://doi.org/https://doi.org/10.1007/978-3-319-46425-1_2
- McGregor, K.G., Anastasio, C., 2001. Chemistry of fog waters in California's Central Valley: 2. Photochemical transformations of amino acids and alkyl amines. *Atmos. Environ.* 35, 1091–1104. [https://doi.org/10.1016/S1352-2310\(00\)00282-X](https://doi.org/10.1016/S1352-2310(00)00282-X)
- Michaud, J.M., Thompson, L.R., Kaul, D., Espinoza, J.L., Richter, R.A., Xu, Z.Z., Lee, C., Pham, K.M., Beall, C.M., Malfatti, F., Azam, F., Knight, R., Burkart, M.D., Dupont, C.L., Prather, K.A., 2018. Taxon-specific aerosolization of bacteria and viruses in an experimental ocean-atmosphere mesocosm. *Nat. Commun.* 9. <https://doi.org/10.1038/s41467-018-04409-z>
- Murray, A.E., Grzymalski, J.J., 2007. Diversity and genomics of Antarctic marine micro-organisms. *Philos. Trans. R. Soc. B Biol. Sci.* 362, 2259–2271. <https://doi.org/10.1098/rstb.2006.1944>
- Murray, A.E., Preston, C.M., Massana, R., Taylor, L.T., Blakis, A., Wu, K., Delong, E.F., 1998. Seasonal and spatial variability of bacterial and archaeal assemblages in the coastal waters near Anvers Island, Antarctica. *Appl. Environ. Microbiol.* 64, 2585–2595. <https://doi.org/10.1128/aem.64.7.2585-2595.1998>
- Norris, S.J., Brooks, I.M., De Leeuw, G., Sirevaag, A., Leck, C., Brooks, B.J., Birch, C.E., Tjernström, M., 2011. Measurements of bubble size spectra within leads in the Arctic summer pack ice. *Ocean Sci.* 7, 129–139. <https://doi.org/10.5194/os-7-129-2011>
- O'Dowd, C.D., Facchini, M.C., Cavalli, F., Ceburnis, D., Mircea, M., Decesari, S., Fuzzi, S., Young, J.Y., Putaud, J.P., 2004. Biogenically driven organic contribution to marine aerosol. *Nature* 431, 676–680. <https://doi.org/10.1038/nature02959>
- Orellana, M. V., Matrai, P.A., Leck, C., Rauschenberg, C.D., Lee, A.M., Coz, E., 2011. Marine microgels as a source of cloud condensation nuclei in the high arctic. *Proc. Natl. Acad. Sci. U. S. A.* 108, 13612–13617. <https://doi.org/10.1073/pnas.1102457108>
- Pinhassi, J., Sala, M.M., Havskum, H., Peters, F., Guadayol, Ò., Malits, A., Marrasé, C., 2004. Changes in bacterioplankton composition under different phytoplankton regimens. *Appl. Environ. Microbiol.* 70, 6753–6766.

<https://doi.org/10.1128/AEM.70.11.6753-6766.2004>

- Poschl, U., Martin, S.T., Sinha, B., Chen, Q., Gunthe, S.S., Huffman, J.A., Borrmann, S., Farmer, D.K., Garland, R.M., Helas, G., Jimenez, J.L., King, S.M., Manzi, A., Mikhailov, E., Pauliquevis, T., Petters, M.D., Prenni, A.J., Roldin, P., Rose, D., Schneider, J., Su, H., Zorn, S.R., Artaxo, P., Andreae, M.O., 2010. Rainforest Aerosols as Biogenic Nuclei of Clouds and Precipitation in the Amazon. *Science* (80-.). 329, 1513–1516. <https://doi.org/10.1126/science.1191056>
- Quinn, P.K., Collins, D.B., Grassian, V.H., Prather, K.A., Bates, T.S., 2015. Chemistry and Related Properties of Freshly Emitted Sea Spray Aerosol. *Chem. Rev.* 115, 4383–4399. <https://doi.org/10.1021/cr500713g>
- Raes, F., Dingenen, R. Van, Elisabetta, V., Wilson, J., Putaud, J.P., Seinfeld, J.H., Adams, P., 2002. Formation and cycling of aerosols in the global troposphere. *Dev. Environ. Sci.* 24, 519–563. [https://doi.org/10.1016/S1474-8177\(02\)80021-3](https://doi.org/10.1016/S1474-8177(02)80021-3)
- Reinfelder, J.R., Kraepiel, A.M.L., Morel, F.M.M., 2000. Unicellular C4 photosynthesis in a marine diatom. *Nature* 407, 996–999. <https://doi.org/10.1038/35039612>
- Reinfelder, J.R., Milligan, A.J., Morel, F.M.M., 2004. The role of the C4 pathway in carbon accumulation and fixation in a marine diatom. *Plant Physiol.* 135, 2106–2111. <https://doi.org/10.1104/pp.104.041319>
- Rinaldi, M., Decesari, S., Carbone, C., Finessi, E., Fuzzi, S., Ceburnis, D., O'Dowd, C.D., Sciare, J., Burrows, J.P., Vrekoussis, M., Ervens, B., Tsigaridis, K., Facchini, M.C., 2011. Evidence of a natural marine source of oxalic acid and a possible link to glyoxal. *J. Geophys. Res. Atmos.* 116, 1–12. <https://doi.org/10.1029/2011JD015659>
- Salter, M.E., Hamacher-Barth, E., Leck, C., Werner, J., Johnson, C.M., Riipinen, I., Nilsson, E.D., Zieger, P., 2016. Calcium enrichment in sea spray aerosol particles. *Geophys. Res. Lett.* 43, 8277–8285. <https://doi.org/10.1002/2016GL070275>
- Saltzman, E.S., Savoie, D.L., Zika, R.G., Prospero, J.M., 1983. Methane sulfonic acid in the marine atmosphere. *J. Geophys. Res.* 88, 10897–10902. <https://doi.org/10.1029/JC088iC15p10897>
- Schlüter, U., Bräutigam, A., Droz, J.M., Schwender, J., Weber, A.P.M., 2019. The role of alanine and aspartate aminotransferases in C4 photosynthesis. *Plant Biol.* 21, 64–76. <https://doi.org/10.1111/plb.12904>
- Stefels, J., Steinke, M., Turner, S., Malin, G., Belviso, S., 2007. Environmental constraints on the production and removal of the climatically active gas dimethylsulphide (DMS) and implications for ecosystem modelling. *Phaeocystis, Major Link Biogeochem. Cycl. Clim. Elem.* 245–275. https://doi.org/10.1007/978-1-4020-6214-8_18
- Teeling, H., Fuchs, B.M., Becher, D., Klockow, C., Gardebrecht, A., Bennis, C.M., Kassabgy, M., Huang, S., Mann, A.J., Waldmann, J., Weber, M., Klindworth, A., Otto, A., Lange, J., Bernhardt, J., Reinsch, C., Hecker, M., Peplies, J., Bockelmann, F.D., Callies, U., Gerdt, G., Wichels, A., Wiltshire, K.H., Glöckner, F.O., Schweder, T., Amann, R., 2012. Substrate-

- controlled succession of marine bacterioplankton populations induced by a phytoplankton bloom. *Science* (80-.). 336, 608–611. <https://doi.org/10.1126/science.1218344>
- Teeling, H., Fuchs, B.M., Bennis, C.M., Krüger, K., Chafee, M., Kappelmann, L., Reintjes, G., Waldmann, J., Quast, C., Glöckner, F.O., Lucas, J., Wichels, A., Gerdt, G., Wiltshire, K.H., Amann, R.L., 2016. Recurring patterns in bacterioplankton dynamics during coastal spring algae blooms. *Elife* 5, 1–31. <https://doi.org/10.7554/eLife.11888>
- Tignat-Perrier, R., Dommergue, A., Thollot, A., Keusch, C., Magand, O., Vogel, T.M., Larose, C., 2019. Global airborne microbial communities controlled by surrounding landscapes and wind conditions. *Sci. Rep.* 9, 1–11. <https://doi.org/10.1038/s41598-019-51073-4>
- Tignat-Perrier, R., Dommergue, A., Thollot, A., Magand, O., Amato, P., Joly, M., Sellegri, K., Vogel, T.M., Larose, C., 2020. Seasonal shift in airborne microbial communities. *Sci. Total Environ.* 716, 137129. <https://doi.org/10.1016/j.scitotenv.2020.137129>
- Timonen, H., Saarikoski, S., Tolonen-Kivimä, O., Aurela, M., Saarnio, K., Petäjä, T., Aalto, P.P., Kulmala, M., Pakkanen, T., Hillamo, R., 2008. Size distributions, sources and source areas of water-soluble organic carbon in urban background air. *Atmos. Chem. Phys.* 8, 5635–5647. <https://doi.org/10.5194/acp-8-5635-2008>
- Tromas, N., Fortin, N., Bedrani, L., Terrat, Y., Cardoso, P., Bird, D., Greer, C.W., Shapiro, B.J., 2017. Characterising and predicting cyanobacterial blooms in an 8-year amplicon sequencing time course. *ISME J.* 11, 1746–1763. <https://doi.org/10.1038/ismej.2017.58>
- Tverberg, V., Skogseth, R., Cottier, F., Sundfjord, Walczowski, W., Inall, M.E., Falck, E., Pavlova, O., Nilsen, F., 2019. Chapter 3: The Kongsfjorden transect: seasonal and inter-annual variability in hydrography.
- van de Poll, W.H., Maat, D.S., Fischer, P., Visser, R.J.W., Brussaard, C.P.D., Buma, A.G.J., 2020. Solar radiation and solar radiation driven cycles in warming and freshwater discharge control seasonal and inter-annual phytoplankton chlorophyll a and taxonomic composition in a high Arctic fjord (Kongsfjorden, Spitsbergen). *Limnol. Oceanogr.* 2014, 1–16. <https://doi.org/10.1002/lno.11677>
- Wang, Q., Garrity, G.M., Tiedje, J.M., Cole, J.R., 2007. Naïve Bayesian classifier for rapid assignment of rRNA sequences into the new bacterial taxonomy. *Appl. Environ. Microbiol.* 73, 5261–5267. <https://doi.org/10.1128/AEM.00062-07>
- Williams, T.J., Wilkins, D., Long, E., Evans, F., Demaree, M.Z., Raftery, M.J., Cavicchioli, R., 2013. The role of planktonic Flavobacteria in processing algal organic matter in coastal East Antarctica revealed using metagenomics and metaproteomics. *Environ. Microbiol.* 15, 1302–1317. <https://doi.org/10.1111/1462-2920.12017>
- Wilson, B., Müller, O., Nordmann, E.L., Seuthe, L., Bratbak, G., Øvreås, L., 2017. Changes in marine prokaryote composition with

- season and depth over an Arctic polar year. *Front. Mar. Sci.* 4, 1–17. <https://doi.org/10.3389/fmars.2017.00095>
- Xing, X., Claustre, H., Blain, S., D'Ortenzio, F., Antoine, D., Ras, J., Guinet, C., 2012. Quenching correction for in vivo chlorophyll fluorescence acquired by autonomous platforms: A case study with instrumented elephant seals in the Kerguelen region (Southern Ocean). *Limnol. Oceanogr. Methods* 10, 483–495. <https://doi.org/10.4319/lom.2012.10.483>
- Xu, J., Bai, Y., Fan, T., Zheng, X., Cai, Y., 2017. Expression, purification, and characterization of a membrane-bound d-amino acid dehydrogenase from *Proteus mirabilis* JN458. *Biotechnol. Lett.* 39, 1559–1566. <https://doi.org/10.1007/s10529-017-2388-0>
- Yokoyama, T., Kan-No, N., Ogata, T., Kotaki, Y., Sato, M., Nagahisa, E., 2003. Presence of free D-amino acids in microalgae. *Biosci. Biotechnol. Biochem.* 67, 388–392. <https://doi.org/10.1271/bbb.67.388>
- Zangrando, R., Barbaro, E., Zennaro, P., Rossi, S., Kehrwald, N.M., Gabrieli, J., Barbante, C., Gambaro, A., 2013. Molecular markers of biomass burning in Arctic aerosols. *Environ. Sci. Technol.* 47, 8565–8574. <https://doi.org/10.1021/es400125r>
- Zeng, Y.X., Zhang, F., He, J.F., Lee, S.H., Qiao, Z.Y., Yu, Y., Li, H.R., 2013. Bacterioplankton community structure in the Arctic waters as revealed by pyrosequencing of 16S rRNA genes. *Antonie van Leeuwenhoek, Int. J. Gen. Mol. Microbiol.* 103, 1309–1319. <https://doi.org/10.1007/s10482-013-9912-6>
- Zhang, G., Liang, S., Shi, X., Han, X., 2015. Dissolved organic nitrogen bioavailability indicated by amino acids during a diatom to dinoflagellate bloom succession in the Changjiang River estuary and its adjacent shelf. *Mar. Chem.* 176, 83–95. <https://doi.org/10.1016/j.marchem.2015.08.001>
- Zhou, J., Richlen, M.L., Sehein, T.R., Kulis, D.M., Anderson, D.M., Cai, Z., 2018. Microbial community structure and associations during a marine dinoflagellate bloom. *Front. Microbiol.* 9, 1–21. <https://doi.org/10.3389/fmicb.2018.01201>

Appendix B

As first author this Elsevier article, I retain the right to include them in this thesis (not for commercial use). Elsevier apply this right to all authors who publish their article as either a subscription article or an open access article. In all cases Elsevier requires to include a full acknowledgement and, if appropriate, a link to the final published version hosted on Science Direct. Here is reported the following published research article:

Photo-oxidation products of α -pinene in coarse, fine and ultrafine aerosol: A new high sensitive HPLC-MS/MS method

In this work it has been developed a new high sensitive method for the quantification of the main photo-oxidation products of α -pinene, in particular pinic acid and cis-pinonic acid, the predominant aerosol products from the photo-oxidation of α -pinene. 14 aerosol samples were collected at Scientific Campus of Ca'Foscari University (Mestre-Venice, Italy) during spring 2016, using the rotating model 120 MOUDI-II cascade impactor. The particle size distribution was obtained for aerodynamic diameter ranging from greater of 18 μm to below 0.056 μm . The configuration of sampler consists to eleven stages with cut sizes at 18, 10, 5.6, 3.2, 1.8, 1.0, 0.56, 0.32, 0.18, 0.10 and 0.056 μm , plus a final back-up filter used to collect particles with $D < 0.056 \mu\text{m}$.

The study aims to improve the existing analytical methods for the determination of pinic and cis-pinonic acid in aerosol in terms of analytical sensitivity and limits of detection (LOD) and quantification (LOQ). The study also attempts to increase the knowledge of the α -pinene photo-oxidation processes by analysing, for the first time, the particle-size distribution up to nanoparticle level.



Contents lists available at ScienceDirect

Atmospheric Environment

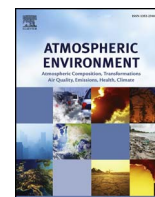
journal homepage: www.elsevier.com/locate/atmosenv

Photo-oxidation products of α -pinene in coarse, fine and ultrafine aerosol: A new high sensitive HPLC-MS/MS method



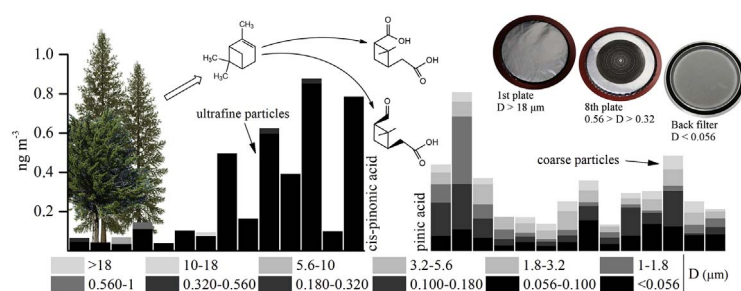
Matteo Feltracco^{a,*}, Elena Barbaro^b, Daniele Contini^c, Roberta Zangrando^b, Giuseppa Toscano^a, Dario Battistel^a, Carlo Barbante^{a,b}, Andrea Gambaro^{a,b}

^a Department of Environmental Sciences, Informatics and Statistics, University of Venice, Ca' Foscari, Via Torino 155, 30172, Venice, Italy

^b Institute for the Dynamics of Environmental Processes CNR, Via Torino 155, 30172, Venice, Italy

^c Institute of Atmospheric Sciences and Climate, ISAC-CNR, 73100, Lecce, Italy

GRAPHICAL ABSTRACT



ARTICLE INFO

Keywords:

Aerosol
Ultrafine particles
HPLC-MS/MS
Cis-pinonic acid
Pinic acid

ABSTRACT

Oxidation products of α -pinene represent a fraction of organic matter in the environmental aerosol. α -pinene is one of most abundant monoterpenes released in the atmosphere by plants, located typically in boreal, temperate and tropical forests. This primary compound reacts with atmospheric oxidants, such as O_3 , O_2 , OH radicals and NO_x , through the major tropospheric degradation pathway for many monoterpenes under typical atmospheric condition. Although several studies identified a series of by-products deriving from the α -pinene photo-oxidation in the atmosphere, such as pinic and cis-pinonic acid, the knowledge of the mechanism of this process is partially still lacking. Thus, the investigation of the distribution of these acids in the different size aerosol particles provides additional information on this regard.

The aim of this study is twofold. First, we aim to improve the existing analytical methods for the determination of pinic and cis-pinonic acid in aerosol samples, especially in terms of analytical sensitivity and limits of detection (LOD) and quantification (LOQ). We even attempted to increase the knowledge of the α -pinene photo-oxidation processes by analysing, for the first time, the particle-size distribution up to nanoparticle level of pinic and cis-pinonic acid. The analysis of aerosol samples was carried out via high-performance liquid chromatography coupled to a triple quadrupole mass spectrometer. The instrumental LOD values of cis-pinonic and pinic acid are 1.6 and 1.2 ng L^{-1} while LOQ values are 5.4 and 4.1 ng L^{-1} , respectively. Samples were collected by MOUDI II™ cascade impactor with twelve cut-sizes, from March to May 2016 in the urban area of Mestre-Venice (Italy).

* Corresponding author.

E-mail address: matteo.feltracco@unive.it (M. Feltracco).

<https://doi.org/10.1016/j.atmosenv.2018.02.052>

Received 13 November 2017; Received in revised form 21 February 2018; Accepted 26 February 2018

Available online 02 March 2018

1352-2310/ © 2018 Elsevier Ltd. All rights reserved.

The range concentrations in the aerosol samples were from 0.1 to 0.9 ng m⁻³ for cis-pinonic acid and from 0.1 to 0.8 ng m⁻³ for pinic acid.

1. Introduction

The formation of secondary organic aerosols (SOA) in the rural atmosphere has attracted growing interest in recent years. The atmospheric formation of new particles and their chemical composition can have an important role for the determination of the global aerosol load and their effect on the climate change (Kulmala et al., 2004).

Monoterpenes are the most abundant biogenic hydrocarbons in troposphere and these compounds affect the oxidising capacity of the atmosphere (Kanakidou et al., 2000). In the last years, considerable studies (Lamb et al., 1987; Larsen et al., 1999; Librando and Tringali, 2005) have been carried out to determine the secondary organic aerosol (SOA) formation from the photo-oxidation of volatile organic compounds (VOCs). In particular, α -pinene is the most important monoterpene released by biogenic sources, particularly conifers. It has an emission rate projected at global scale of about 127 Tg y⁻¹ (Guenther et al., 1995) and it has been shown to give high SOA yields in laboratory smog chamber research (Kahnt et al., 2014; Lamb et al., 1987; Larsen et al., 1999). The emission on global scale of total monoterpenes from the vegetation has been estimated between 120 and 480 Tg y⁻¹ (Fehsenfeld et al., 1992), therefore the α -pinene fraction represent a large part of global monoterpenes, by considering its emission rate. α -pinene is a primary ingredient of pine resin and it is also found other conifers and non-coniferous plants. Nevertheless, the atmospheric degradation proceeds through a very complex mechanism that is still not totally identified, and this leads to form an abundance of reaction products (Glasius et al., 2000, 1999; Iinuma et al., 2016, 2004; Kristensen et al., 2013; Larsen et al., 1999; Librando and Tringali, 2005; Zhang et al., 1992, 2015).

The innovative purpose of this work is to present an evaluation of the distribution of cis-pinonic and pinic acid, known as water-soluble organic compounds (WSOC) (Ion et al., 2005; Kitanovski et al., 2011; Pio et al., 2006; Zhang et al., 2010), in aerosols as a function of particle size focusing on the ultrafine fractions. To our knowledge, the photo-oxidation products of α -pinene in the ultrafine fraction have never been investigated. The quantitative performance of HPLC coupled to triple quadrupole API 4000 were carried out to determine these acids in environmental samples at trace levels. Recently, photo-oxidation products of α -pinene have been investigated using GC-MS and LC-MS methods (Ding et al., 2008; Iinuma et al., 2007; Ion et al., 2005; Kitanovski et al., 2011; Parshintsev et al., 2010; Pio et al., 2006; Reinnig et al., 2008; Sheesley and Kenski, 2004; Zhang et al., 2010). GC-MS is a widely used method for the separation, identification and quantification of individual organic compounds in aerosol samples, even though low-volatile polar substances have to be derivatized prior to injection (Haque et al., 2016; Ion et al., 2005; Szmigielski et al., 2007) and some compounds might decompose during analysis. HPLC/MS methods were used by some authors to measure oxidation products from terpenes in atmospheric samples and with chamber experiments (Anttila et al., 2005; Reinnig et al., 2008; Zhang et al., 2010). Anttila et al. (2005) investigated the environmental aerosol matter with reversed phase chromatography applied to HPLC system, coupled to an ion-trap mass spectrometer using an electro-spray ionisation (ESI) interface in negative ionisation mode. Besides, Renning et al. (2008) carried out the ozonolysis of α -pinene in a smog chamber and the samples were investigated using reversed phase chromatography coupled with ion-trap mass spectrometer though an APCI source operating in positive mode. Zhang et al. (2010), analysed aerosol samples using C18 column placed in a HPLC system coupled with a hybrid Qq-TOF mass spectrometer. The benefit of HPLC is the suitability for polar and non-volatile

compounds as well as the conditions through the analysis, while mass spectrometer allows high sensitivity and selectivity. The main objective of this work is to develop and quantify some of the main photo-oxidation products of α -pinene, pinic and pinonic acids, in different particle size fractions of aerosol collected in the urban area of Mestre-Venice (Italy). A sensitive improvement of analytical method is necessary due to the high fractionation of aerosol in twelve different size ranges.

2. Experimental section

2.1. Reagents and standard solutions

Ultra-grade methanol (MeOH) and ultra-grade acetonitrile (ACN) were purchased from Romil[®] LTD (Cambridge, UK), Ultrapure water (18.2 M Ω , 1 ppb TOC) was produced using a Purelab Ultra System (Elga[®], HighWycombe, UK), formic acid ($\geq 98\%$) eluent additive for HPLC system was obtained from Fluka (Sigma Aldrich[®], Buchs, Switzerland). Cis-pinonic acid (Sigma-Aldrich, Saint Louis, Missouri, USA) and pinic acid (Santa Cruz Biotechnology[®], Dallas, Texas, USA), were prepared by solid standard (purity $\geq 98\%$) and diluted in ultrapure water. Isotopically labelled vanillin¹³C₆ (VAH*) was obtained from Sigma Aldrich[®].

Ultrapure water produced using the Purelab system was further purified with LC-Pak[®] cartridge (Merck KGaA, Darmstadt, Germany) to obtain higher water quality with a TOC level below 1 ppb. The LC-Pak[®] cartridge uses a reversed-phase silica purification media to remove traces of neutral organics.

2.2. HPLC-ESI-MS/MS

An Agilent 1100 Series HPLC Systems (Waldbronn, Germany) with a binary pump, vacuum degasser, autosampler and thermostated column compartment was coupled with an API 4000 Triple Quadrupole Mass Spectrometer (Applied Biosystem/MSD SCIEX, Concord, Ontario, Canada) using a Turbo V electrospray source (ESI) that operated in negative mode. The chromatographic separation used for the sample determination of cis-pinonic acid and pinic acid was conducted using a Zorbax Extend-C18 column (Rapid Resolution, 4.6–150 mm, 3.5 mm; Agilent Technologies). Elution was achieved by a linear gradient using as mobile phase water with 0.01% of formic acid (eluent A) and MeOH/ACN 80:20 (eluent B). The binary elution program with flow rate of 0.5 mL min⁻¹ was as follows: 0–1 min, 20% eluent B; 8–25 min, 100% eluent B; 25–35 min, equilibration with 20% eluent B; 100 μ L of sample was injected for analysis. The mass spectrometer's parameters were set as follows: temperature 650 °C, ion spray voltage –4500 V, GS1 40 psi, GS2 60 psi, CUR 15 psi, CAD 8 psi and EP -8 V. Data were collected with multiple reaction monitoring (MRM) mode. The first quadrupole (Q1) selected the molecular ion, while the third quadrupole (Q3) selected the fragment. Both Q1 and Q3 were set at unit resolution with peak width of 0.7 \pm 0.1 amu at 50% of maximum peak height. To improve the sensitivity, declustering potential (DP), cell energy (CE) and cell exit potential (CXP) were set, using direct infusions of 1 mg L⁻¹ of each individual standard. The voltage of the orifice was controlled by the DP parameter, the CE was the amount of energy that the precursor ions received as they were accelerated into the collision cell, and the CXP was used to focus and accelerate the ions after leaving the collision cell. The monitored transition and instrumental parameters for each compound are shown in Table S-1. Analyst Software version 1.5.2 (Applied Biosystems MDS SCIEX Instruments) was used for the identification and quantification of the target compounds.

2.3. Sample collection

14 aerosol samples were collected at Scientific Campus of Ca' Foscari University (45°28'47"N, 12°15'12"E, Mestre-Venice, Italy) during spring 2016, using the rotating model 120 MOUDI-II™ cascade impactor. The particle size distribution was obtained for aerodynamic diameter (D) ranging from greater of 18 μm to below 0.056 μm. The configuration of sampler consists to eleven stages with cut sizes at 18, 10, 5.6, 3.2, 1.8, 1.0, 0.56, 0.32, 0.18, 0.10 and 0.056 μm, plus a final back-up filter used to collect particles with D < 0.056 μm. The impaction plates, 11 μm thick aluminium substrate having a diameter of 47 mm, were prepared in the laboratory and inserted into the impactor at the time of use. The substrates were made using aluminium foils cut with a hollow cutter. Finally, the collection of ultrafine atmospheric particles in the last stage was carried out with a quartz fibre filters (QFF) (SKC Inc., Eighty-Four, To-13 model).

The duration of the sampling was about 160 h for most of the samples, with an average flow rate of $30 \pm 1 \text{ L min}^{-1}$. The air flow at the inlet was measured with a flowmeter before and after each sampling. The sampling period was chosen to obtain enough matter even for weighting. In fact, one of the most important features of MOUDI II™ is the possibility of the weighing of each aluminium substrate, thanks to their restrained diameter. After conclusion of sampling, the substrates were stored separately at -20°C until chemical analysis. The sampler was placed on the roof of a building at a height of 20 meters, to avoid direct human contaminations and to minimize the influence of the urban layout that may affect the wind pathways.

The weather information was provided by station FISTEC-Mestre (IUAV, Venice - Environmental engineering physics laboratory, website: fistec.iuav.it). Precipitation has a great variability especially in spring due to the high humidity, in fact there were a significant precipitation events from 9th to 12th of March (22.8 mm) and a minor from 13th to 15th of April (4.2 mm) and from 11th to 13th of May (3.2 mm). The range humidity was included between 22% (4th May) and 98.5% (most of the data). Moreover, the sampling period was conditioned by the medium-high temperature ranging (from 4 °C to 25 °C) and the prevailing winds were from NW and SW with wind speed between 1 and 7 m s^{-1} (Figure S-2 and S-3, supporting material).

The impactor with the rotation of the nozzle and impaction plates at 1 rpm, formed a near-uniform particle deposit on each substrate.

2.4. Sample treatment

To determine and quantify cis-pinonic acid and pinic acid, airborne aerosol was collected on aluminium plates pre-cleaned with MeOH, and on quartz filter, decontaminated with a pre-combustion (4 h at 400 °C in a muffle furnace). Before the closing inside in a clean aluminium foil, the aluminium plates were weighted to allow the calculation of the collected aerosol.

Aluminium plates and filters were removed from the storage package in a laminar flow hood, broken up into small pieces and placed in a 15 mL vial (previously cleaned with ultra-pure water by sonication at 25 °C) with steel tweezers. 50 μL of isotopically labelled vanillin¹³C₆ (78 ng absolute weight) and 4.95 mL of ultrapure water was added to the substrate before cold-ultrasonically extracting at 10 °C to avoid the volatilization of the analytes. The extract has been filtrated through a 0.45 mm PTFE filter (Minisart® Sartorius SRP25, Goettingen, Germany) to remove particulate and filter traces before instrumental analysis.

During the sampling periods, three field blanks were taken at the beginning, during and end of the sampling period. Blank samples were collected by loading, carrying and installing the filter holder in the instrument with the air pump turned off.

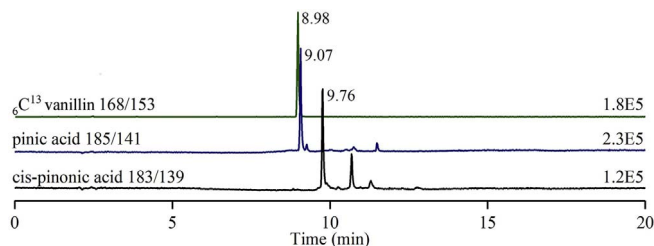


Fig. 1. Chromatograms of the target acids and their internal standard from 0 to 20 min. Each ion chromatogram is related to most intense ions of MRM method.

3. Result and discussion

3.1. Quantitative performance

Fig. 1 shows the chromatographic separations carried out with a Zorbax Extend-C18 column of cis-pinonic and pinic acid and ¹³C₆ vanillin (internal standard) using the chromatographic method. The chromatographic method was achieved studying retention time (t_R), peak width (W), number (N), height (HEPT) of theoretical plates, asymmetry (A_s), resolution (R_s) and selectivity (α). It was used as mobile phase water with 0.01% of formic acid and MeOH/ACN 80:20. Elution was achieved by a linear gradient using as mobile phase water with 0.01% of formic acid (eluent A) and MeOH/ACN mixtures (eluent B). Three different eluent B composition were investigated to improve the chromatographic performance: pure MeOH (method 1), 80:20 MeOH/ACN (method 2) and 50:50 MeOH/ACN (method 3). All the chromatographic investigations are shown in Supporting material.

The analytical procedure was validated through linear range, instrumental limit of detection (LOD), instrumental limit of quantification (LOQ), procedural blank, method detection limit (MDL), method quantification limit (MQL), trueness, repeatability and extraction yield. The internal standard method by isotope dilution was used to quantify cis-pinonic and pinic acids and labelled ¹³C₆ vanillin was chosen as internal standard because it demonstrated similar instrumental and pre-analytical behaviour. The linearity of the calibration curves for cis-pinonic acid and pinic acid with labelled ¹³C₆ vanillin as internal standard was evaluated using a series of standard solutions prepared in ultrapure water at average concentrations from 0.01 to $50 \mu\text{g L}^{-1}$ and a constant concentration of labelled ¹³C₆ vanillin ($15.5 \mu\text{g L}^{-1}$). By considering the ratio between concentration of target acids and internal standard and the ratio between the relative peak areas, linearity was evaluated obtaining $R^2 \geq 0.9997$. LOD and LOQ values are calculated as three and ten times the signal-to-noise ratio of the known absolute amounts of the analysed target compound in a standard solution (Bliesner, 2006). The LOD values of cis-pinonic and pinic acid are 1.6 and 1.2 ng L^{-1} while LOQ values are 5.4 and 4.1 ng L^{-1} , respectively. Parshintsev et al. (2010) obtained a LOD value of 27 and $12 \mu\text{g L}^{-1}$, while Zhang et al. (2010) obtained 3.3 and $0.35 \mu\text{g L}^{-1}$, respectively for cis-pinonic acid and pinic acid. In both of cases the studies were carried out via HPLC-MS systems and the LOD values of this study are considerable lower than reported literature. Furthermore, to our knowledge, the method has the lowest LOD values compared to previous studies. The instrumental precision was evaluated and CV% value (reported as a percentage and calculated from the average (A) and standard deviation (SD), calculated as $(\text{SD}/A) \times 100$) was below of 10%. Due to the lack of certified reference materials for cis-pinonic and pinic acid in the aerosol or dust, we estimated trueness, precision and recovery by analyzing five spiked cleaned aluminium plate and QFF with 63 ng of cis-pinonic acid, 45 ng of pinic acid and 78 ng of ¹³C₆ vanillin. The quantification was carried out using a response factor in order to avoid the instrumental signal fluctuations.

Trueness is an important parameter to evaluate during method validation. It refers to the degree of closeness of the determined value to

the known “true” value. It is expressed as a percent error, calculated as $(Q - T)/T \times 100$ where Q is the determined value and T is the “true value”. The error for cis-pinonic acid and pinic acid was calculated performing the same pre-analytical procedure achieved with the environmental samples. For the evaluation of the extraction yield to estimate the procedural extraction efficiency the isotopically labelled $^{13}\text{C}_6$ vanillin was added after the PTFE filtration. Table 1 shows the validation values just described for cis-pinonic acid and pinic acid. The internal standard method provided an error percentage and CV $\% < \pm 10\%$ for each compound. The recovery of the analytical procedure for the investigated acids ranged between 66 ± 7 and $85 \pm 5\%$; Parshintsev et al. (2010) reached extraction levels from 77 ± 9 to $96 \pm 4\%$: the values are close with the extraction levels of QFF, but they are higher than aluminium plates. This means that QFF is a better substrate for extraction. In Table 1 is reported the mean absolute blank amount which was subtracted from the analytical results. MDL and MQL were evaluated through 5 procedural blanks, i.e. 5 aluminium substrates and 5 quartz substrates in which it has been added only the $^{13}\text{C}_6$ vanillin after the extraction. The MDL and the MQL were evaluated as 3 and 10 times the standard deviation of these field blanks. Even though the fiber filter has a higher MDL compared to the aluminium plate due its porosity, the values are quite similar to the procedural blanks, demonstrating a minimal contamination during the operation before and after the sampling.

3.2. Cis-pinonic and pinic acid in the urban atmospheric aerosol

Cis pinonic and pinic acids were determined in the atmospheric aerosol collected in the urban area of Mestre-Venice (Italy) from 14th March to 13th May 2016. The total concentration of each acid, calculated as the sum of their size distributions in all aerosol samples, has an average value of 0.3 ng m^{-3} . Cis-pinonic acid was usually found in the ultrafine fraction ($< 56 \text{ nm}$), and its concentrations ranged from below MDL to 0.9 ng m^{-3} . Instead pinic acid concentrations ranged from below MDL to 0.8 ng m^{-3} . The concentration values found in this study are lower of an order of magnitude than the investigation reported in literature (Fu et al., 2009; Kavouras et al., 1998; Kavouras and Stephanou, 2002; Kitanovski et al., 2011; Kristensen et al., 2013; Sheesley and Kenski, 2004; Yu et al., 1999; Zhang et al., 2010) (Table 2). These authors collected the samples very close to conifers and deciduous areas, while in the present study the sampling site was just near a restrict area of deciduous trees. Lamb et al. (1987) demonstrated how monoterpenes are mostly formed near coniferous and deciduous trees. However, the formation of the photo-oxidation products follows a partially unknown mechanism, developing an abundance of SOA compounds with a wide range particles diameter. The urban location of aerosol site certainly influences the relative concentrations of photo-oxidation products of α -pinene, because fine and ultra-fine particles can be transferred for long distances, according to the atmospheric conditions. Considering the huge distance from coniferous sources and the features of the long-range particles, the sampling site gives information about the atmospheric transformations and SOA aging (Robinson et al., 2007; Rudich et al., 2007). In literature it is demonstrated that the highest concentrations for cis-pinonic acid and pinic acid are measured in spring and summer months (Kitanovski et al., 2011; Sheesley and Kenski, 2004; Zhang et al., 2010). The results of this study agree with these observations (Fig. 2) for cis-pinonic acid, because it increased its concentrations from March to May, while pinic acid has a different behaviour. The major concentrations of cis-pinonic acid have been found in the three samples of April 26–29 and May 3–6 and May 10–13, while pinic acid is most concentrated in the collecting periods of March 14–18, 18–22 and May 3–6.

It is known how cis-pinonic acid is a high/semi-volatile compound (Zhang et al., 2010) and it was detected in the gas and particulate phase in forests atmosphere (Kavouras et al., 1999, 1998; Kavouras and Stephanou, 2002; Pio et al., 2001). Fig. 2 and the box-plot diagram of

Fig. 3 show that cis-pinonic acid was only found in the ultrafine particles (mostly distributed below 56 nm diameter) and this suggests that it is a typical first-generation reaction product (Jimenez et al., 2009) with a gas-to-particle process (Anttila et al., 2005; Pio et al., 2006), due to its abundant presence in the gas phase.

Several studies explained that pinic acid derives from pinonic acid thought photo-oxidation processes (Lamb et al., 1987; Larsen et al., 1999; Librando and Tringali, 2005; Noziere et al., 1999). This is well described in recent smog-chamber experiments where pinic acid concentration continues to increase after α -pinene is consumed. This suggests an additional production pathway, with cis-pinonic acid as a precursor (Zhang et al., 2015). The scientific literature describes pinic acid as low/semi-volatile compounds that is mainly present in the submicrometer fraction of ambient aerosols (Alves et al., 2000; Müller et al., 2012; Pio et al., 2006). Pinic acid can not act as cloud condensation nuclei (CCN) as the saturation vapour pressure ($9.5 \times 10^{-6} \text{ Pa}$ at 24°C) is significantly above the limit of $1.2 \times 10^{-8} \text{ Pa}$ (Bilde and Pandis, 2001; Bonn and Moortgat, 2003). Considering that cis-pinonic acid constitutes efficient CCN in the atmosphere (Huff Hartz et al., 2005; O'Dowd et al., 2002), it can undergo the photo-oxidation in the nucleation mode creating pinic acid that grows forming fine aerosol with a greater diameter, up to $1 \mu\text{m}$ (Spurny, 2000). Coarse particles (diameter $> 1 \mu\text{m}$) are mostly emitted to the atmosphere during mechanical processes from both natural and anthropogenic sources. A further explanation of the presence of pinic acid in coarse particles might be the result of condensation of pinic acid, produced by the gas-phase photo-oxidation of cis-pinonic acid, onto larger existing aerosol particles or of particle coagulation, especially during long-range transport (Herckes et al., 2006; Wang et al., 2009; Zangrando et al., 2016, 2013). The feature of the urban area may allow the atmospheric aging of cis-pinonic acid, as the oxidation of this gas-phase precursor can generate pinic acid via homogeneous or heterogeneous reaction of oxidants such as OH, ozone and NO_x (Rudich et al., 2007; Seinfeld and Pankow, 2003). Cis-pinonic acid is mainly distributed in the nucleation mode ($D < 56 \text{ nm}$). Indeed, it is a high/semi-volatile compound and does not enhance in terms of dimension or is transformed to by-products, as the distance from the source areas likely allow the photo-oxidation degradation. Cis-pinonic acid, being also a first-generation reaction product (Jimenez et al., 2009) with a gas-to-particle process (Anttila et al., 2005; Pio et al., 2006), continues to be distributed in the ultrafine particles undergoing the long-range transport. Conversely, pinic acid follows the nucleation (Aitken, particle diameter $< 0.1 \mu\text{m}$), accumulation (particle diameter: $0.1 \mu\text{m} < D < 1 \mu\text{m}$) and coarse (particle diameter $> 1 \mu\text{m}$) modes (Fig. 3).

In this study cis-pinonic acid and pinic acid don't have a clear correlation with temperature (Figure S-4), probably due to the different atmospheric conditions undergo by the particles during the transport processes. Moreover, there is not a clear relationship among the trend concentrations of the acids and precipitations, relative humidity and

Table 1
Average errors (%), recovery (%), CV%, blank (ng), MDL and MQL (ng).

Compound	Error %	Recovery %	CV%	Blank (ng)	MDL (ng)	MQL (ng)
Aluminium						
Cis-pinonic acid	5.9	77 ± 1	2	2.3 ± 0.2	0.7	2.5
Pinic acid	-9.2	66 ± 7	10	3.1 ± 0.4	1.2	4.1
Quartz QFF						
Cis-pinonic acid	2.3	80 ± 2	2	3.0 ± 0.8	2.3	7.5
Pinic acid	0.9	85 ± 5	6	2.7 ± 0.6	1.9	6.2

Table 2
Average TSP concentration compared with other studies.

Compound	Average conc. ng m ⁻³	Location, sampling period
Cis-pinonic acid	0.3 ± 0.3	Mestre-Venice, Italy, March–May 2016 (this study)
	6.26 ± n.d.	Alaska, Spring 2009 (Haque et al., 2016)
	6.1 ± 0.6	Sierra Nevada Mountains, California, September 2007 (Kristensen et al., 2013)
	11 ± 5.6	Sierra Nevada Mountains, California, July 2009 (Kristensen et al., 2013)
	5.4 ± 3.5	Ljubljana, Slovenia, February and August 2010 (Kitanovski et al., 2011)
	1.22 ± 1.33	Mainz, Germany, May 2006–June 2007 (Zhang et al., 2010)
	0.069 ± 0.023	Canadian Arctic, February–June 1991 (Fu et al., 2009)
	18 ± 31	SMEARII station, Finland, August 2007 (Parshintsev et al., 2010)
	40.5 ± 67.5	Alabama, USA, May 2004–April 2005 (Sheesley and Kenski, 2004)
	9.7 ± 11	Pertouli, Greece, August 1998 (Kavouras and Stephanou, 2002)
Pinic acid	0.3 ± 0.2	Mestre-Venice, Italy, March–May 2016 (this study)
	5.97 ± n.d.	Alaska, Spring 2009 (Haque et al., 2016)
	7.6 ± 4.0	Sierra Nevada Mountains, California, September 2007 (Kristensen et al., 2013)
	7.1 ± 3.0	Sierra Nevada Mountains, California, July 2009 (Kristensen et al., 2013)
	1.4 ± 1.4	Ljubljana, Slovenia, February and August 2010 (Kitanovski et al., 2011)
	2.32 ± 2.72	Mainz, Germany, May 2006–June 2007 (Zhang et al., 2010)
	0.51 ± 0.40	Canadian Arctic, February–June 1991 (Fu et al., 2009)
	1 ± 9	SMEARII station, Finland, August 2007 (Parshintsev et al., 2010)
	0.54 ± n.d.	Nova Scotia, Canada, July 1996 (Yu et al., 1999)
	0.5 ± n.d.	San Bernadino, Canada, September 1998 (Yu et al., 1999)
2.4 ± 1.5	Pertouli, Greece, August 1998 (Kavouras and Stephanou, 2002)	

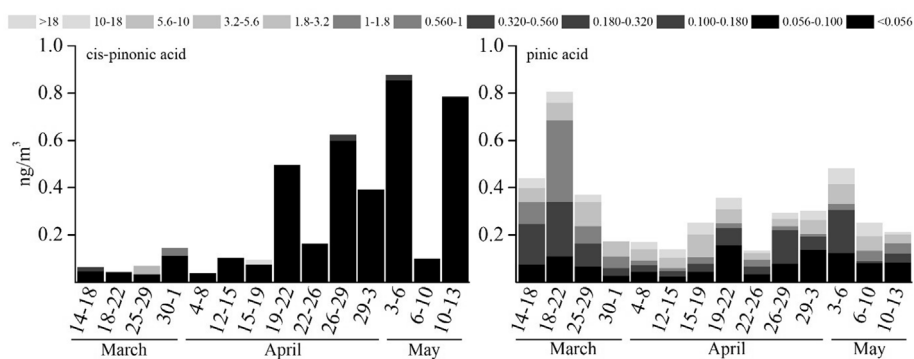


Fig. 2. Monthly variations (ng m⁻³) and fractions distribution (μm) of target acids.

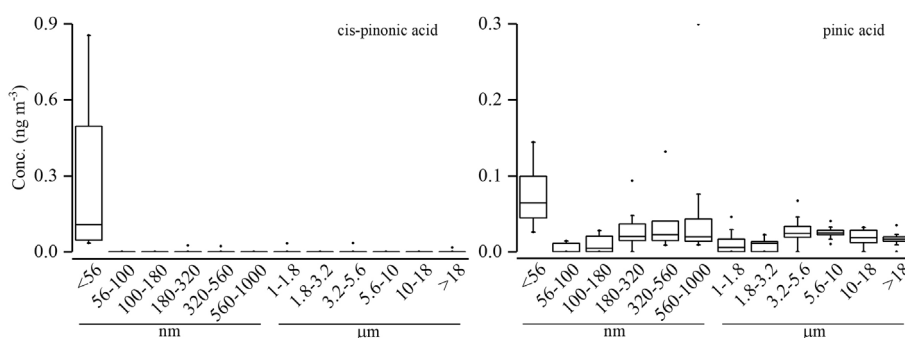


Fig. 3. Box-plot diagram of cis-pinonic acid and pinic acid according to the particles diameter. The line inside the box is referred to the median.

wind directions and intensity (relative humidity, precipitation and wind rose are shown in the [supporting material, Figure S-2 and S-3](#)). Pio et al. (2006) has shown, using a cascade impactor, how pinonic and pinic acids appeared mainly in fine particles (< 0.69 μm diameter): the distribution differences with this study are due to the distance from the sources. To our knowledge this is the first study in which we can observe the behaviour of cis pinonic acid and pinic acid in aged aerosol in an urban environment.

Clear differences in the concentration values and in the dimensional distribution of the two acids were observed, suggesting that the

concentrations and the size distributions of these WSOC depend on the source area and on the age of aerosol (Timonen et al., 2008).

4. Conclusions

In this study a method for the quantification in particulate matter of two terpenic acid, cis-pinonic acid and pinic acid, using a HPLC-ESI (-)-MS/MS system was developed. We obtained a sensitive method with instrumental detection limits of 1.6 and 1.2 ng L⁻¹, respectively. To our knowledge, this is the most sensitive method to quantify these

target acids. The analytical procedure was validated to accurately quantify these compounds in the aerosol samples through the estimation of trueness, repeatability and recovery.

The HPLC-MS/MS method developed in this study was applied to the atmospheric samples collected in Mestre-Venice, to characterise particle size distribution of cis-pinonic acid and pinic acid. The sampling was conducted using a MOUDI II cascade impactor to discriminate the particle size from 18 µm to < 0.056 nm. This is the first study about the characterization of the pinic and cis-pinonic in the ultrafine particles. During the spring 2017 fourteen different samples demonstrated that cis-pinonic acid is mostly distributed in the ultra-fine fraction (below 56 nm diameter) while pinic acid show a steady distribution among the 12 fractions. Both acids did not show a clear correlation with the temperature.

Acknowledgements

The research was supported by the National Research Council of Italy (Consiglio Nazionale delle Ricerche, CNR). The research leading to these results has received funding from the European Research Council under the European Union's Seventh Framework Programme (FP7/2007-2013)/ERC Grant agreement n° 267696 – EARLYhumanIMPACT. The authors also acknowledge Elga Lab Water (High Wycombe, UK) for providing the ultrapure water systems. Data and information on local meteorology were obtained from FISTEC-Mestre (IUAV, Venice - Environmental engineering physics laboratory, website: fistec.iuav.it). We would also like to thank Dr. Natalie M. Kehrwald for the revision of our manuscript.

Appendix A. Supplementary data

Supplementary data related to this article can be found at <http://dx.doi.org/10.1016/j.atmosenv.2018.02.052>.

References

- Alves, C.A., Pio, C., Duarte, A.C., 2000. Particulate size distributed organic compounds in a forest atmosphere. *Environ. Sci. Technol.* 34, 4287–4293.
- Anttila, P., Hyötyläinen, T., Heikkilä, A., Jussila, M., Finell, J., Kulmala, M., Riekkola, M.L., 2005. Determination of organic acids in aerosol particles from a coniferous forest by liquid chromatography-mass spectrometry. *J. Sep. Sci.* 28, 337–346. <https://doi.org/10.1002/jssc.200401931>.
- Bilde, M., Pandis, S.N., 2001. Evaporation rates and vapor pressures of individual aerosol species formed in the atmospheric oxidation of α - and β -pinene. *Environ. Sci. Technol.* 35, 3344–3349. <https://doi.org/10.1021/es001946b>.
- Bliessner, D.M., 2006. *Validating Chromatographic Methods: a Practical Guide*. Brochure 1–297.
- Bonn, B., Moortgat, G.K., 2003. Sesquiterpene ozonolysis: origin of atmospheric new particle formation from biogenic hydrocarbons. *Geophys. Res. Lett.* 30 (1585). <https://doi.org/10.1029/2003GL017000>.
- Ding, X., Zheng, M., Yu, L., Zhang, X., Weber, R.J., Yan, B., Russell, A.G., Edgerton, E.S., Wang, X., 2008. Spatial and seasonal trends in biogenic secondary organic aerosol tracers and water-soluble organic carbon in the southeastern United States. *Environ. Sci. Technol.* 42, 5171–5176. <https://doi.org/10.1021/es7032636>.
- Fehsenfeld, F., Calvert, J., Fall, R., 1992. Emissions of volatile organic compounds from vegetation and the implications for atmospheric chemistry. *Global Biogeochem. Cycles* 6, 389–430.
- Fu, P.Q., Kawamura, K., Pochanart, P., Tanimoto, H., Kanaya, Y., Wang, Z.F., 2009. Summertime contributions of isoprene, monoterpenes, and sesquiterpene oxidation to the formation of secondary organic aerosol in the troposphere over Mt. Tai, Central East China during. *Atmos. Chem. Phys. Discuss.* 9, 16941–16972. <https://doi.org/10.5194/acpd-9-16941-2009>.
- Glasius, M., Duane, M., Larsen, B.R., 1999. Determination of polar terpene oxidation products in aerosols by liquid chromatography-ion trap mass spectrometry. *J. Chromatogr. A* 833, 121–135. [https://doi.org/10.1016/S0021-9673\(98\)01042-5](https://doi.org/10.1016/S0021-9673(98)01042-5).
- Glasius, M., Lahaniati, M., Calogirou, A., Di Bella, D., Jensen, N.R., Hjorth, J., Kotzias, D., Larsen, B.R., 2000. Carboxylic acids in secondary aerosols from oxidation of cyclic monoterpenes by ozone. *Environ. Sci. Technol.* 34, 1001–1010. <https://doi.org/10.1021/es990445r>.
- Guenther, A., Hewitt, C., Erickson, D., 1995. A global model of natural volatile organic compound emissions. *J. Geophys. Res.* 100, 8873–8892.
- Haque, M.M., Kawamura, K., Kim, Y., 2016. Seasonal variations of biogenic secondary organic aerosol tracers in ambient aerosols from Alaska. *Atmos. Environ.* 130, 95–104. <https://doi.org/10.1016/j.atmosenv.2015.09.075>.
- Herckes, P., Engling, G., Kreidenweis, S.M., Collett, J.L., 2006. Particle size distributions of organic aerosol constituents during the 2002 Yosemite aerosol characterization study. *Environ. Sci. Technol.* 40, 4554–4562. <https://doi.org/10.1021/es0515396>.
- Huff Hartz, K.E., Rosenørn, T., Ferchak, S.R., Raymond, T.M., Bilde, M., Donahue, N.M., Pandis, S.N., 2005. Cloud condensation nuclei activation of monoterpene and sesquiterpene secondary organic aerosol. *J. Geophys. Res. Atmos.* 110, 1–8. <https://doi.org/10.1029/2004JD005754>.
- Iinuma, Y., Böge, O., Gnauk, T., Herrmann, H., 2004. Aerosol-chamber study of the α -pinene/O₃ reaction: influence of particle acidity on aerosol yields and products. *Atmos. Environ.* 38, 761–773. <https://doi.org/10.1016/j.atmosenv.2003.10.015>.
- Iinuma, Y., Keywood, M., Herrmann, H., 2016. Characterization of primary and secondary organic aerosols in Melbourne airshed: the influence of biogenic emissions, wood smoke and bushfires. *Atmos. Environ.* 130, 54–63. <https://doi.org/10.1016/j.atmosenv.2015.12.014>.
- Iinuma, Y., Müller, C., Berndt, T., Böge, O., Claeys, M., Herrmann, H., 2007. Evidence for the existence of organosulfates from β -pinene ozonolysis in ambient secondary organic aerosol. *Environ. Sci. Technol.* 41, 6678–6683. <https://doi.org/10.1021/es070938t>.
- Ion, A.C., Vermeylen, R., Kourtchev, I., Cafmeyer, J., Chi, X., Gelencsér, A., Maenhaut, W., Claeys, M., 2005. Polar organic compounds in rural PM_{2.5} aerosols from K-puszta, Hungary, during a 2003 summer field campaign: sources and diurnal variations. *Atmos. Chem. Phys. Discuss.* 5, 1863–1889. <https://doi.org/10.5194/acpd-5-1863-2005>.
- Jimenez, J.L., Canagaratna, M.R., Donahue, N.M., Prevot, A.S.H., Zhang, Q., Kroll, J.H., DeCarlo, P.F., Allan, J.D., Coe, H., Ng, N.L., Aiken, A.C., Docherty, K.S., Ulbrich, I.M., Grieshop, A.P., Robinson, A.L., Duplissy, J., Smith, J.D., Wilson, K.R., Lanz, V.A., Hueglin, C., Sun, Y.L., Tian, J., Laaksonen, A., Raatikainen, T., Rautiainen, J., Vaattovaara, P., Ehn, M., Kulmala, M., Tomlinson, J.M., Collins, D.R., Cubison, M.J., Dunlea, J., Huffman, J.A., Onasch, T.B., Alfarra, M.R., Williams, P.I., Bower, K., Kondo, Y., Schneider, J., Drewnick, F., Borrmann, S., Weimer, S., Demerjian, K., Salcedo, D., Cottrell, L., Griffin, R., Takami, A., Miyoshi, T., Hatakeyama, S., Shimono, A., Sun, J.Y., Zhang, Y.M., Dzepina, K., Kimmel, J.R., Sueper, D., Jayne, J.T., Herndon, S.C., Trimborn, A.M., Williams, L.R., Wood, E.C., Middlebrook, A.M., Kolb, C.E., Baltensperger, U., Worsnop, D.R., 2009. Evolution of organic aerosols in the atmosphere. *Science* (80-.) 326, 1525–1529. <https://doi.org/10.1126/science.1180353>.
- Kaht, A., Iinuma, Y., Blockhuys, F., Mutzel, A., Vermeylen, R., Kleindienst, T.E., Jaoui, M., Offenberg, J.H., Lewandowski, M., Böge, O., Herrmann, H., Maenhaut, W., Claeys, M., 2014. 2-hydroxyterpenylic acid: an oxygenated marker compound for α -pinene secondary organic aerosol in ambient fine aerosol. *Environ. Sci. Technol.* 48, 4901–4908. <https://doi.org/10.1021/es500377d>.
- Kanakidou, M., Tsigaridis, K., Dentener, F.J., Crutzen, P.J., 2000. Human-activity-enhanced formation of organic aerosols by biogenic hydrocarbon oxidation. *J. Geophys. Res.* 105, 9243–9254. <https://doi.org/10.1029/1999JD901148>.
- Kavouras, I.G., Mihalopoulos, N., Stephanou, E.G., 1999. Formation and gas/particle partitioning of monoterpenes photo-oxidation products over forests. *Geophys. Res. Lett.* 26, 55–58. <https://doi.org/10.1029/1998GL900251>.
- Kavouras, I.G., Mihalopoulos, N., Stephanou, E.G., 1998. Formation of atmospheric particles from organic acids produced by forests. *Nature* 372, 683–686. <https://doi.org/10.1038/27179>.
- Kavouras, I.G., Stephanou, E.G., 2002. Direct evidence of atmospheric secondary organic aerosol formation in forest atmosphere through heteromolecular nucleation. *Environ. Sci. Technol.* 36, 5083–5091. <https://doi.org/10.1021/es025811c>.
- Kitanovski, Z., Grgić, I., Veber, M., 2011. Characterization of carboxylic acids in atmospheric aerosols using hydrophilic interaction liquid chromatography tandem mass spectrometry. *J. Chromatogr. A* 1218, 4417–4425. <https://doi.org/10.1016/j.chroma.2011.05.020>.
- Kristensen, K., Enggrob, K.L., King, S.M., Worton, D.R., Platt, S.M., Mortensen, R., Rosenoern, T., Surratt, J.D., Bilde, M., Goldstein, A.H., Glasius, M., 2013. Formation and occurrence of dimer esters of pinene oxidation products in atmospheric aerosols. *Atmos. Chem. Phys.* 13, 3763–3776. <https://doi.org/10.5194/acp-13-3763-2013>.
- Kulmala, M., Vehkamäki, H., Petäjä, T., Dal Maso, M., Lauri, A., Kerminen, V.M., Birmili, W., McMurry, P.H., 2004. Formation and growth rates of ultrafine atmospheric particles: a review of observations. *J. Aerosol Sci.* 35, 143–176. <https://doi.org/10.1016/j.jaerosci.2003.10.003>.
- Lamb, B., Guenther, A., Gay, D., Westberg, H., 1987. A national inventory of biogenic hydrocarbon emissions. *Atmos. Environ.* 21, 1695–1705. [https://doi.org/10.1016/0004-6981\(87\)90108-9](https://doi.org/10.1016/0004-6981(87)90108-9).
- Larsen, B.R., Di Bella, D., Glasius, M., Winterhalter, R., Jensen, N.R., Hjorth, J., 1999. Gas-phase ozone oxidation of Monoterpenes: gaseous and particulate products. *J. Atmos. Chem.* 38, 207–258. <https://doi.org/10.1023/A:1006254930583>.
- Librando, V., Tringali, G., 2005. Atmospheric fate of OH initiated oxidation of terpenes. Reaction mechanism of α -pinene degradation and secondary organic aerosol formation. *J. Environ. Manag.* 75, 275–282. <https://doi.org/10.1016/j.jenvman.2005.01.001>.
- Müller, L., Reinnig, M.C., Naumann, K.H., Saathoff, H., Mentel, T.F., Donahue, N.M., Hoffmann, T., 2012. Formation of 3-methyl-1,2,3-butanetricarboxylic acid via gas phase oxidation of pinonic acid - a mass spectrometric study of SOA aging. *Atmos. Chem. Phys.* 12, 1483–1496. <https://doi.org/10.5194/acp-12-1483-2012>.
- Nozière, B., Barnes, I., Becker, K., 1999. Product study and mechanisms of the reactions of α -pinene and of pinonaldehyde with OH radicals. *J. Geophys. Res.* 104, 23645–23656. <https://doi.org/10.1029/1999JD900778>.
- O'Dowd, C.D., Aalto, P., Hmeri, K., Kulmala, M., Hoffmann, T., 2002. Atmospheric particles from organic vapours. *Nature* 416, 497–498.
- Parshintsev, J., Hyötyläinen, T., Hartonen, K., Kulmala, M., Riekkola, M.L., 2010. Solid-phase extraction of organic compounds in atmospheric aerosol particles collected with the particle-into-liquid sampler and analysis by liquid chromatography-mass

- spectrometry. *Talanta* 80, 1170–1176. <https://doi.org/10.1016/j.talanta.2009.09.004>.
- Pio, C., Alves, C., Duarte, A., 2001. Organic components of aerosols in a forested area of central Greece. *Atmos. Environ.* 35, 389–401. [https://doi.org/10.1016/S1352-2310\(00\)00135-7](https://doi.org/10.1016/S1352-2310(00)00135-7).
- Pio, C., Alves, C., Carvalho, A., Santos, C., 2006. Size distribution characteristics of organic species in atmospheric particulate matter from Finnish and German rural sites with variable anthropogenic influence. *Environ. Eng. Sci.* 23, 933–941. <https://doi.org/10.1089/ees.2006.23.933>.
- Reinnig, M.C., Müller, L., Warnke, J., Hoffmann, T., 2008. Characterization of selected organic compound classes in secondary organic aerosol from biogenic VOCs by HPLC/MSn. *Anal. Bioanal. Chem.* 391, 171–182. <https://doi.org/10.1007/s00216-008-1964-5>.
- Robinson, A.L., Donahue, N.M., Shrivastava, M.K., Weitkamp, E.A., Sage, A.M., Grieshop, A.P., Lane, T.E., Pierce, J.R., Pandis, S.N., 2007. Rethinking organic aerosols: semi-volatile emissions and photochemical aging. *Science* (80) 315, 1259–1262. <https://doi.org/10.1126/science.1133061>.
- Rudich, Y., Donahue, N.M., Mentel, T.F., 2007. Aging of organic aerosol: bridging the gap between laboratory and field studies. *Annu. Rev. Phys. Chem.* 58, 321–352. <https://doi.org/10.1146/annurev.physchem.58.032806.104432>.
- Seinfeld, J.H., Pankow, J.F., 2003. Organic atmospheric particulate material. *Annu. Rev. Phys. Chem.* 54, 121–140. <https://doi.org/10.1146/annurev.physchem.54.011002.103756>.
- Sheesley, R.J., Kenski, D., 2004. Trends in secondary organic aerosol at a remote site in Michigan's upper peninsula. *Environ. Sci. Technol.* 38, 6491–6500.
- Spurny, K.R., 2000. *Aerosol Chemical Processes in the Environment*. Lewis Publishers.
- Szmigielski, R., Surratt, J.D., Gómez-González, Y., van der Veken, P., Kourtchev, I., Vermeylen, R., Blockhuys, F., Jaoui, M., Kleindienst, T.E., Lewandowski, M., Offenberg, J.H., Edney, E.O., Seinfeld, J.H., Maenhaut, W., Claeys, M., 2007. 3-methyl-1,2,3-butanetricarboxylic acid: an atmospheric tracer for terpene secondary organic aerosol. *Geophys. Res. Lett.* 34, 2–7. <https://doi.org/10.1029/2007GL031338>.
- Timonen, H., Saarikoski, S., Tolonen-Kivimä, O., Aurela, M., Saarnio, K., Petäjä, T., Aalto, P.P., Kulmala, M., Pakkanen, T., Hillamo, R., 2008. Size distributions, sources and source areas of water-soluble organic carbon in urban background air. *Atmos. Chem. Phys.* 8, 5635–5647. <https://doi.org/10.5194/acp-8-5635-2008>.
- Wang, G., Kawamura, K., Lee, M., 2009. Comparison of organic compositions in dust storm and normal aerosol samples collected at Gosan, Jeju Island, during spring 2005. *Atmos. Environ.* 43, 219–227. <https://doi.org/10.1016/j.atmosenv.2008.09.046>.
- Yu, J., Griffin, J., Cocker, R., Flagan, R.C., Seinfeld, J.H., 1999. Observation of gaseous and particulate products of monoterpene oxidation in forest atmosphere. *Geophys. Res. Lett.* 26, 1145–1148.
- Zangrando, R., Barbaro, E., Vecchiato, M., Kehrwald, N.M., Barbante, C., Gambaro, A., 2016. Levoglucosan and phenols in Antarctic marine, coastal and plateau aerosols. *Sci. Total Environ.* 544, 606–616. <https://doi.org/10.1016/j.scitotenv.2015.11.166>.
- Zangrando, R., Barbaro, E., Zennaro, P., Rossi, S., Kehrwald, N.M., Gabrieli, J., Barbante, C., Gambaro, A., 2013. Molecular markers of biomass burning in Arctic aerosols. *Environ. Sci. Technol.* 47, 8565–8574. <https://doi.org/10.1021/es400125r>.
- Zhang, S.H., Shaw, M., Seinfeld, J.H., Flagan, R.C., 1992. Photochemical aerosol formation from α -pinene- and β -pinene. *J. Geophys. Res.* 97, 20717–20729. <https://doi.org/10.1029/92JD02156>.
- Zhang, X., McVay, R.C., Huang, D.D., Dalleska, N.F., Aumont, B., Flagan, R.C., Seinfeld, J.H., 2015. Formation and evolution of molecular products in α -pinene secondary organic aerosol. *Proc. Natl. Acad. Sci. Unit. States Am.* 112, 14168–14173. <https://doi.org/10.1073/pnas.1517742112>.
- Zhang, Y.Y., Müller, L., Winterhalter, R., Moortgat, G.K., Hoffmann, T., Pöschl, U., 2010. Seasonal cycle and temperature dependence of pinene oxidation products, dicarboxylic acids and nitrophenols in fine and coarse air particulate matter. *Atmos. Chem. Phys.* 10, 7859–7873. <https://doi.org/10.5194/acp-10-7859-2010>.

Acknowledgements

I would like to express my special appreciation and thanks to my supervisor Professor Andrea Gambaro, you have been a formidable mentor for me. I would like to thank you for encouraging my research and for allowing me to grow as a research scientist. Your advice on both research as well as on my career have been invaluable.

I would also like to thank the "external expert", Dr. Elena Barbaro for helping me and supporting me when I needed it. I also want to thank you for your brilliant comments and suggestions. I thank all the colleagues with whom I collaborated, Dr. Catherine Larose for the research experience in Lyon and Dr. Andrea Spolaor for the opportunities you gave me.

A special thanks to my family. Words can not express how grateful I am. I would also like to thank to Sabrina. Thank you for supporting me for everything, and especially I can not thank you enough for encouraging me throughout this experience.



Università
Ca' Foscari
Venezia

DEPOSITO ELETTRONICO DELLA TESI DI DOTTORATO

DICHIARAZIONE SOSTITUTIVA DELL'ATTO DI NOTORIETA'

(Art. 47 D.P.R. 445 del 28/12/2000 e relative modifiche)

Io sottoscritto Matteo Feltracco

nat o. a Asolo (prov. TV) il 03/09/1988

residente a Asolo in Via Castellana n. 31

Matricola (se posseduta) 816906 Autore della tesi di dottorato dal titolo:
Chemical characterization of Arctic aerosol for investigating the multi-annual profile of
anthropogenic and biogenic markers

Dottorato di ricerca in Scienze Ambientali

(in cotutela con

Ciclo 33°


Anno di conseguimento del titolo 2021

DICHIARO

di essere a conoscenza:

- 1) del fatto che in caso di dichiarazioni mendaci, oltre alle sanzioni previste dal codice penale e dalle Leggi speciali per l'ipotesi di falsità in atti ed uso di atti falsi, decado fin dall'inizio e senza necessità di nessuna formalità dai benefici conseguenti al provvedimento emanato sulla base di tali dichiarazioni;
- 2) dell'obbligo per l'Università di provvedere, per via telematica, al deposito di legge delle tesi di dottorato presso le Biblioteche Nazionali Centrali di Roma e di Firenze al fine di assicurarne la conservazione e la consultabilità da parte di terzi;
- 3) che l'Università si riserva i diritti di riproduzione per scopi didattici, con citazione della fonte;
- 4) del fatto che il testo integrale della tesi di dottorato di cui alla presente dichiarazione viene archiviato e reso consultabile via Internet attraverso l'Archivio Istituzionale ad Accesso Aperto dell'Università Ca' Foscari, oltre che attraverso i cataloghi delle Biblioteche Nazionali Centrali di Roma e Firenze;
- 5) del fatto che, ai sensi e per gli effetti di cui al D.Lgs. n. 196/2003, i dati personali raccolti saranno trattati, anche con strumenti informatici, esclusivamente nell'ambito del procedimento per il quale la presentazione viene resa;
- 6) del fatto che la copia della tesi in formato elettronico depositato nell'Archivio Istituzionale ad Accesso Aperto è del tutto corrispondente alla tesi in formato cartaceo, controfirmata dal tutor, consegnata presso la segreteria didattica del dipartimento di riferimento del corso di dottorato ai fini del deposito presso l'Archivio di Ateneo, e che di conseguenza va esclusa qualsiasi responsabilità dell'Ateneo stesso per quanto riguarda eventuali errori, imprecisioni o omissioni nei contenuti della tesi;
- 7) del fatto che la copia consegnata in formato cartaceo, controfirmata dal tutor, depositata nell'Archivio di Ateneo, è l'unica alla quale farà riferimento l'Università per rilasciare, a richiesta, la dichiarazione di conformità di eventuali copie;

Data 03/11/2020

Firma 

NON AUTORIZZO

l'Università a riprodurre ai fini dell'immissione in rete e a comunicare al pubblico tramite servizio on line entro l'Archivio Istituzionale ad Accesso Aperto la tesi depositata per un periodo di 12 (dodici) mesi a partire dalla data di conseguimento del titolo di dottore di ricerca.

DICHIARO

- 1) che la tesi, in quanto caratterizzata da vincoli di segretezza, non dovrà essere consultabile on line da terzi per un periodo di 12 (dodici) mesi a partire dalla data di conseguimento del titolo di dottore di ricerca;
- 2) di essere a conoscenza del fatto che la versione elettronica della tesi dovrà altresì essere depositata a cura dell'Ateneo presso le Biblioteche Nazionali Centrali di Roma e Firenze dove sarà comunque consultabile su PC privi di periferiche; la tesi sarà inoltre consultabile in formato cartaceo presso l'Archivio Tesi di Ateneo;
- 3) di essere a conoscenza che allo scadere del dodicesimo mese a partire dalla data di conseguimento del titolo di dottore di ricerca la tesi sarà immessa in rete e comunicata al pubblico tramite servizio on line entro l'Archivio Istituzionale ad Accesso Aperto.

Specificare la motivazione:

motivi di segretezza e/o di proprietà dei risultati e/o informazioni sensibili dell'Università Ca' Foscari di Venezia.

motivi di segretezza e/o di proprietà dei risultati e informazioni di enti esterni o aziende private che hanno partecipato alla realizzazione del lavoro di ricerca relativo alla tesi di dottorato.

dichiaro che la tesi di dottorato presenta elementi di innovazione per i quali è già stata attivata / si intende attivare la seguente procedura di tutela:

.....;

Altro (specificare):

.....
.....
.....

A tal fine:

- dichiaro di aver consegnato la copia integrale della tesi in formato elettronico tramite auto-archiviazione (upload) nel sito dell'Università; la tesi in formato elettronico sarà caricata automaticamente nell'Archivio Istituzionale ad Accesso Aperto dell'Università Ca' Foscari, dove rimarrà non accessibile fino allo scadere dell'embargo, e verrà consegnata mediante procedura telematica per il deposito legale presso la Biblioteca Nazionale Centrale di Firenze;

- consegno la copia integrale della tesi in formato cartaceo presso la segreteria didattica del dipartimento di riferimento del corso di dottorato ai fini del deposito presso l'Archivio di Ateneo.

Data 03/11/2020

Firma 

La presente dichiarazione è sottoscritta dall'interessato in presenza del dipendente addetto, ovvero sottoscritta e inviata, unitamente a copia fotostatica non autenticata di un documento di identità del dichiarante, all'ufficio competente via fax, ovvero tramite un incaricato, oppure a mezzo posta.

Firma del dipendente addetto

Ai sensi dell'art. 13 del D.Lgs. n. 196/03 si informa che il titolare del trattamento dei dati forniti è l'Università Ca' Foscari - Venezia.

I dati sono acquisiti e trattati esclusivamente per l'espletamento delle finalità istituzionali d'Ateneo; l'eventuale rifiuto di fornire i propri dati personali potrebbe comportare il mancato espletamento degli adempimenti necessari e delle procedure amministrative di gestione delle carriere studenti. Sono comunque riconosciuti i diritti di cui all'art. 7 D. Lgs. n. 196/03.

Estratto per riassunto della tesi di dottorato

Studente: Matteo Feltracco

matricola: 816906

Dottorato: Scienze Ambientali

Ciclo: 33°

Titolo della tesi:

Chemical characterization of Arctic aerosol for investigating the multi-annual profile of anthropogenic and biogenic markers

Abstract (english version):

The present PhD thesis provides a broad information about the chemical characterization of the Arctic aerosol from 2013 to early 2019 collected at Ny Ålesund, Svalbard Island, Norway. Here, the size-distributions, transport processes and source apportionment of major ions, organic acids, free and combined amino acids, sugars and phenolic compounds were studied in the Arctic aerosols. The thesis also aimed to develop a new method for the determination of combined amino acids and photo-oxidation products of α -pinene in aerosol to understand differences and analogies with free amino acids and to understand the possible emission sources of these biomarkers.

The results of this study explained that the water-soluble compounds were influenced by biomass burning events occurred in Northern Russia and Canada, together with a strong contribution from sea particles and phytoplankton bloom, especially deriving from the fjord (Kongsfjorden) which is located 1.2 km from the sampling site.

Abstract (versione in italiano):

La presente tesi di dottorato fornisce un approfondito studio della composizione chimica dell'aerosol artico atmosferico raccolto dal 2013 al 2019 a Ny Ålesund, Isole Svalbard, Norvegia. È stata studiata la distribuzione dimensionale dell'aerosol, i processi di trasporto e il source apportionment di ioni maggiori, acidi organici, amminoacidi liberi e combinati, zuccheri e composti fenolici. È stato inoltre sviluppato un nuovo metodo per la determinazione di amminoacidi combinati e prodotti di foto-ossidazione dell' α -pinene in aerosol, per comprendere differenze e analogie con gli amminoacidi liberi e le possibili fonti di emissione di questi biomarcatori.

I risultati di questo studio spiegano come i composti idrosolubili siano stati influenzati da eventi di combustione di biomasse che si sono verificati nel nord della Russia e in Canada, assieme ad un forte contributo delle particelle marine e della fioritura del fitoplancton, soprattutto derivante dal fiordo (Kongsfjorden) antistante al sito di campionamento.

Firma dello studente

